

Flexible AC/DC Grids in Dymola/ Modelica

**Modeling and Simulation of Power Electronic Devices and
Grids**



Andreas Olenmark and Jens Sloth

Division of Industrial Electrical Engineering and Automation
Faculty of Engineering, Lund University

ABSTRACT

The research of the thesis was aimed towards investigating the possibility of implementing different control strategies for power electronic converters in a simulation environment. The different control modes were fitted into flexible models that were interconnected in various grid topologies. The software used in order to develop the simulation environment is called Dymola and presently does not include any form of control of power electronic units. The library used is the Modelica Electric Power Library (EPL) where some power electronic converters were already implemented. The grid was controlled and kept stable for various scenarios using the developed controlled converter models.

The converter models were tested separately in order to verify that the models acted in the desired manner. The models were then interconnected into a grid and simulated for different scenarios in order to get grid models that could be fitted into multiple grid applications. To further prove this, models from external Modelica libraries were used in the grid setups. The results of the simulations clearly show that constructed models support the implementation of scalable and controllable grids in Dymola.

ACKNOWLEDGMENTS

Throughout the thesis support, help and useful inputs have been given by a number of people. These people deserve a special recognition for their encouragement and patience.

Therefore we would like to express our gratitude to Francisco Marquez for all useful and knowledgeable advice and constructive ideas. To Jörgen Svensson who has enabled this project and helped along the way with interesting ideas and helpful advice.

Thanks also goes out to Anna Johnsson at Modelon AB for all the technical support concerning Dymola/Modelica. Finally we would like to thank Carl Wilhelmsson and Modelon AB for guidance and for making this project possible.

Andreas Olenmark & Jens Sloth

TABLE OF CONTENT

Abstract.....	2
Acknowledgments.....	2
1 Introduction.....	6
1.1 Background.....	6
1.2 Problem description.....	6
1.3 Method of approach.....	7
1.4 Modeling tools.....	7
1.5 Goals and Limitations.....	8
1.6 Why are these grids needed.....	8
1.7 Report outline.....	11
2 Power Electronic Theory.....	12
2.1 Modulation.....	12
2.2 The Buck Converter.....	14
2.3 The Boost Converter.....	17
2.4 H-bridge DC/DC Converter.....	18
2.4.1 Dymola Implementation of the H-bridge.....	18
2.5 Diode Rectifier.....	19
2.6 The Three Phase Converter.....	21
2.6.1 Dymola Implementation of the Three Phase Converter.....	24
2.7 Active Front End (AFE).....	26
2.7.1 Background.....	26
2.7.2 General function.....	26
2.7.3 Mathematical Description of the system.....	28
2.7.4 Dymola Implementation of the Active Front End.....	32
3 Control Methodology and Verification.....	33
3.1 The PI-controller.....	33
3.1.1 Dymola Implementation.....	33
3.2 H-Bridge Control.....	34
3.2.1 Dymola Implementation of the H-Bridge Power Control.....	35
3.2.2 Simulation Results of the Power Controlled H-Bridge.....	36
3.2.3 Discussion.....	38
3.3 Active Front End DC Voltage Control.....	39
3.3.1 Dymola Implementation of Active Front End Voltage Control.....	40
3.3.2 Simulation Results of the Voltage Controlled AFE.....	43

3.3.3	Discussion.....	47
3.4	AC/DC Converter Power Control.....	48
3.4.1	Dymola Implementation of the AC/DC Inverter with Power Control.....	50
3.4.2	Simulation Results of the Power Controlled AC/DC Converter.....	52
3.4.3	Discussion.....	55
3.5	AC/DC Converter Droop Control.....	56
3.5.1	Dymola Implementation of the AC/DC Converter with Droop Control.....	58
3.5.2	Simulation Results of the Droop Controlled AC/DC Converter.....	60
3.5.3	Discussion.....	63
3.6	Open Loop AC Voltage Control of the AC/DC Converter.....	64
3.6.1	Dymola Implementation of the Open Loop AC Voltage Control.....	66
3.6.2	Simulation Results of the Open Loop AC Voltage Control.....	67
3.6.3	Discussion.....	69
3.7	Reactive Power Compensation in an Internal AC Grid.....	70
3.7.1	Dymola Implementation of the Reactive Power Compensation.....	71
3.7.2	Simulation results of the reactive compensation block.....	72
3.7.3	Discussion.....	75
4	Model Flexibility.....	76
4.1	Multi controller.....	76
4.2	Records.....	79
5	Grid Setups.....	81
5.1	Cable Theory.....	81
5.1.1	AC Cables.....	81
5.1.2	Inductance Dimensioning in a Realistic Three Phase AC Grid.....	81
5.1.3	DC Cables.....	82
5.2	Internal DC Grid.....	82
5.2.1	Back-To-Back Converter and Mtdc Grids.....	83
5.2.2	Dymola Implementation and Simulation Results of DC Grids with Switched Converters.....	84
5.3	DC Grid with Wind Power and Smart House Libraries.....	100
5.3.1	Dymola Implementation of the DC Grid with External Models.....	100
5.3.2	Discussion.....	102
5.3.3	Droop Controlled DC Grid with External Models in Dymola.....	103
5.3.4	Discussion.....	105
5.3.5	High Voltage Scenario.....	105

5.4	Internal AC Grid	109
5.4.1	AC-Grid Topology	109
5.4.2	Dymola Implementation of the AC Grid	110
6	Conclusions	118
6.1	Future Work	118
7	Nomenclature.....	119
8	List of Figures.....	122
9	List of Tables.....	126
10	Acronyms	127
11	References	127
	Appendix A.....	130
	Appendix B.....	130
	Appendix C.....	131
	Appendix D	133

1 INTRODUCTION

1.1 BACKGROUND

The need for electrical energy is increasing continuously and in order for these needs to be met the electrical grid has to be able to handle the energy which is to be transferred. In addition to this, renewable energy sources are increasingly introduced in the electrical grid which contributes to the grid dependence on external conditions. This applies to electrical grids of all sizes whether it is a large national grid or a smaller household grid. Common for these grid setups are that several units are coupled together and need to be controlled in some manner in order to keep the grid operational in the desired voltage level and meet the grid specifications. The units are power electronic devices e.g. converters which can operate either in alternating current (AC) or in direct current (DC) which also offers the option of controllability. This means that the converter can transform AC given from an AC power source to a DC grid or consumer, and vice versa, and has the ability to control power flow, voltage, current etc. Thereby a simulation model of arbitrary size which implements these devices will enable the introduction of smart grid control. A smart grid would to a large extent offer a flexible and adaptive grid which would benefit the introduction of renewable energy sources in the electrical grid.

1.2 PROBLEM DESCRIPTION

The main part of the project is to build an extended library of simulation models using Modelica [16] which can be interconnected into an electric grid. These models, mainly power electronic converters, should be connected into a grid and each unit supplies the grid with energy from an arbitrary source of power. In order for this to act as an electrical grid energy consumers must also be included in the grid. A general setup of the grid topology that will be used in this thesis is shown in figure 1.1.

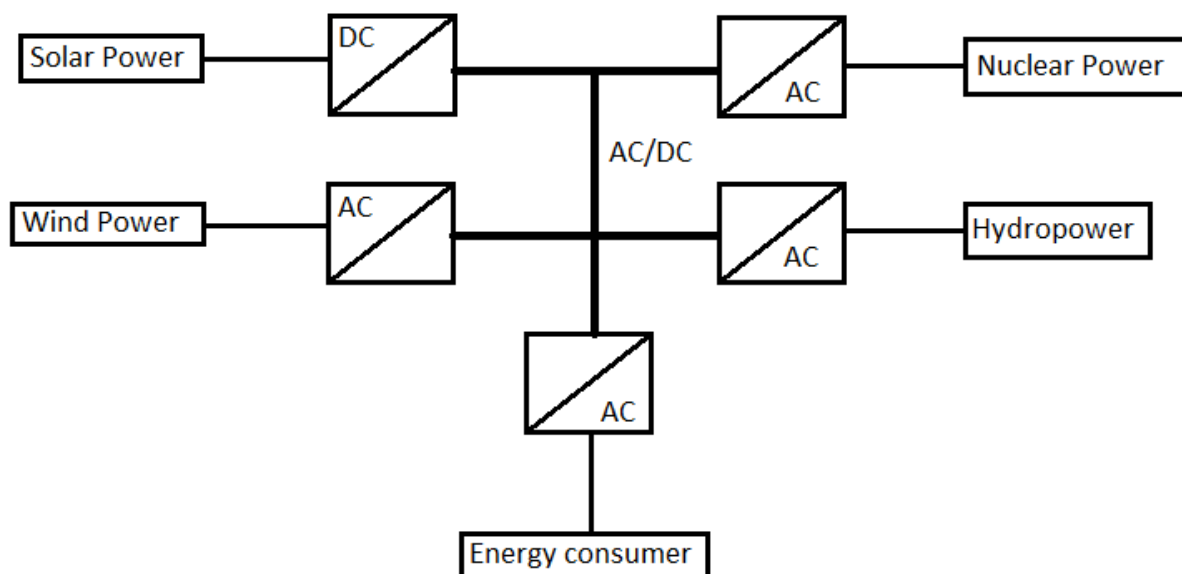


Figure 1.1 The figure illustrates the general grid structure with power electronic devices connected to it.

The system should be scalable and able to operate in either AC or DC. This means that some power sources and consumers can be replaced or removed depending on the size of the grid. The general idea is to make units easily replaceable and scalable in order to implement the sought net for a specific application. Currently the Electrical Power Library (EPL) in Dymola lacks models of an electrical grid built with power electronic converters which could be scaled and coupled to different sources of power.

1.3 METHOD OF APPROACH

To reach an electrical grid simulation model, sub models first has to be constructed such as converters and grid representations. The Modeling language Modelica and the software Dymola will be used to construct and build Modelica models. In Dymola components can be modeled using sub-components from EPL or from other Modelica Libraries.

Firstly the converter models must be built. This includes implementing control algorithms for the converters so that the correct voltage and frequency is kept at the output. Converters and rectifiers are verified using ideal voltage sources. Later on these sources are partly substituted with already existing models for different types of electricity generation.

Next step of inquiry is the grid representation. Here the grid should be represented properly to enable interconnections of the power electronic units. The properties of the grid should be fitted into a model and key variables should be identified for both AC and DC operation. Since no storage of electricity is available the amount of power consumed at any time must be injected by the power sources. When these steps are taken the work will consist of merging the models into a system. By appropriate control of the converters, voltage stability can be reached and power balance between consumer and source can be maintained.

In order for this grid simulation model to be useful the model has to be flexible. The flexibility lies within the option that either internal AC or DC grid models can be constructed using different control modes for the converters. The scalability is shown by connecting the model in different scenarios for each AC and DC. The scenarios handle different voltage levels where the power flows and currents differ as well. The scenarios are chosen to represent practical implementations and will be further discussed later.

1.4 MODELING TOOLS

To construct models and test them in a computerized environment the simulation software Dymola is used in this thesis. Dymola (Dynamic Modeling Laboratory) is a simulation tool that can be used in several engineering areas such as electrical, thermodynamical, mechanical etc. The software can be used when working in different engineering areas simultaneously and has interfaces between the different areas. Dymola incorporates graphical programming, but can also be used in a conventional programming manner [17]. Dymola is based on the Modelica language, which is a free equation-based object-oriented language. The Modelica language was especially developed for modeling dynamical systems. Electric power library (EPL) which is used to model power electronic units and power systems is an external Modelica library developed for Dymola. [18]

1.5 GOALS AND LIMITATIONS

The main goal is to implement a scalable controllable grid model representation. This representation will consist of different units which are scalable and adjustable in order to create flexible electrical grids that could be used in many different applications. Milestones of this are:

- Construction of simulation models of converters, this will include
 - AC/DC converters
 - DC/DC converters
- Implementation of control principles for the different units, this will include
 - AC/DC converter with current and DC voltage control
 - AC/DC converter with AC voltage control
 - AC/DC converter with droop control
 - AC/DC converter with current and power control allowing bidirectional power flow
 - DC/DC converter with current and power control allowing bidirectional power flow
- Construct one converter model where all the above mentioned control modes are included as options. In this Multi Controller it will be possible to choose between different voltage and power levels.
- Create a model of the grid to which the converters etc will be connected.
- Connect the models to components from other Modelica libraries.
- Testing of converter and grid models in different scenarios.
- Analysis of simulation results.

The thesis does not include calculations of losses in the converters or thermal losses developed in the system components. These kinds of losses in the system are of course important when constructing these kinds of units and grids, but will not be taken into account. For high voltages simulations (HVDC) only one three phase converter is used in the converter models. In reality this is not possible since the maximum voltage that a transistor (IGBT) can withstand is around 4000 V. The assumption is that the converters can be stacked in a formation so that the IGBT is operating at rated voltage levels. In the models this formation is represented as one three phase converter.

1.6 WHY ARE THESE GRIDS NEEDED

The idea of having a grid that only has converters connected is based on the fact that the grid structure needs to change in order to introduce new forms of generating electricity. The conventional grid structure is based upon having few points of generation which branches out to the consumers as shown in figure 1.2. With new electricity sources which are suitable for being placed at the consumer, e.g. solar power, wind power plants etc, rather than having a large generation at one point only, shifts the grid structure compared to the conventional structure. The grid structure shifts because the consumers now are not only consumers of electricity but could also be a source of electricity generation.

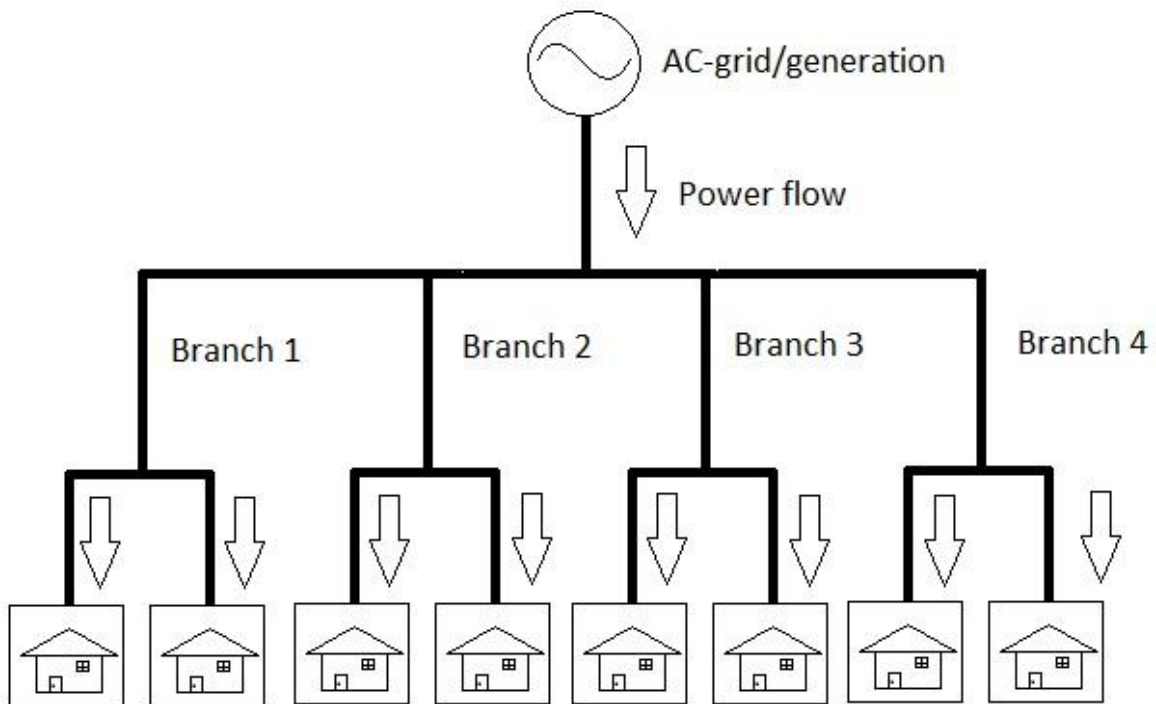


Figure 1.2 The figure shows the conventional grid structure with generation at a common point and all consumers act as pure loads.

The topology of the grid stays the same since the conductor layout is already in place. The structural shift is more an issue of where generation takes place as can be seen in figure 1.3. The power electronic converters, that are the topic of this project, are placed inside the consumer block shown in figure 1.3. Although the converters could be inserted anywhere in the structure the consumer block is the most logical place to start this implementation. The power electronic devices are implemented here in order to, internally in the consumer block, create an electrical sub-grid where the generation, grid connection and the pure load are interconnected. This enables the consumer to both consume and supply power to the main grid. Power electronic devices enables the internal sub-grid to operate in either DC or AC. By doing this the DC-grids and DC-components can be inserted into the main grid. However, the largest benefit of using power electronic converters is that the main grid and the local sub-grid are decoupled. The decoupling is due to the power electronic devices, more specifically the *Active Front End (AFE)* where an AC-voltage input creates a DC-voltage output or vice versa. The control of the AFE offers the opportunity to control the active and the reactive power. Where the reactive power consumed from or supplied to the grid can be chosen freely and the active power control is dependent on the load. This means that the power consumed from and supplied to the main grid can be limited to active power since this is the desired scenario. This is since the power electronic devices can create an almost arbitrary switched AC-voltage.

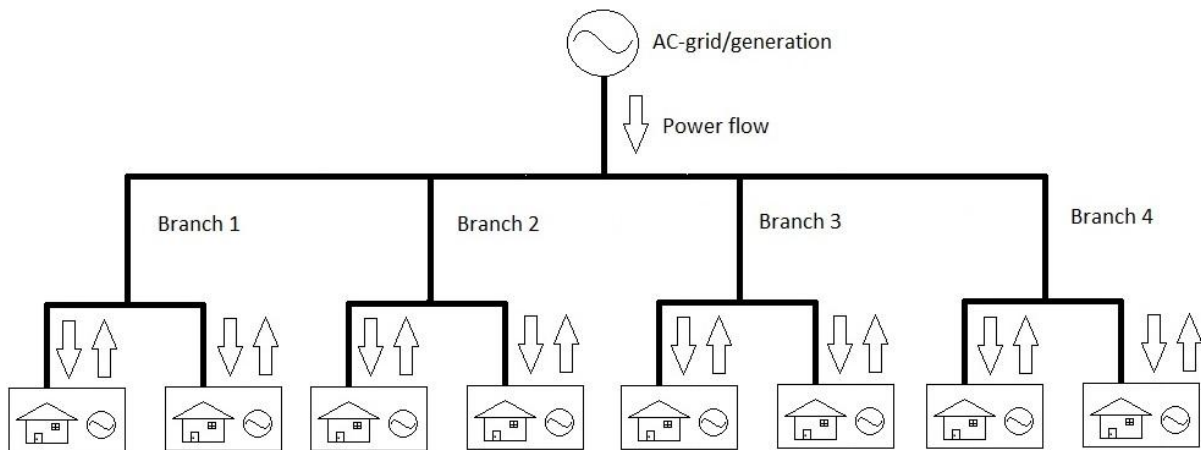


Figure 1.3 The new grid structure that allows consumers to feed back power onto the grid.

Another application where this kind of grid structure and control can be implemented is in the introduction of electric vehicles [1]. Electric cars need to be charged when not used to ensure that a sufficient amount of energy is available when starting to drive. To simplify this, large charging stations could be placed at malls, offices and such in order to charge the car batteries while doing other activities since it takes some time to charge the car batteries. These charging stations are small grids in their self since there are loads in the form of cars and power supply in the form of the outside connected grid. In addition wind power plants or/and PV-cells can be connected to these grids. This means that the charging stations can be viewed upon as both consumers and suppliers of energy. The electric car can be considered as both a load and source itself as well since the energy stored in the car can be retracted if needed. This could be the case if for example three nearly fully charged cars are connected to the charging station and will stay plugged in for some time. A new car connects to the charging station and needs to be charged quickly. Instead of consuming a huge amount of power from the outside connected grid, the power can flow from the three nearly fully charged cars and from the grid. This would make the power consumption from the outside connected grid constant to a larger extent. Hence, the grid would not be as stressed when connecting a large load to the grid compared to before.

However, these kind of electric vehicle grids are still to be implemented in a larger scale in the future. A present example of where the consumer-supply chain changes is in the hybrid cars that are increasingly popular. Since the battery and, at least, the electrical propulsion system are interconnected some kind of converter has to be placed in the interface between these units. The internal combustion engine coupled generator is commonly connected to this grid point as well [4]. The electrical propulsion system is also able to generate power when the wheels are rolling and a negative traction torque is applied to them e.g. when breaking. A grid with the internal combustion engine coupled generator, the battery and the electrical propulsion system is formed where the latter unit can either consume or supply power. Furthermore, the battery commonly operates in DC meaning that converters have to be used in order to get the generator and the electrical propulsion system to interact properly with the battery.

An internal grid in the vehicle industry is however not narrowed down to car applications but quite the opposite. Ships use electricity in various forms in different places across the vessel. There has been a notion that ships could decrease the fuel consumption, increase payload, just

by implementing internal DC grids and converters [2]. Furthermore, this grid structure allows installment of large batteries, solar power or even wind power on ships, which could further reduce the fuel consumption and therefore the fuel cost.

A large area where DC grids are implemented currently is in large wind power parks where many wind power plants are interconnected through DC cables [3]. This might seem odd since wind power plants produce alternating electricity, but the reason for this is that maximum power at any wind speed is desired. This requires the wind turbines to spin in different speed depending on the speed of the wind outside. This means that the different wind turbines rotate with different speeds. In order to interconnect them the rotating frequency has to be decoupled. This is done using a converter which converts AC into DC making the different wind turbines easy to interconnect. The internal DC grid needs to be connected to the distribution grid in order to supply power to the main grid. Since the power supplied by the wind turbines varies with the wind speed the power control of the converters has to be just as fast as the variation in the power generated.

Industries with industrial drives could also benefit from having internal DC grids. Instead of having force commuted rectifiers with filters in front of every electrical drive line, it could be more effective to have one AFE rectifier connected to the utility grid. By doing this power could be fed, via the DC grid, to all other power electronic devices controlling the electrical drivelines. This could provide advantages in terms of efficiency, cost and flexibility, [13].

Despite all the above mentioned areas of where these kinds of grids can be used, the internal grid implementation of distributed systems still remains mostly a topic only for research.

1.7 REPORT OUTLINE

In chapter 2 the theory and purpose of the power electronic units are highlighted and then the Dymola implementations of the units are described. In Chapter 3 the control algorithms of the converters and the Dymola implementations of these are presented. Test benches are set up to test and verify the control behavior followed by a brief discussion. Chapter 4 describes the flexibility of the models and how this is implemented in the software. In chapter 5 the DC and AC grid theory are presented and the converters are connected into DC and AC grid setups. Different scenarios are simulated and the results of the simulations are evaluated. Chapter 5 also comprises the incorporation of other Modelica libraries. The discussions of all the simulation results form the overall conclusion that is presented in chapter 6. In chapter 6 potential improvements and further developments of the models are also highlighted.

2 POWER ELECTRONIC THEORY

Power electronic converters are used for many different applications such as AC/DC transformation, DC/DC conversion etc. It provides precise controllability and keeps high energy efficiency and is therefore an important component in the electrical grid.

2.1 MODULATION

In order to create the switching duty-cycle signals for the various power electronic units some form of modulation is needed. This is generally done using a triangular wave (so called carrier wave), the DC voltage and the voltage reference that is to be modulated. The frequency of the carrier wave corresponds to the switching frequency of the power electronic unit. The voltage reference is compared to the carrier in order to determine when the transistors should be active and not. This is done in the manner shown in figure 2.1 for a Buck converter. The voltage reference is compared to the carrier wave using a comparator and when the voltage reference exceeds the value of the carrier wave a signal telling the transistor to conduct is sent from the comparator to the transistor. This results in a voltage as can be seen in the lower part of figure 2.1. The average voltage in one switching period across the load will then be equal to the reference voltage since the load voltage is the full DC voltage during on-state and zero during off-state, which is illustrated in the lower part of figure 2.1. This is explained further in chapter 2.2. [5]

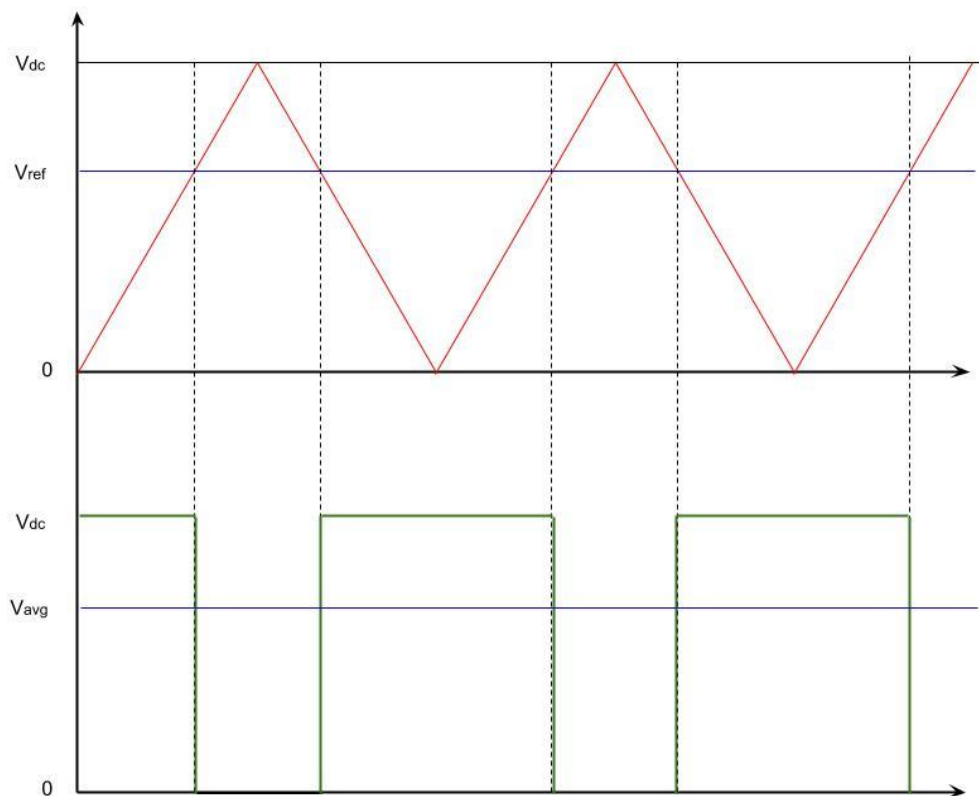


Figure 2.1 The figure shows the simple modulation of a Buck converter.

If AC voltage is desired as an output the voltage reference instead will be two AC voltages with half the amplitude and the same frequency as the desired output voltage. These reference voltages are counter phased to each other, meaning that one is shifted 180 degrees compared to the other [5]. Since the voltage references now can assume negative values an offset has to be added to the voltage references in order to place it into the carrier wave. Alternatively the triangular wave can be moved in order make it oscillate around zero seen in figure 2.3. However, the peak-to-peak voltage of the carrier wave should not be altered. The type of power electronic unit has to be changed in order to supply a negative voltage across the load [6]. For a single phase modulation, as described in figure 2.3, an H-bridge which can be seen in figure 2.2 is sufficient. The voltage across the load is the difference in potential between node 1 and node 2 in figure 2.2. In order to get the desired output voltage the two different potentials need to be controlled separately and it is achieved using two voltage references. One voltage reference is compared to the carrier wave and the output from the comparator is sent to one of the H-bridge legs, the other counter shifted voltage reference is compared in the same manner and the output is sent to the other H-bridge leg. This will result in the switched AC voltage across the load shown in the bottom part of figure 2.3.

In practical uses there is also implemented a short glitch (so called dead time) before applying the voltage across the load. Consider the transistor pair connected to node 2 in figure 2.2. Before turning on the top transistor it has to be ensured that the bottom transistor is turned off to avoid large currents rushing through the circuit. This is why the dead-band time is implemented. The result of these glitches is that the width of the pulses, the switched AC voltage shown in figure 2.3, would be smaller. This feature is implemented in the EPL components [18].

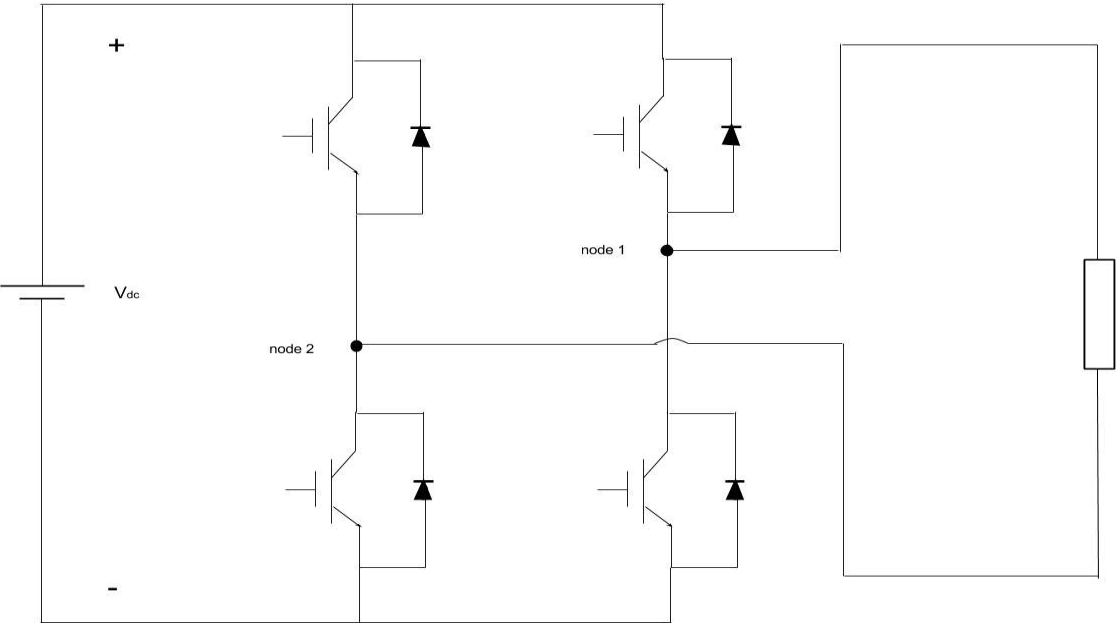


Figure 2.2 The electric schematic of the H-bridge.

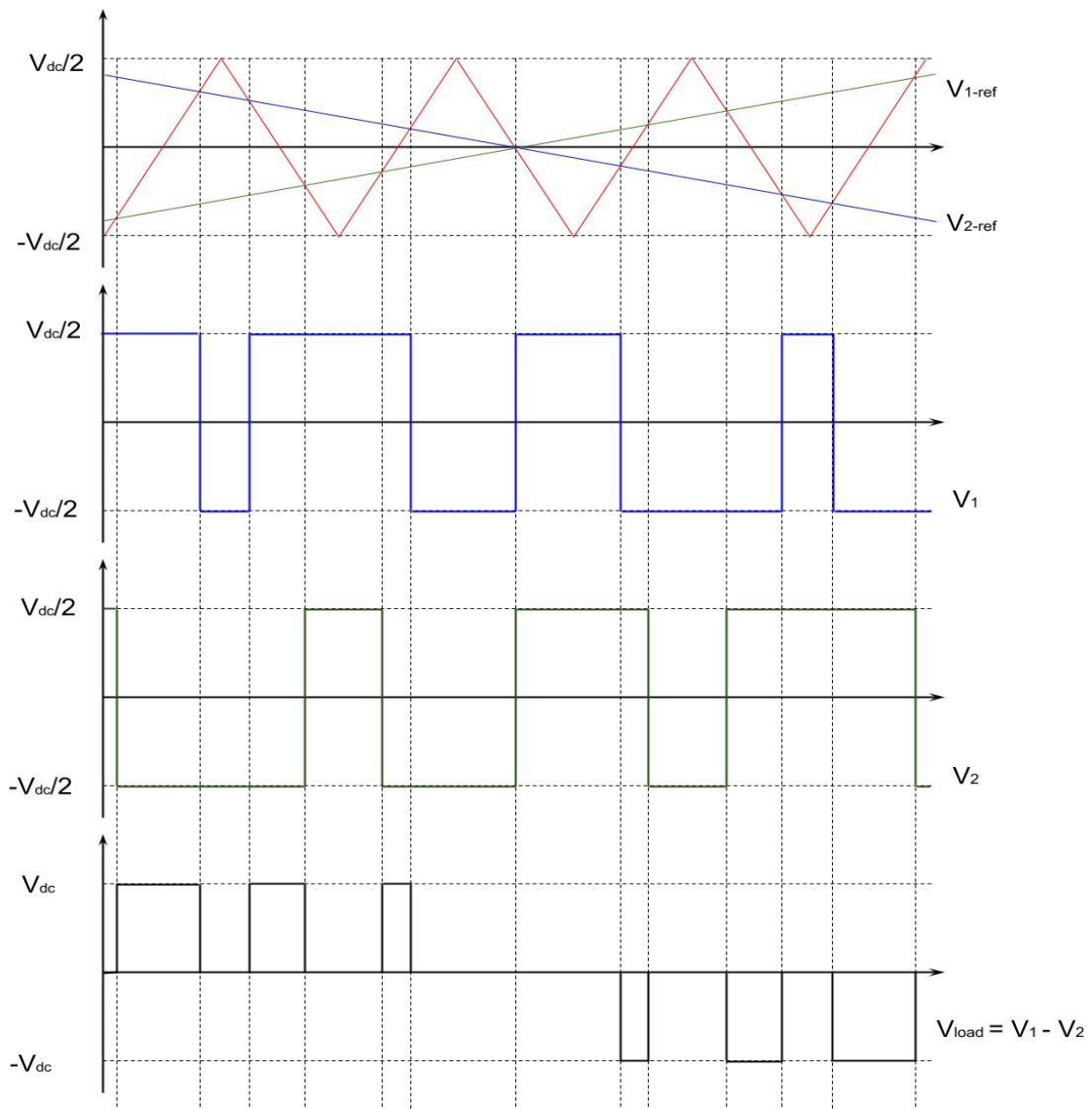


Figure 2.3 The modulation of the H-bridge when the H-bridge is used to create an AC voltage.

2.2 THE BUCK CONVERTER

A Buck-converter also called a step-down converter is used, as the name implies, to convert a certain input DC voltage to a lower output DC voltage. This is achieved by using a transistor, an inductor and a diode in the configuration shown in figure 2.4. The idea is to chop the input voltage using the transistor with a certain frequency making the output voltage in average lower than the input. Consider the transistor in figure 2.4 being active and thus making the transistor act like a (ideally) short circuit, from the input point of view. The voltage in node 1 in figure 2.4 will then be equal to the input voltage. When the transistor is inactive the voltage in node 1 will be equal to zero [5].

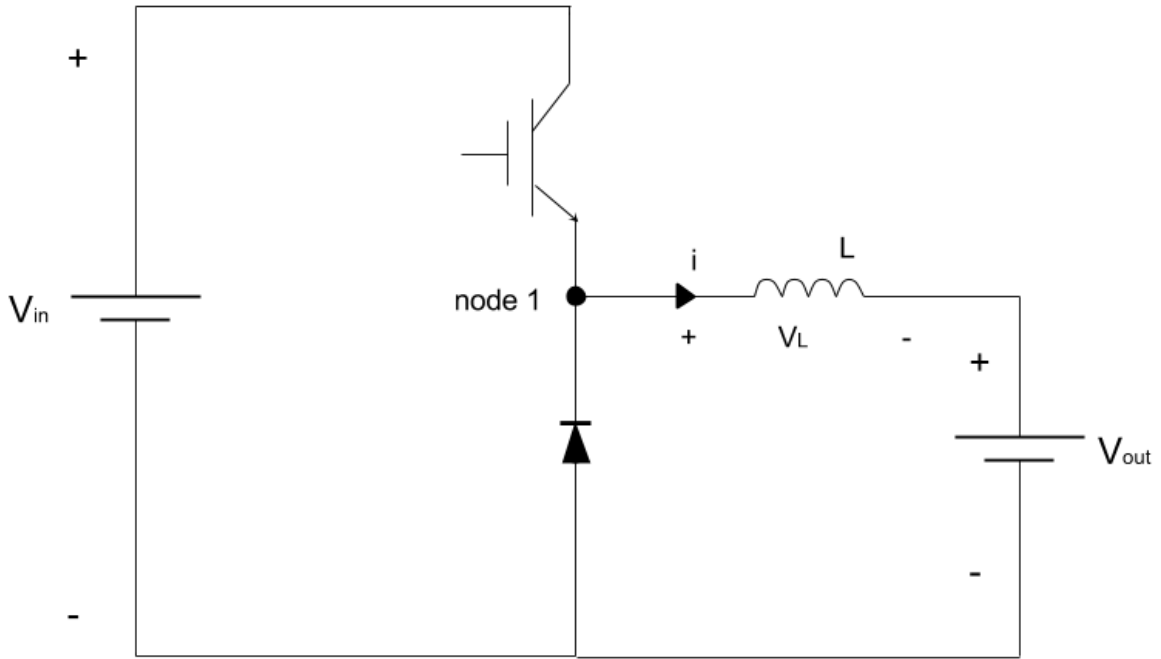


Figure 2.4 The electric schematic of the Buck converter.

The average voltage in node 1 (V_1) from figure 2.4 during one switching period will be the sum of on-state voltage and off-state voltage. Equation 2.1 describes this mathematically.

$$V_1 = \frac{t_{on}}{T_{sw}} * V_{in} + \frac{t_{off}}{T_{sw}} * 0 = \frac{t_{on}}{T_{sw}} * V_{in} \quad (2.1)$$

The ratio between on-state time (t_{on}) and switching period (T_{sw}) is called the duty-cycle and denoted D . Since the off-state time (t_{off}) is related to the switching period and the on-state time, the off-state time can also be expressed through the duty-cycle as follows

$$\frac{t_{off}}{T_{sw}} = \frac{T_{sw} - t_{on}}{T_{sw}} = 1 - \frac{t_{on}}{T_{sw}} = 1 - D \quad (2.2)$$

However, the output voltage is at this point a square wave and the current would also be a square wave if connected here. Therefore an inductor is placed in between the output and node 1 into which some energy could be stored. During the transistor on-state the inductor is charged due to the current that flows through it and during the off-state of the transistor the current is kept higher due to the inductor discharging [5]. It is in the discharging sequence the diode is important. The diode allows an alternate path for the current to flow through when the transistor is switched off. At this time the current goes from a positive value to zero making the current derivative theoretically negatively infinite. The voltage across the inductor is given by equation 2.3.

$$v_L = L \frac{di}{dt} \quad (2.3)$$

This would make the voltage across the inductor theoretically negatively infinite as well. However, due to the diode a current could now be pushed through the output and the diode back

to the inductor, thus completing a circuit in the off-state as well. This gives the current a smoother behavior acting more like a direct current. Despite this the current will still have a ripple which is related mostly to the size of the inductor and the switching frequency for a certain output current.

Using Kirchhoff's voltage law (KVL) the circuit can be analyzed and the current ripple can be determined. The voltage drop across the transistor is typically very small in comparison to the input voltage and therefore it could be set to zero when analyzing [5]. This assumption is also valid for the voltage drop of the diode. Further the output voltage could be viewed upon as constant by setting the switching period much smaller than the time constant of the output.

First of the on-state circuit is examined. Using KVL equation 2.4 is given.

$$V_{in} = v_L + V_{out} \rightarrow v_L = V_{in} - V_{out} \quad (2.4)$$

Combining this with equation 2.3 and assuming the current to be linear during this period equation 2.5 is given.

$$L \frac{\Delta i}{\Delta t} = V_{in} - V_{out} \rightarrow \Delta i = \frac{V_{in} - V_{out}}{L} * \Delta t \quad (2.5)$$

The maximum current difference occurs when switching from on-state to off-state at time $\Delta t = t_{on} = D * T_{sw}$, and thereby the current difference is given through equation 2.6.

$$\Delta i = \frac{V_{in} - V_{out}}{L} * D * T_{sw} \quad (2.6)$$

Using the same procedure the off-state current difference could also be calculated. Equation 2.4 could still be used where $V_{in} = 0$ instead. This result in equation 2.5 where $V_{in} = 0$. This will be true for the entire off-state time meaning that the current decreases during:

$$\Delta t = t_{off} = (1 - D) * T_{sw} \quad (2.7)$$

Corresponding to equation 2.6, equation 2.8 is formed.

$$\Delta i = \frac{-V_{out}}{L} * (1 - D) * T_{sw} \quad (2.8)$$

In steady-state operation the current will return to the same value after a full period which is expressed in equation 2.9. From this equation 2.9 is obtained and into it equation 2.7 and 2.8 is inserted. From this an alternate expression for the duty-cycle in steady-state is obtained equation 2.10.

$$\Delta i_{on} + \Delta i_{off} = 0 \quad (2.9)$$

$$\rightarrow \frac{V_{in} - V_{out}}{L} * D * T_{sw} = \frac{V_{out}}{L} * (1 - D) * T_{sw} \rightarrow$$

$$D = \frac{V_{out}}{V_{in}} \quad (2.10)$$

2.3 THE BOOST CONVERTER

Similar to the Buck converter the Boost converter is used to transform DC voltage to another DC voltage level. For the boost converter, also called step-up converter, the objective is to raise the voltage to a higher level. This can be done using the same type of components as for the Buck converter, namely a transistor, an inductor and a diode. The setup of the Boost converter is shown in figure 2.5. The input voltage in this case is lower than the output voltage making the operation of Boost converter quite different compared to the Buck converter. The idea here is to use the inductor as storage of energy in order to push current from a lower potential to a higher potential.

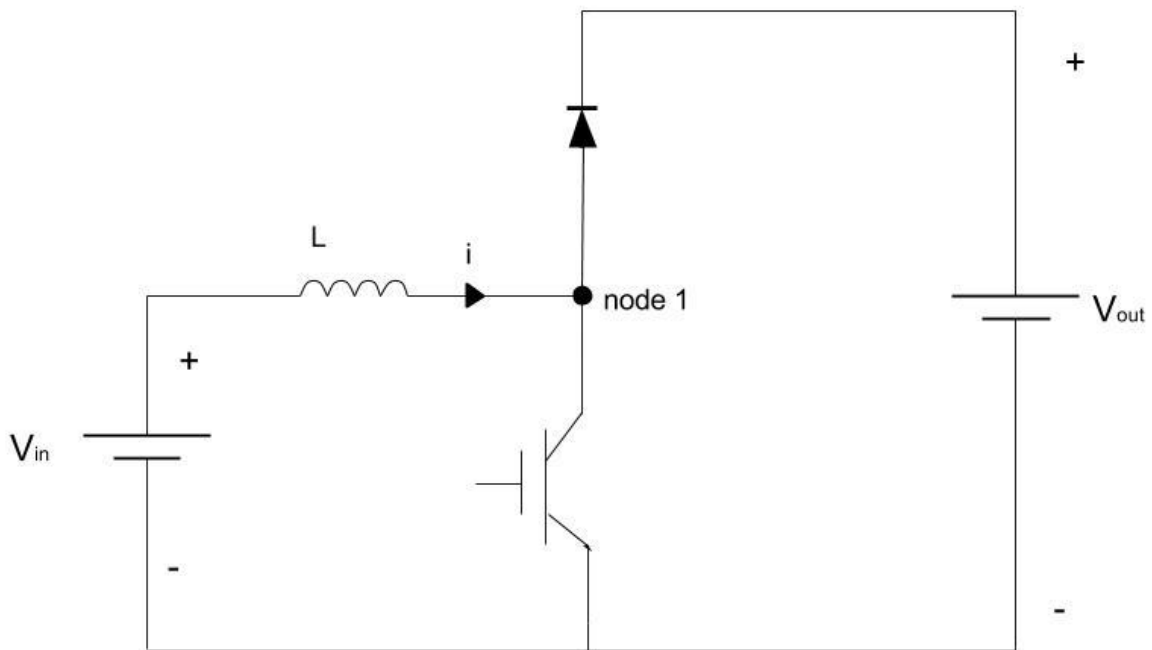


Figure 2.5 The electric schematic of the Boost converter.

When the transistor is in its on-state mode the transistor is ideally short circuited making the voltage in node 1 from figure 2.5 $V_1=0$. Since the diode blocks the current that would flow from the output voltage, the output is in this moment disconnected. This means that the only current flowing through the circuit is the current supplied by the input, flowing from the input through the inductor and transistor in a completed circuit. As it was in the case of the Buck converter the voltage drop across the transistor is neglected making the voltage across the inductor equal to the input voltage. When combining this with equation 2.3, equation 2.11 is formed.

$$V_{in} = L \frac{di}{dt} \quad (2.11)$$

If, again, the current is assumed to be linear during the on-state period and the time of on-state is expressed through duty cycle and switching period $\Delta t = D \cdot T_{sw}$, the rise in current can be determined as seen in equation 2.12.

$$L \frac{\Delta i}{\Delta t} = V_{in} \rightarrow \Delta i = \frac{V_{in}}{L} * D * T_{sw} \quad (2.12)$$

However, when the transistor is switched off there is no longer a path for the current to flow in. The current derivative will in this instant be theoretically negatively infinite and this causes the voltage across the inductor increase forcing current through diode. Examining the full circuit using KVL and neglecting the voltage drop across the diode equation 2.13 is reached, where the current difference during $\Delta t = t_{off} = (1-D) * T_{sw}$ can be calculated. Note that the output voltage is larger than the input voltage causing the current to decrease.

$$V_{in} - v_L = V_{out} \rightarrow \Delta i = \frac{V_{in} - V_{out}}{L} * (1 - D) * T_{sw} \quad (2.13)$$

In steady-state operation the same expression for the current ripple applies as in the case of the Buck converter, giving an alternate expression for the Boost converter duty cycle as seen in equation 2.14.

$$\Delta i_{on} + \Delta i_{off} = 0 \rightarrow \frac{V_{in}}{L} * D * T_{sw} + \frac{V_{in} - V_{out}}{L} * (1 - D) * T_{sw} = 0 \rightarrow D = 1 - \frac{V_{in}}{V_{out}} \quad (2.14)$$

2.4 H-BRIDGE DC/DC CONVERTER

The H-bridge DC/DC converter is the most versatile DC/DC converter because of its structure. The H-bridge, shown in figure 2.6, combines the properties of the Buck and Boost converter. In addition it also offers the possibility of choosing the direction of the current and the polarity of the voltage applied over the output. This means that power can flow both from input to output and vice versa. In order for this configuration to work the output voltage has to be lower than the input voltage. However, this does not pose a big problem since the converter could be flipped when higher output voltage is required.

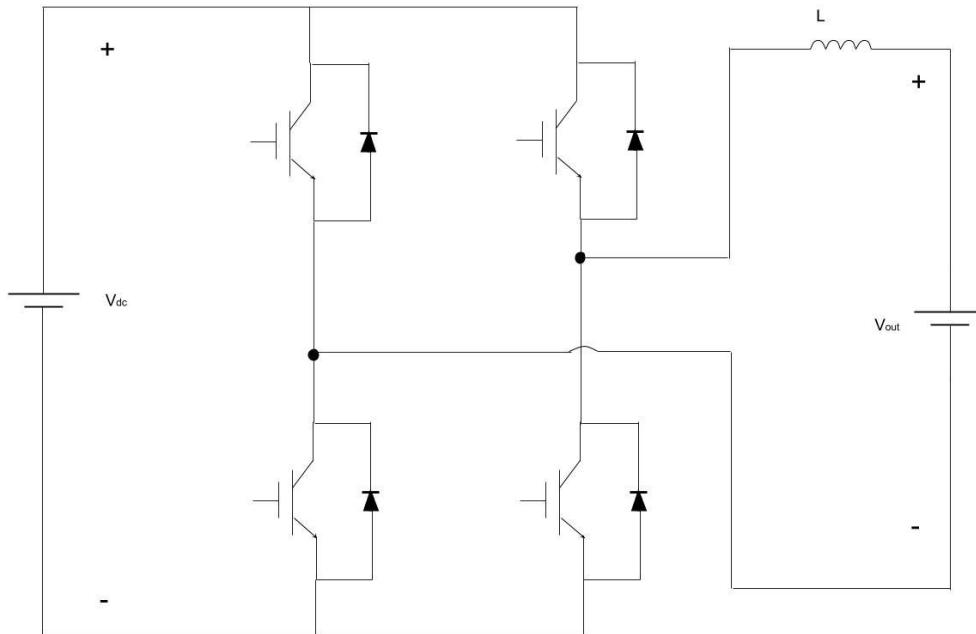


Figure 2.6 The electric schematic of the H-bridge.

2.4.1 DYMOLA IMPLEMENTATION OF THE H-BRIDGE

The Dymola implementation of the H-bridge is quite straight forward. The legs of the converter are already implemented in EPL. A leg is the transistor pair connected to each side of the output.

Two of these legs were connected in the manner seen in figure 2.6, and an inductance in series with a current sensor was connected at the output side. The measured current was connected to an output in order for it to be used in the control of the converter. To each side of the converter DC-link capacitors were connected in order to make it compatible with the DC grid and also to smoothen out the voltage to the load. The inputs to the transistor gates are generated by modulator outside the H-bridge model. The full Dymola model of the H-bridge can be seen in figure 2.7. Note that the diamond shaped connectors consists of two conductors one positive and one negative. These conductors can be divided into single ones which are seen in figure 2.7.

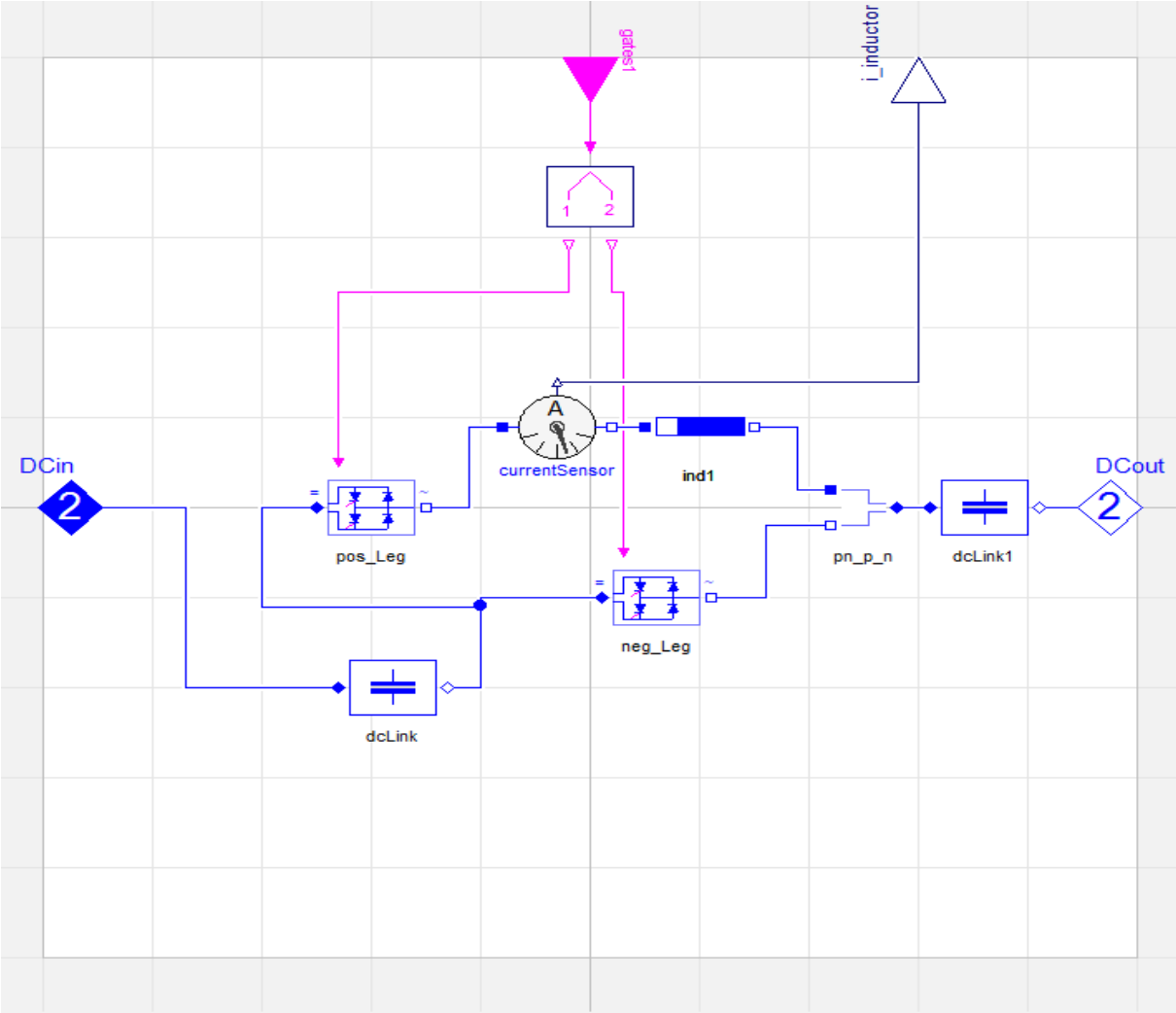


Figure 2.7 The Dymola implementation of the H-bridge.

2.5 DIODE RECTIFIER

The previously mentioned units operate in DC to DC meaning that both input and output are DC. When converting AC to DC a diode rectifier is a simple and effective way to carry out the conversion. The diode rectifier consists of four diodes working in pairs coupled in the configuration seen in figure 2.8 for a single phase operation. When the AC voltage is positive the top left diode (D1 in figure 2.8) has a positive potential on its anode making it biased. The current flows through the load and the bottom right diode (D4 in figure 2.8), since the potential of this diode cathode is negative. Further, when the AC voltage is negative the top right diode (D2 in figure 2.8) anode has positive potential making it able to conduct. The bottom left diode

(D3 in figure 2.8) cathode now has negative potential also making it able to conduct. Thus, the circuit is complete and the current direction is the same both when the alternating source is positive and negative.

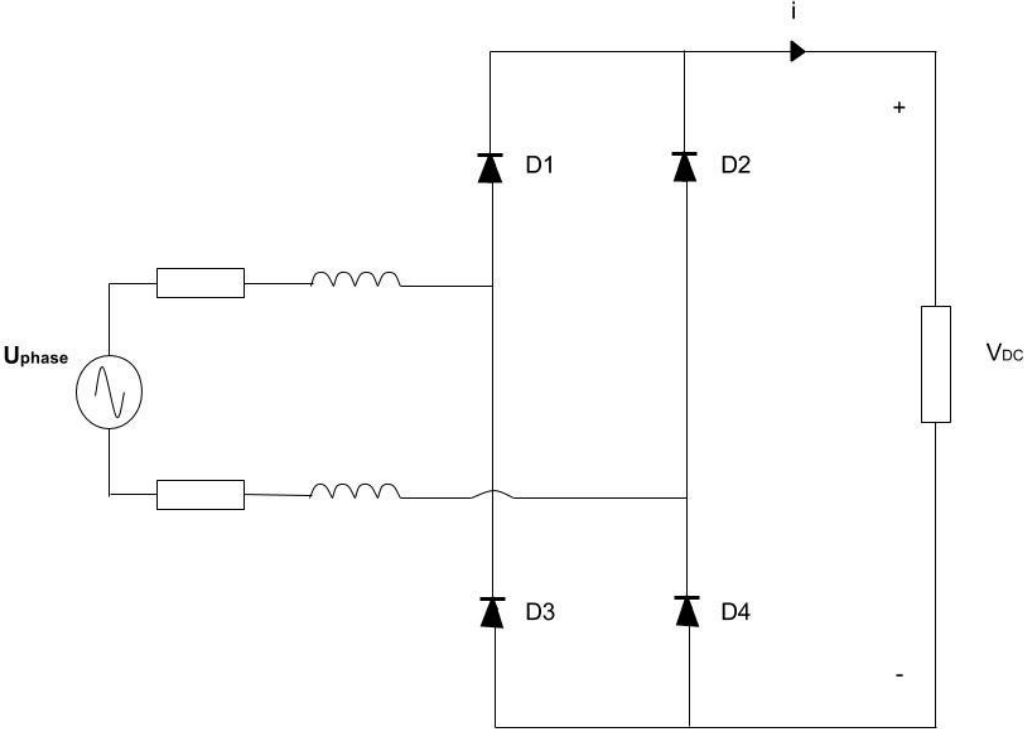


Figure 2.8 The electric schematic of the one phase diode rectifier.

This can be expanded into symmetrical three-phase applications by connecting two diodes to each phase in similar configuration, as can be seen in figure 2.9. The DC voltage across the load can be calculated through equation 2.15 for single-phase applications and through equation 2.16 for symmetrical three-phase applications, using the RMS phase-to-neutral voltage (E_{PN}) and the RMS phase-to-phase voltage (E_{PP}) respectively [5].

$$V_{DC} = \frac{2\sqrt{2}}{\pi} E_{PN} \tag{2.15}$$

$$V_{DC} = \frac{3\sqrt{2}}{\pi} E_{PP} \tag{2.16}$$

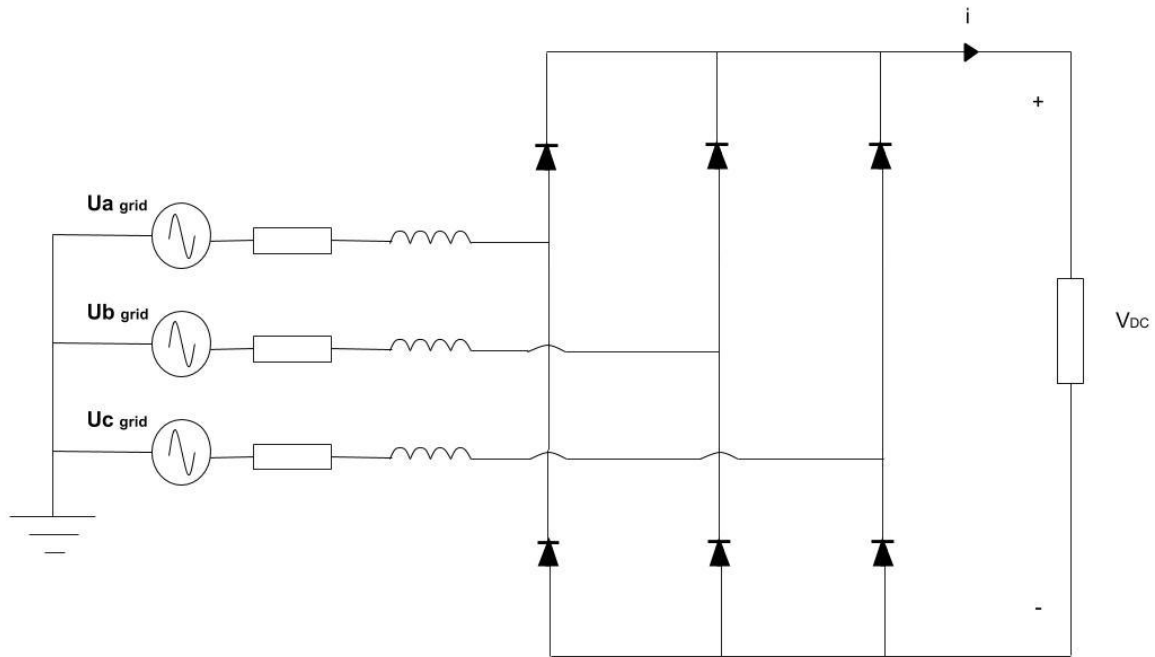


Figure 2.9 The electric schematic of the three phase diode rectifier.

However, this kind of rectifiers will consume quite some harmonic currents from the grid due to the non-linear behavior of the diodes [10]. This in turn will affect the grid negatively since current harmonic residue will remain in the grid current. These effects can be compensated for using an AFE, which is described in chapter 2.7, or with an active or passive filter.

2.6 THE THREE PHASE CONVERTER

A three phase converter consists of six transistors (implemented as IGBTs) and in parallel with each transistor there is a freewheeling diode connected (see figure 2.10). It can be divided into three transistor half-bridges where each can be seen as a switch. The diodes are needed to provide a path for the inductor currents when the transistors switch off. As in the single phase case Pulse Width Modulation (PWM) is used to form a switch pattern that is creating an output voltage used for controlling e.g. specific machines, eliminate harmonics when connected to the utility grid (AFE see chapter 2.7), uninterruptable power supplies (UPS) etc.

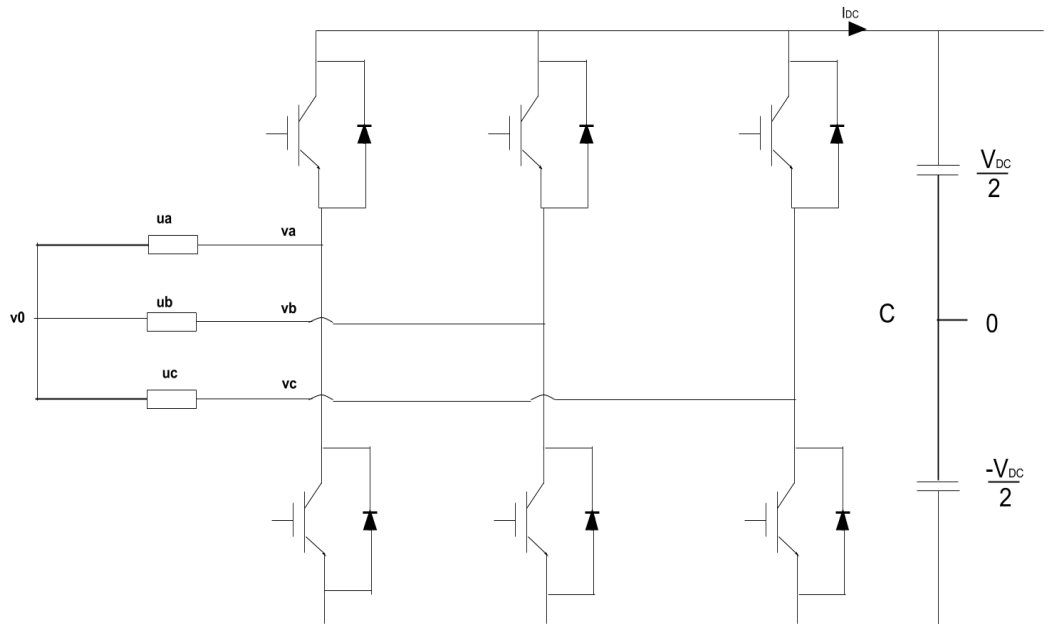


Figure 2.10 The electric schematic of the three phase converter connected to a load.

The phase potential on each leg of the inverter can have two values: either $\frac{U_{dc}}{2}$ or $-\frac{U_{dc}}{2}$, and with three phase legs there are $3^2 = 8$ different voltage vectors that can be applied (see figure 2.11).

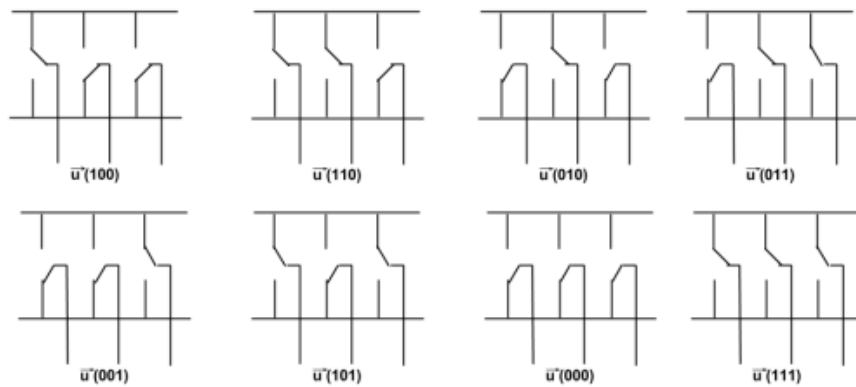


Figure 2.11 In the illustration the different possible switch positions are shown [5].

Which vector that is to be used depends on the value of the phase references and the selected modulation scheme, see figure 2.12.

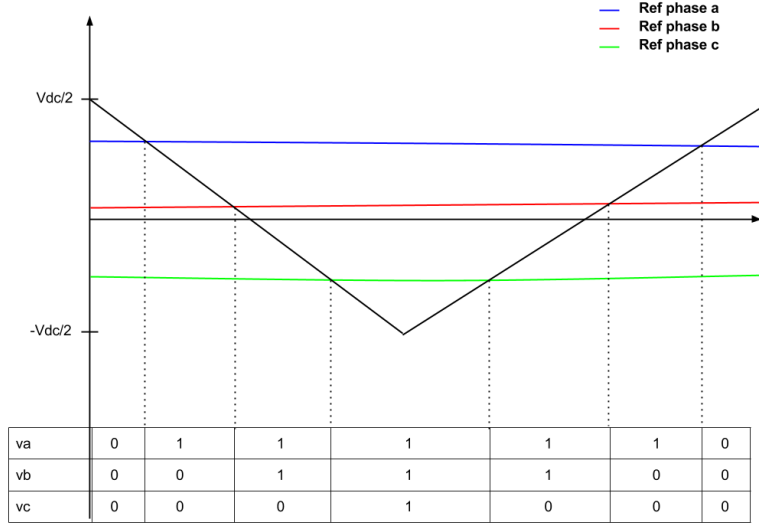


Figure 2.12 The carrier wave and the sinusoidal voltage references together with the corresponding switching states over one switching period [5].

The zero potential is the mean value of the phase potentials and since the phase potential switches between $\pm \frac{U_{dc}}{2}$ the zero potential is not zero but $v_0 = \frac{1}{3}(v_a + v_b + v_c)$, where $v_{a,b,c} = \pm \frac{U_{dc}}{2}$. The phase voltage of the converter output $u_{a,b,c}$ is the difference between the phase potential and the zero potential v_0 [5].

If $\vec{u}(100)$ is applied it means that the phase voltages expressed in a, b, c coordinates are:

$$u_a = v_a - \frac{1}{3}(v_a + v_b + v_c) = \frac{U_{dc}}{2} - \frac{1}{3}\left(\frac{U_{dc}}{2} - \frac{U_{dc}}{2} - \frac{U_{dc}}{2}\right) = \frac{2U_{dc}}{3} \quad (2.17)$$

$$u_b = v_b - \frac{1}{3}(v_a + v_b + v_c) = -\frac{U_{dc}}{2} - \frac{1}{3}\left(\frac{U_{dc}}{2} - \frac{U_{dc}}{2} - \frac{U_{dc}}{2}\right) = -\frac{U_{dc}}{3} \quad (2.18)$$

$$u_c = v_c - \frac{1}{3}(v_a + v_b + v_c) = -\frac{U_{dc}}{2} - \frac{1}{3}\left(\frac{U_{dc}}{2} - \frac{U_{dc}}{2} - \frac{U_{dc}}{2}\right) = -\frac{U_{dc}}{3} \quad (2.19)$$

Applying the phase voltage expressed in α, β coordinates (Clark Transformation see chapter 2.7.3):

$$\vec{u}_{\alpha\beta} = u_\alpha + ju_\beta = \sqrt{\frac{3}{2}}u_a + j\frac{1}{\sqrt{2}}(u_b - u_c) = \sqrt{\frac{2}{3}} \cdot U_{dc} \quad (2.20)$$

By applying these equations for each state the absolute value and angle of the voltage vectors can be calculated. The different voltage vectors are shown in figure 2.13.

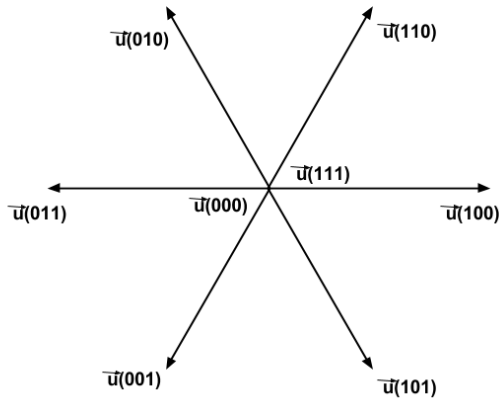


Figure 2.13 The 8 voltage vectors plotted in the complex plane [5].

The time that a certain vector is applied corresponds to the distance between two consecutive crosses between the voltage references and the triangular carrier wave (see figure 2.13). There are different modulation types such as symmetrical, sinusoidal, Bus-clamping etc. depending on how the reference voltage signals are manipulated. In this thesis sinusoidal modulation is used. The maximum output voltage which can be applied for all angles is illustrated in figure 2.14:

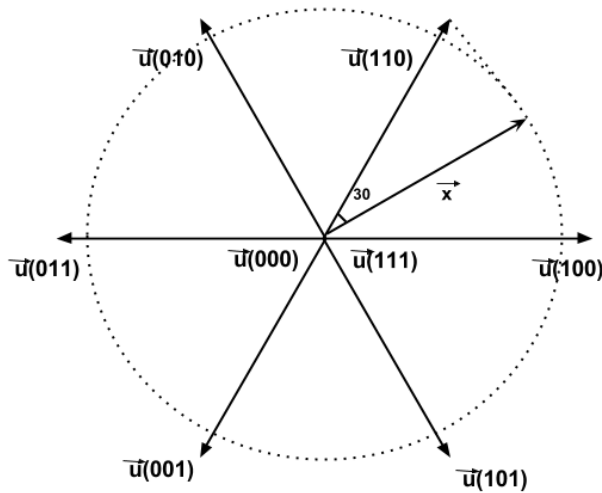


Figure 2.14 An illustration of the maximum AC output voltage, shown in the circle, of the three phase converter.

Where:

$$|\vec{x}| = \cos(30) \cdot \sqrt{\frac{2}{3}} \cdot U_{dc} = \frac{U_{dc}}{\sqrt{2}} \quad (2.21)$$

2.6.1 DYMOLA IMPLEMENTATION OF THE THREE PHASE CONVERTER

In EPL there are two different types of converters to choose between. One that neglects the switching effects and one that does not. The one that accounts for switching effects, shown in figure 2.16, is closest to reality but it slows down the simulations. If a close up study of the signals is needed then it is enough with a short simulation to verify that everything works. For

longer simulations the time average model, seen in figure 2.15, is a better choice. The average behavior of the signals is the same but in the time average model the signals are continuous whereas they are discontinuous in the switched model.

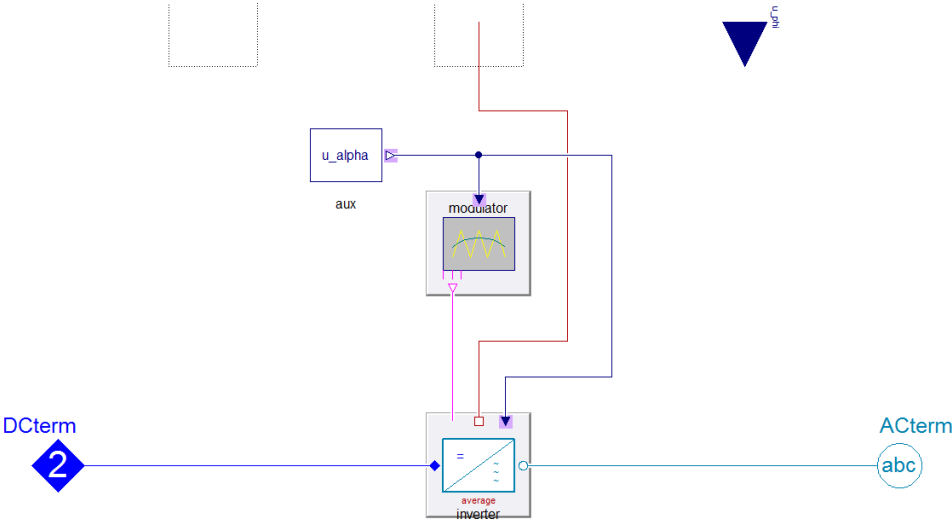


Figure 2.15 The figure illustrates the time average converter implemented in EPL with modulator.

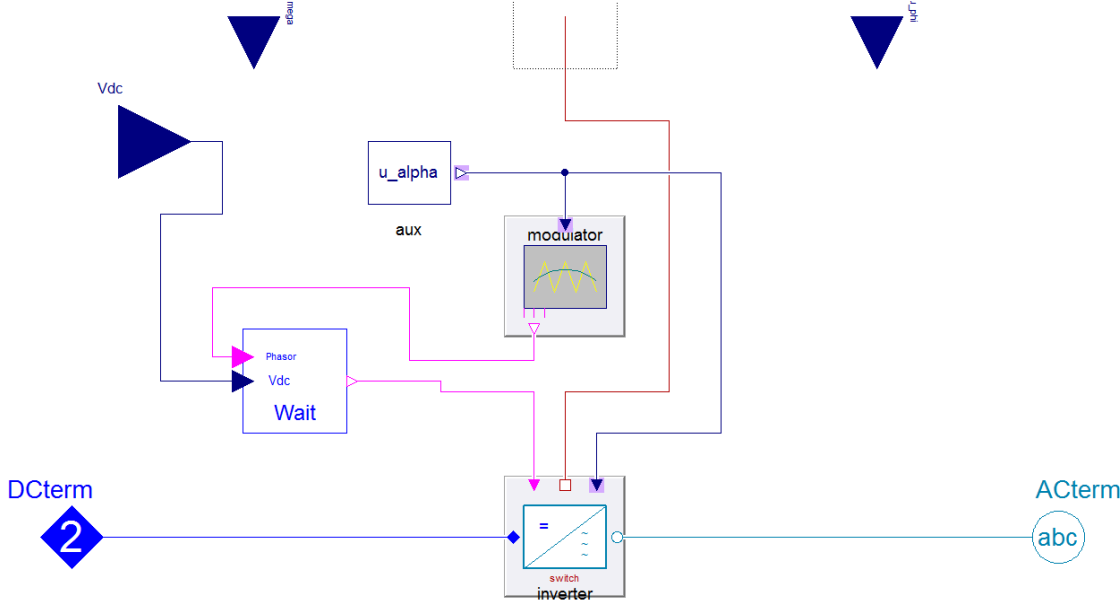


Figure 2.16 The figure shows the switched three phase converter implemented in EPL with modulator.

Using the switched converter one can choose from three different models; modular, switched equation and switched equation with no diodes. The signals are almost identical for the modular and switched equation model the only difference is that in the switched equation model average values are used during the initial startup but after a tenth of a second they are identical. The model without diodes has not been used in this thesis. A modification has been implemented in the switched models in EPL; a wait block (see figure 2.16) has been added that keeps the

transistors open until a specified dc voltage level has been reached. This means that the converter will act as a rectifier for a while. The reason for this is that the converter needs a certain DC voltage to be controllable. This modification is not implemented in the average model since the modulator is only a dummy and has no impact on the converter. The Modelica code for both the average and switched converter can be studied in Appendix D. The frequency of the created voltage is set in the modulator and, in its default value, it is equal to the outer system frequency. The frequency can however be chosen arbitrarily by changing the parameter responsible for the frequency. If this is done an additional input becomes available where the frequency of the voltage to be created can be fed into the model.

The modulator block provides several different modulation types to choose from and as mentioned earlier sinusoidal asynchronous modulation is used throughout the thesis.

2.7 ACTIVE FRONT END (AFE)

2.7.1 BACKGROUND

Electrical drives consume a large amount of the total energy production in Sweden. Among these are variable speed drives often controlled by the use of power electronic devices which provides accurate control while achieving energy high efficiency and thus reducing energy costs. Usually, these devices are supplied with DC voltage, conventionally obtained by rectifying the grid voltage using a diode or a thyristor rectifier bridge. The problem with these rectifiers is that they introduce harmonic content in the current drawn from the grid and also lower the power factor due to its nonlinear properties. This result in a decrease in the power transferred across the line. The European standard IEC 61000-3-2 concerns the limitation of the current harmonic content that is allowed to be injected to the grid [see figure A1 in Appendix A][11]. If the amount of harmonics exceeds a certain limit penalties will be given. During the years different solutions has been provided to eliminate the current harmonics. One example is to install a passive filter in conjunction with the rectifier but this may create other problems such as those related to cost and size. Another solution to eliminate the harmonics and improve the power quality is to use an AFE [10].

2.7.2 GENERAL FUNCTION

An AFE is a three phase converter connected to the utility grid (see figure 2.17). Between the converter and the grid an inductance is placed to provide the voltage boosting feature and also filter the currents. On the DC side the capacitors are needed to provide energy storage and to smooth the dc voltage. The AFE can be seen as a 4 quadrant DC/DC Boost Converter meaning that it can boost up the DC voltage side to a suitable level and power can flow in both directions [10]. The DC voltage can then be switched using the transistors creating an in average sinusoidal voltage. By controlling the switching of the transistors the currents passing through the inductors are controlled. In that way the DC voltage can be controlled at the same time as the currents can be tuned to eliminate harmonics and keep the power factor equal to one.

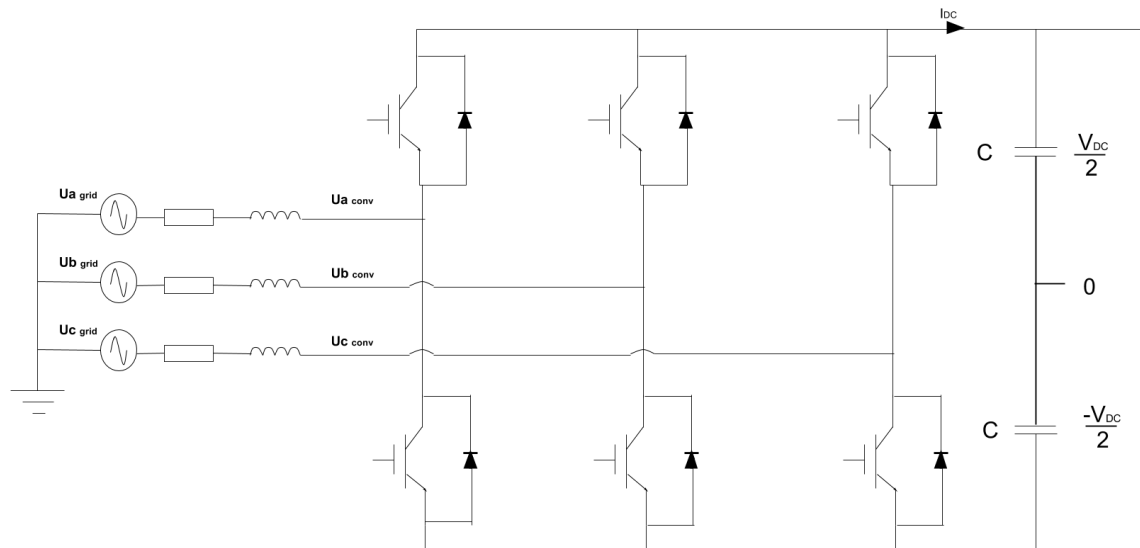


Figure 2.17 The AFE connected to the utility grid.

Figure 2.18 is an illustration of the grid and converter voltages modeled as sources and in figure 2.19 the phasor diagram shows the direction of the voltage phasors providing unity power factor (UPF).

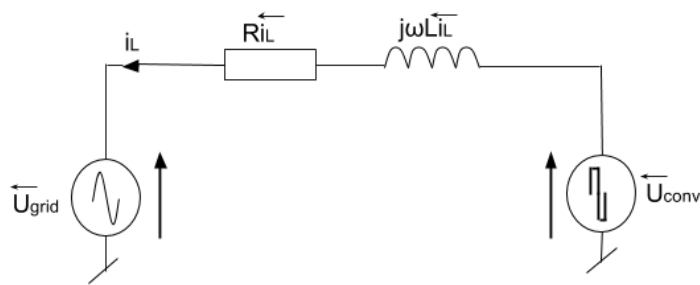


Figure 2.18 The connection point between the AFE and the grid with voltage phasors.

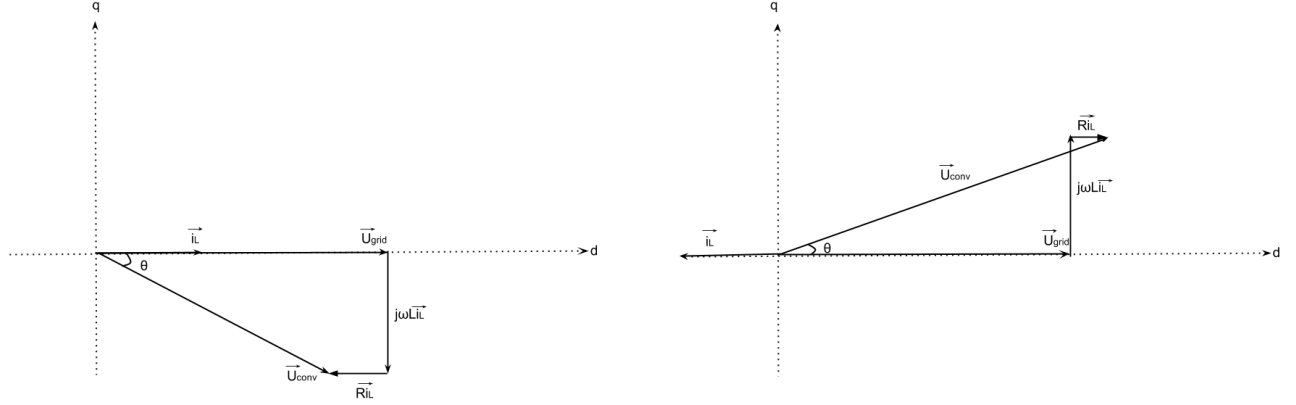


Figure 2.19 Phasor diagram showing the voltage phasors during regeneration (to the left) and rectification (to the right) while having the power factor equal to one.

The phase angle θ and amplitude of the current \vec{i}_L can be controlled by changing the phase angle and amplitude of the converter voltage \vec{U}_{conv} . This is true since the current is originated by the voltage drop over the inductance i.e. the difference between the grid voltage \vec{U}_{grid} and the converter voltage \vec{U}_{conv} . Therefore the average value and sign of the current (I_{DC}) is controllable and also the active power flowing through the converter which in an ideal loss-less case is the same on the AC side as on the DC side. The reactive power can be set to zero separately by a phase shift in the current with respect to the grid voltage. The DC voltage is also subject to control and since the filter inductances also provide the boost character of the converter, the DC voltage can be regulated to levels much higher than the rectified AC voltage. [9]

2.7.3 MATHEMATICAL DESCRIPTION OF THE SYSTEM

2.7.3.1 Power Transfer

The apparent power flowing from the grid through the inductance and the AFE can be expressed in the following way [6]:

$$\vec{S}_{grid} = P_{grid} + jQ_{grid} = \frac{U_{grid}^2 \cdot e^{j\frac{\pi}{2}} - U_{grid} \cdot U_{conv} \cdot e^{j(\theta_{grid} - \theta_{conv} + \frac{\pi}{2})}}{\omega L_{conv}} \rightarrow \quad (2.22)$$

$$\begin{cases} \text{Re}\{\vec{S}_{grid}\} = P_{grid} = \frac{U_{grid} \cdot U_{conv} \cdot \sin(\theta_{grid} - \theta_{conv})}{\omega L_{conv}} \\ \text{Im}\{\vec{S}_{grid}\} = Q_{grid} = \frac{U_{grid}^2 - U_{grid} \cdot U_{conv} \cdot \cos(\theta_{grid} - \theta_{conv})}{\omega L_{conv}} \end{cases} \quad (2.23)$$

From equation 2.23 it can be seen that the amount of active power that is transferred is due to the difference in phase angle ($\theta_{grid} - \theta_{conv}$). If the difference is zero the transferred active power is zero.

The reactive power is not affected if the angle difference is zero since $\cos(0) = 1$. Instead it is the difference in voltage magnitude that transfers reactive power.

The wave for the modulator is sinusoidal and for phases a , b and c it is given by:

$$m_a = \hat{m}_a \cdot \sin(\omega t - \theta_{conv}) \quad (2.24)$$

$$m_b = \hat{m}_b \cdot \sin(\omega t - \theta_{conv} + \frac{2\pi}{3}) \quad (2.25)$$

$$m_c = \hat{m}_c \cdot \sin(\omega t - \theta_{conv} + \frac{4\pi}{3}) \quad (2.26)$$

Thus by changing the magnitude (\hat{m}_a) and phase angle (θ_{conv}) of the reference signal the reactive and active power flow through the AFE can be controlled.

2.7.3.2 Transform from abc to $\alpha\beta$ coordinates (Clarke Transformation)

In a symmetrical three phase system the summation of the phase currents is always equal to zero. This means that the system is over determined and the three phase equations can be solved knowing only two of current variables. As the matter of fact the whole three phase system can instead be described using two complex components one real and one imaginary (α, β) by means of the Clarke transformation [6].

This state space vector denoted \vec{s} is defined as [9]:

$$\vec{s}_{\alpha\beta} = s_\alpha + js_\beta = \frac{2}{3} \cdot K \left[s_a + s_b e^{j\frac{2\pi}{3}} + s_c e^{j\frac{4\pi}{3}} \right] \quad (2.27)$$

Where K is a constant that scales the equations depending on if either the amplitude ($K = 1$)-, power ($K = \sqrt{\frac{3}{2}}$)- or RMS ($K = \frac{1}{\sqrt{2}}$) invariant transformation is used [9].

Further on the power invariant transformation will be used which means that the instantaneous power should be the same for both the three phase and two phase systems [6]:

$$p(t) = u_a \cdot i_a + u_b \cdot i_b + u_c \cdot i_c = u_\alpha \cdot i_\alpha + u_\beta \cdot i_\beta \quad (2.28)$$

This gives

$$\vec{s}_{\alpha\beta} = s_\alpha + js_\beta = \sqrt{\frac{2}{3}} \left[s_a + s_b e^{j\frac{2\pi}{3}} + s_c e^{j\frac{4\pi}{3}} \right] = \sqrt{\frac{3}{2}} s_a + j \frac{1}{\sqrt{2}} (s_b - s_c) \quad (2.29)$$

Where symmetrical condition is assumed i.e. $s_a + s_b + s_c = 0$.

The line voltage is then given by ($u_{a \text{ grid}} = e_a, u_{b \text{ grid}} = e_b, u_{c \text{ grid}} = e_c$):

$$\vec{e}_{\alpha\beta} = e_\alpha + je_\beta = \sqrt{\frac{3}{2}} e_a + j \frac{1}{\sqrt{2}} (e_b - e_c) \quad (2.30)$$

Applying Kirchhoff's voltage law in the connection point using α, β coordinates gives the following equation:

$$\vec{e}_{\alpha\beta} = \vec{u}_{\alpha\beta} - R \cdot i_{\alpha\beta} - L \frac{di_{\alpha\beta}}{dt} \quad (2.31)$$

Where $\vec{u}_{\alpha\beta}$ is the output voltage from the converter and $i_{\alpha\beta}$ is the line current.

2.7.3.3 Transform from $\alpha\beta$ to dq coordinates (Park Transformation)

Since the α, β vectors are rotating in the complex plane it can be difficult to implement a control strategy without a stationary error. A possible solution to the problem is to perform a Park transformation where the space vectors are transformed to DC quantities that can be controlled without any stationary error with a Proportional Integral (PI) controller [9]. This new coordinate system denoted as the dq plane is rotating together with the space vector and the

latter can thus be seen as a DC quantity. When using the Park transformation block in EPL the d-axis is aligned with the voltage and the q axis is 90 degrees ahead.

$$\vec{s}_{dq} = \vec{s}_{\alpha\beta} \cdot e^{-j\theta} \rightarrow \quad (2.32)$$

$$\begin{aligned} \vec{e}_{dq} \cdot e^{j\theta} &= \vec{u}_{dq} \cdot e^{j\theta} - R \cdot i_{dq} \cdot e^{j\theta} - L \frac{di_{dq} \cdot e^{j\theta}}{dt} \leftrightarrow \\ \vec{e}_{dq} \cdot e^{j\theta} &= \vec{u}_{dq} \cdot e^{j\theta} - R \cdot i_{dq} \cdot e^{j\theta} - L \cdot e^{j\theta} \cdot \left[j\omega \cdot i_{dq} + \frac{di_{dq}}{dt} \right] \leftrightarrow \\ \vec{e}_{dq} &= \vec{u}_{dq} - R \cdot i_{dq} - L \left[j\omega \cdot i_{dq} + \frac{di_{dq}}{dt} \right] \end{aligned} \quad (2.33)$$

Finally separating the real and imaginary parts:

$$\begin{cases} \vec{e}_d = -Ri_d - L \frac{di_d}{dt} + L\omega i_q + \vec{u}_d \\ \vec{e}_q = -Ri_q - L \frac{di_q}{dt} - L\omega i_d + \vec{u}_q \end{cases} \quad (2.34)$$

During a small time interval such as a switching period the rotating dq frame is slowly changing a can be considered to be constant. Then equation 2.34 can be approximated to:

$$\begin{cases} \frac{\vec{u}_d - \vec{e}_d}{L} = \frac{di_d}{dt} \\ \frac{\vec{u}_q - \vec{e}_q}{L} = \frac{di_q}{dt} \end{cases} \quad (2.35)$$

The voltage vector $\vec{u} - \vec{e}$ determines the sign of the current ripple. The size of the inductance impacts the magnitude of the current ripple as well. A larger inductance reduces the current ripple but it also decreases the maximum current/power that can be transferred through the converter.

2.7.3.4 Power in terms of dq quantities

As mentioned earlier the power invariant transformation is chosen which gives [9]:

$$\begin{aligned} v_{\alpha\beta} \cdot i_{\alpha\beta}^* &= v_{dq} \cdot i_{dq}^* = \left(\frac{2}{3} \cdot K\right)^2 \left[v_a + v_b e^{j\frac{2\pi}{3}} + v_c e^{j\frac{4\pi}{3}} \right] \cdot \left[i_a + i_b e^{j\frac{2\pi}{3}} + i_c e^{j\frac{4\pi}{3}} \right] = \\ \left(\frac{2}{3} \cdot K\right)^2 &\left[v_a i_a + v_b i_a + v_c i_c + j \frac{1}{\sqrt{3}} (v_a (i_c - i_b) + v_b (i_a - i_c) + v_c (i_b - i_a)) \right] \end{aligned} \quad (2.36)$$

The active and reactive powers are then taken by separating the real and imaginary parts:

$$\begin{cases} P = \frac{2}{3K^2} \text{Re}\{v_{dq} \cdot i_{dq}^*\} = v_a i_a + v_b i_b + v_c i_c \\ Q = \frac{2}{3K^2} \text{Im}\{v_{dq} \cdot i_{dq}^*\} = \frac{1}{\sqrt{3}} (v_a (i_c - i_b) + v_b (i_a - i_c) + v_c (i_b - i_a)) \end{cases} \quad (2.37)$$

$$K = \sqrt{\frac{3}{2}} \rightarrow P = 1 \cdot \text{Re}\{v_{dq} \cdot i_{dq}^*\} = v_a i_a + v_b i_b + v_c i_c \quad (2.38)$$

$$Q = 1 \cdot \text{Im}\{v_{dq} \cdot i_{dq}^*\} = \frac{1}{\sqrt{3}} (v_a (i_c - i_b) + v_b (i_a - i_c) + v_c (i_b - i_a)) \quad (2.39)$$

The grid voltage and current expressed in dq are:

$$e_{dq} = e_q + je_q \quad (2.40)$$

$$i_{dq} = i_q + ji_q \quad (2.41)$$

Then the active and reactive powers are:

$$e_{dq} \cdot i_{dq}^* = (e_d + je_q)(i_d - ji_q) = e_d i_d + e_q i_q - je_d i_q + je_q i_d \rightarrow \quad (2.42)$$

$$\begin{cases} P = \text{Re}\{e_{dq} \cdot i_{dq}^*\} = e_d i_d + e_q i_q \\ Q = \text{Im}\{e_{dq} \cdot i_{dq}^*\} = e_q i_d - e_d i_q \end{cases} \quad (2.43)$$

Since the grid voltage is aligned with the d axis it means that $e_q = 0$ and by controlling i_q to zero the reactive power becomes zero.

$$P = \text{Re}\{S\} = e_d i_d \quad (2.44)$$

$$Q = \text{Im}\{S\} = 0 \quad (2.45)$$

The power factor is defined as $\cos \theta$ and unity power factor occurs when $\cos \theta = 1$ since:

$$\theta = \arctan\left(\frac{Q}{P}\right) \quad (2.46)$$

$$Q = 0 \rightarrow \theta = 0 \rightarrow \cos(0) = 1$$

Thus by controlling the dq current separately unity power factor can be achieved. [9]

2.7.3.5 DC quantities

In steady state the active power on the AC side is equal to the active power on DC side (at zero losses) this gives:

$$P_{AC} = e_d i_d + e_q i_q = P_{DC} = V_{DC} \cdot I_{DC} \leftrightarrow \quad (2.47)$$

$$I_{DC} = \frac{e_d i_d + e_q i_q}{V_{DC}} \quad (2.48)$$

2.7.3.6 Maximum current

The voltage across the impedance is as large as possible when the converter output voltage is 180 degrees shifted compared to the grid voltage. This gives a maximum current in one phase (I_{max}) corresponding to equation 2.49. As mentioned in chapter 2.6 the maximum converter output voltage vector is $\frac{U_{dc}}{\sqrt{2}}$, hence the maximum current is given by Ohm's law:

$$|I_{max}| = \frac{|U_{grid}| - |U_{conv}|}{|Z|} = \frac{|U_{grid}| - \frac{U_{dc}}{\sqrt{2}}}{\sqrt{R^2 + (\omega L)^2}} \quad (2.49)$$

2.7.4 DYMOLA IMPLEMENTATION OF THE ACTIVE FRONT END

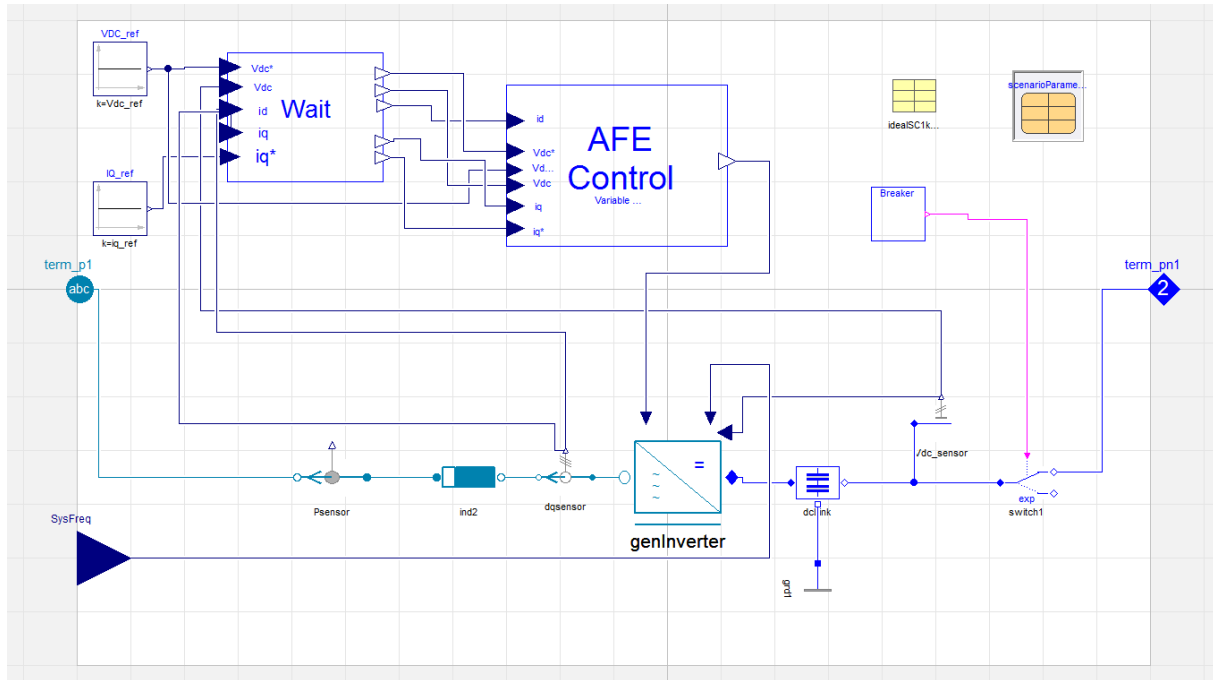


Figure 2.20 The figure shows the Dymola implementation of the AFE.

On the three-phase AC side an inductance (ind2) is connected in series with the converter as seen in figure 2.20. The inductance is needed as energy storage to boost up the DC voltage as well as to filter the currents. It is the current that passes through the inductance that is controlled and the current sensor placed in series with the inductance to measure the three phase current and transforms it to dq quantities according to the park transformation explained in chapter 2.7.3. This is a nice feature in EPL, it saves a lot of time to have a sensor already implemented that transforms from abc to dq coordinates. A PVI-meter is also added to provide information about the power and voltage levels at the AC side.

The DC-link is added in parallel with the converter. It consists of two capacitors with a neutral point in between. The DC link can be seen as an energy storage that helps smooth the DC voltage. Since it is the DC voltage that is controlled a voltage sensor is included in parallel to the DC link measure the difference in potential between the two DC lines. A breaker is also added to the DC side to provide the possibility to disconnect the model from the DC grid.

The wait-block and control- block will be explained in chapter 3.3.

3 CONTROL METHODOLOGY AND VERIFICATION

3.1 THE PI-CONTROLLER

A basic unit in control theory is the Proportional Integral controller (PI-controller). The PI-controller consists of a proportional and an integral action, as it can be seen in equation 3.2. These parts operate with the error as an input, where the error is the difference in between the reference value and the actual value of the controlled magnitude, equation 3.1.

$$e(t) = u_{ref}(t) - u_{act}(t) \quad (3.1)$$

$$y_o(t) = K_p \left(e(t) + \frac{1}{T_i} \int e(t) dt \right) \quad (3.2)$$

If no integral part is added in the control the proportional part simply multiplies the gain value with the error to generate a control signal. Unless the controlled object has integrator characteristic, this causes a stationary error that cannot be eliminated fully with a simple P-controller [14]. In order to eliminate this stationary error an integral part is added. By integrating the error, the stationary error in time will be accounted for and the correct reference can be reached at least for a step input signal. When the integral part is added it is also necessary to add some form of anti-windup unit. This prevents the integral part from creating a very large output value that would be impossible for the actuator to supply [14]. In this thesis both P-controllers and PI-controllers will be used in different configurations in order to control the power electronic units.

3.1.1 DYMOLA IMPLEMENTATION

In the Modelica standard library [19] used in Dymola, a PID-control block with anti-windup and limited output is already implemented. The block can be modified in the user interface to run in P-control, PI-control, PD-control or PID-control. The block structure was modified in order to be able to change the limits of the output signal dynamically, and the resulting block structure is shown in figure 3.1. This was done in order to improve the function of the anti-windup and in order to scale the limits to the desired DC-link voltage.

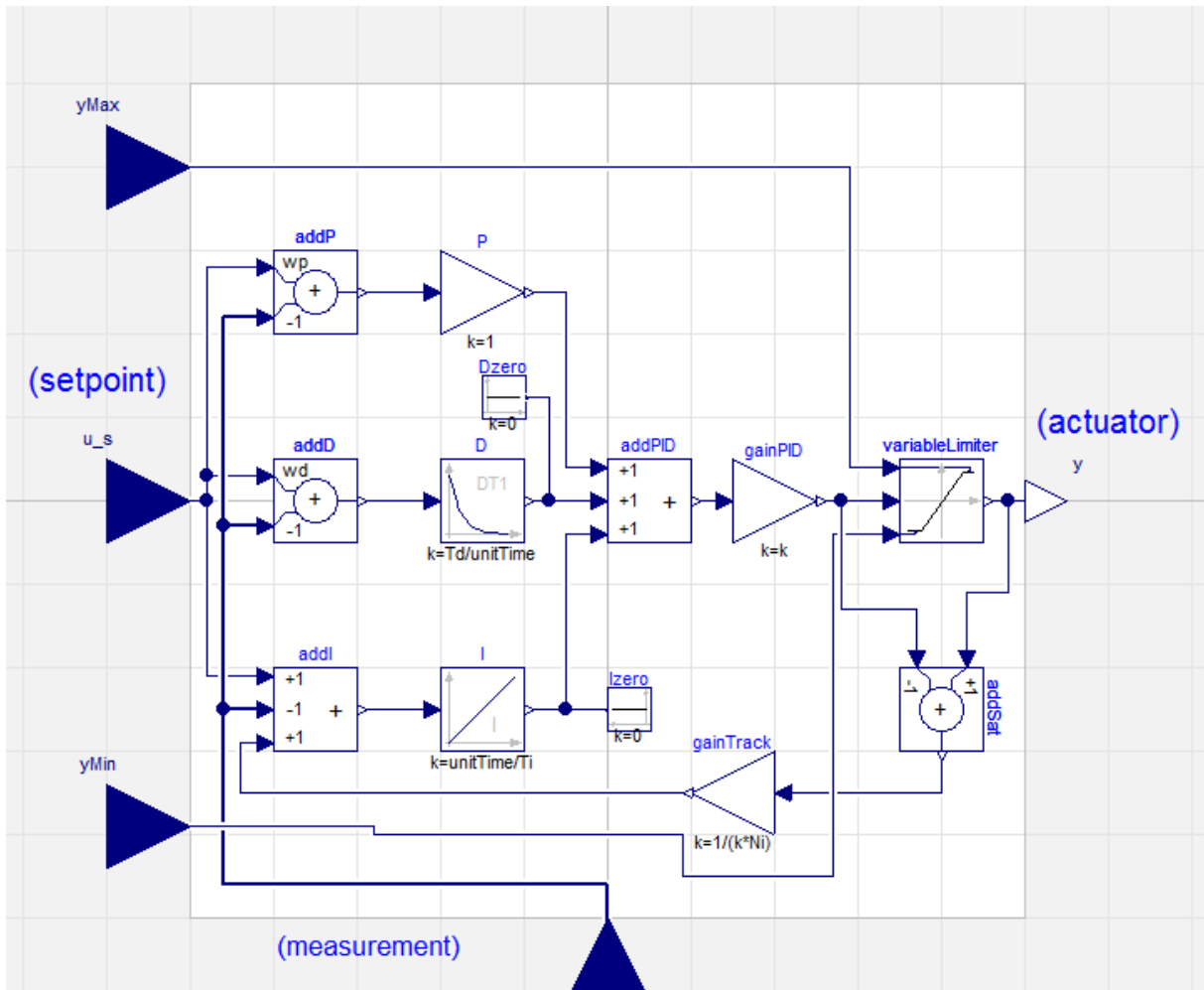


Figure 3.1 The Dymola implementation of the modified PID-controller block.

3.2 H-BRIDGE CONTROL

The H-bridge is in this thesis used to supply power to a stiff DC-grid where the voltage in the grid is set by either another converter or by a DC source. Therefore the power supplied to or drawn from the grid needs to be controlled. Power is controlled by affecting the transistors in the converter and by doing this allowing a current to flow to the grid or a load. Since the voltage is kept constant the power will be proportional to the current according to equation 3.3.

Therefore a power reference and the measured power are sent into a PI-controller. The output from this controller will be a current reference. The input to the modulator which switches transistors on and off is however a voltage reference as described in chapter 2.1. This means that the current reference needs to be sent into another controller where the current error is calculated and an output, in form of voltage reference, is generated and sent to the modulator.

$$P = U * I \tag{3.3}$$

The resulting control loop block diagram of the system can be seen in figure 3.2. Notable is that the current controller only uses a proportional gain and no integral part. This causes no problem since the stationary error in the current will be accounted for by the integral part of the power controller. If the power controller would output a current reference that cannot be met by the current controller, the power controller will simply increase the current reference until enough current flows through the circuit.

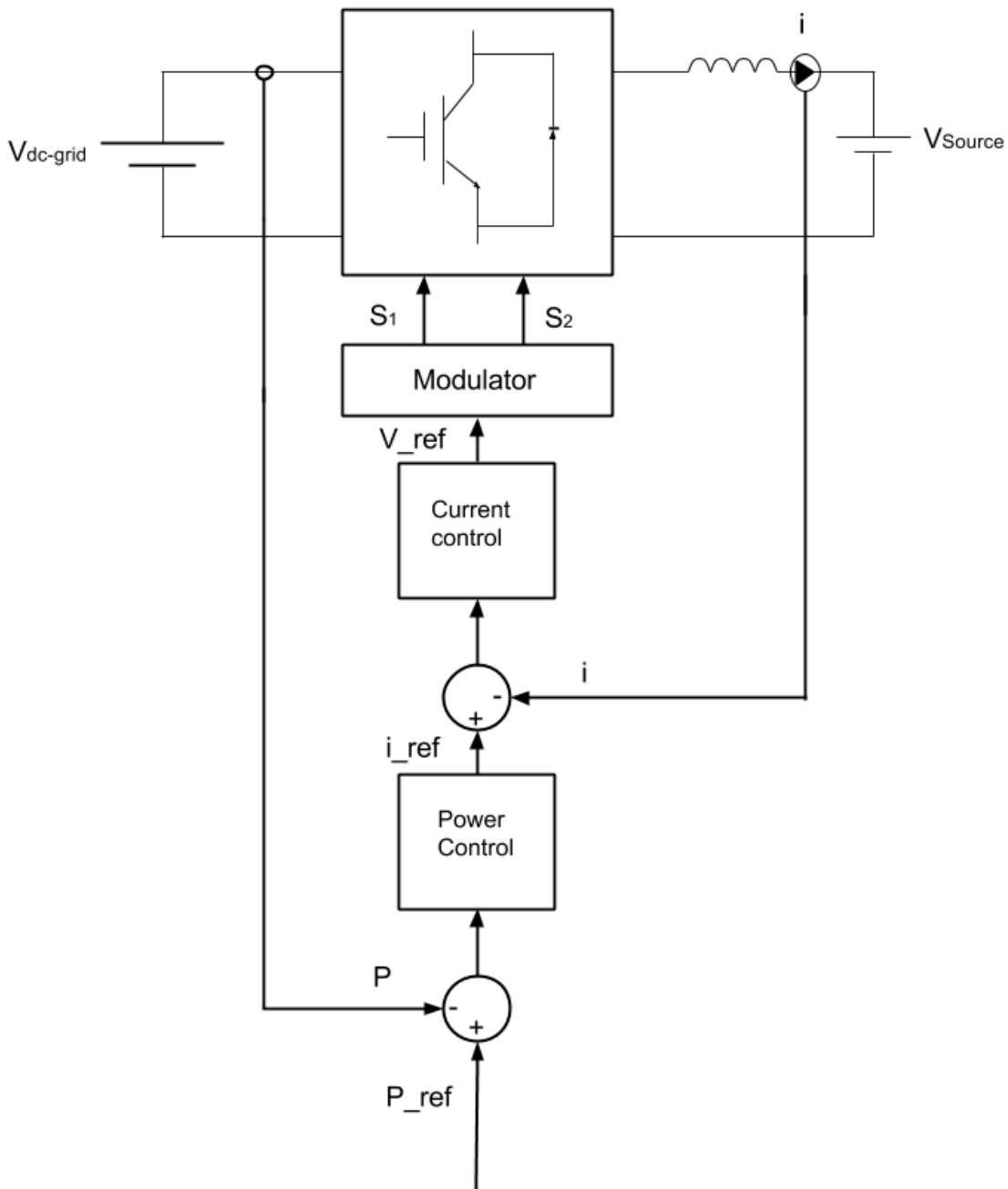


Figure 3.2 The figure shows the control block of the power controlled H-bridge

3.2.1 DYMOLA IMPLEMENTATION OF THE H-BRIDGE POWER CONTROL

The corresponding Dymola control loop, corresponding to the one seen in figure 3.2, is shown in figure 3.3. The controllers used are the PID-controllers of the Modelica standard library, described in chapter 3.1.1, set to be a PI-control for the power controller and a P-control for the current controller. The modulator, named “pwm” in figure 3.3, takes two inputs; one that corresponds to the length of the voltage vector to be modulated and one describing the angle of the voltage vector. Since the H-bridge, in this application, operates in DC the rotation variable is set to zero throughout the simulation. The length of the voltage vector is generated by the current controller and fed to the modulator. The appropriate voltage is achieved by switching

according to table 3.1. In table 3.2 the system parameters such as inductor, capacitor and resistor values in the converter are also listed.

Requirements for the H-bridge are:

- Power should be able to flow in both directions.
- The converter should be able to supply 5 kW to the grid and consume 10 kW
- The current ripple should be significantly small.
- The power should reach its reference in 0.1 s
- The power should not have any overshoot.
- The current has to be able to respond to large changes rapidly.

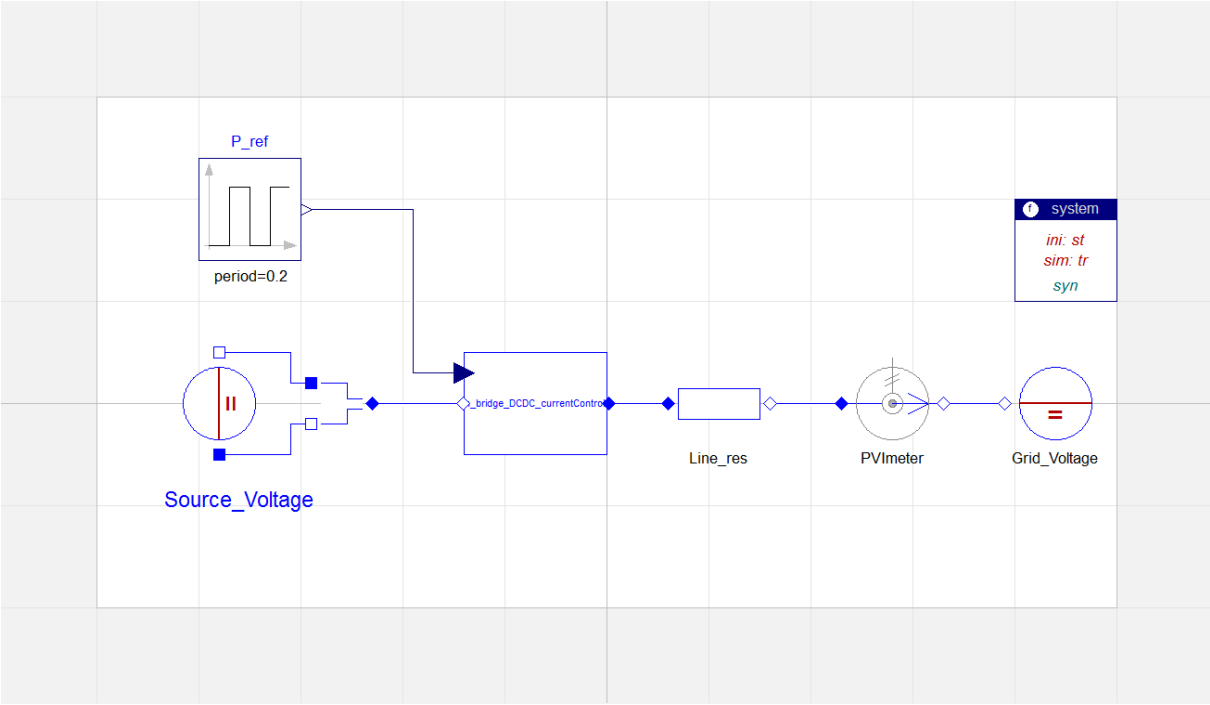


Figure 3.4 The Dymola test bench for the power controlled H-bridge.

Power control proportional gain	Power control integral gain	Current control proportional gain
$K_p=0.0003$	$T_p=0.001$	$K_c=20$

Table 3.1 The table lists the control parameters set to the test bench.

Inductance	Resistor	Source DC-link capacitor	Grid DC-link capacitor
100 mH	1 Ω	250 μ F	300 μ F

Table 3.2 The table lists the system parameters set to the test bench.

In figure 3.5 performance of the current and power controller is shown, acting on the power reference generated by the square wave. Note that the measured power signal to the controller is filtered. The unfiltered measured power is shown in figure 3.6, where the ripple in power is shown.

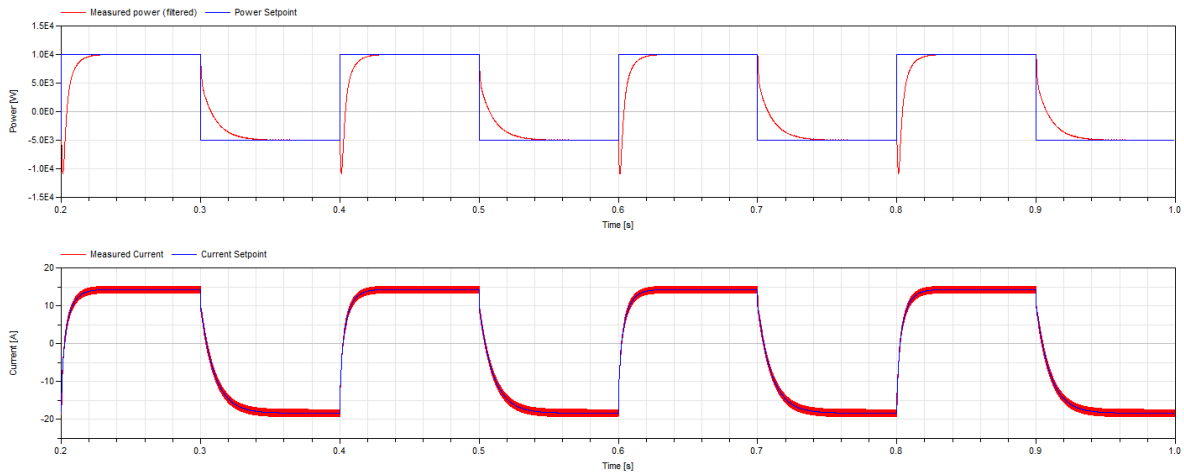


Figure 3.5 The graphs show the filtered power (top graph) and current (bottom graph) acting on their respective references.

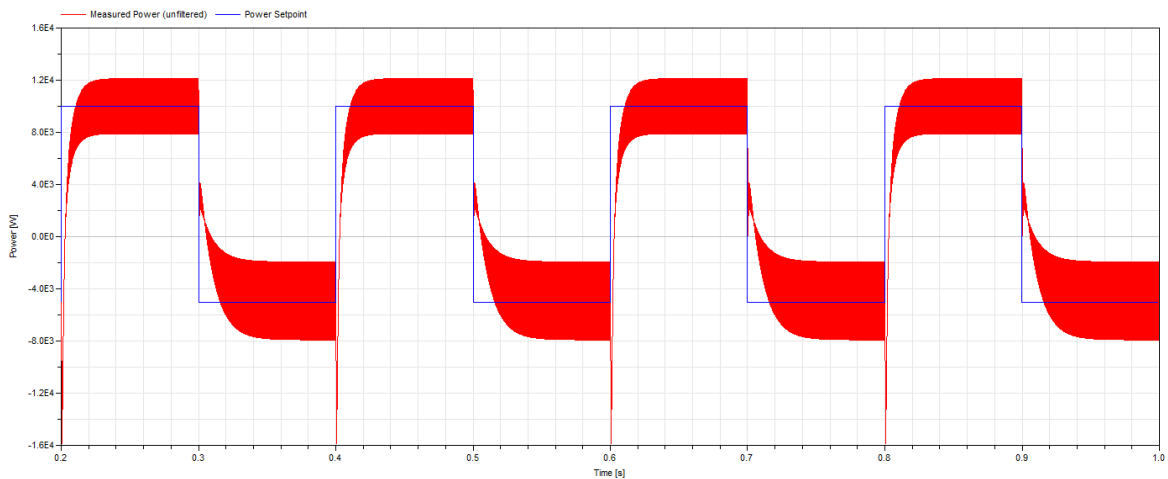


Figure 3.6 The graph show the unfiltered power acting on its reference.

3.2.3 DISCUSSION

From figure 3.5 it can be concluded that:

- Power can flow in both directions.
- The inverter is able to deliver 5 kW to the grid and consume 10 kW
- The current ripple is significantly small.
- The power reaches its reference in just 0.1 s, with no overshoot.
- The current responds sufficiently fast to changes in current reference.

The results show that the power regulation reaches its stationary value faster when acting upon a positive flank of the power reference than a negative flank as can be seen in figure 3.5. The reason for this is that the stationary value after negative flank is a negative value. This means that the power source actually supplies power to the grid. This requires that the boost-properties of the converter are used in order to push current into the grid. The inductor has to be charged for a longer time and the inductor discharges much faster, due to the larger voltage at the grid side [6]. Since the discharging time is the same time that current is pushed to the grid a longer response time is to be expected. Because of this the limit of transferred power to the grid is lower than the power that could be consumed.

The ripple in power is directly correlated with the ripple in current as described by equation 3.3. The ripple in current is unavoidable as described in chapter 2.2 and chapter 2.3 and will always be present in these kinds of power electronic units. However, the current ripple could be decreased, as the inductance stands in the denominator of equation 2.6 and equation 2.12 (chapter 2), by increasing the value of the inductance. This is valid in both boost and buck operation. To increase the inductance value will however change the dynamics of the system causing the control parameters to change. In order to find the new control parameters a series of new simulations are required, alternatively a transfer function of the full system has to be derived and the parameters be identified through this. Further work could be done in this area, to identify these parameters through transfer functions and implementing them in the simulation models.

3.3 ACTIVE FRONT END DC VOLTAGE CONTROL

The AFE can be used in different operation modes, but in this section the AFE is used to control the DC voltage and it is connected to an AC grid. This mode can be used to control the grid voltage of an internal DC grid or to keep constant voltage across a load. The voltage across a load is given by Ohm's Law, equation 3.4, and since the load is in a DC grid the load is purely resistive. Given this the voltage across the load is proportional to the current flowing through it, which is why the current is used to control the voltage.

$$U = R * I \tag{3.4}$$

The full voltage control loop can be seen in figure 3.7 and as the figure suggests the DC voltage is controlled through the active component of the current i.e. i_d . The voltage is controlled through this component because the power drawn from the grid, in order to maintain the correct DC voltage, should only be active power. Since it is desired to only consume active power, in most cases, from the AC grid the reactive current component is set to zero by setting i_{q_ref} in figure 3.7 to zero. Notable in figure 3.7 is that the controllers are of different types. The voltage controller is a PI-controller, the d current controller is a P-controller and the q current controller is a PI-controller. The integral part of the voltage controller takes care of any stationary error in the voltage and the integral part of the reactive current controller ensures that no reactive power is drawn from the grid. Note also that the transformation from ABC -reference frame to dq -reference frame is carried out internally in the EPL current sensor.

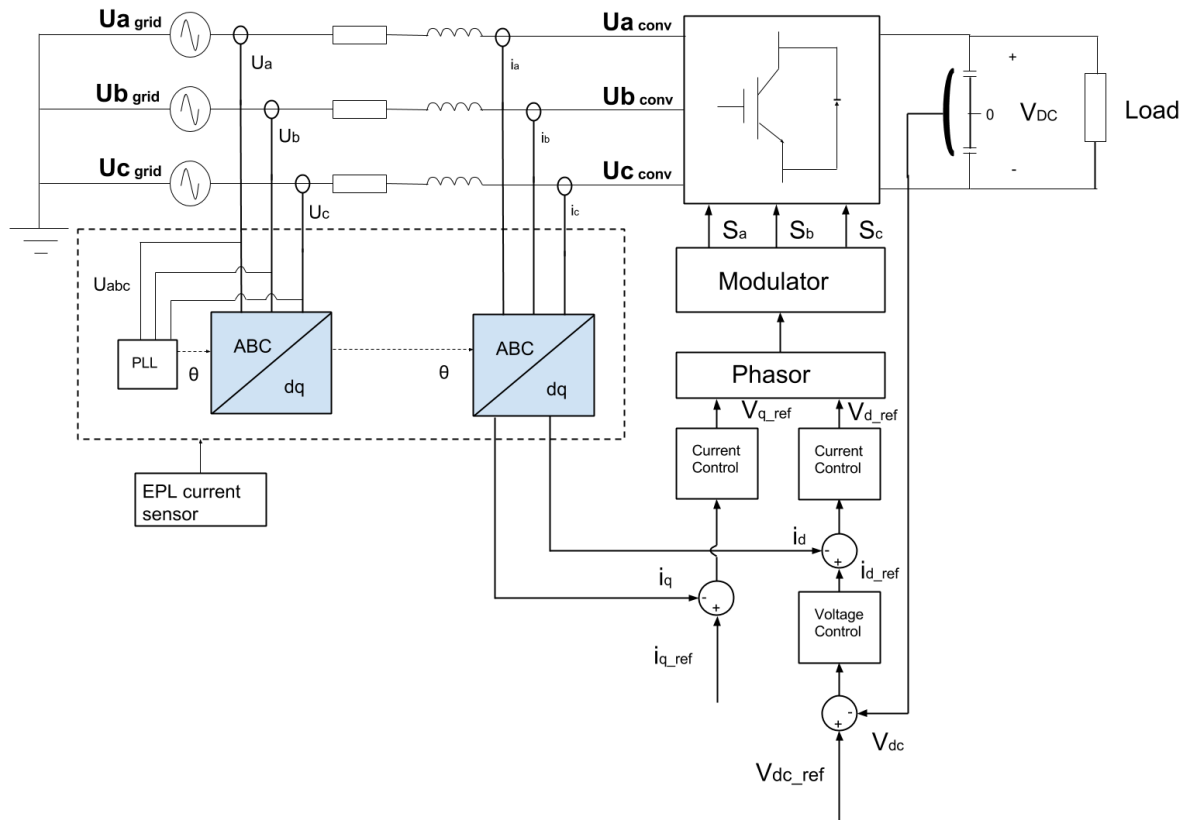


Figure 3.7 The control loop with voltage control in the outer loop and current control in the inner loop.

3.3.1 DYMOLA IMPLEMENTATION OF ACTIVE FRONT END VOLTAGE CONTROL

The control block at top level has the measured values of the DC voltage, d-current and q-current, plus the DC voltage reference and q-current reference as inputs. All signals pass through a wait block before they enter the control block. The DC voltage reference bypasses the wait block as can be seen in figure 3.8. Since it is not possible for the inverter to perform any switching without a DC voltage, the wait block is needed to prevent the controllers to wind up. This feature is combined with a wait block inside the converter (see chapter 2.6.1) that sets the gates to false meaning that the inverter will only rectify the current until the DC voltage is large enough before the voltage regulation starts. Hysteresis is implemented in both wait blocks to avoid chattering. The Modelica code for these wait-blocks can be studied in Appendix D.

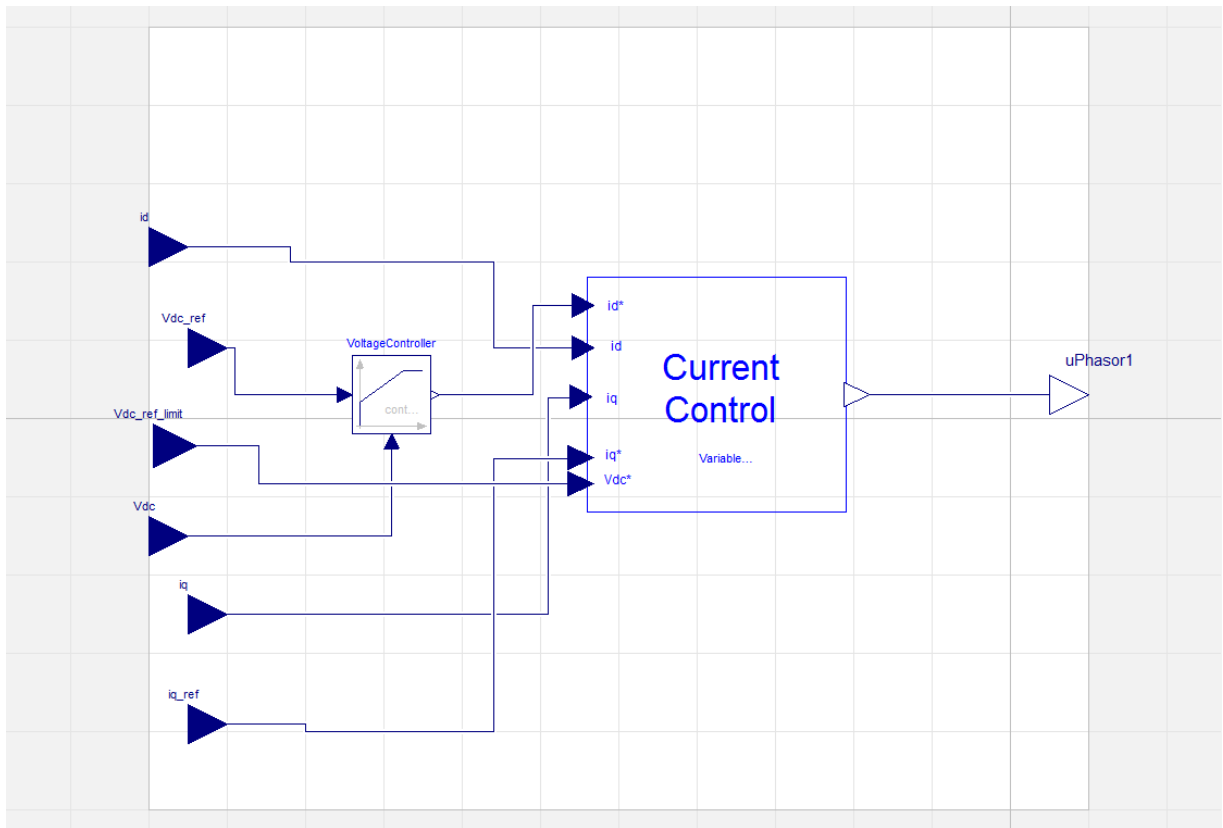


Figure 3.9 The inside of the AFE control block from figure 3.8 compare with figure 3.7.

The DC voltage reference is also sent to the current controllers where it is used as output limits. This is why the DC voltage reference also bypasses the wait block in figure 3.8.

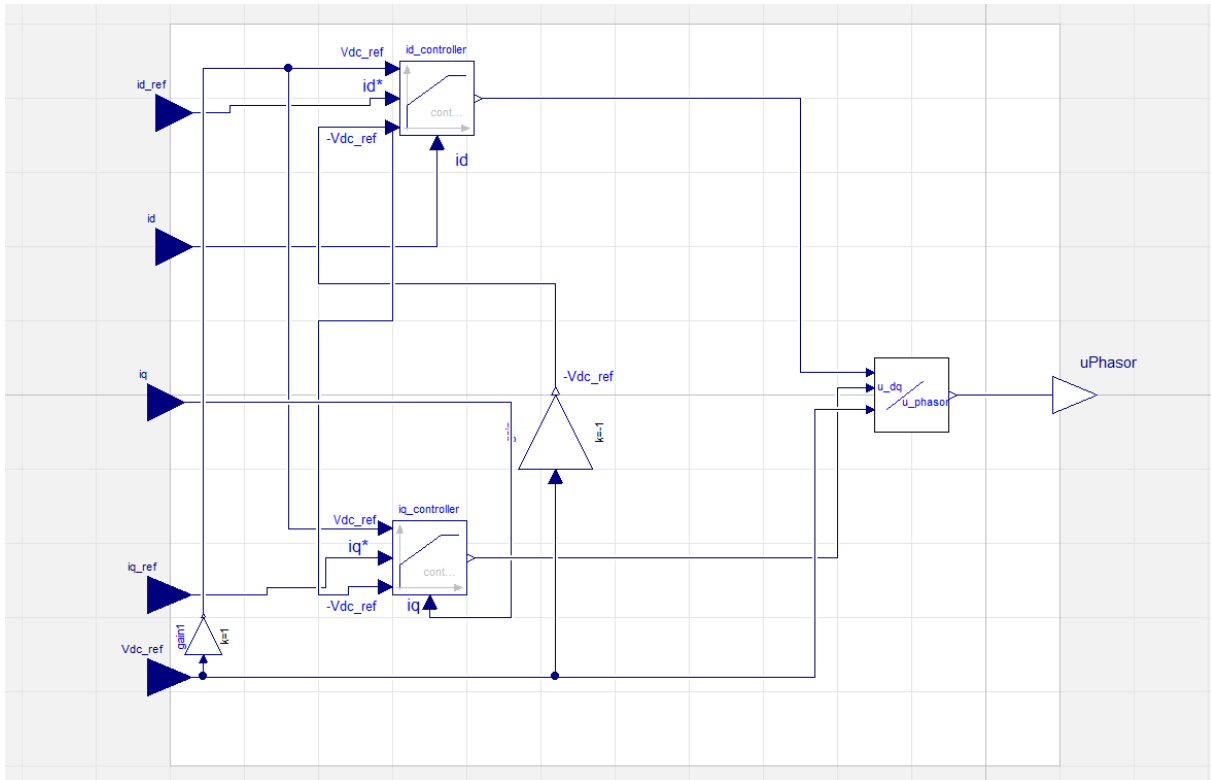


Figure 3.10 The content of the “Current Control”-block in figure 3.9

At the third level the two current controllers are located. The d-current controller is a P controller since it is coupled to the voltage controller which is a PI. The q-current is controlled by a PI controller and the output of the current controllers is an AC voltage reference. As mentioned before the output of the controllers is limited to the maximum amplitude of the switched voltage that can be generated by the converter.

Since the input of the converter, where the modulator of the converter is located, is a voltage phasor with length and angle, the voltage references are transformed to a phasor inside the phasor block (the block on the right in figure 3.10) and then send to the converter. The phasor-block simply calculates the length of the vector and scales it to the DC voltage. The angle of the vector in reference to the d-axis of the dq -frame is also calculated in this block.

3.3.2 SIMULATION RESULTS OF THE VOLTAGE CONTROLLED AFE

The model described in figure 3.8 is connected to an AC-source together with a line inductance representing a stiff 50 Hz 400 V grid. The DC link is connected to a variable resistor representing a load with variable power consumption. The test bench setup is illustrated in figure 3.11. A square wave is connected to the variable resistor which is varying between 1100Ω and 100Ω with a 0.3 seconds period, which alters the current flowing through the load corresponding to a pulsed power consumption between 4 - 40 kW. The DC-voltage reference was set to 2000 V. The control parameters for the controllers are presented in table 3.3 and the system parameters in table 3.4. All parameters have been empirically optimized. The grid inductance has been calculated according to the formulas derived in chapter 5.1.1.

The requirements are:

- The start voltage for the DC link shall be zero and the DC link voltage shall reach the reference value (2000 V) in a few milliseconds.
- In steady state the DC link voltage should have a maximum ripple of less than 1 %.
- The controllers shall react quickly to changes.
- No reactive power shall be consumed in the connection point.
- The three phase grid current shall be sinusoidal i.e. the current harmonics shall be reduced significantly.

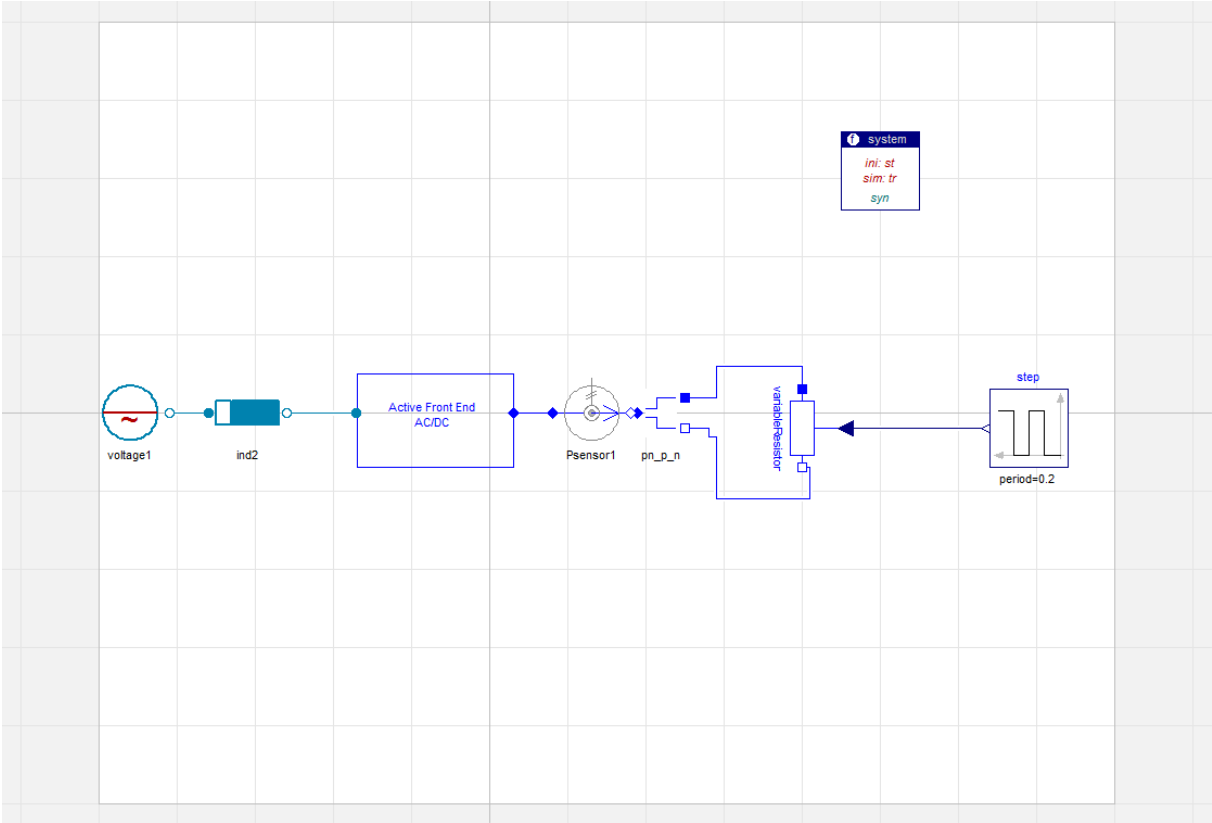


Figure 3.11 The test bench for the voltage controlled AFE.

Gain (Voltage)	Time constant (voltage)	Gain (d current)	Gain (q current)	Time constant (q current)
$K_V = -1$	$T_{iv} = 0.01$	$K_{id} = 5000$	$K_{iq} = 100$	$T_{iq} = 0.00001$

Table 3.3 The control parameters for the test bench.

Inductance	Resistance	DC-link capacitance
$L_{conv} = 9.5 \text{ mH}$	$R_{conv} = 0.00005 \Omega$	$C_{dlink} = 0.8 \text{ mF}$
$L_{grid} = 0.101 \text{ mH}$	$R_{grid} = 0.00005 \Omega$	

Table 3.4 The system parameters for the test bench.

In figure 3.12 the performance of the voltage controller is shown, together with the change in resistance. In figure 3.13 a close up of the DC voltage is shown where the maximum and minimum values of the voltage ripple can be seen. In figure 3.14 the startup phase of the boost

DC voltage is illustrated. Figure 3.15 shows how the current controllers react to the current references. The power consumed by the load can be seen in figure 3.16. Figure 3.17 shows the three-phase AC current for phase A during steady state where the load is consuming constant power of 40 kW. Finally, the last figure 3.18 is a frequency analyze of the current harmonics for frequencies up to 4800 HZ.

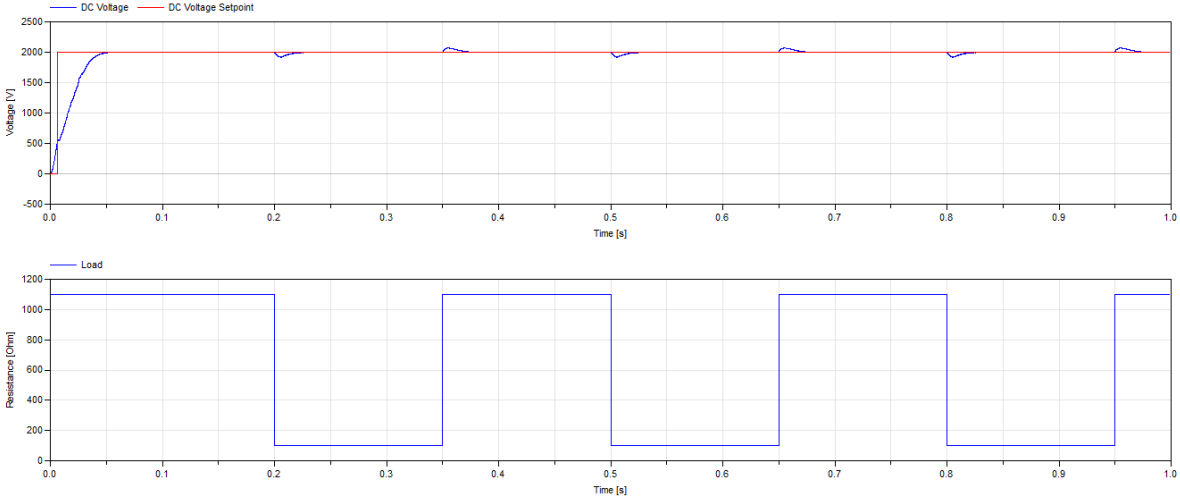


Figure 3.12 The graphs shows the performance of the voltage controller (top graph) and also the change in resistive value of the load (bottom graph).

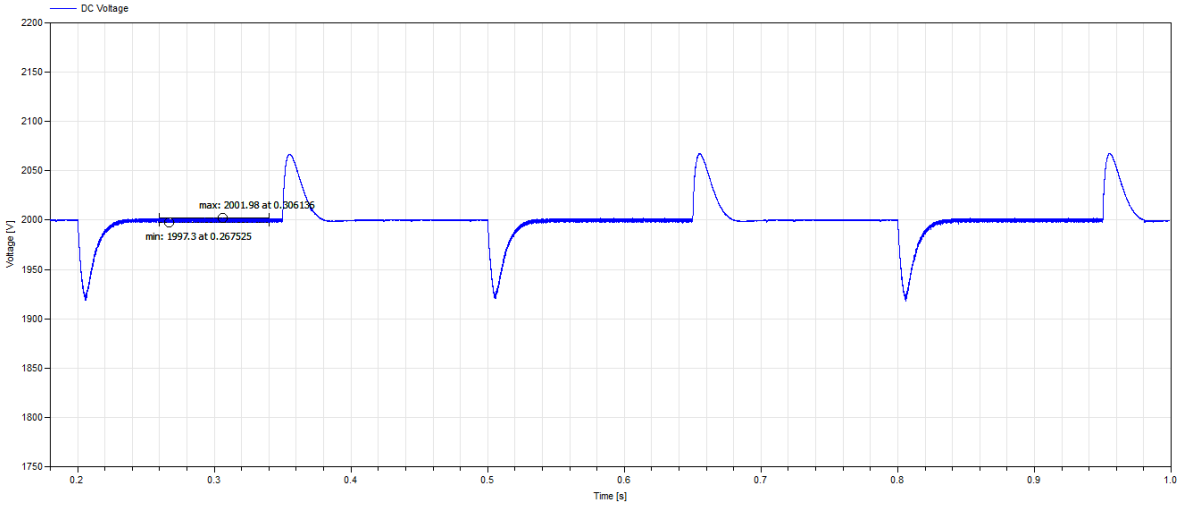


Figure 3.13 A close up of the voltage controller with maximum and minimum values of the voltage ripple.

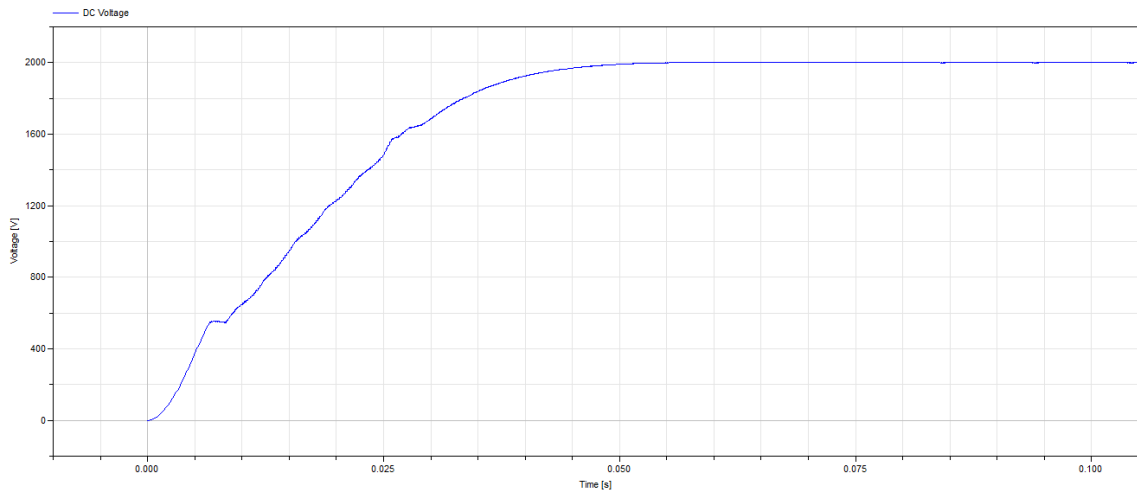


Figure 3.14 The startup phase where the DC link voltage is controlled from 0 V to 2000 V. It can also be seen that the transistors are open until the DC link voltage reaches 550 V.

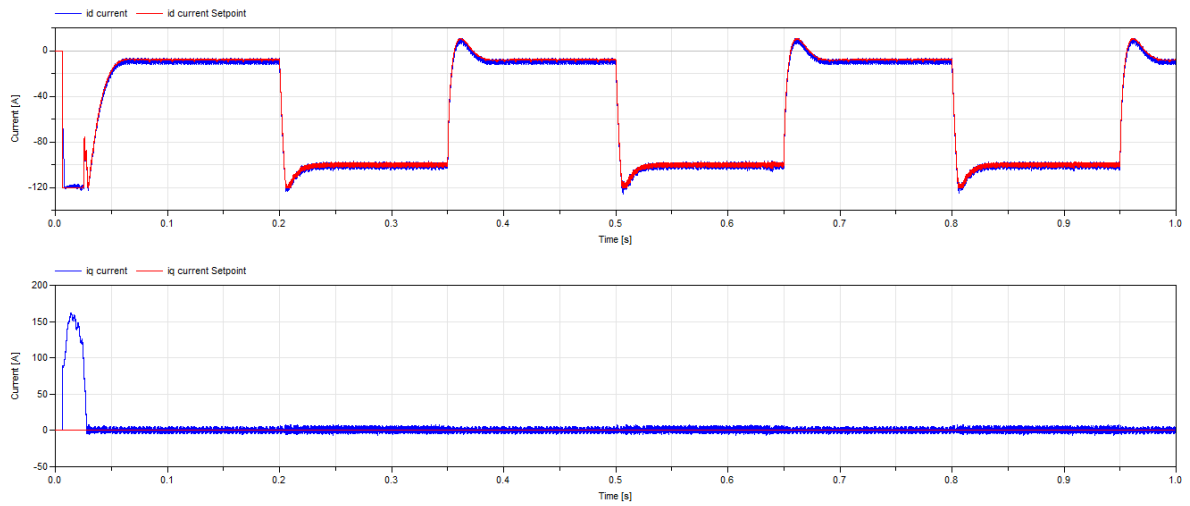


Figure 3.15. The d, q currents and their setpoints.

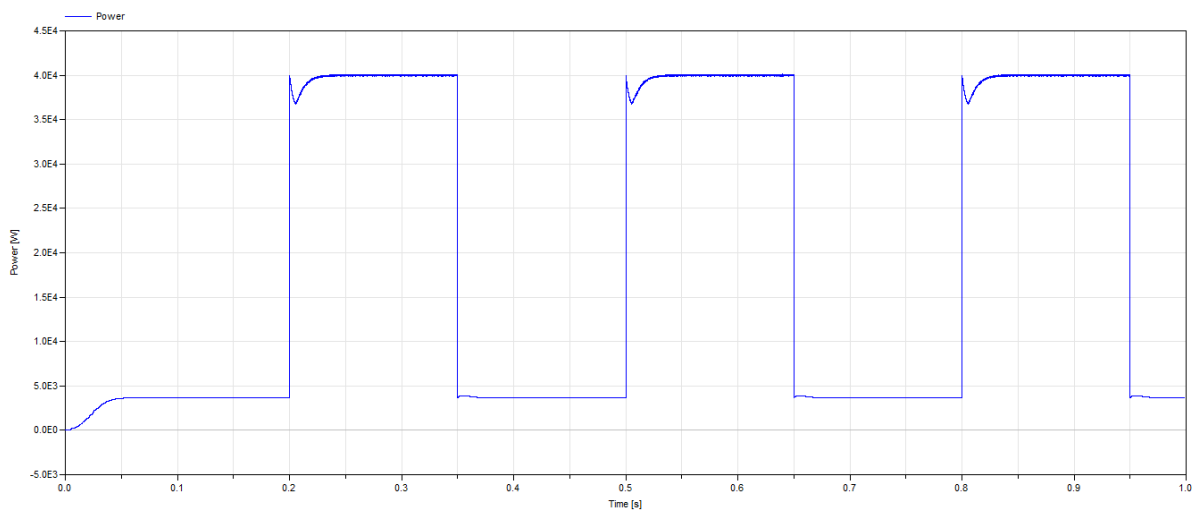


Figure 3.16 The corresponding power consumption in the load.

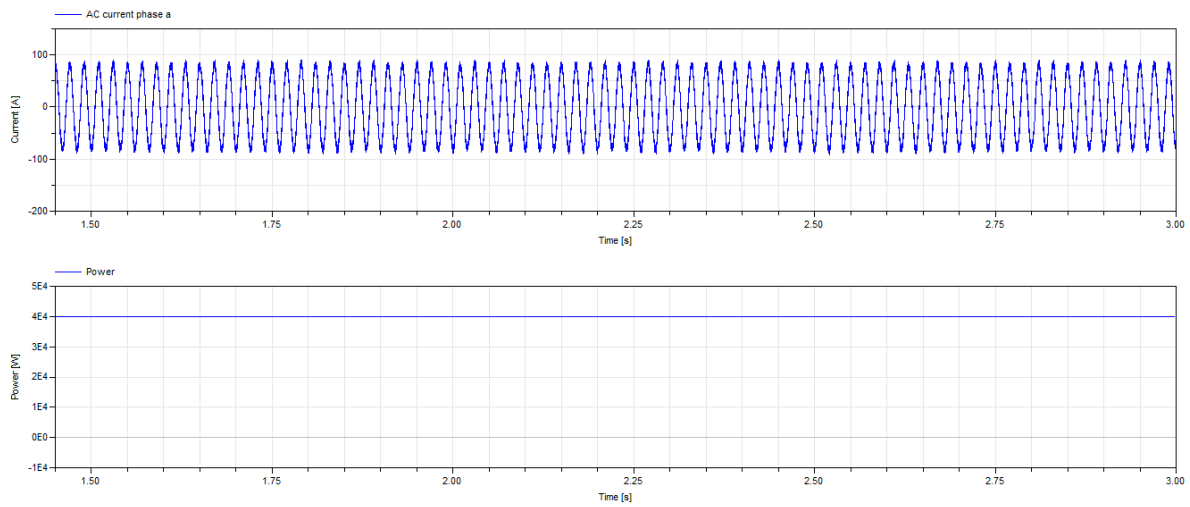


Figure 3.17 The AC current in phase A with corresponding power consumption of 40 kW during steady state simulation.

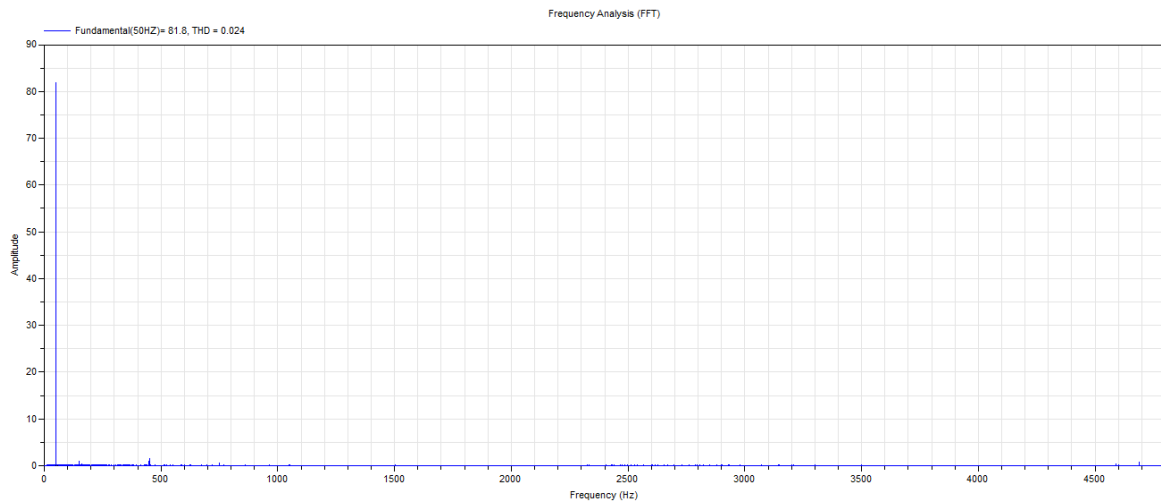


Figure 3.18 The current harmonics content for 40 kW load in phase A for frequencies up to 4800 Hz.

3.3.3 DISCUSSION

In the startup phase all transistors are open and the controllers are turned off meaning that the AFE works in rectifying mode. This can be seen in figure 3.14 where the DC voltage is smooth up to 550 V and then transistors start switching. This feature is necessary since it is not possible to perform controlled switching if the DC voltage is too low. The voltage limit has been empirically derived and is set to 550 V since the regulation should start as quickly as possible.

Comments to the requirements:

- The DC voltage reference reaches the reference value in 55 milliseconds which is relatively fast (see figure 3.14).
- The maximum DC voltage ripple in steady state is 0.234 % which is below the requirements that were set to 1% (see figure 3.13).
- During each pulse the controller has to adjust the amount of current that is drawn from the grid in order to keep the DC link voltage around 2000 V. After each pulse it takes

around 30 milliseconds for the DC voltage to reach the reference value again (figure 3.13). This implies that the control performance is robust and response quickly to changes.

- By studying the i_q current in figure 3.15 it can be seen that it is controlled to zero which implies that no reactive power is drawn from the grid connection point.
- The AC current in phase A is sinusoidal in steady state simulation as can be seen in figure 3.17. The current harmonics up to the 39th harmonic is plotted in figure 3.18. Here it can be seen that all harmonics are filtered.

The requirements that were set are fulfilled. Some notations can be made such as the i_d current controller has a small stationary error since it is a P-controller which was predicted. The small power dips in the beginning of each pulse in figure 3.16 is due to the voltage drop in the DC link. The power is given by the $P = \frac{U_{DC}^2}{R}$ and since the voltage is lower than 2000 V for a short time the power will drop. Dymola can only perform FFT analysis for frequencies up to around 5000 HZ. Due to this the higher order harmonics could not be plotted.

3.4 AC/DC CONVERTER POWER CONTROL

The theory for describing this model is the same as for the DC voltage controlled AFE (see chapter 2.7). The AFE is controlling the DC voltage by injecting or withdrawing active power from the AC utility grid. Instead of controlling the DC voltage by the use of the active current component i_d , the same current can be used to control active power. In the same way the reactive power can be controlled by controlling the i_q current. See figure 3.19.

The converter is always connected in a back-to-back configuration (see chapter 5.2.1) with an AFE rectifier that controls the DC voltage by exchanging power from the utility grid. The AC side of the converter can be connected to almost any kind of source or load; such as wind power plants, hydro power, individual drives or industrial plants. A nice feature with this formation is that power can flow in both directions and the excess energy can be sent back to the utility grid.

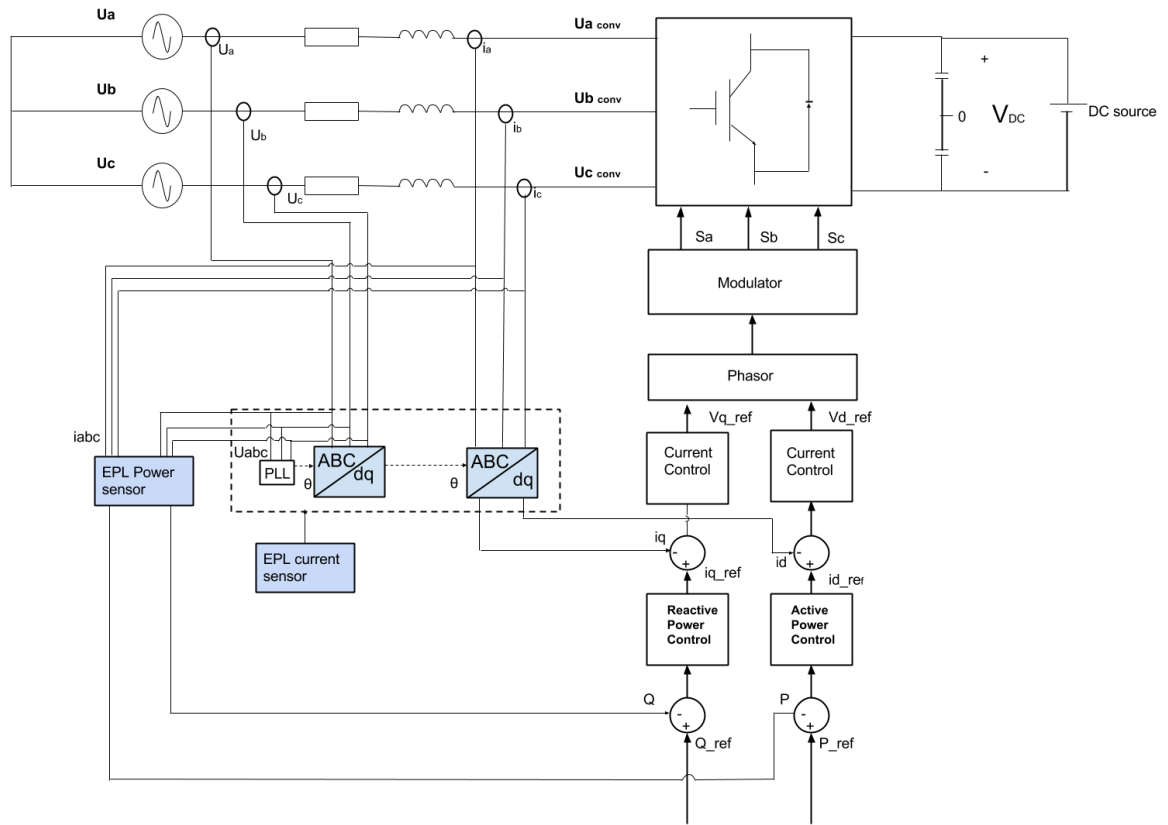


Figure 3.19 An illustration of the implemented power controller. The outer loop is controlling the power and the inner loop is controlling the current.

3.4.1 DYMOLA IMPLEMENTATION OF THE AC/DC INVERTER WITH POWER CONTROL

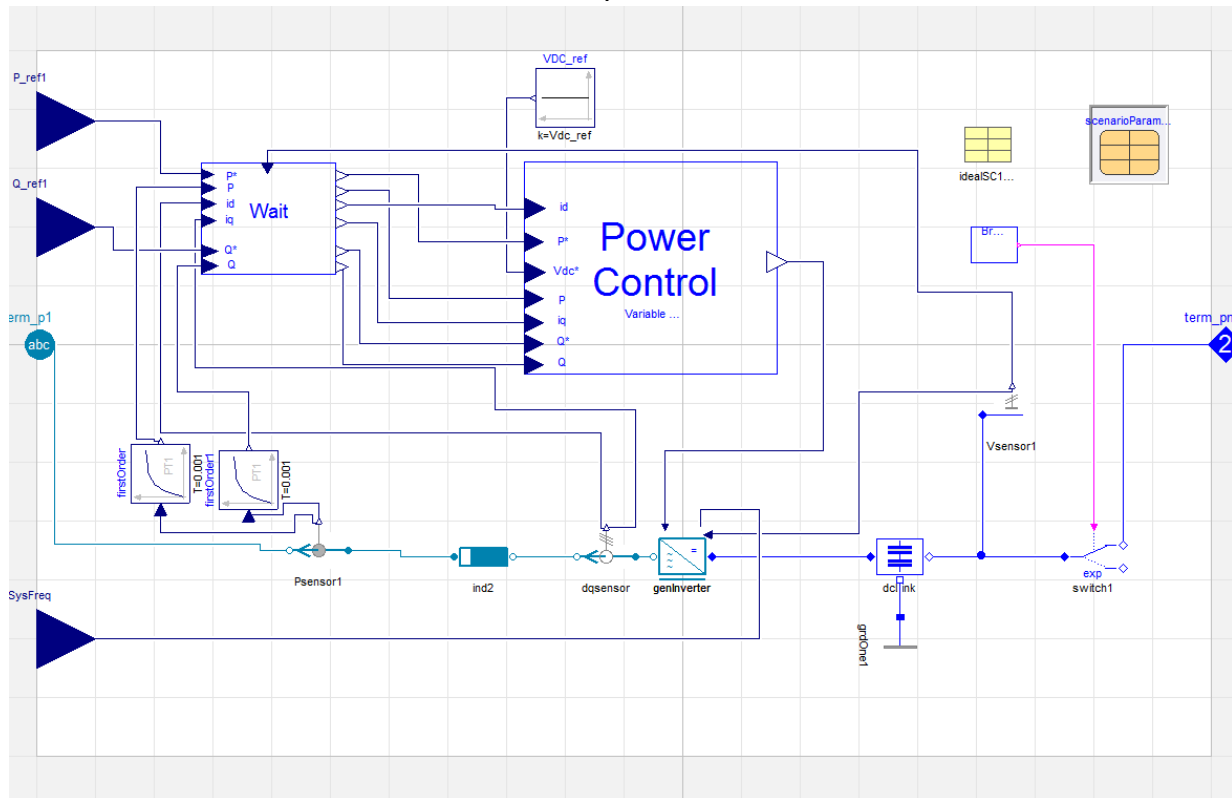


Figure 3.20 The Dymola implementation of the power controlled AC/DC converter which corresponds to the control configuration in figure 3.19.

The structure at the top level is almost identical with the DC voltage controller. The difference compared to the DC voltage controller is that active and reactive power is measured on the AC side and sent to a first order transfer function that suppresses the higher frequencies. The DC voltage is measured and sent to the wait block in order to determine when the power control should start.

The control block at top level has the active power (reference and signal), reactive power (reference and signal), d-current, q-current and DC voltage reference as inputs. All signals except the DC voltage reference passes through a wait block before they enter the control block. The DC voltage needs to be sufficiently high to be able to perform power control. There is also a wait block inside the inverter with the same DC voltage limit. When the DC voltage is large enough the signals are sent to the “Power Control”-block in figure 3.20.

Inside the “Power Control”-block, seen in figure 3.21, the active power and reactive power signals are sent to two PI controllers. The output from the active power controller is the d-current reference and the output from the reactive power controller is the q-current reference. These current references, along with the measured currents and the DC voltage reference are sent to the current control block as can be seen in figure 3.21.

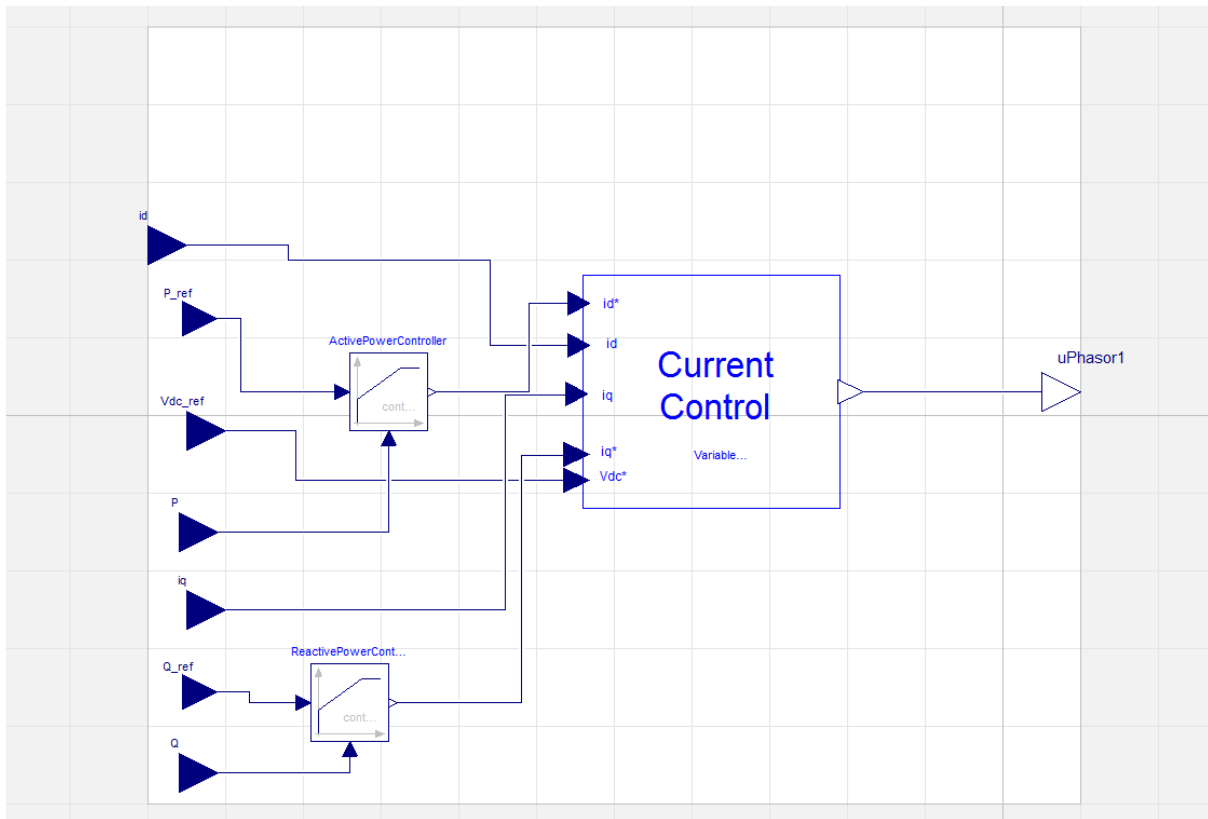


Figure 3.21 The power control block model seen in figure 3.20.

The current control block, seen in figure 3.22, is the same as in the DC voltage controller but with P controllers in both components, since both outer loops feature PI controllers. The output from the current controller is limited by the maximum DC-link voltage and sent to the phasor block. The phasor block calculates, with the input voltage references, the voltage vector length scaled to the DC-link voltage and the angle of the vector in respect to the d-axis in the dq-frame. These two values are sent to the “genInverter”-block in figure 3.20, where they are fed to the modulator block.

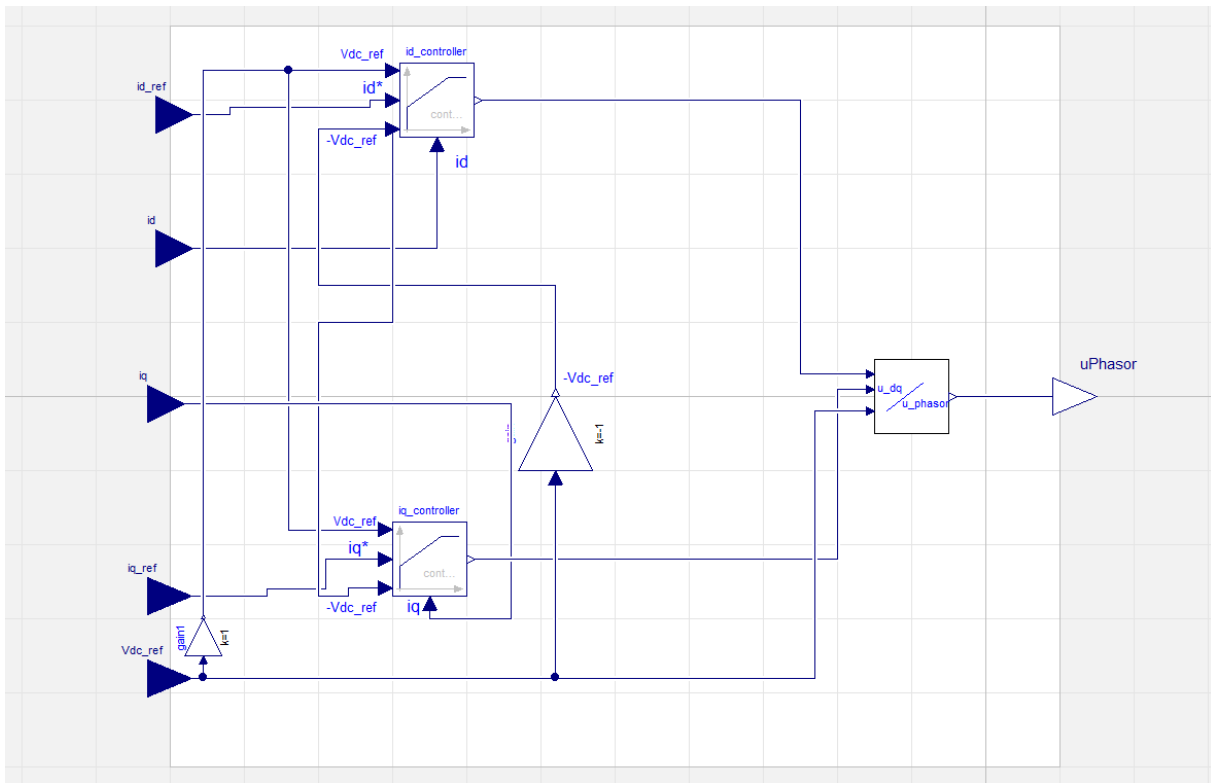


Figure 3.22 The current control block

3.4.2 SIMULATION RESULTS OF THE POWER CONTROLLED AC/DC CONVERTER

The simulation configuration presented in figure 3.23 and as it can be seen in the figure the inverter is connected to voltage sources at each side. The AC voltage source represents a stiff three-phase AC grid with 50 Hz grid frequency and 400 V line-to-line voltages. The DC voltage represents a stiff DC grid and is set to 2 kV. The power references are generated by square waves each with an amplitude of 60 kW/kVA, an offset of -30 kW/kVA and a period of 0.2 s. Having a negative reference to the power controllers corresponds to supplying power to the DC grid. The square wave corresponding to the reactive power reference, “Q_ref” in figure 3.23, is delayed 0.1 s. The parameters for the controllers are specified in table 3.5 and the system parameters for the model are listed in table 3.6.

Requirements for the power controlled AC/DC converter are:

- Power should be able to flow in both directions.
- Reactive and active power can be regulated separately.
- The inverter should be able to supply/consume 30 kW/kVA to/from the grid
- The current ripple should be significantly small.
- The power should reach its reference in 0.05 s
- The current has to be able to respond to large changes rapidly.

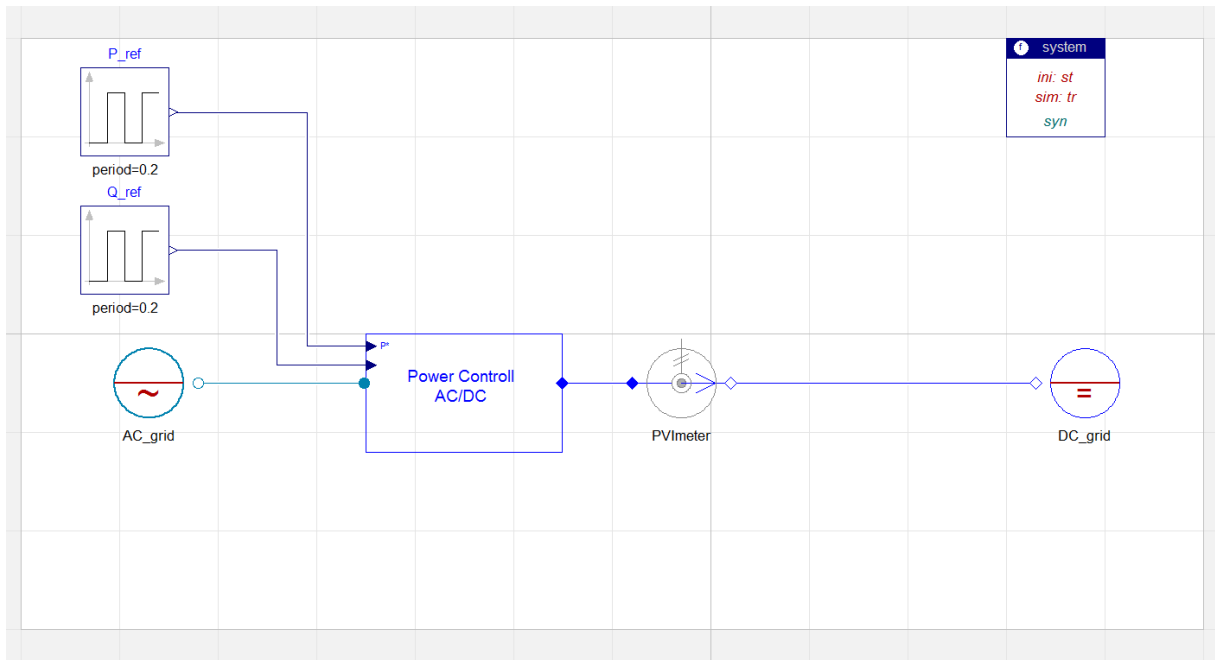


Figure 3.23 The test bench of the power controlled AC/DC converter connected to two stiff grids.

Active Power Gain	Active Power Integral Gain	Reactive Power Gain	Reactive Power Integral Gain	d-current Gain	q-current Gain
$K_{AP}=0.0005$	$T_{AP}=0.001$	$K_{RP}=-0.0001$	$T_{RP}=0.0001$	$K_{id}=5000$	$K_{iq}=5000$

Table 3.5 The parameters for the controllers in the test bench.

Inductance	Resistance	DC-link capacitor
$L = 15.9 \text{ mH}$	$R = 0.00005 \Omega$	$C = 0.1 \text{ mF}$

Table 3.6 The system parameters set for the test bench

In figure 3.24 the performance of the active and reactive power controllers is shown. Note that the measured power is filtered before going into the controller. Figure 3.25 shows the unfiltered power drawn from and supplied to the AC-grid. Note that consuming reactive power from the AC grid into a DC grid structure is highly peculiar since in the DC operation only active power is available, but since the performance of the controllers are to be studied this reference was used anyway. The current controllers are shown in figure 3.26 and the close resemblance to the power is notable.

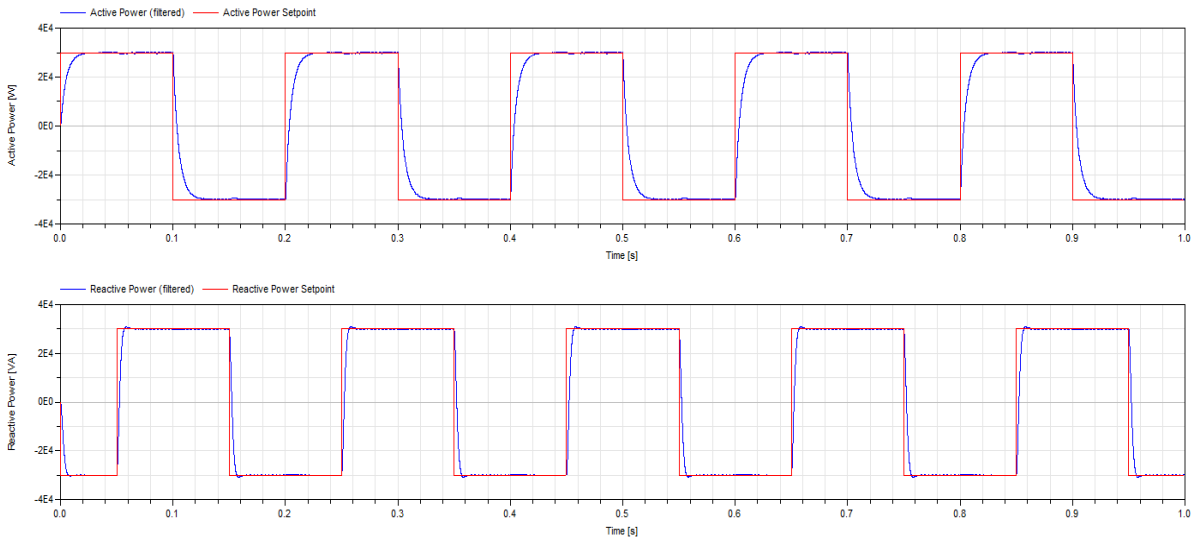


Figure 3.24 The graphs show the performance of the active (top graph) and reactive (bottom graph) power control. The signals are filtered in in this graphs.

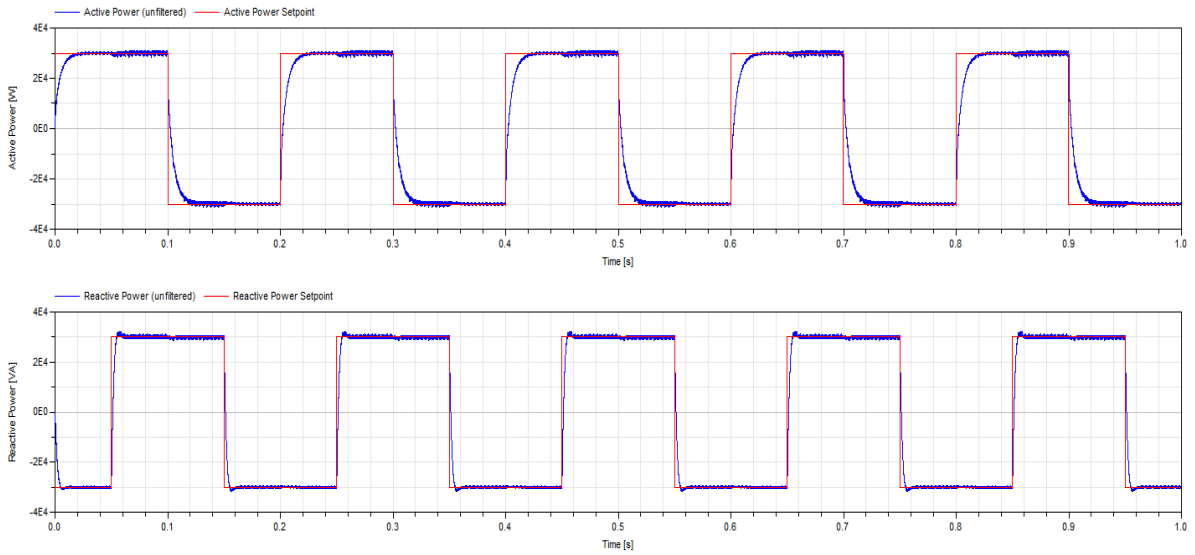


Figure 3.25 The unfiltered active (top graph) and reactive (bottom graph) power is shown in the figure compared to the power references.

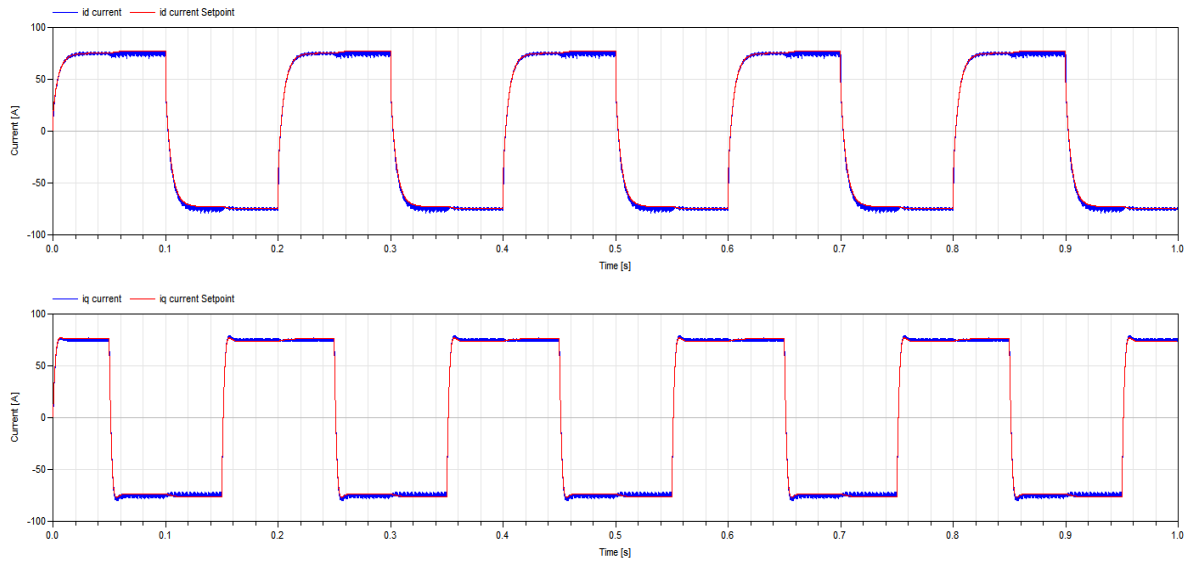


Figure 3.26 The current controllers responding to the reference generated by the active and reactive power controllers.

3.4.3 DISCUSSION

With use of figure 3.24, 3.25 and 3.26 it can be determined that:

- Power can flow in both directions.
- Reactive and active power can be controlled independently.
- The converter can consume 30 kW/kVA from the grid and also supply 30 kW/kVA to the grid.
- The current ripple is considered to be significantly small.
- The power reaches its reference in just 0.05 s.
- The current responds sufficiently fast to changes in current reference.

From both figure 3.24 and figure 3.25 the power control can be concluded to be accurate. The power reaches its reference and responds to step changes sufficiently fast. From these figures it is also seen that the reactive and active power can be controlled separately as the references vary differently. As mentioned in previous chapter the excessive consumption of reactive power from the AC is highly irregular, but since this test is used to evaluate the performance of the controllers this only shows that the controller is stable. The ripple in power seen in figure 3.24 is lower than the ripple seen in figure 3.25, which is due to the filtering of signals also seen in figure 3.20. The ripple in power is unavoidable in switched environments and is related to the ripple in current. The ripple is however acceptably small compared to the power reference. The current follows the same pattern as the corresponding power as can be seen by comparing figure 3.25 and figure 3.26, where the q-current follow the behavior of the reactive power and the d-current follows the active power.

When examining the power closely in figure 3.25 one can see that the active power changes somewhat when changing the reactive power and vice versa. This is because the reactive and active power are not completely independent of each other as can be seen in chapter 2.7.3.4, equation 2.43. This could be handled in the power control algorithm of the AC/DC converter, however it is not included in this thesis since the effects of this is not imminently large.

The rise time of the active and reactive power controllers also differs somewhat as can be seen in figure 3.24. The two different controllers are tuned separately which may be the origin of their different performance. The controllers could be tuned further in order to get the exact same behavior for both components, but since the controllers are sufficiently fast and do not produce instabilities this can be overlooked.

3.5 AC/DC CONVERTER DROOP CONTROL

In a back-to back multi terminal system such as an internal DC grid implemented in chapter 5.2.1 it is the AFE DC voltage controller that is responsible for keeping the DC voltage on the correct level. If the DC voltage controller for some reason is disconnected from the internal DC grid there is no converter in control of the voltage meaning that the DC grid is operating in islanding mode. Depending on whether the other controllers are generating or drawing power the DC link voltage will either be too high or too low and finally the internal DC grid will crash. A solution to this problem is presented in this section.

The overall setup scheme for the AC/DC inverter is the basically the same as for the AFE, the difference is the control structure. By measuring the DC voltage the controller get information on whether to perform active power or DC voltage control. If the magnitude of the DC voltage is increasing or decreasing too much the controllers will start controlling the DC voltage to the correct level. If it is the utility grid causing the disconnection it is generally only a matter of seconds until the power is back and the controllers could start in normal operation mode again.

The circuit and control structure can be seen in figure 3.27.

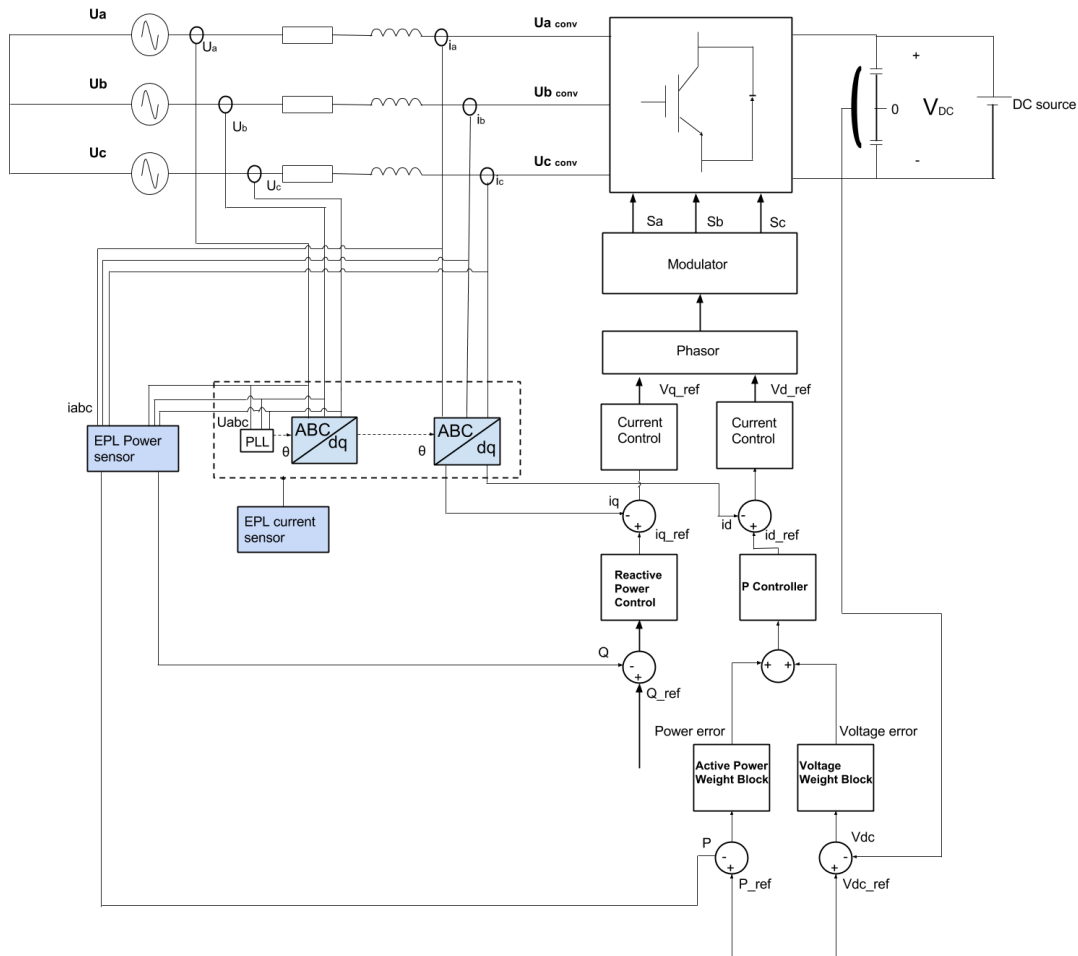


Figure 3.27 The droop control structure.

The idea is to use two blocks that add a weight to the power and voltage errors which decide the importance of each error. The two errors are then added and sent to a P controller, the signal that deviates most will be subject of control. Since it could be a multilevel system with perhaps many controllers only P control is used in the outer loop to prevent the different controllers from working against each other.

The weight blocks in figure 3.27 can also be used to set DC voltage limits for when turning on and off the power control. If the DC voltage is close to the reference power control is turned on and if the DC voltage deviates too much, power control it is turned off and voltage control is turned on. This is done by setting the weight to zero or one depending on the DC voltage. A hysteresis has been implemented in the weight block to avoid chattering.

The rest of the control structure is basically the same as for the AC/DC power control.

3.5.1 DYMOLA IMPLEMENTATION OF THE AC/DC CONVERTER WITH DROOP CONTROL

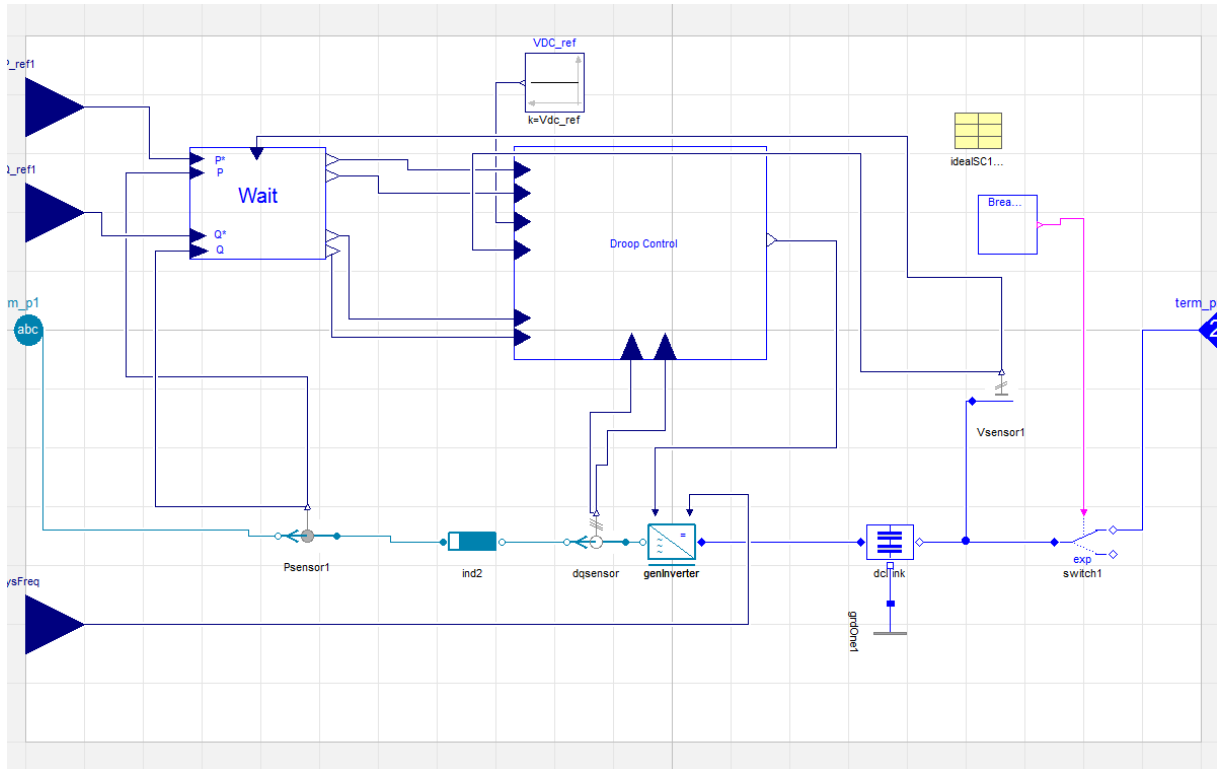


Figure 3.28 Illustration of the AC/DC droop control loop implemented in Dymola

The AC/DC droop controller is only used in longer simulations and has therefore only been implemented as a Time Average model. As mentioned before the signals are in average the same as for the switched models but the simulation time is much faster. The only components that will be discussed in this model are the droop control on the second level (see figure 3.29) since the rest of the blocks are the same as for the AC/DC power controller. It should also be mentioned that since there are no transistors to turn off in a Time Average model that feature is removed inside the “genInverter” model.

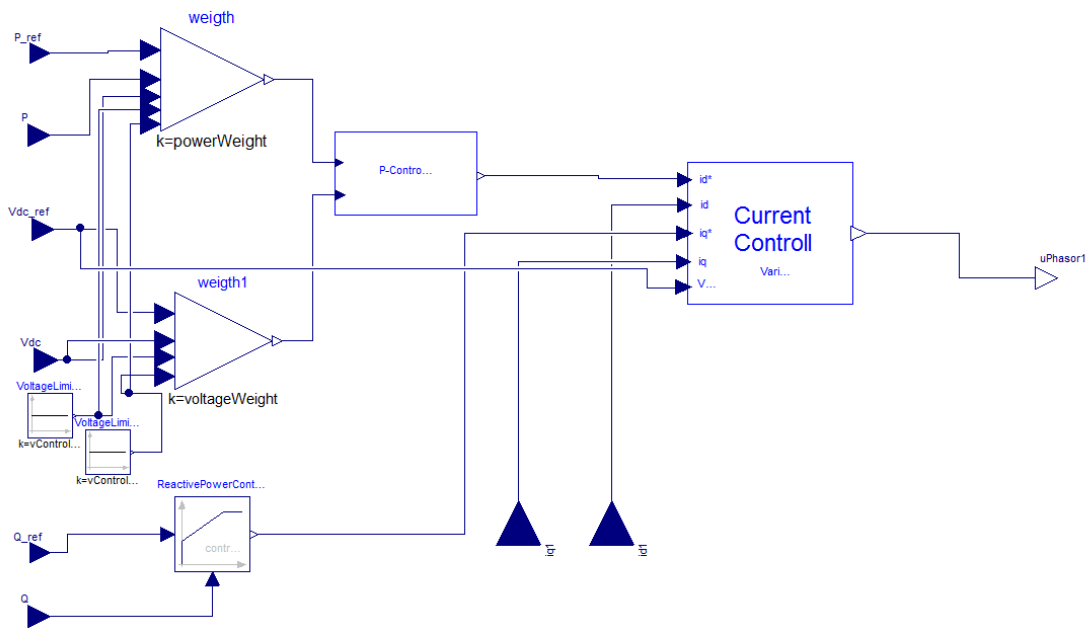


Figure 3.29 The figure illustrates the inside of the “Droop Control”-block seen in figure 3.28.

In figure 3.29 the Dymola implementation of the droop control structure can be seen. The subtraction between the reference and measured quantity is made inside the weight blocks for both power and voltage. The errors are then added together inside the P Controller block as seen in figure 3.30.

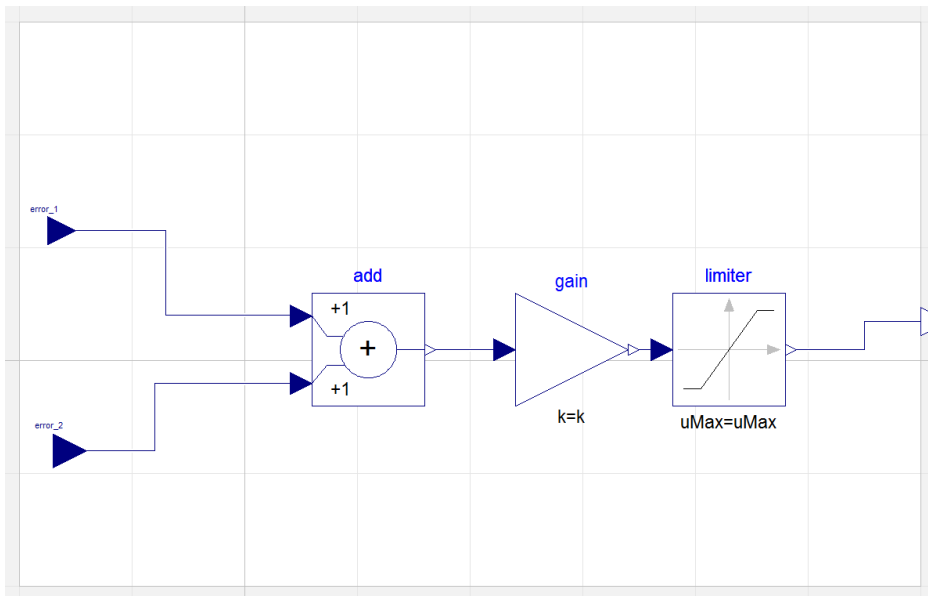


Figure 3.30 The figure shows the power P-controllers.

3.5.2 SIMULATION RESULTS OF THE DROOP CONTROLLED AC/DC CONVERTER

The test bench can be seen in figure 3.31. The AC/DC droop controller is connected to an ideal DC source via a resistance (symbolizing the DC grid resistance) and a DC breaker. The AC voltage source connected to the droop controller represents a stiff three phase power source with a frequency of 50 Hz and 400 V line-to-line voltages. The power reference for the droop control is set to 20 kW, since it should not be possible to supply power to the source. A variable resistor is connected to the DC grid acting as a load. The load is varied to consume power in pulses of approximately 30 kW. The idea is to test how well the droop controller can maintain the DC voltage level when the DC source is disconnected after 0.2 seconds from the DC grid. The test will include two cases; when the subject of control depends on DC voltage limits and one where the magnitude of the errors decides which controller that shall be used. Controller parameters for the droop control are listed in table 3.7 and the system parameters are listed in table 3.8.

The requirements for both tests are:

- The droop controller should be able to maintain the DC voltage level over the load when the DC source is disconnected from the grid while the load is pulsing.
- If the DC voltage is too high the droop controller should decrease the amount of power generated by the energy source to decrease the DC link voltage.
- If the DC link voltage is too low the droop controller should increase the amount of power generated by the energy source to increase the DC link voltage.
- If the DC link voltage is on a reasonable level the droop controller should try to keep the power reference of 20 kW.

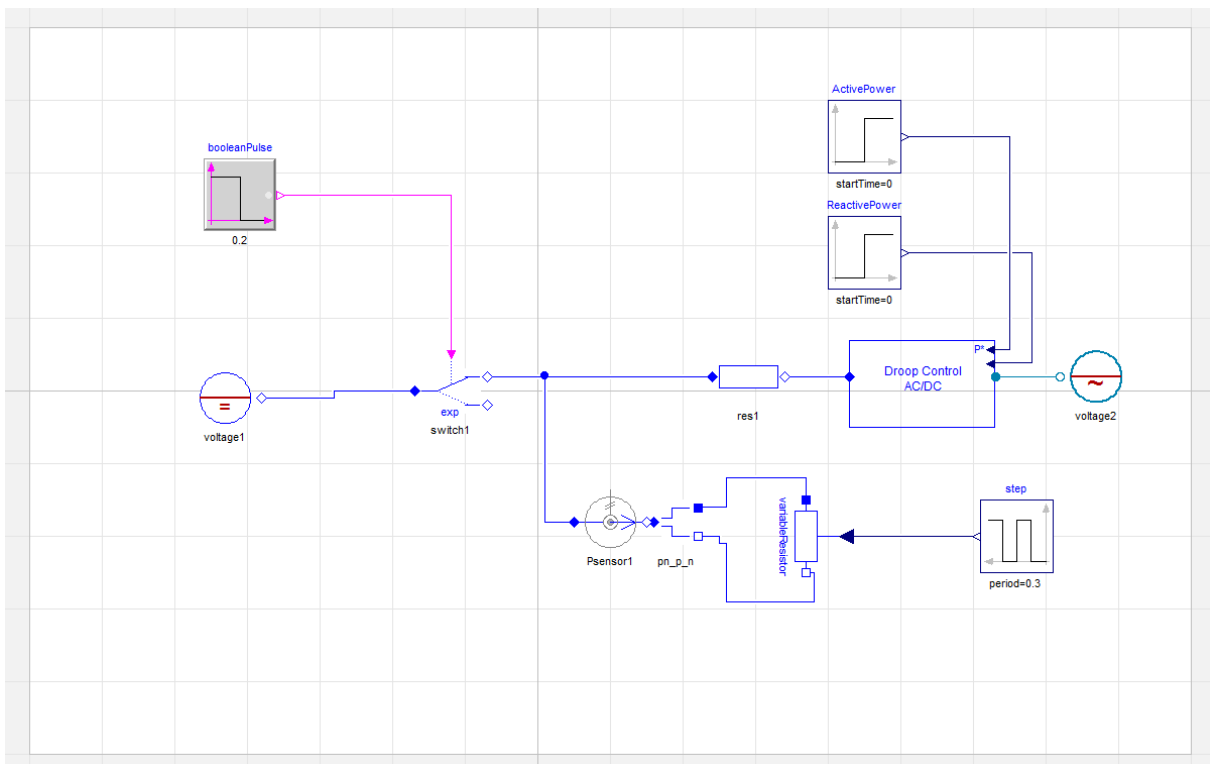


Figure 3.31 Test bench for droop control with a load connected to the DC grid consuming power in pulses of 30 kW.

P controller Gain	Reactive Power Gain	Reactive Power Integral Gain	d-current Gain	q-current Gain
$K_{droop}=5$	$K_{droop}=-0.0001$	$T_{droop}=0.0001$	$K_{droop}=500$	$K_{droop}=500$

Table 3.7 The control parameters for the droop control test bench.

Inductance	Resistance	DC-link capacitor
$L_{droop} = 6.4 \text{ mH}$	$R_{droop} = 0.00005 \Omega$	$C = 0.8 \text{ mF}$

Table 3.8 The system parameters for the droop control test bench.

TEST 1 DROOP CONTROL USING VOLTAGE LIMITS:

DC Voltage Limit Low	1992V
Hysteresis Low	$0.98 \cdot 1992 \text{ V} = 1952 \text{ V}$
DC Voltage Limit High	2008 V
Hysteresis High	$1.02 \cdot 2008 \text{ V} = 2048.6 \text{ V}$

Table 3.9 The voltage limits for the droop control.

As mentioned before hysteresis is implemented to avoid chattering. The limits are seen in table 3.9. When the DC voltage is low and increases above 1992 V power control starts. When the DC voltage increases above 2048.6 V power control will stop and when it decreases again below 2008 V power control will start again and continue until the DC voltage is below 1952 V.

Remark: The power sensor of the droop controller is pointing towards the source i.e. negative power is flowing towards the DC link. The power sensor before the load is pointing towards the load i.e. the power is positive when the load is consuming power.

The top plot in figure 3.32 is showing the DC voltage over the load and DC voltage reference and the bottom plot is showing the power generated by the energy source, when the DC source is disconnected after 0.2 s. The power consumed by the load can be seen in figure 3.33. The same results for test 2 can be seen in figure 3.34 and figure 3.35. The reactive power is controlled to zero in both tests and is not plotted.

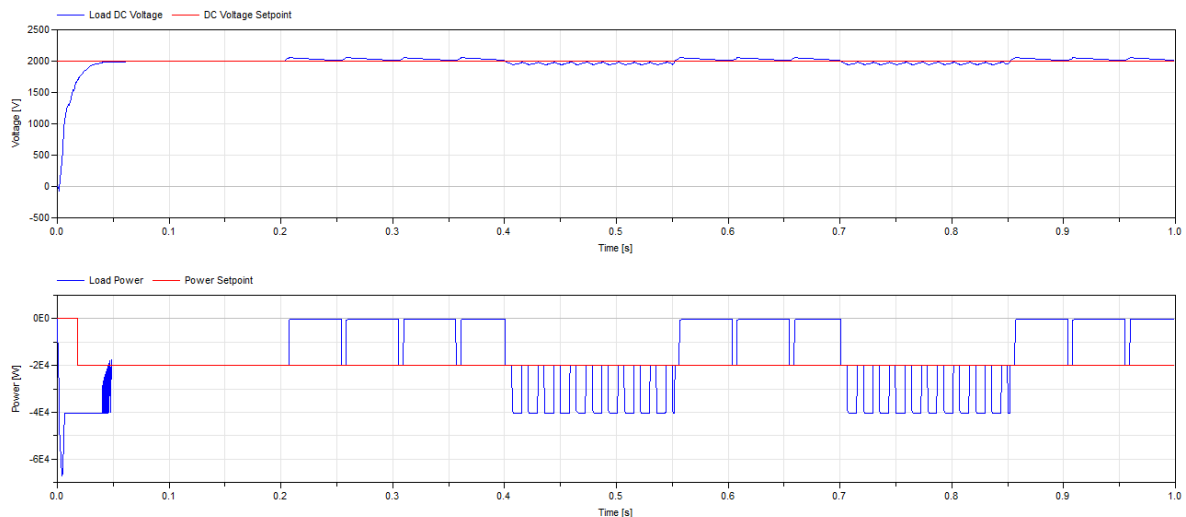


Figure 3.32 Test 1: DC voltage over the load and power generated by the source when the DC source is disconnected after 0.2 s.

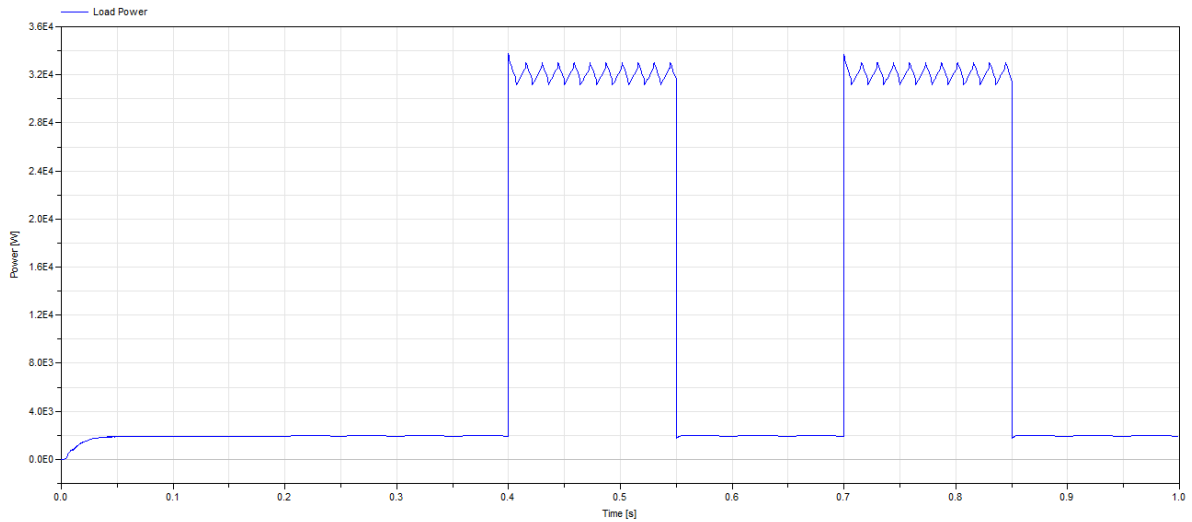


Figure 3.33 Load consuming power in pulses of approximately 30 kW for test 1.

TEST 2 DROOP CONTROL USING ERROR DEVIATION:

In test 2 the largest error deviation decides the control type of the droop controller. The weights were set according to table 3.10.

Voltage	9.9
Power	0.01

Table 3.10 The weights of the droop control.

All parameters are the same as in test 1.

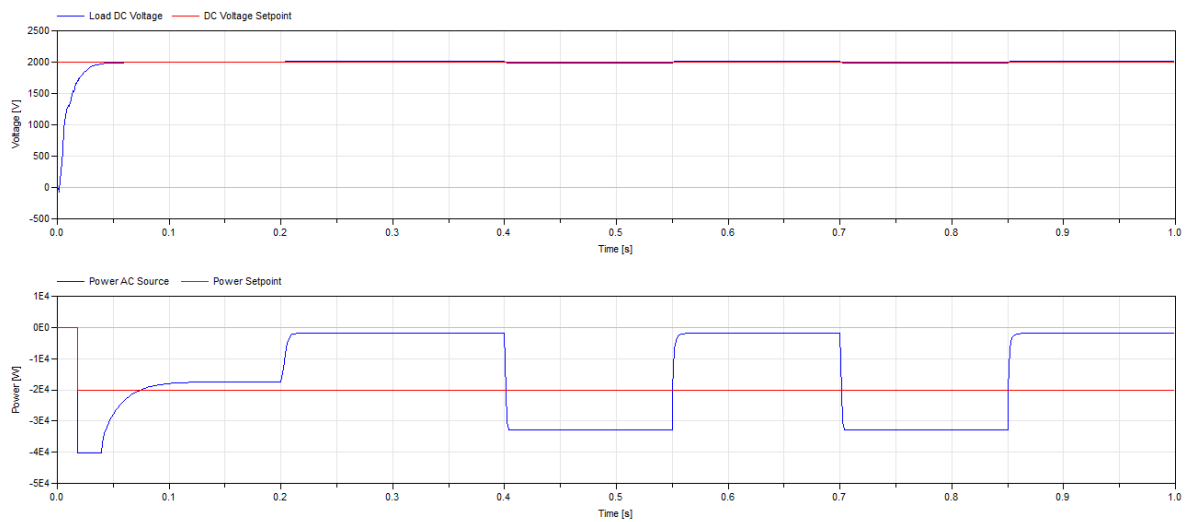


Figure 3.34 Test 2: DC voltage over the load and power generated by the source when the DC source is disconnected after 0.2 s.

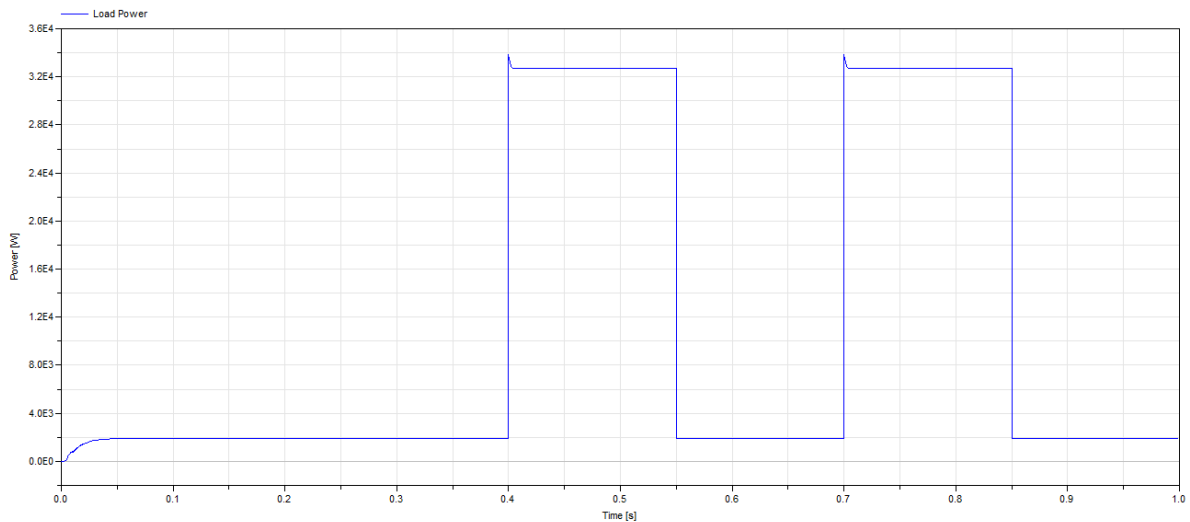


Figure 3.35 Load consuming power in pulsing of approximately 30 kW for test 2.

3.5.3 DISCUSSION

Test 1 (figure 3.32 and figure 3.33): When the DC source is disconnected after 0.2 s the load is not pulsing and therefore power is flowing to the DC grid increasing the DC voltage over the load since the droop controller is holding the power reference of 20 kW. When the voltage is exceeding the upper voltage limits the droop control shifts to voltage control. Since it is not possible for the power to flow to the source the controller decreases the power flow to the grid as much as possible. When the voltage is below the upper voltage limit the controller tries to control the power again but only until the upper voltage limits has been crossed once again. This explains the ripple after the disconnection from the DC source.

When the load pulse starts the DC voltage starts decreasing and when it crosses the lower voltage limit the droop controller tries to rise up the voltage by increasing the amount of power injected to the grid. Since the controller is a P controller it does not succeed to increase the voltage to the reference level. When the load pulse ends the DC voltage increases again and the droop controller alternates between power and voltage control. The same behavior is then repeated over one more pulse.

Test 2 (figure 3.34 and figure 3.35): The weight points used in table 3.10 differ quite much. This is done in order to compensate for the fact that the magnitude of the power is higher than the voltage and also to prioritize the DC voltage control. When the DC source is disconnected the DC voltage starts increasing at the same time the droop control tries to compensate for this by decreasing the power. When the load starts pulsing the DC voltage decreases and the controller tries to inject more power but it is not enough to reach the reference level. The error in voltage and power was 17 V and 3000 W respectively.

Comments to the requirements:

The overall behavior of the droop control structures in both tests seem to work. Power is injected when the DC voltage is too low and the amount of injected power is decreasing when the DC voltage is too high. The first method managed to reach the power reference at some short time and it kept the DC voltage closer to the reference but at the same time it was not that smooth. The second method is smoother but it does not reach the reference values of either

power or voltage. In both testes the first priority was to prevent the DC voltage from plummeting which was successfully performed by both controllers. In this thesis the second alternative is chosen due to the smooth but still quite accurate control performance.

3.6 OPEN LOOP AC VOLTAGE CONTROL OF THE AC/DC CONVERTER

The previously mentioned voltage controller maintains DC voltage in the internal DC grid. However, if the internal grid instead operates in AC, a converter has to be responsible for the AC voltage at the common point of connection in the internal AC grid. This converter must ensure constant voltage amplitude and constant frequency. To the AC grid, in this thesis, only power electronic converters are connected which makes the voltage regulation in the common point of connection somewhat unique. In a conventional AC grid the frequency of the system is affected by the inertias of generators and loads. However, these inertias are decoupled when placing back-to-back converters between them and the internal AC grid i.e. no inertias are connected directly to the internal AC grid. This implies that the frequency of the internal grid can be chosen freely and is also unaffected by the power consumption and supply.

The control of the AC voltage is an open loop voltage control since the desired amplitude and frequency of the voltage is known. By providing this information to the modulator the specified voltage can be created by the converter. But when connecting units in any grid formation there will always be some form of impedance in the line between the unit and the common point of connection. This impedance causes a voltage drop and a phase shift in the current and voltage, and these no longer lie in phase with the modulated voltage in the point of common connection. Besides, this cannot be altered due to the characteristics of the impedance. In the connection point it is eligible to have a current and voltage aligned with one of the dq-frame axes. If it is assumed that the line impedance is known and symmetrical it is fairly simple to compensate for the voltage drop of the line impedance.

A typical line is shown in figure 3.36 and consists of a resistor and an inductor. To compensate for the voltage drop across the line impedance the current has to be measured. The voltage across the line impedance is calculated through Ohm's law, equation 3.5, and since the current is alternating it has both d- and q-component.

$$U_{line} = (R + j\omega L) * i = (R + j\omega L) * (i_d + ji_q) = Ri_d - \omega Li_q + j(Ri_q + \omega Li_d) \quad (3.5)$$

By using KVL equation 3.6 is obtained, and since the voltages are also alternating they are composed of d- and q-components.

$$U_{grid} = U_{conv} - U_{line} \rightarrow \begin{pmatrix} U_{d\ grid} \\ U_{q\ grid} \end{pmatrix} = \begin{pmatrix} U_{d\ conv} \\ U_{q\ conv} \end{pmatrix} - \begin{pmatrix} U_{d\ line} \\ U_{q\ line} \end{pmatrix} \quad (3.6)$$

When combining equation 3.5 and equation 3.6 the d- and q-components of the grid voltage can be expressed separately as is the case in equation 3.7.

$$\begin{pmatrix} U_{d\ grid} \\ U_{q\ grid} \end{pmatrix} = \begin{pmatrix} U_{d\ conv} \\ U_{q\ conv} \end{pmatrix} - \begin{pmatrix} Ri_d - \omega Li_q \\ Ri_q + \omega Li_d \end{pmatrix} \rightarrow \begin{pmatrix} U_{d\ conv} \\ U_{q\ conv} \end{pmatrix} = \begin{pmatrix} U_{d\ grid} \\ U_{q\ grid} \end{pmatrix} - \begin{pmatrix} Ri_d - \omega Li_q \\ Ri_q + \omega Li_d \end{pmatrix} \quad (3.7)$$

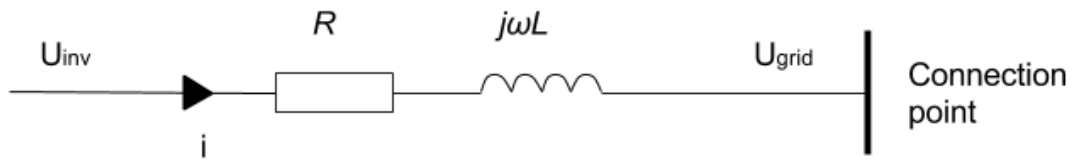


Figure 3.36 Typical line representation in an AC-grid

If the current is measured and the grid voltage is set to be aligned to the d-axis with a certain magnitude the d- and q-converter voltages can be calculated through equation 3.8.

$$\begin{pmatrix} U_{d \text{ conv}} \\ U_{q \text{ conv}} \end{pmatrix} = \begin{pmatrix} U_{line-line} \\ 0 \end{pmatrix} - \begin{pmatrix} Ri_d - \omega Li_q \\ Ri_q + \omega Li_d \end{pmatrix} \quad (3.8)$$

The open loop AC voltage control regulation principle is illustrated in figure 3.37. The outcome of equation 3.8 is sent to a phasor-block that calculates the appropriate voltage representation for the modulator.

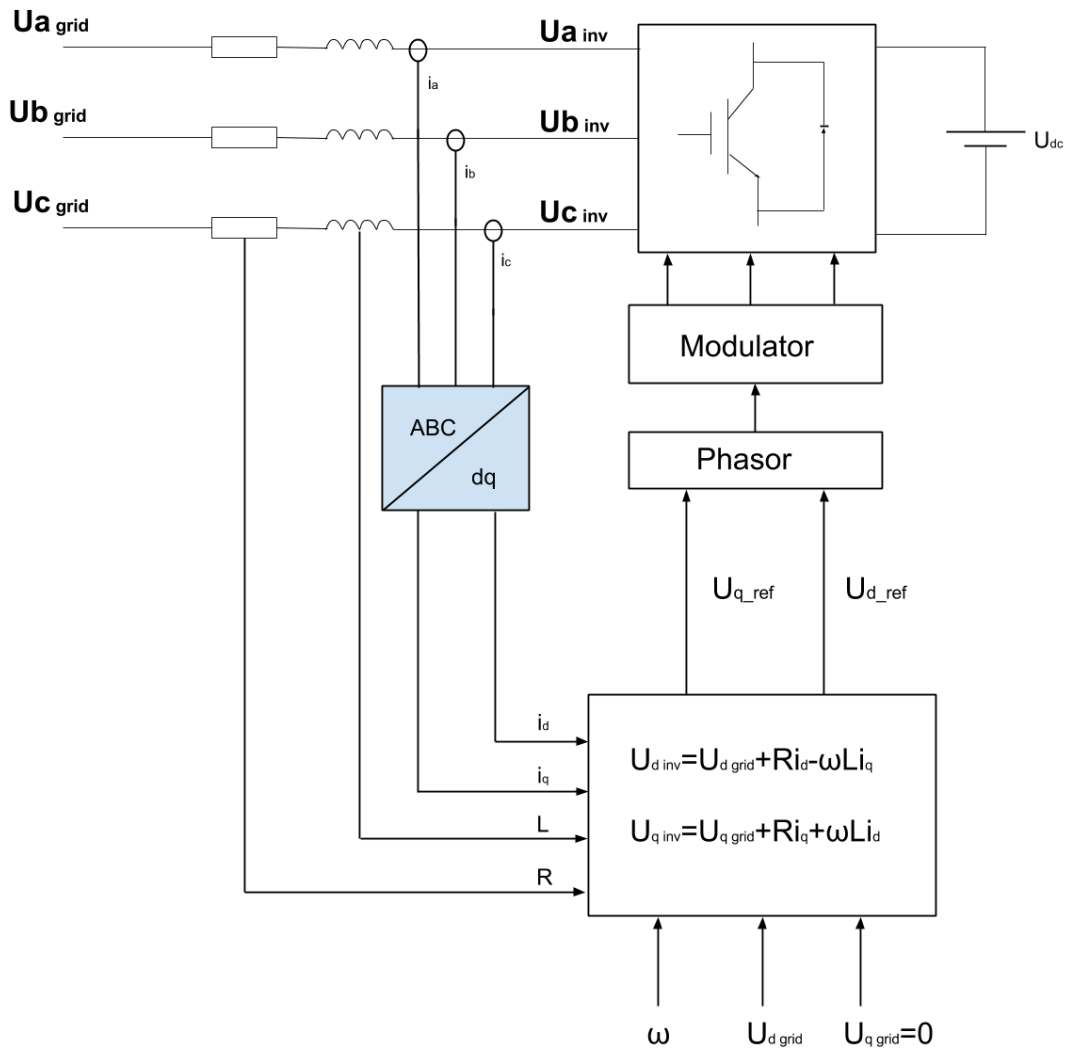


Figure 3.37 Illustration of the open loop AC voltage control setup.

3.6.1 DYMOLA IMPLEMENTATION OF THE OPEN LOOP AC VOLTAGE CONTROL

The implementation in Dymola of the open loop AC voltage control is fairly straight forward since only mathematical operators are used. The exception to this is that the current has to be measured. The open loop AC voltage control is shown in figure 3.38 and is fitted into a block. Note that the input “Ind-Line” in figure 3.38 is the line inductance multiplied with the angular frequency (ω) of the system. The phasor-block is once again used to scale and convert the d- and q-voltage references into a suitable representation for the modulator of the converter. In order for the phasor-block to scale the voltage reference properly the DC voltage reference is needed as an input as well. The voltage amplitude in line-to-line RMS unit is determined from the values set in the blocks “d_ref” and “q_ref”. If the line-to-line RMS voltage is desired to be placed along the d-axis “q_ref” is set to zero and “d_ref” is set to the desired voltage amplitude.

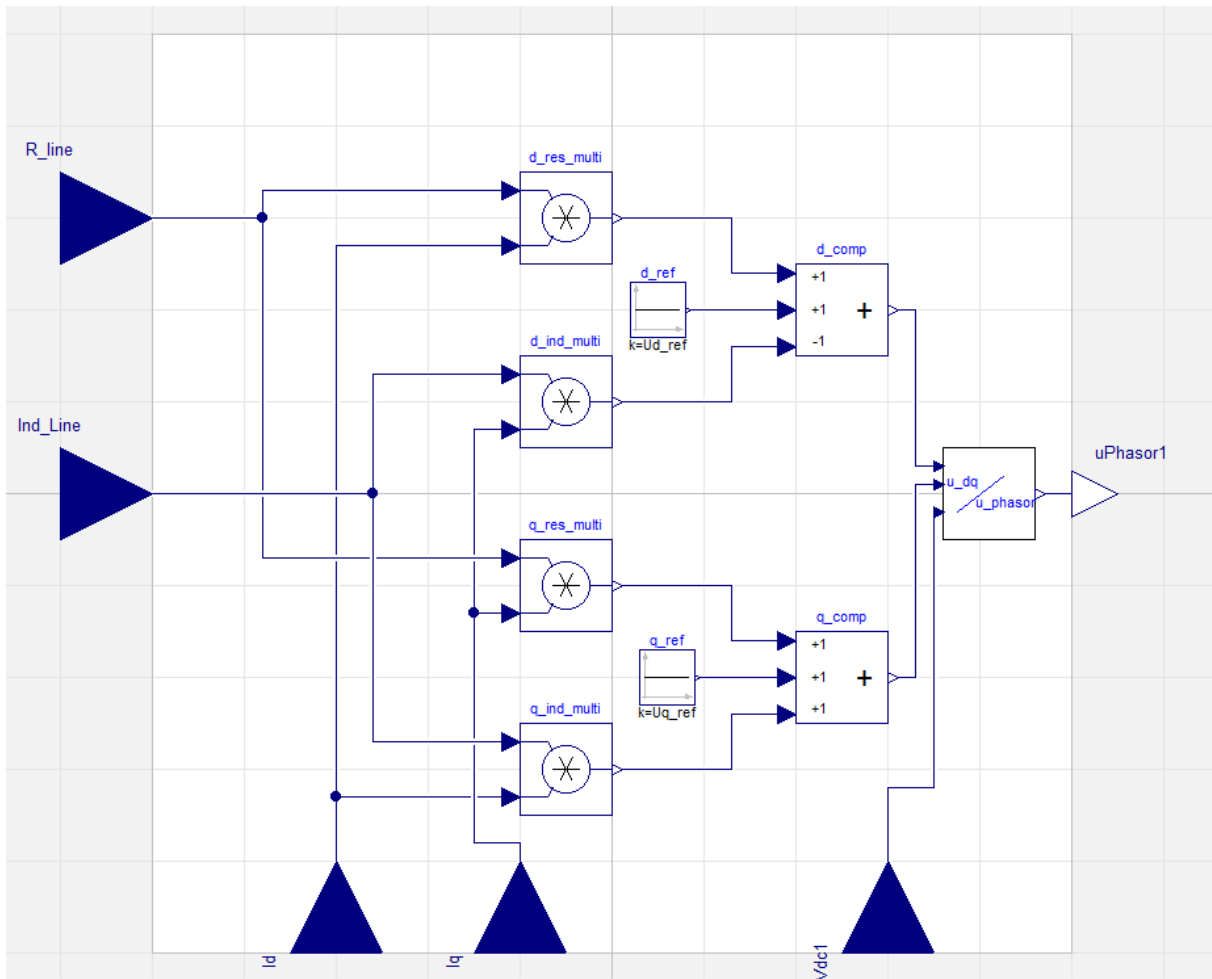


Figure 3.38. The control block of the open loop AC voltage control implemented in Dymola.

3.6.2 SIMULATION RESULTS OF THE OPEN LOOP AC VOLTAGE CONTROL

The simulation test bench for the open loop AC voltage control is constructed in the manner shown in figure 3.39. The DC voltage reference for the control block is in this case the measured voltage of the DC source. The DC source is set to 2 kV and connected to the DC side of the time average converter. The AC side of the converter is connected to a current sensor which measures the currents and transforms them into d- and q-component. The line impedance is placed between the converter and the connection point and the characteristics of the impedance are fed to the control block. Note that the “InductanceLine”-block outputs the product of the line inductance and the angular frequency. The connection point is connected to ground via an inductive load. The inductive load, much like the line impedance, is a resistor in series with an inductor. The load inductance varies sinusoidally between 0-1 mH with frequency 5 Hz. The load resistance varies between 10 and 20 Ω in 0.2 s intervals. Note that if the load inductance is not set to zero, the voltage will not be in phase with the current in the connection point.

The requirements of the open loop AC voltage control are:

- Three phase voltage with amplitude 400 V line-to-line in the connection point placed along the d-axis.
- Voltage and current frequency of 50 Hz.
- Voltage and current in phase in the connection point, when load is purely resistive.

- The voltage amplitude in the connection point and frequency should be kept when changing the load resistance and inductance. This also applies to the current frequency.

The system parameters for the test can be seen in table 3.11.

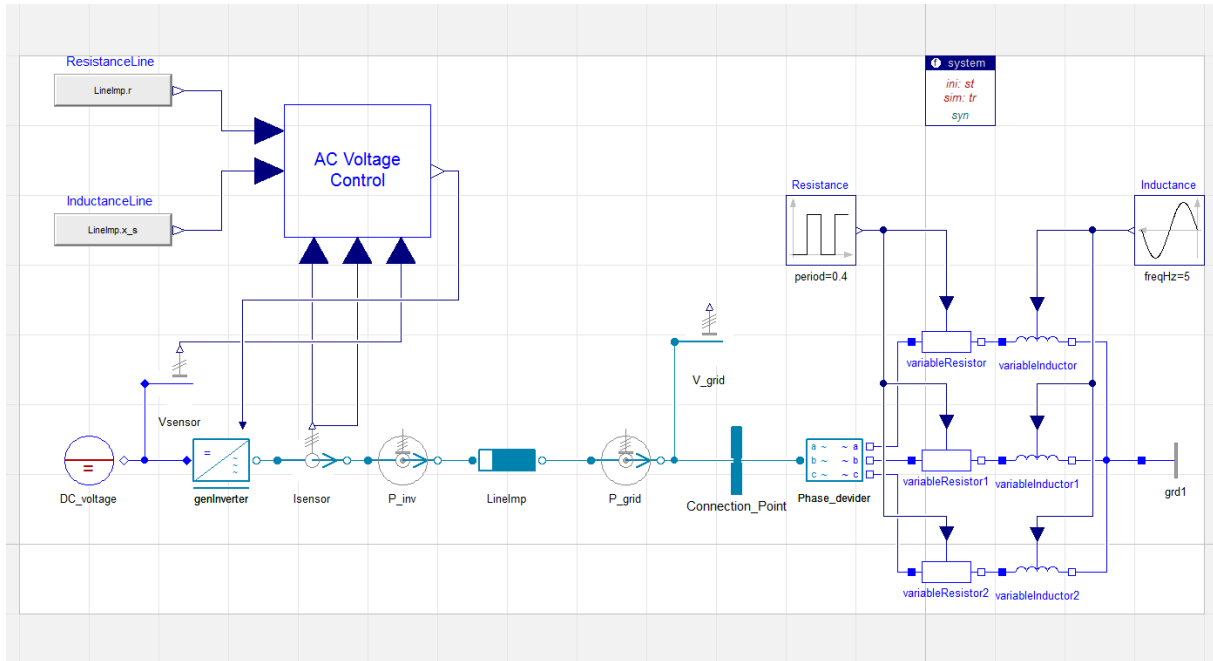


Figure 3.39 The test bench for the open loop AC voltage control implemented in Dymola.

	Line inductance	Line resistance	Load inductance	Load resistance
Test 1	$L_{line} = 50 \mu\text{H}$	$R_{line} = 1 \text{ m}\Omega$	$L_{load} = 0\text{-}1 \text{ mH}$	$R_{load} = 10\text{-}20 \Omega$

Table 3.11 The system parameters for the open loop AC voltage control.

In figure 3.40 the alignment of the voltage and current vector in the connection point in comparison to the d-axis is shown. The maximum deviation of the voltage angle to the d-axis is also shown. In the upper graph the length of the voltage vector d- and q-component (line-to-line voltage) is also shown and the alignment of the voltage vector and d-axis can be verified. The phase voltages (line-to-neutral) in the connection point can be studied in figure 3.41 as well as the phase currents.

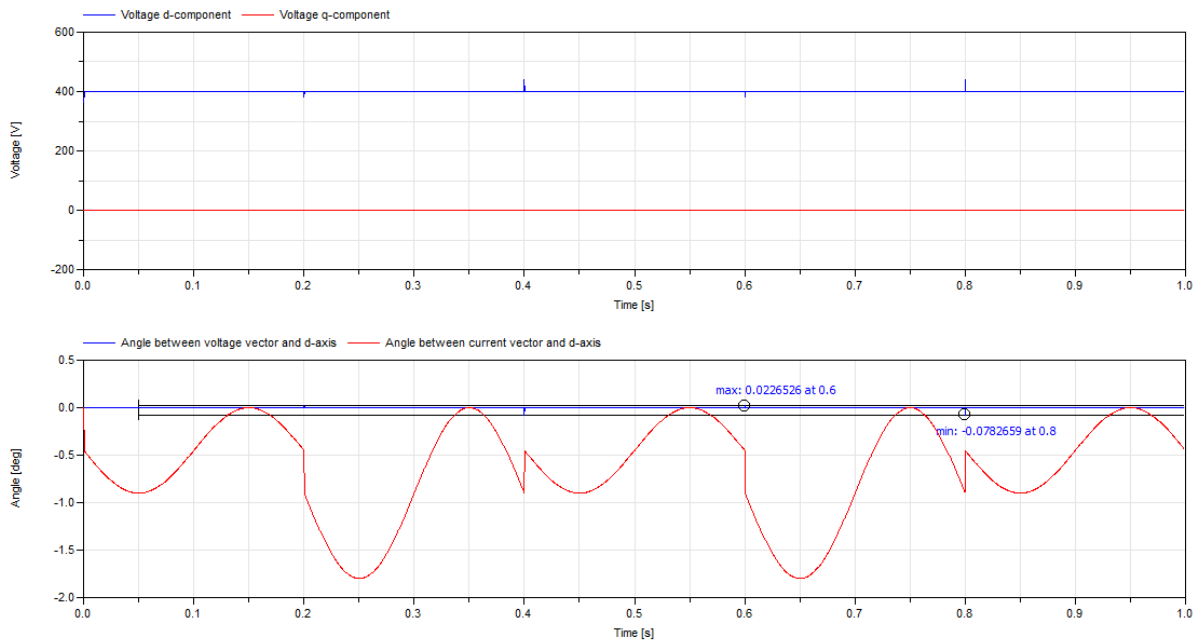


Figure 3.40 The length of the voltage d- and q-component and also the angle of the voltage/current vectors to the d-axis.

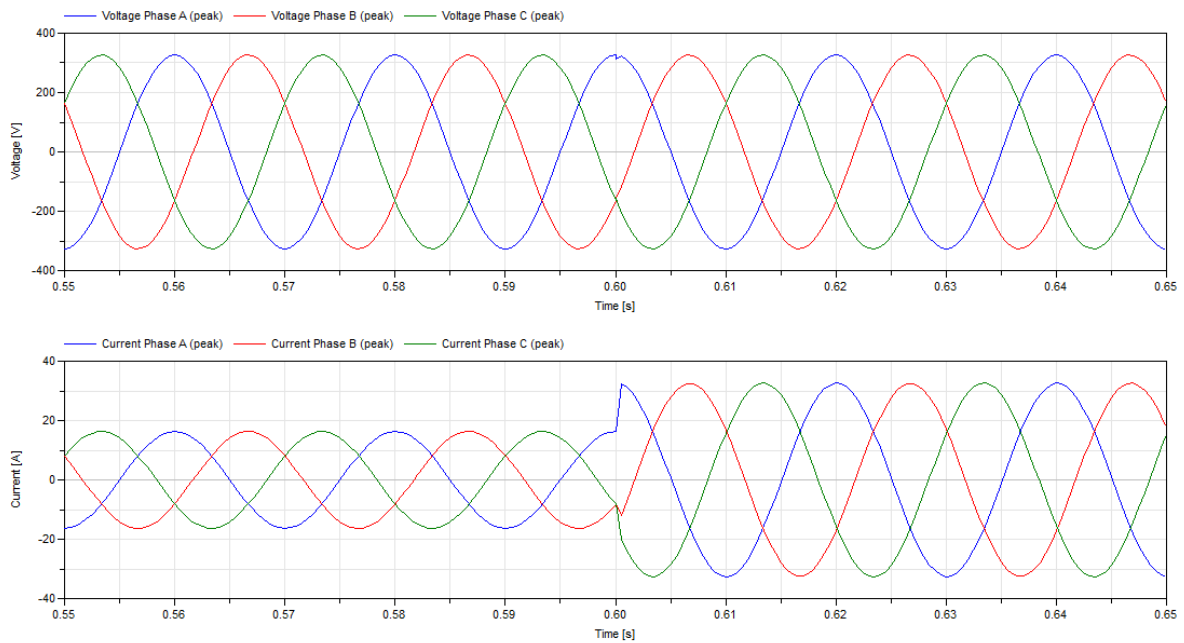


Figure 3.41 The phase voltages and currents in the connection point.

3.6.3 DISCUSSION

From the figures 3.40 and 3.41 it is able to conclude that the control operates as expected. It is also concluded that the requirements established in the simulation chapter are met.

- The controller keeps the line-to-line RMS voltage at 400 V seen both in; figure 3.40 where the voltage vector is kept at 400 V line-to-line and figure 3.41 where the phase voltages is kept at 326.6 V line-to-neutral which corresponds to 400 V line-to-line.
- The frequency of the voltage and current is 50 Hz as can be seen in figure 3.41 where the periods of the voltage and current is equal to 0.02 s.

- From figure 3.40 it can be concluded that the current and voltage vectors are aligned with each other and with the d-axis when inductance is zero.
- The frequency and amplitude of the voltage is kept when changing the load properties. The frequency of the current is also kept throughout load changes. This can be seen in figure 3.41.

Furthermore, the voltage control is very fast, since the only input supplied to the controller that is affected by the system dynamics is the current. All operations are purely mathematical, therefore the controller directly supplies the correct voltage reference to the modulator. The phase shift caused by the load is unavoidable in this configuration, but could be handled by implementing some form of reactive power compensation at the load. Such compensation will be discussed further in next chapter.

3.7 REACTIVE POWER COMPENSATION IN AN INTERNAL AC GRID

In the common point of connection the voltage and current should be aligned with each other and the d-axis. This is the basis from which the reactive power compensation operates. By supplying some reactive power, equal to the reactive power consumption of the line between connection point and load, from the load converter, it is possible to keep the voltage and current in the connection point aligned. If the impedance of the load line is known and symmetrical this can be solved in the same manner as for the open loop AC voltage control. The apparent power consumed by the load line impedance is derived from equation 3.9 and using equation 3.5 from chapter 3.6 an expression for the apparent power using only current and impedance is reached [5][6].

$$\begin{cases} S_{line} = U_{line} * i^* \\ U_{line} = (R + j\omega L) * i \end{cases} \rightarrow S_{line} = (R + j\omega L) * i * i^* \rightarrow$$

$$S_{line} = (Ri_d^2 + Ri_q^2) + j(\omega Li_d^2 - \omega Li_q^2) \quad (3.9)$$

The reactive power consumption is the imaginary part of the expression in equation 3.9 which can be seen in equation 3.10.

$$Q_{line} = Im(S_{line}) = \omega L(i_d^2 - i_q^2) \quad (3.10)$$

Since the currents i_d and i_q are already measured in both DC voltage control and power control, the reactive power consumption of the line (Q_{line} in equation 3.10) is simply added to the reactive power reference and then sent to the power control. This can be applied for the DC voltage control as well since the DC voltage is related to the current d-component only and the reactive power is governed by the current q-component. In this case a reactive power controller is added and the reference fed into this controller is the reactive power compensation. For the AC/DC power control the reactive power controller is already available and it is used for the compensation. The control loop for the compensated system can be viewed in figure 3.42. Note that the inputs of the power/DC voltage control are not included in figure 3.42 and also note that in the DC voltage control a reactive power controller is added.

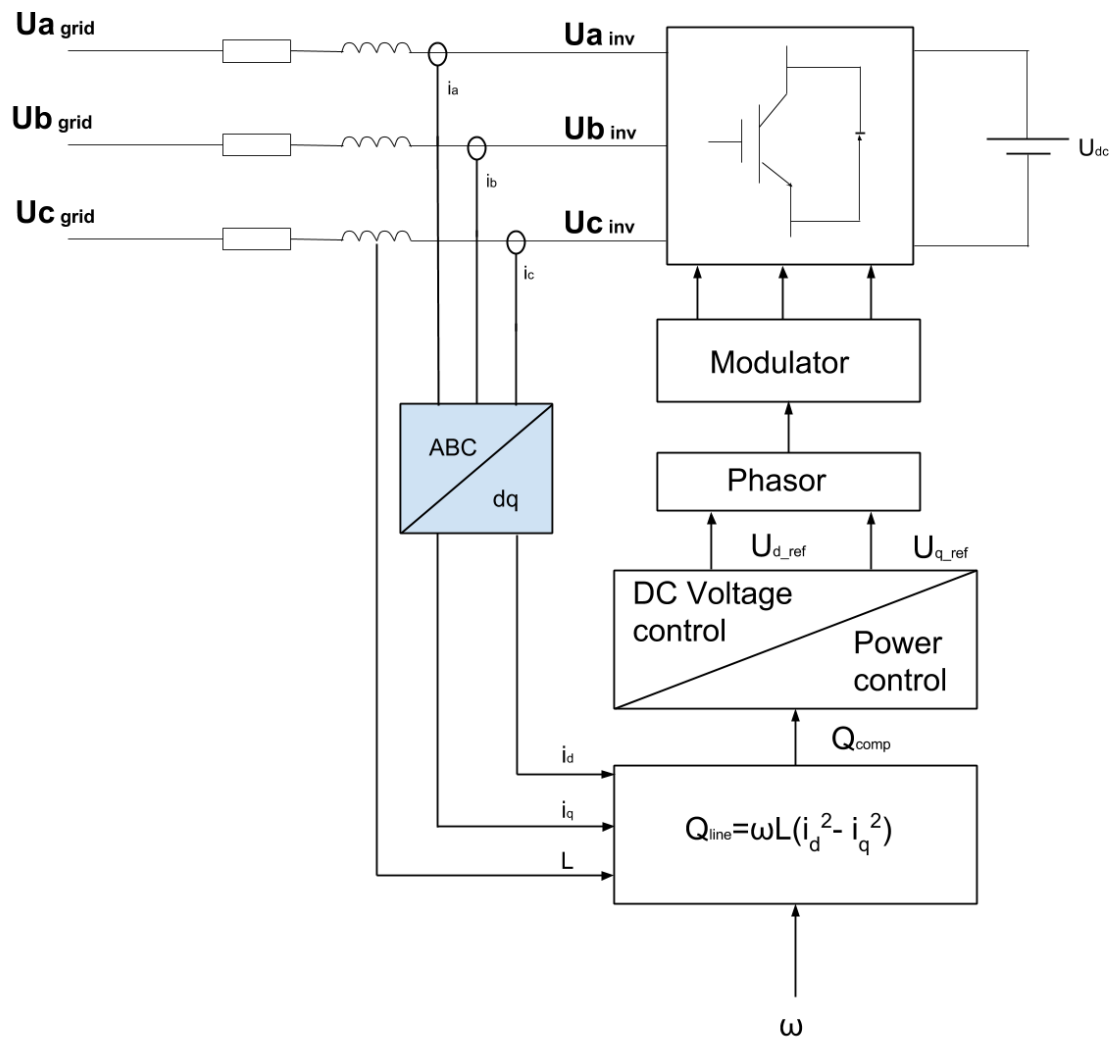


Figure 3.42 The compensation made for reactive power shown in both DC voltage control and power control.

3.7.1 DYMOLA IMPLEMENTATION OF THE REACTIVE POWER COMPENSATION

The calculation of the reactive power compensation is fitted into a compensation block shown in figure 3.43. In this block the d- and q-currents are squared and then the squared q-current is subtracted from the squared d-current. This value is then multiplied with the inductance and the angular frequency of the system. Note that the input “Ind-line” is the line inductance multiplied with the angular frequency. Besides, the reactive power compensation is added to the present reactive power reference.

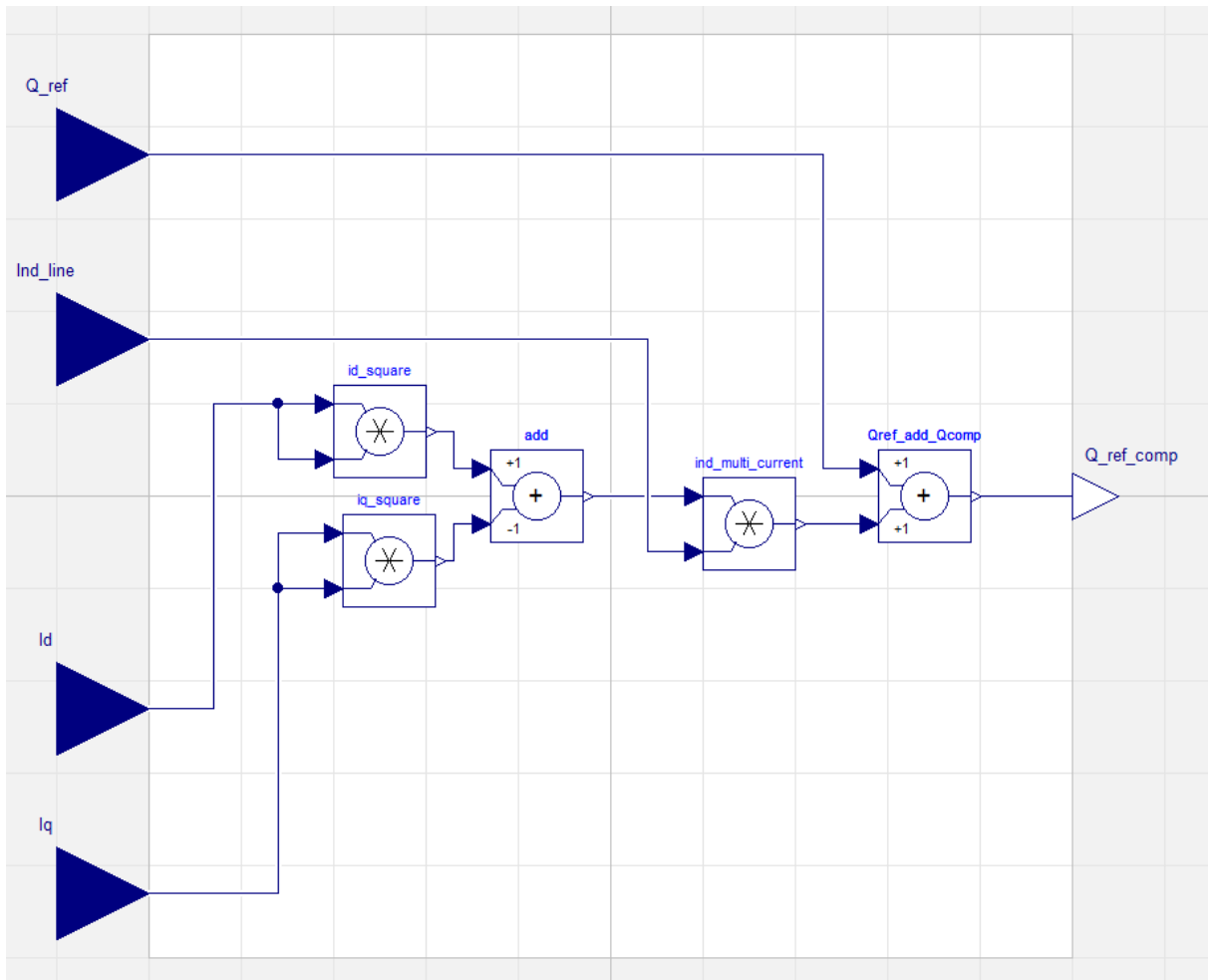


Figure 3.43 The Dymola implementation of the reactive power compensation block.

3.7.2 SIMULATION RESULTS OF THE REACTIVE COMPENSATION BLOCK

The simulation of the reactive power compensation in Dymola is carried out in the test bench shown in figure 3.44. When the reactive power compensation is tested it is connected to a power controlled AC/DC converter. The converter is connected to the connection point via a variable line impedance. The inductance of the line impedance varies between 0-0.5 mH sinusoidally with a frequency of 5 Hz. The resistance of the line impedance varies between 0.1-0.3 Ω and is repeated every 0.4 s. The reactive power compensation block is fed with; the inductance multiplied with the angular frequency of the AC grid, the measured d- and q-currents and also the reactive power reference. The desired reactive power to be consumed from the grid is set to zero. The active power consumed from/supplied to the grid is set to 30 kW, which corresponds to a load/generator depending on whether it consumes or supplies power. The load is set to switch between being a load and generator every 0.15 s. The load DC voltage is set to be 2 kV. The AC voltage in the connection point is regulated by a converter using open loop AC voltage control. The line impedance between the connection point and the AC voltage controlled converter is kept constant, with a resistance of 0.01 Ω and an inductance of 0.5 mH. The DC grid voltage is set to 2 kV.

Requirements of the reactive power compensation are:

- Current and voltage in the connection point should be aligned with the d-axis, when changing the characteristics of the line between load and connection point and when changing power consumed from and supplied to the grid.
- The connection point voltage amplitude and frequency should be kept, when changing power consumed from and supplied to the grid and when changing the characteristics of the line between load and connection point.
- The reactive power should be able to follow the continuous changes in reactive power reference sufficiently fast.
- The correct active power should be consumed from/supplied to the grid.

The control parameters of the simulation are listed in table 3.12 and the parameters of the power converter are shown in table 3.13.

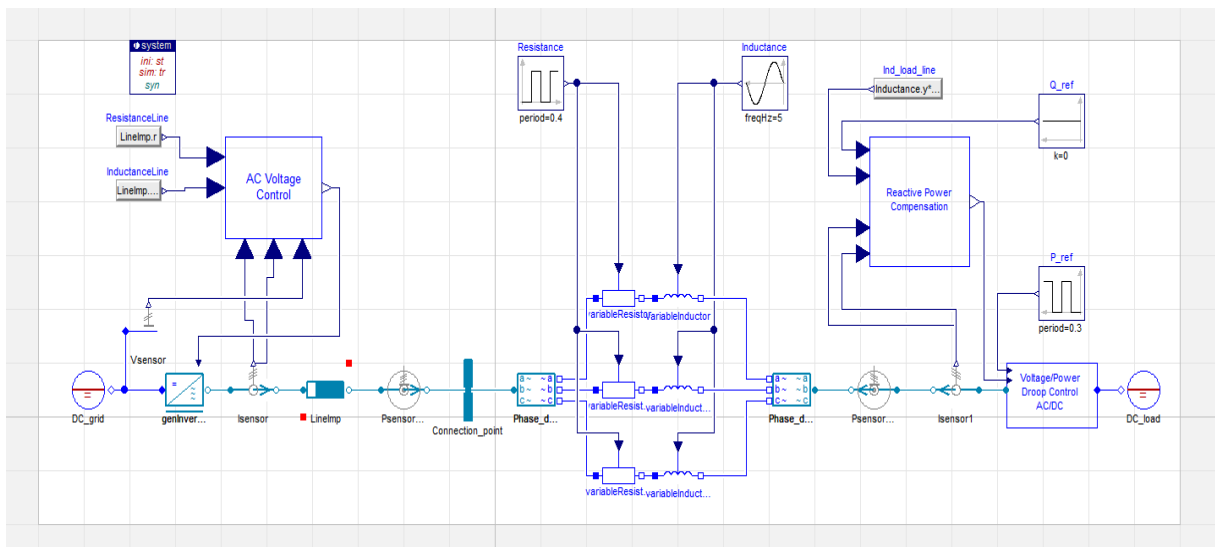


Figure 3.44 The test bench using power compensation for the power controlled AC/DC inverter.

Active Power Gain	Active Power Integral Gain	Reactive Power Gain	Reactive Power Integral Gain	d-current Gain	q-current Gain
$K_{AP}=0.0005$	$T_{AP}=0.001$	$K_{RP}= -0.00001$	$T_{AP}= 0.00005$	$K_{id}= 500$	$K_{iq}= 500$

Table 3.12 The control parameters of the power controlled converter in the test bench.

Inverter inductance	Inverter resistance	DC-link capacitor
$L = 15.9 \text{ mH}$	$R = 0.00005 \Omega$	$C = 0.1 \text{ mF}$

Table 3.13 The system parameters of the power controlled converter in the test bench.

In figure 3.45 the active and reactive power regulation results are shown. In figure 3.46 the alignment of the voltage and current vectors towards the d-axis is shown. Note that the current vector is dependent on the power flow direction. In figure 3.47 the phase peak voltages in the connection point are shown.

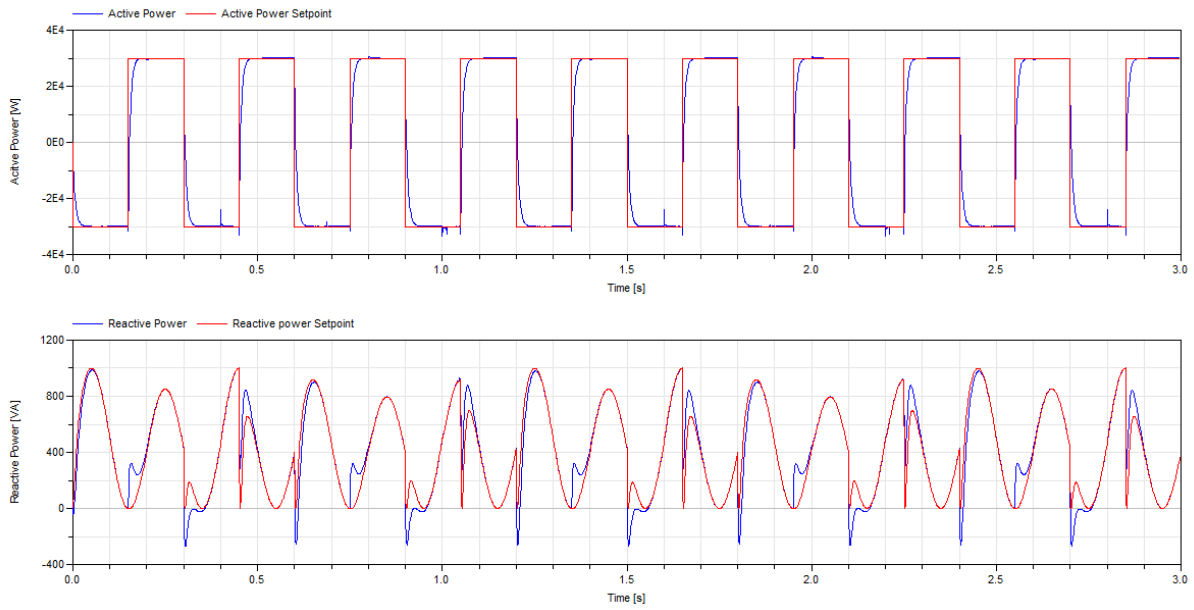


Figure 3.45 The performance of the active (top graph) and reactive (bottom graph) power regulation.

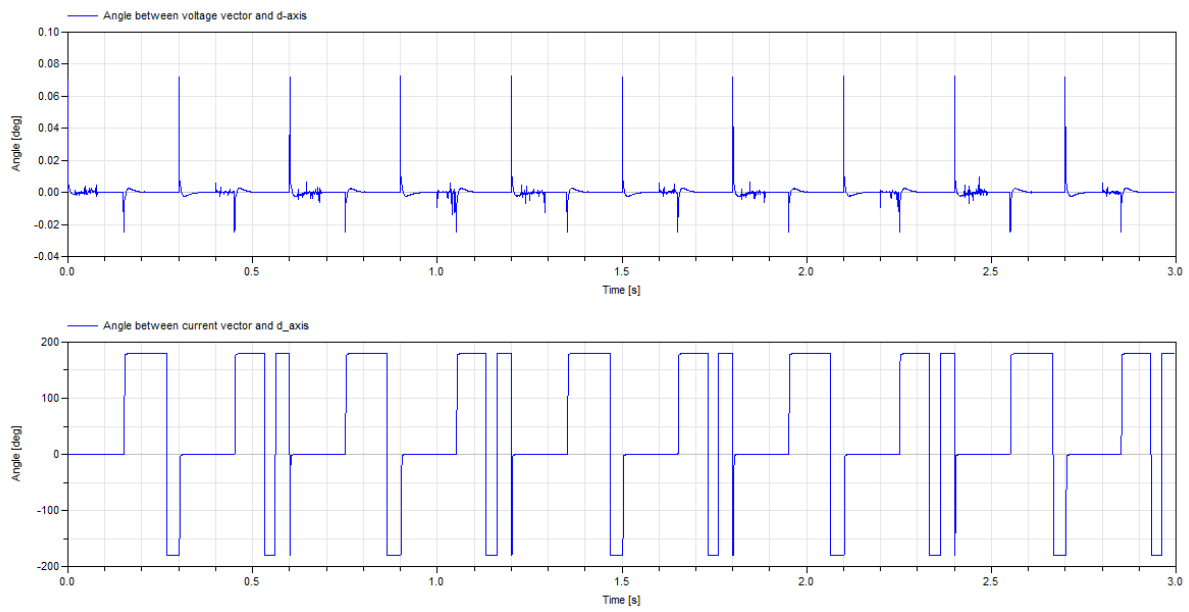


Figure 3.46 The alignment of the current (bottom graph) and voltage (top graph) vector towards the d-axis.

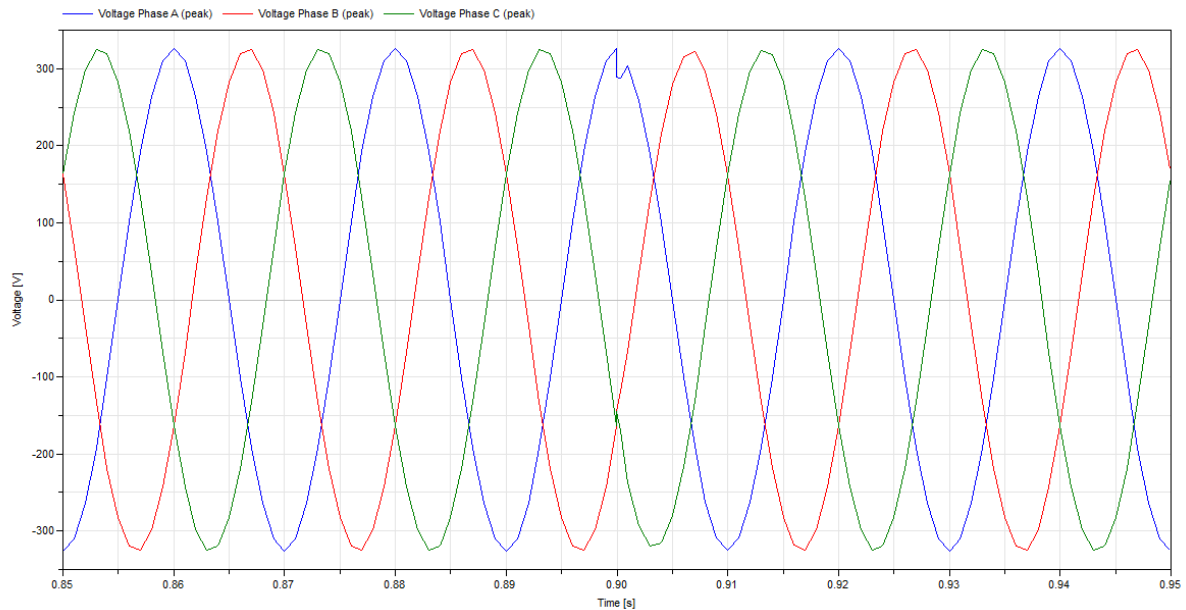


Figure 3.47 The instantaneous phase voltages in the connection point.

3.7.3 DISCUSSION

A study of the previous results shows that:

- The current and voltage vectors are aligned with the d-axis in the connection point at all times as seen in figure 3.46. The current vector is aligned with the d-axis but is either positive or negative depending on the power flow direction. The current angle switches between 180 degrees or -180 degrees phase shift as it can be seen in figure 3.46, which corresponds to the same direction in the dq-frame. The spikes seen in the voltage vector angle is due to the changes in the resistance of the line between the load and the connection point, and also when the load changes from consuming to generating power. Since the current will rapidly change when this happens the AC voltage regulator needs to apply a different voltage in order to keep the voltage vector aligned with the d-axis. The reaction is nearly immediate which is desirable. The spikes are however not considerably large and only shift the voltage vector 0.07 degrees momentarily.
- Figure 3.47 shows the phase voltages amplitude (peak) and frequency. From this figure it is possible to conclude that the voltage amplitude and frequency is kept constant throughout the simulation. The voltage amplitude is affected when changing the load properties and it stabilizes in the same manner as the angle of the voltage vector.
- The reactive power follows the reactive power reference well and is mainly affect by the sudden changes in active power as seen in figure 3.45. The reason for this is that the reactive power compensation block uses the d-current component as an input when calculating compensation action. Since the d-current changes when the active power controller tries to reach its reference value, the performance of the reactive power controller is limited by the performance of the active power controller. The active power controller reaches its reference value in 0.03 s which is very fast.
- The active power controller is able to reach its desired value sufficiently fast and without any overshoot as can be seen in figure 3.45.

4 MODEL FLEXIBILITY

The purpose of this thesis is to have flexible models which can operate in different control modes and in different power levels. By doing this a flexible grid can be developed, which can be modified in order to work in different applications where the voltage levels of the internal grid and the power flowing in the grid are arbitrary. In chapter 3, the different control modes in which the power electronic units can operate are described. In order to make a flexible converter model these regulation loops have to be fitted into a single converter model where the type of control and voltage level are chosen through the GUI. The grid and converter models must also be able to work with models from other libraries in order to keep the flexibility and practicality of the developed models.

To fulfill these requirements the multi-controlled converter is developed. The Multi Controller is done for the Time Average AC/DC converter models. The DC/DC converter is only implemented with power control; hence no switching between different control-modes is needed and is kept as described in chapter 3.3. The Multi Controller is only implemented in the Time Average converter models since longer simulations could be done with these models within a reasonable period of time. Further work can be done in order to implement the multi-control strategy into the switched models as well. The multi-control implementation is described in chapter 4.1.

The Multi Controller and the power controlled DC/DC converter uses records for their control and system parameters. The record is used to easily change the parameters of the model to fit the power level that is to be simulated. The records will be described in chapter 4.2.

4.1 MULTI CONTROLLER

The Multi Controller model is shown in figure 4.1 and its structure is similar to that of the controllers described for the AC/DC converters in chapter 3. The model differs somewhat in order to include all the features. The reactive-power-compensation block is located outside the control block since the compensation modifies the reactive power reference. The compensation block is only active if an inductive line is present between the Converter and the connection point of the AC grid. This is done by setting the parameter “inductiveLine” to true in the GUI and has to be done manually by the user. The same rule applies for the input of the line inductance called “Ind_Line1” in figure 4.1. This input has an additional condition since the line inductance is also used in the open loop AC voltage control. The latter condition is also used for the input “R_Line1” which is the resistance of the line. The line impedance inputs are connected to a switch block which simply sets the inputs to the control block to zero when open loop AC voltage control is not active. When the open loop AC voltage control is active the inductance of the inverter has to be neglected in order to create the correct voltage at the connection point of the internal AC grid. This is why there is a dummy inductor bypassing the converter inductance which has zero impedance. The dummy inductor is only active in open loop AC voltage control.

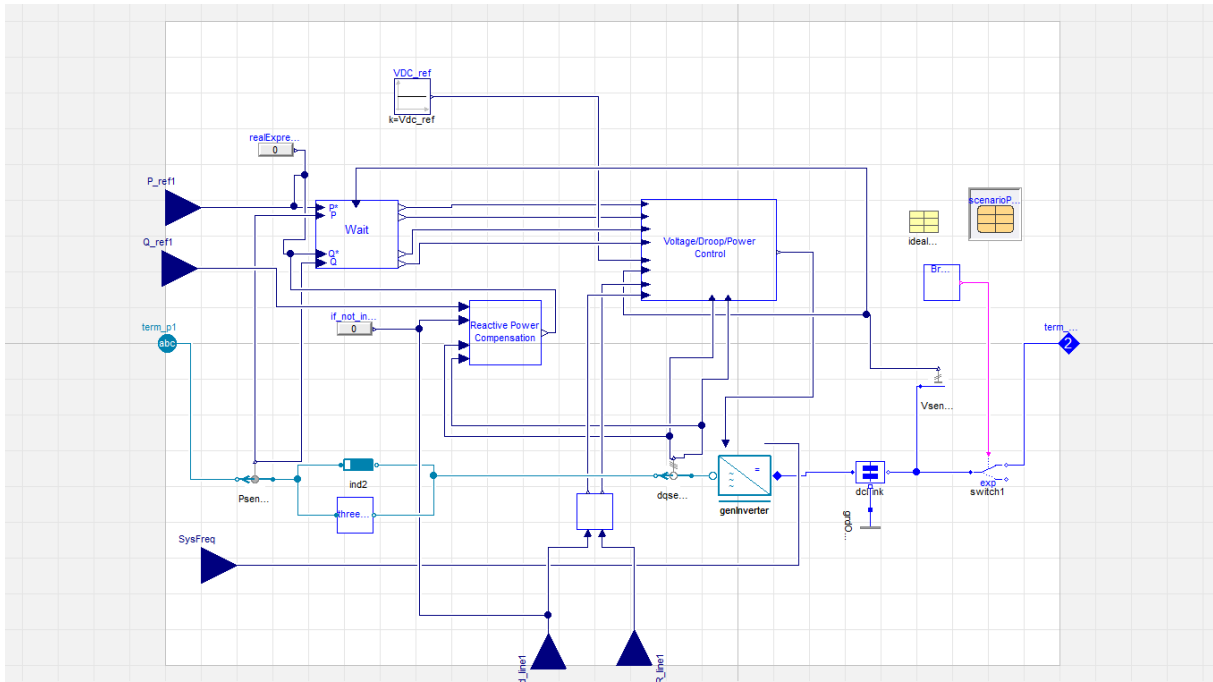


Figure 4.1 The Multi Controller that incorporate all control loops for the AC/DC converter implemented in Dymola.

The contents of the control block, seen in figure 4.1, can be studied in figure 4.2 where all the control functions related to the AC/DC converter described in chapter 3 are implemented. The droop, DC voltage and reactive/active power control are connected to a switch which feeds the current control with the appropriate current references. The switch keeps track of in which control mode the converter is, and outputs the current references corresponding to the control mode. The output of the current control is connected to yet another switch, which ensures that there is no conflict in the output to the modulator. It should be mentioned that the different control modes are chosen before the simulation and cannot be changed dynamically. The control mode is chosen through the GUI seen in figure 4.3. The Multi Controller will be used in different scenarios and control modes in chapter 5.

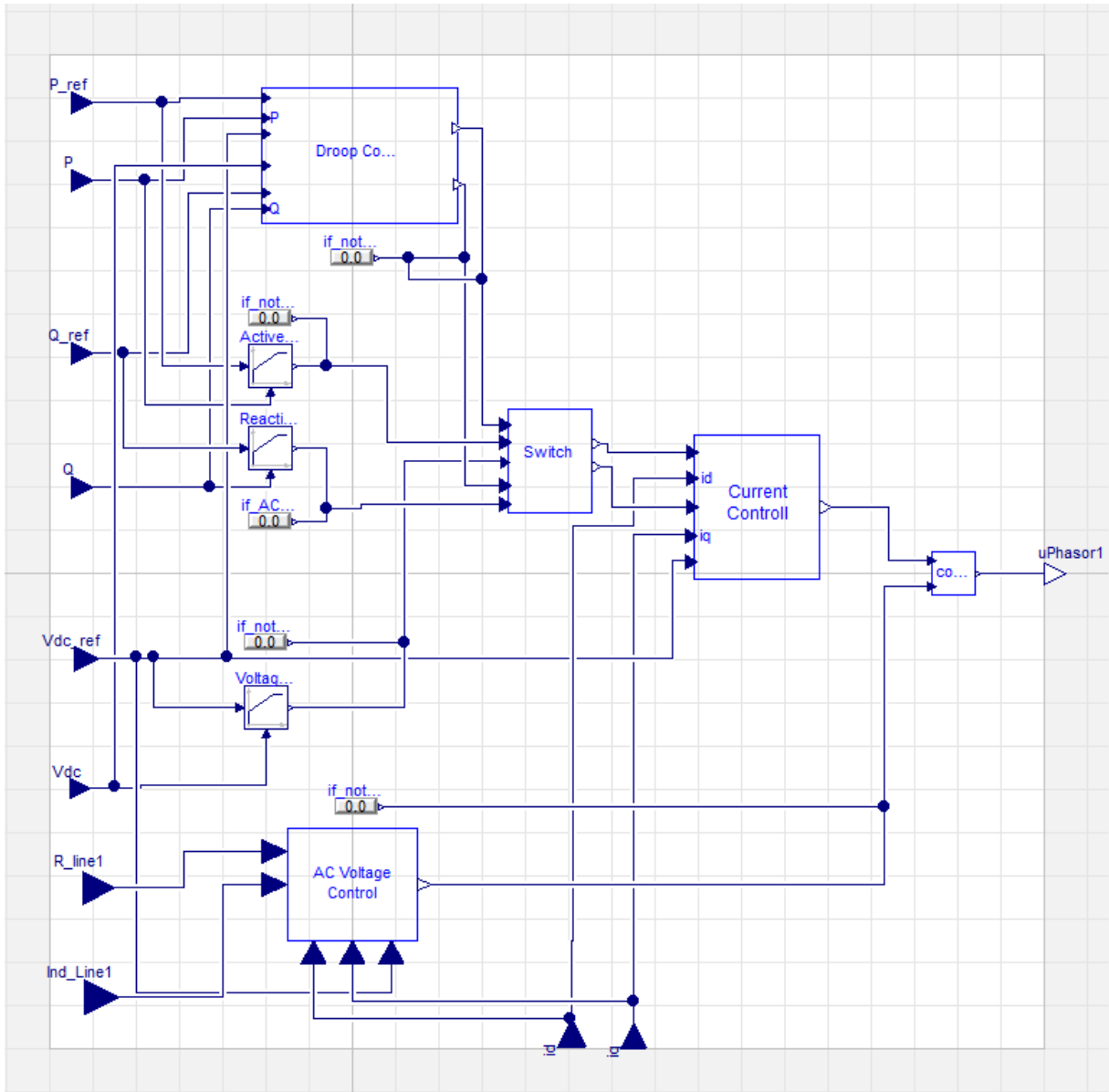


Figure 4.2 The content of the control block seen in figure 4.1.

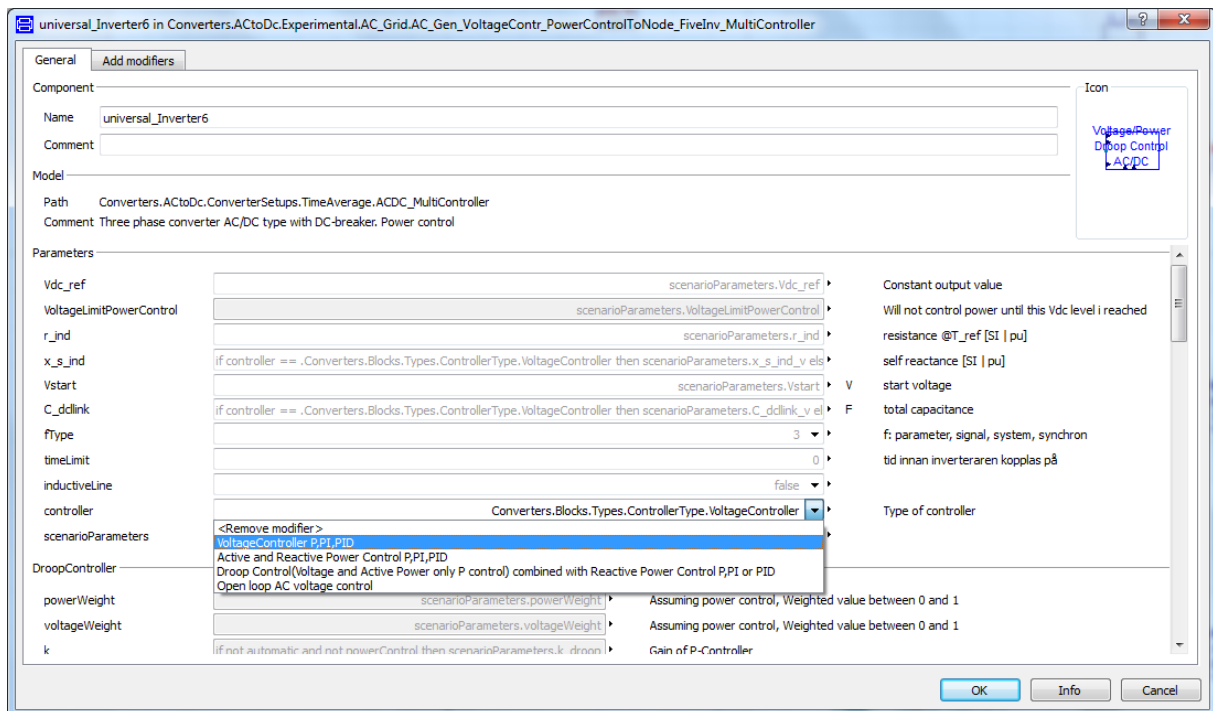


Figure 4.3 The different control modes that can be chosen in Multi Controller user interface.

4.2 RECORDS

A record is basically a list of variables (scenarioParameters in figure 4.1 and the Modelica code in Appendix D) where the values of the model parameters are stored and can be retrieved and copied into the corresponding parameter in the model. The record is a type of model that is placed inside the model where the parameters are implemented. Each parameter of the model then retrieves the corresponding parameter from the record by referring to the record and the name of the parameter in the record. To make the model flexible by using records a base record is create, where all the parameters are declared. Another record is then introduced which extends the base record, containing all the default parameters, and changes their value to suit the scenario at hand. The base record is placed in the model where the parameters are to be used. When using the model, suitable parameters for the scenario are applied through changing the record through a GUI as can be seen in figure 4.4.

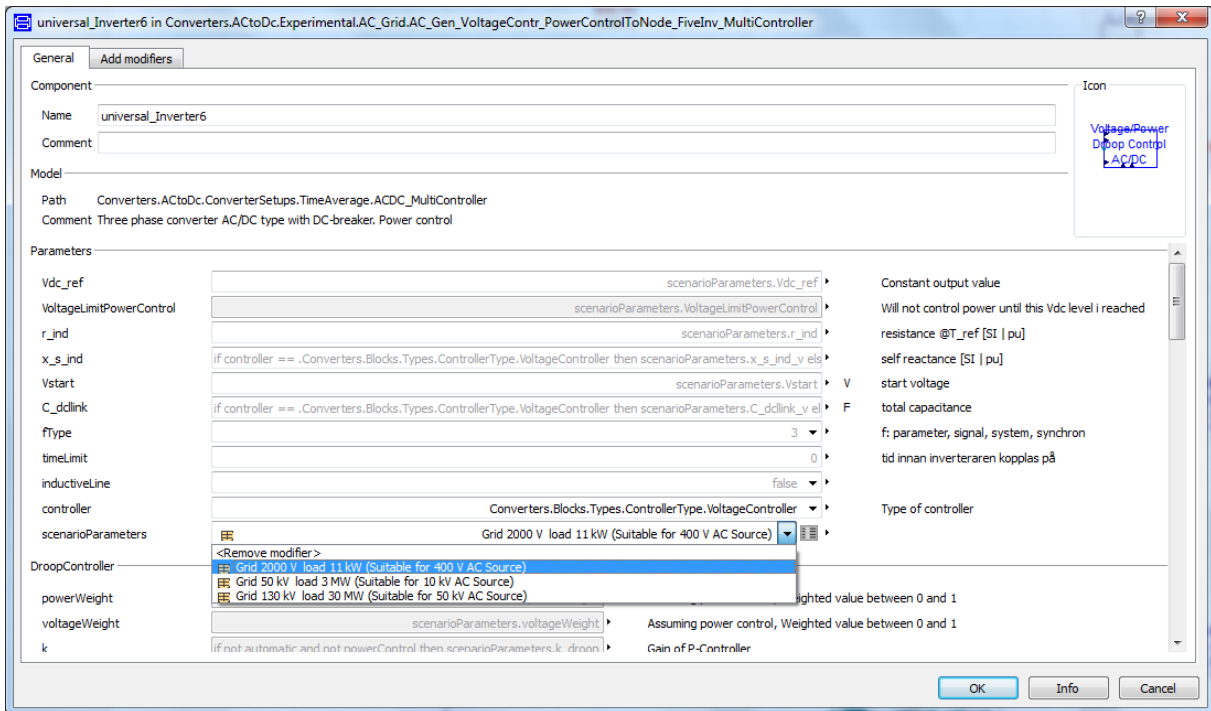


Figure 4.4 The different power levels that can be chosen.

5 GRID SETUPS

In this chapter the converters are connected to each other forming internal AC or DC grids. These grids operate on different power levels and in different formations. The grids are simulated in different scenarios. When doing this the properties of the cables should be accounted for. A short theory of the cables and the dimensioning of them are presented.

5.1 CABLE THEORY

5.1.1 AC CABLES

When an electrical grid is constructed it is obvious that lines for carrying the electricity are needed. The grid can be interconnected in several ways in this section deals mainly with the properties of the lines that are used for transportation of electricity.

The electrical properties of the lines are dependent on the material of which the line is constructed, the cross section of the line, length of the line and the orientation of the lines towards the other phase lines. The electrical properties that could be applied to the line are line resistance, inductance and capacitance. The resistance of the line is affected by the shape and length of the line, as well as the material of the line [7]. The inductance of the line is a result of the current flowing through the line. This current causes electromagnetic flux both in the line itself and around the line. Both these fluxes add to the inductance value of the line. Since the symmetrical three-phase AC grid has several lines placed side by side the flux from one line will affect the other lines [7]. In the same way as the inductance, the capacitance of the line is related to the orientation of the lines towards each other and the capacity of the lines [7].

The properties of the line are commonly represented in a so called π -equivalent circuit shown in appendix B and it is used in simulation applications electrical analysis. This circuit aims to generate a symmetrical distribution of the impedance throughout the line. When analyzing and simulating electrical power systems the capacitance of the line impedance is often neglected since it is small in comparison to the other impedance units. Therefore the line is only modeled with a resistance in series with an inductance.

5.1.2 INDUCTANCE DIMENSIONING IN A REALISTIC THREE PHASE AC GRID

When a conventional three phase transformer is short-circuited there is a parameter u_{cc} that describes the input voltage as a fraction of the nominal voltage V_N the transformer needs to be able to reach nominal current when short-circuited. In most cases the parameter u_{cc} is equal to 5 %, [15].

In this thesis three different transformer levels are used.

1: When the nominal voltage is $V_N = 230 V$ the rated power from the transformer S_N is set to 250 kW. The nominal current I_N is then given by:

$$I_N = \frac{S_N}{\sqrt{3} \cdot V_{LL}} = \frac{250 \text{ kW}}{\sqrt{3} \cdot 400} = 360.84 \text{ A} \quad (5.1)$$

A test condition for a short circuit is given by:

$$\omega \cdot L_{grid} \cdot I_N = u_{cc} \cdot V_N \leftrightarrow$$

$$L_{grid} = \frac{u_{cc} \cdot V_N}{\omega \cdot I_N} = \frac{0.05 \cdot 230 \cdot \sqrt{3} \cdot 400}{2\pi \cdot 50 \cdot 250 \cdot 10^3} = 101 \mu H \quad (5.2)$$

2: $V_{LL} = 10000 V \rightarrow V_N = 5733 V$ and the rated power is set to 10 MW:

$$I_N = \frac{S_N}{\sqrt{3} \cdot 10000} = \frac{10MW}{\sqrt{3} \cdot 10000} = 577 A \quad (5.3)$$

$$L_{grid} = \frac{u_{cc} \cdot V_N}{\omega \cdot I_N} = \frac{0.05 \cdot 5733 \cdot \sqrt{3} \cdot 10000}{2\pi \cdot 50 \cdot 10 \cdot 10^6} = 1.58 mH \quad (5.4)$$

3: $V_{LL} = 50000 V \rightarrow V_N = 28868 V$ and the rated power is set to 100 MW:

$$I_N = \frac{S_N}{\sqrt{3} \cdot 50000} = \frac{100MW}{\sqrt{3} \cdot 50000} = 577.4 A \quad (5.5)$$

$$L_{grid} = \frac{u_{cc} \cdot V_N}{\omega \cdot I_N} = \frac{0.05 \cdot 28868 \cdot \sqrt{3} \cdot 50000}{2\pi \cdot 50 \cdot 100 \cdot 10^6} = 3.97 mH \quad (5.6)$$

5.1.3 DC CABLES

The cables of the DC grid are mainly resistive and capacitive and in which extent depends on the length and size of the cable. In this thesis the cable capacitance will be neglected and the size of the resistance will be calculated according to [8]:

$$R = 0.01 \Omega/km$$

5.2 INTERNAL DC GRID

The introduction included examples of where and why internal DC grids could and should be used. Better controllability, lower energy losses, decoupling and filter costs have been mentioned. The structure of the DC grid depends on where it is implemented:

- High Voltage Direct Current (HVDC, 30 kV – 400 kV)
- Medium Voltage Direct Current (MVDC, 1500 V – 30 kV)
- Low Voltage Direct Current (LVDC, up to 1500 V)

HVDC grids are normally used when transferring power over long distances to reduce the power losses. It could be power transferred from e.g. large offshore wind power plants, hydro power plants, nuclear plants etc. and distributed all over the country. It could also be used in the other direction to supply power from the electricity network to off shore gas platforms [13].

MVDC grids could also be used to distribute power from producers to consumers but for shorter distances and on lower power levels. It can also be placed in industries to deliver power to electrical drive lines or it can be used on off shore wind power plants [13].

LVDC can be used as power supply to electrical cars or hybrid cars that are normally charged while connected to the utility grid. It can also be used in simple households that have their own energy production in terms of solar panels or wind power which provides the possibility to inject power into the utility grid [13].

5.2.1 BACK-TO-BACK CONVERTER AND MTDC GRIDS

The DC grid could consist of several converters connected (seen in figure 5.2) in parallel (MTDC) or it could be only two converters connected together. Regardless of the amount of devices, they are always connected in a Back- to- Back formation (see figure 5.1). There has to be at least one converter that is responsible for keeping a constant DC voltage level on the DC grid. The one controlling the DC voltage is called the master terminal and all other terminals controlling power to the different units are slave terminals. It is the master terminal that maintains the power flow balance in the DC grid. To avoid severe under or over DC Voltages, the slave controllers should be able to stabilize the DC voltage if the master for some reason is disconnected. That control method called droop control has been explained in chapter 3.5 [8].

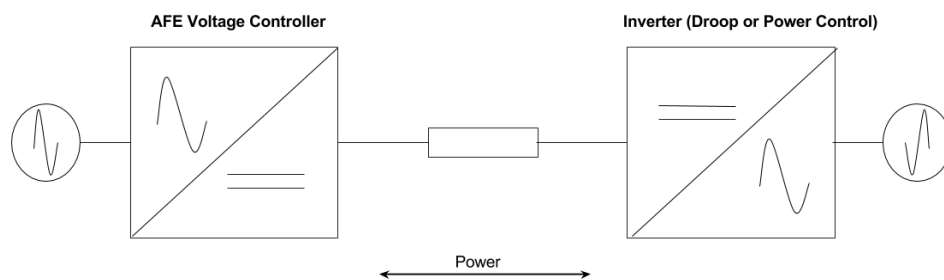


Figure 5.1 Two power electronic converters connected in a Back-to-Back configuration.

The AFE which has been mentioned earlier in the report (chapter 2.7) should provide sinusoidal grid currents without harmonics and at the same time be the master terminal i.e. responsible for keeping a constant DC voltage. The other power controllers are similar to the AFE in terms of structure and inner loop current control. This means that the slaves could also be connected to another part of the AC utility grid and provide sinusoidal current while controlling the active power flow instead. By having three phase converters connected in a Back-to Back formation power can be transferred in both directions. Depending on if it is a load or a source the required energy could be absorbed or produced power could be sent back to the utility grid.

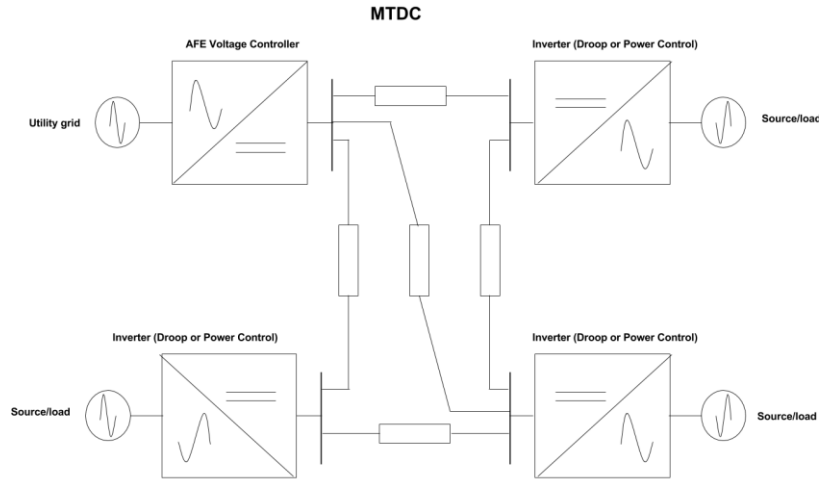


Figure 5.2 Illustration of a MTDC grid.

5.2.2 DYMOLA IMPLEMENTATION AND SIMULATION RESULTS OF DC GRIDS WITH SWITCHED CONVERTERS

Several different DC grid setups will be demonstrated. To provide a close up study of the behavior of the switched signals different scenarios of the switched DC grid will be simulated. Then different scenarios will be simulated using time average models to study the signals behavior over a longer period. The performance of the droop controllers will also be studied using time average models.

In all simulations the inductance corresponding to the three phase utility grid will be calculated according to the formulas provided in chapter 5.1.2. Other energy sources and loads will be modeled as a stiff three phase AC grids with a frequency of 50 Hz if nothing else is mentioned.

5.2.2.1 Simulation of the Back-to-Back converter

In the first test bench, seen in figure 5.3, the behavior of the Back-to-Back converter will be studied on a MVDC level of 2000 V. Here the AFE is connected to the three phase utility grid (400 V line-to-line). The AC/DC power controller is connected to another part of the same level of the AC grid, working both as a source and a load. The distance between the converters is around 1 km.

Since these converters have been tested already separately it has been proven that they can perform fast and accurate control. But the dynamics change when they are connected together and the test bench will show if the controllers work as intended. The reference for the active power controller is a ± 30 kW pulse with a period of 0.2 s. The current and power sensors are pointing towards the AC grids thus negative power is flowing towards the DC link. The control parameters are listed in table 5.1 and 5.2 and the system parameters are listed in table 5.3.

The requirements are:

- Power flow in both directions.
- $P_{in} = P_{ut}$ i.e. what comes out form one side of the grid must come out in the other (neglecting the losses).
- All controllers shall be fast and robust and keep their reference values.

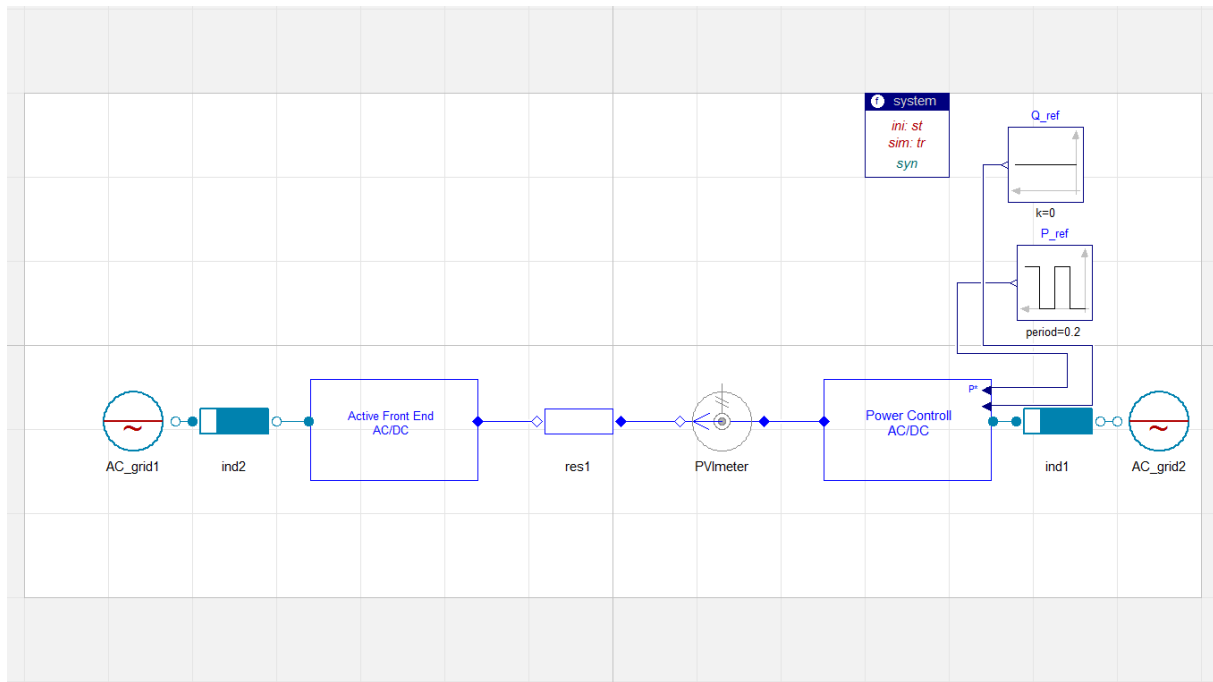


Figure 5.3 Test bench for the Back- to Back setup.

Active Power Gain	Active Power Integral Gain	Reactive Power Gain	Reactive Power Integral Gain	d-current Gain	q-current Gain
$K_{AP}=0.0005$	$T_{AP}=0.001$	$K_{RP}=-0.0001$	$T_{RP}=0.0001$	$K_{id}=5000$	$K_{iq}=5000$

Table 5.1 Power control parameters for the test bench.

Gain (Voltage)	Time constant (voltage)	Gain (d current)	Gain (q current)	Time constant (q current)
$K_V=-1$	$T_{iv}=0.01$	$K_{id}=5000$	$K_{iq}=100$	$T_{iq}=0.00001$

Table 5.2 Voltage control parameters for the test bench.

	Inductance	Resistance	DC-link capacitor
Power Controller	$L = 15.9 \text{ mH}$	$R = 0.00005 \Omega$	$C = 0.1 \text{ mF}$
AFE	$L = 6.4 \text{ mH}$	$R = 0.00005 \Omega$	$C = 0.8 \text{ mF}$
Grid	$L = 0.101 \text{ mH}$	$R = 0.00005 \Omega$	

Table 5.3 System parameters for the converters in the test bench.

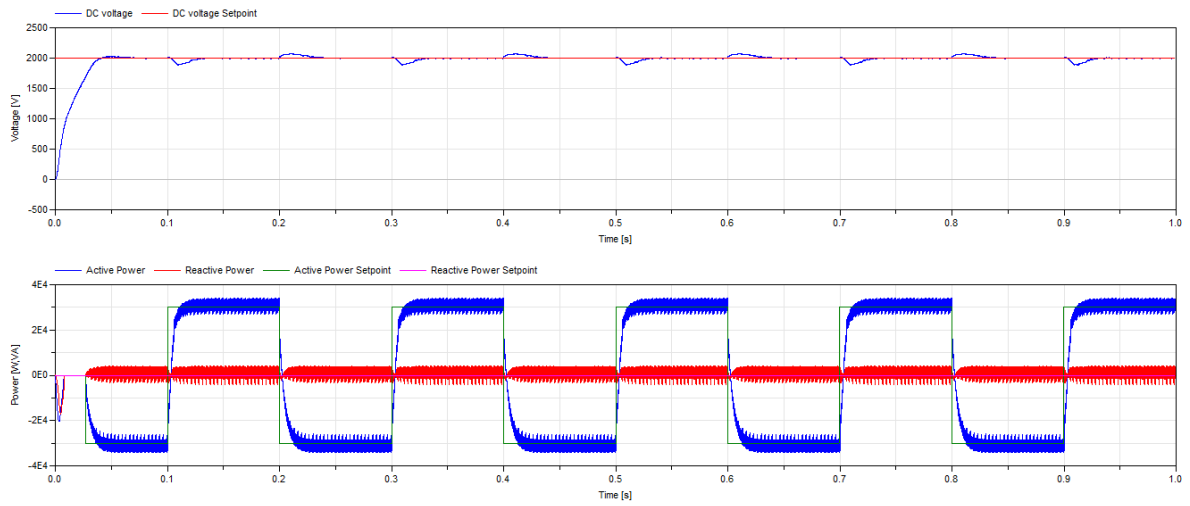


Figure 5.4 The DC link voltage (top graph), active power (bottom graph in blue) and reactive power (bottom graph in red) and references.

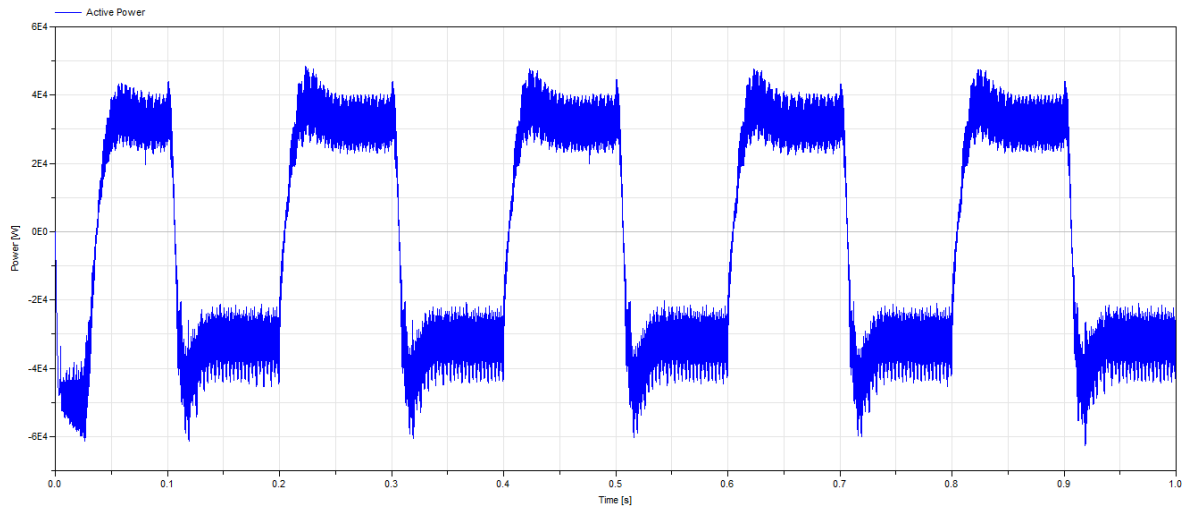


Figure 5.5 The active power on the AC side of the AFE DC voltage controller.

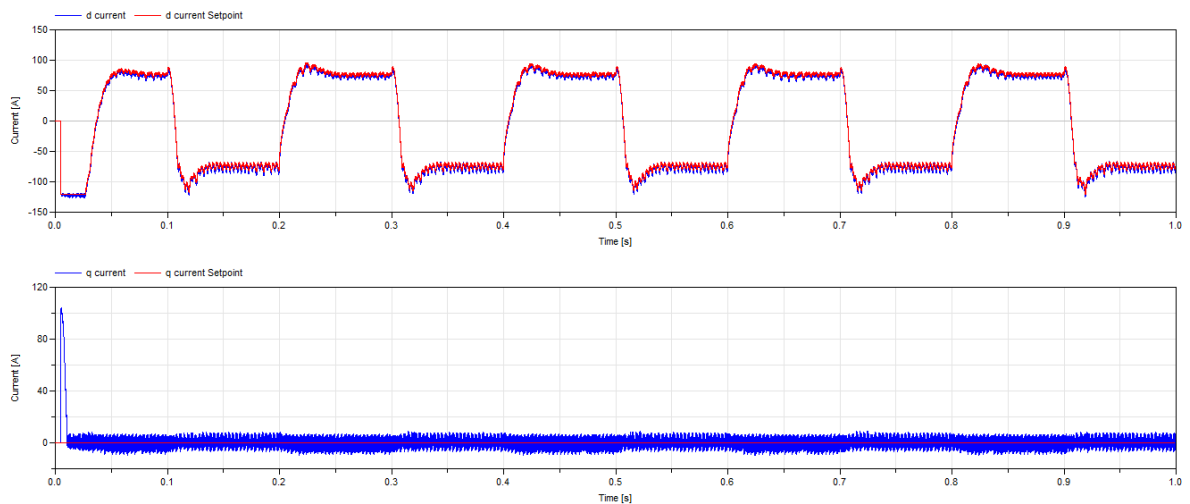


Figure 5.6 The top graph show the d-current control and the bottom graph shows q-current control used in the AFE.

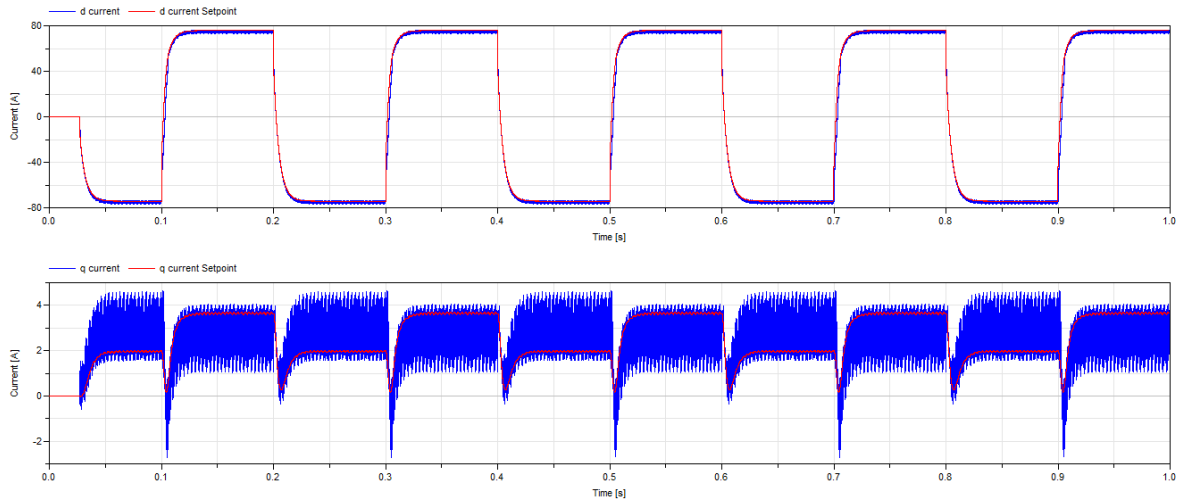


Figure 5.7 The top graph show the d-current control and the bottom graph shows q-current control used with the power controller.

5.2.2.2 Discussion

- From figure 5.4 and figure 5.5 it can be seen that $P_{in} = P_{out}$ when power is generated from the power controller to the DC link it flows out on the AC grid at the AFE side and vice versa.
- It can be seen in each figure that the controllers are reaching their reference values.

Studying the d current (figure 5.6) for the DC voltage controller it can be seen that it is a bit jumpy. This is due to the DC voltage controller. Since power is flowing in and out through the capacitors on the DC link the DC voltage fluctuates. Since the DC voltage controller tries to compensate for these fluctuations the d current reference changes all the time and the current controller follows the reference.

It can also be seen that the q current (figure 5.7) in the power controller is not zero, this is due to the grid inductance. Since it is the reactive reference that is zero it has to provide a small q current to ensure that no reactive power is drawn from the connection point. It can also be seen that active and reactive power are affecting each other (figure 5.4), when the active power increases the ripple of the reactive power increases. This is expected when studying equation 2.43 in chapter 2.7.3.4.

5.2.2.3 MTDC

In the following test benches MTDC grids will be simulated. Three different scenarios will be tested. The specifications of the scenarios are seen in table 5.4.

Note: Due to the switched system which causes a significant amount of computation time the simulations will be done just for a 1 s time span. All power and current sensors are pointing towards the three phase AC side i.e. positive power is generated to the AC grid. All control parameters can be seen in table C1 in appendix C.

	Scenario 1	Scenario 2	Scenario 3
DC voltage internal grid	1500 V	2000 V	50 kV
AC voltage amplitude (line-line) of main AC-grid, loads and generators	400 V	400 V	10 kV
Consumed power by loads	11 kW	80 kW	4.5 MW
Power supplied by generators	11 kW	0 kW	1 MW

Table 5.4 The specifications of the three scenarios.

The requirements for all three scenarios are:

- The starting voltage for the DC link should be zero and the DC link voltage shall reach the reference value in a few milliseconds.
- In steady state the DC link voltage should have a maximum ripple of less than 1 %.
- The controllers should react quickly to changes.
- No reactive power should be consumed in the connection point.
- The three phase grid current should be sinusoidal in steady state if possible.
- $P_{in} = P_{out}$ i.e. the power generated at one side of the grid must be consumed in other parts of the grid (neglecting the losses)
- If more power is produced than consumed the excess should be sent to the utility grid.

5.2.2.3.1 MTDC Scenario 1

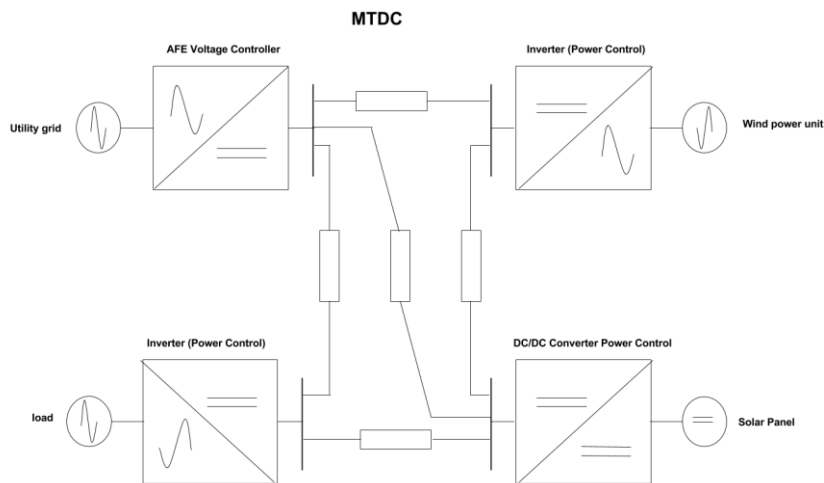


Figure 5.8 Scenario 1: MTDC for LVDC grid with an AFE DC voltage controller connected to the utility grid. DC voltage level is 1500 V. A wind power unit and solar panels are generating power of 11 kW and 2 kW. A load is connected to one of the converters consuming power between 1kW to 11 kW.

The grid structure can be seen in figure 5.8. The reference to the DC/DC controller is a sine wave which intends to resemble the sun coming and going. The wind power reference is also a sinus wave which should resemble the wind changes. The load is pulsing from 1 kW to 11 kW. The line resistances are set to $R = 0.01 \Omega$ which symbolizes a distance of 1 km between the converters. The Dymola implementation of this scenario is shown in figure 5.9.

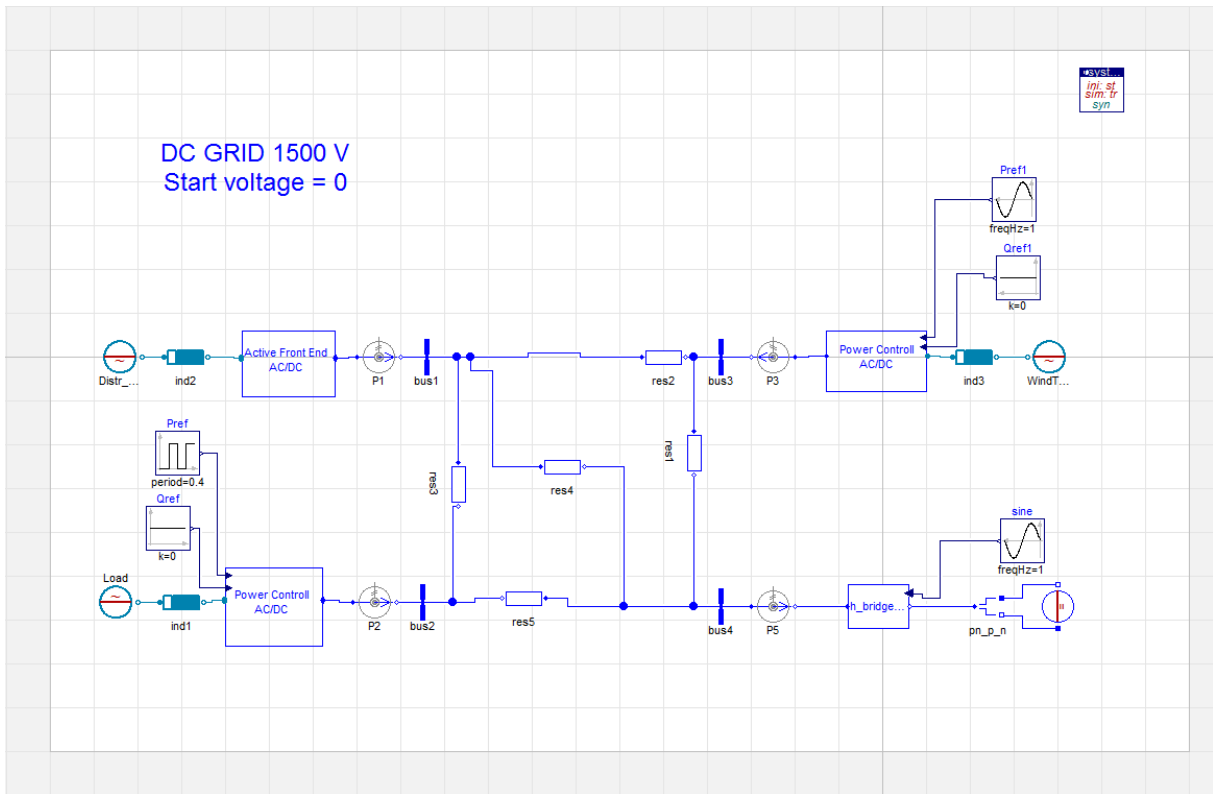


Figure 5.9 Dymola implementation of scenario 1.

The top figure in figure 5.10 shows the DC link voltage and in the bottom figure the d, q currents on the three phase AC grid are plotted. In Figure 5.11 the ripple of the DC link voltage can be seen and in Figure 5.12 and Figure 5.13 the power flow through each converter is shown. Figure 5.13 is also showing the AC grid current for phase A and an FFT analysis of the current harmonics.

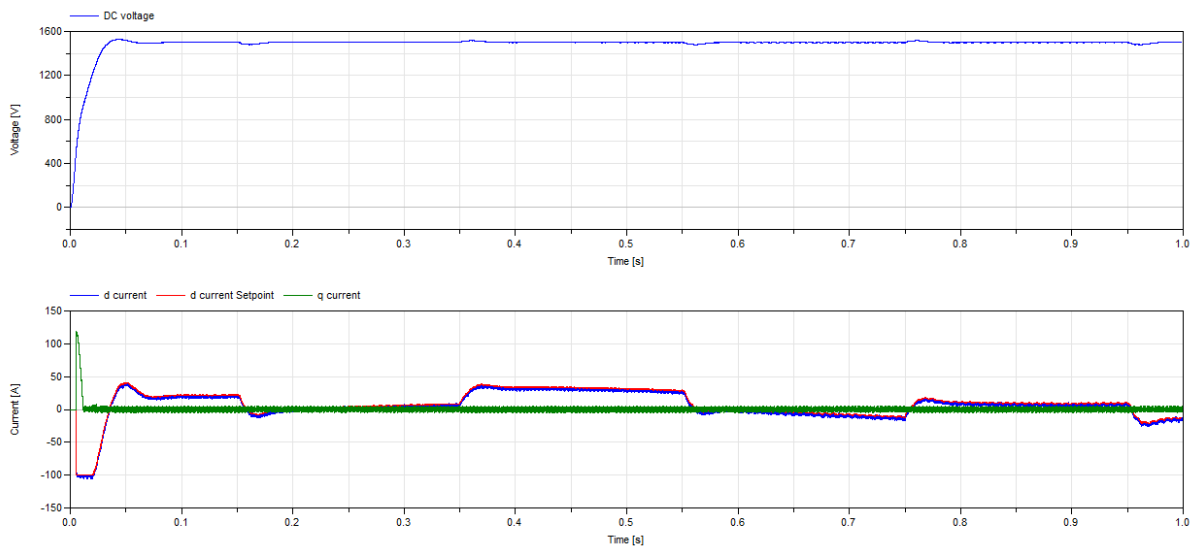


Figure 5.10 DC link voltage of 1500 V in the top figure and in the lower figure the d, q currents of the DC voltage controller can be seen.

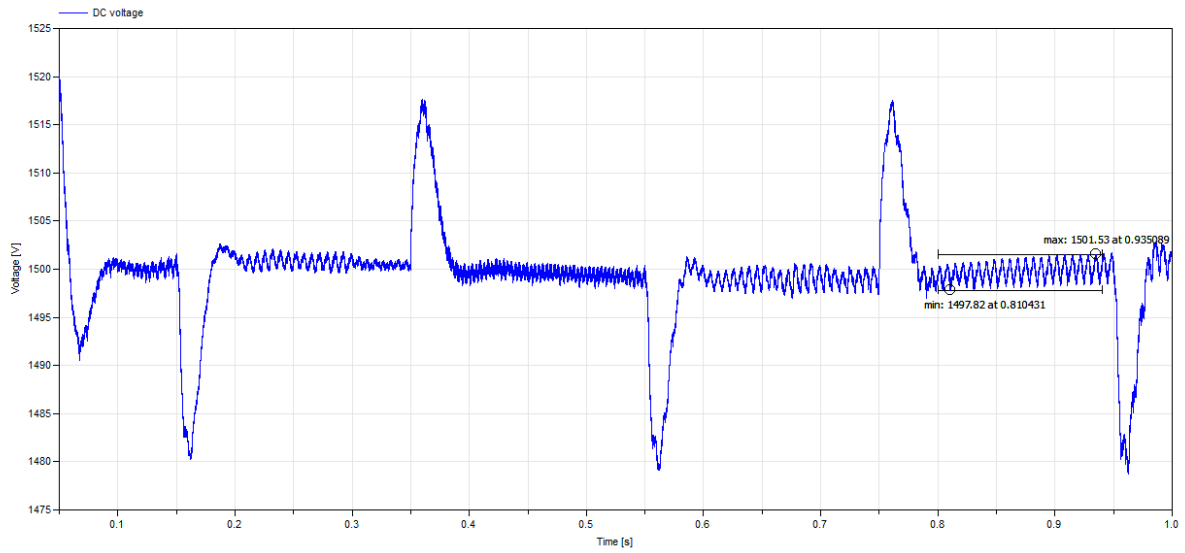


Figure 5.11 DC-link voltage in close up with minimum and maximum values of the ripple.

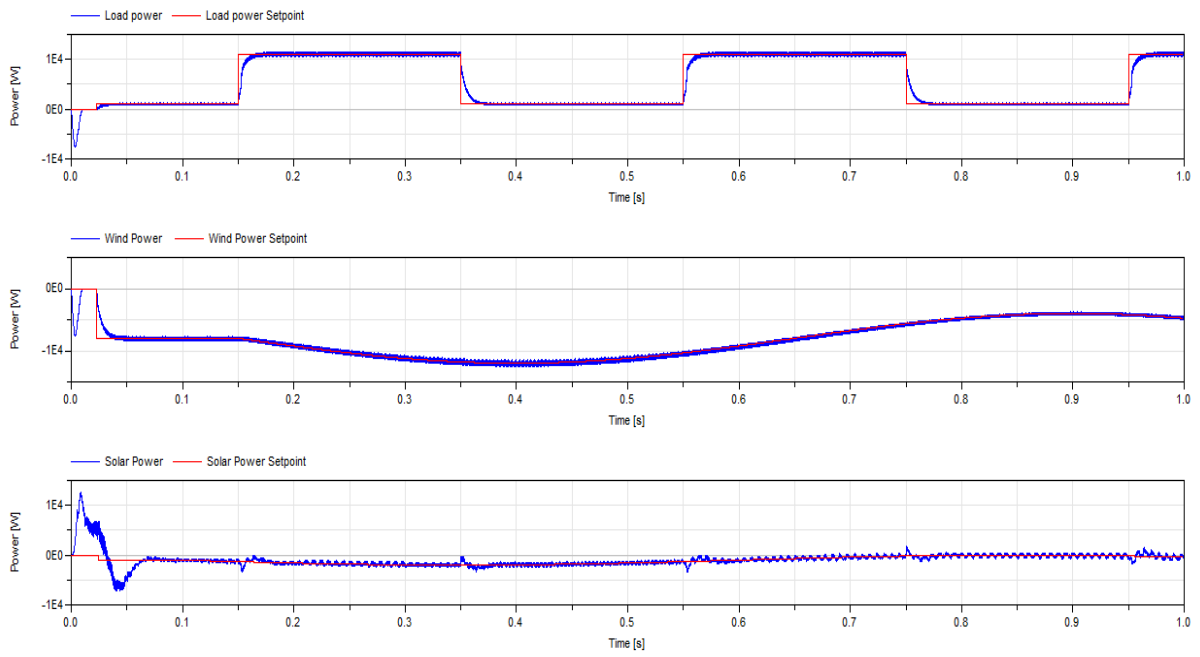


Figure 5.12 Produced and consumed power from the load, wind power unit and solar panel.

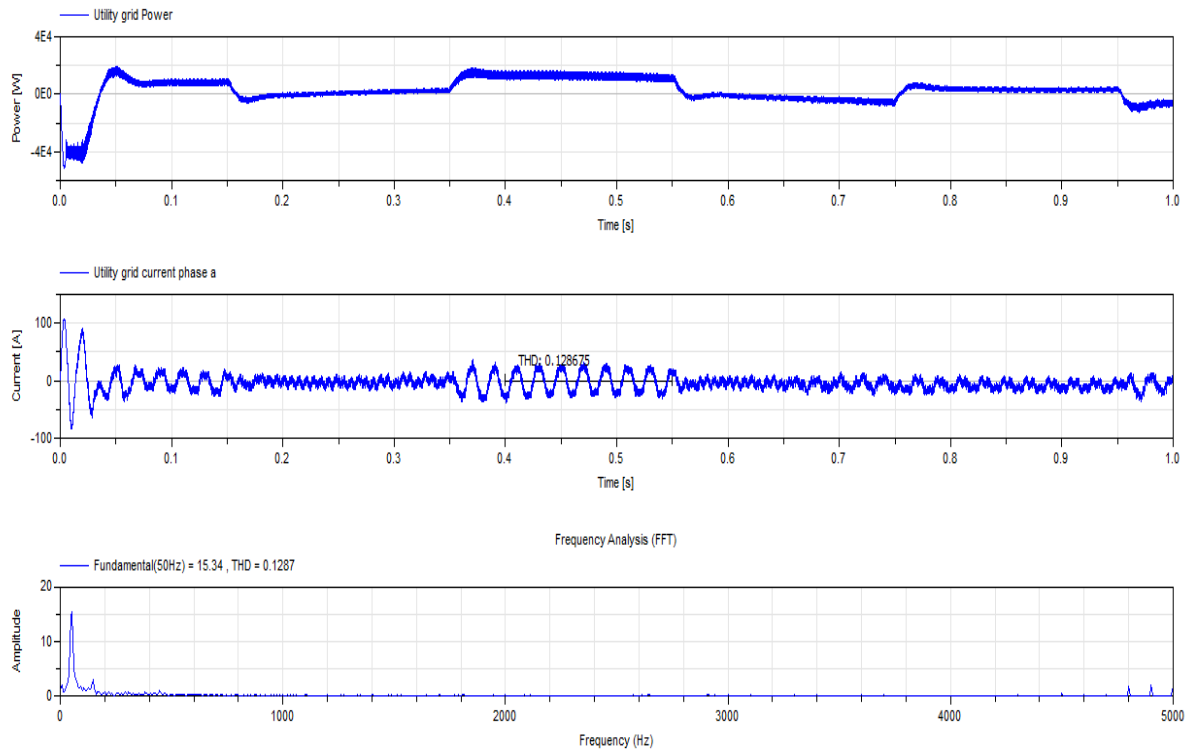


Figure 5.13 Top figures are showing the power and current (phase A) on the utility grid. The bottom figure is showing a FFT analysis of the current in phase a performed in the time interval 0.4-0.55 s.

5.2.2.3.2 Discussion

Comments to the requirements:

- The DC voltage reaches the reference in approximately 50 ms. It has a small overshoot but since the wind power is pushing power to the DC link at the same time it is within desirable limits. (See figure 5.10).
- The maximum ripple of the DC voltage in steady state is 0.247 % which is below the requirements (1 %). (See Figure 5.11)
- The DC voltage controller is fast and robust and responds quickly to changes when power is consumed or injected in the DC link. (See Figure 5.11)
- The power controllers for the load and wind power unit are reaching their references fast and accurate see Figure 5.12.
- The measured power in the DC/DC controller is jumpy but in average it is keeping the reference value.
- By studying the i_q current in Figure 5.10 it can be seen that it is controlled to zero which implies that no reactive power is drawn from the grid at the connection point.
- The AC current in phase A is only sinusoidal in the time interval 0.37-0.55 s. The current harmonics up to the 39th harmonic are plotted in Figure 5.13. Here it can be seen that all harmonics are not filtered.
- Studying the power flow in Figure 5.12 and Figure 5.13 it can be seen that when the produced power is exceeding the power consumed by the load the excessed injected in the utility grid.

According IEC 61000-3-2 (see appendix A) approved FFT analysis shall be performed after 10 s when the signals have reached steady state and it shall be performed during 1.5

seconds. In this simulation the power demand changes during the time of the analysis which has impacts on the FFT result. The reason why the current only is sinusoidal in a certain interval is due to the magnitude of the current and the DC link voltage controller. Small changes in the DC link voltage will have a significant effect in the current reference computed by the DC voltage controller. If the magnitude of the current is small then these changes will have a larger impact on the current amplitude which will change up and down creating a non-sinusoidal current.

The measured power in the DC/DC converter is a bit jumpy. The reason for this is that it is measured on the DC link where the power is flowing in and out of the capacitors.

5.2.2.3.3 MTDC Scenario 2:

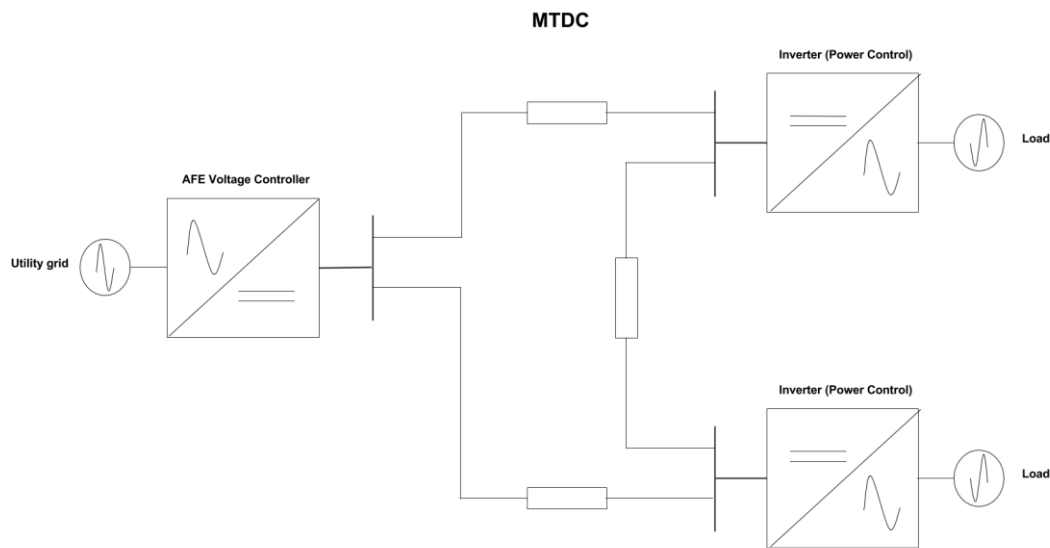


Figure 5.14 Scenario 2: MTDC for MVDC grid with an AFE controlling the DC voltage connected to the utility grid. DC voltage level is 2000 V. Two loads are connected to two of the converters consuming a total power of 80 kW. This could resemble an industry with an internal DC grid.

The second scenario is a MVDC grid with a DC link voltage of 2000 V. The setup is shown in figure 5.14 and could resemble an industry with an internal DC grid. Each load is pulsing from 30 kW to 40 kW i.e. the total power consumption is 80 kW. The line resistances are set to $R = 0.01 \Omega$ which symbolizes a distance of maximum 1 km between the converters. The Dymola implementation is shown in figure 5.15.

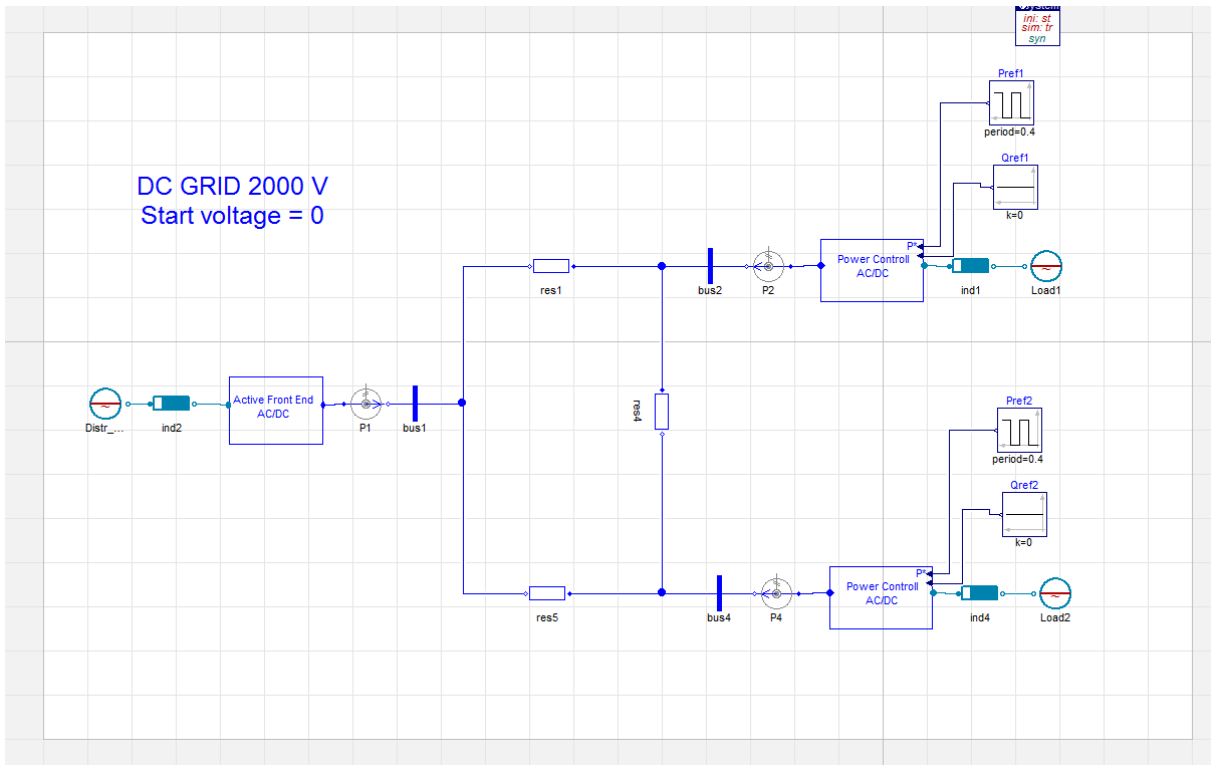


Figure 5.15 Dymola implementation of scenario 2.

The top figure in Figure 5.16 shows the DC link voltage and in the bottom figure the d, q currents on the three phase AC grid are plotted. In Figure 5.17 the ripple of the DC link voltage can be seen and in Figure 5.18 and Figure 5.19 the power flow through each converter is shown. Figure 5.19 is also showing the AC grid current for phase A.

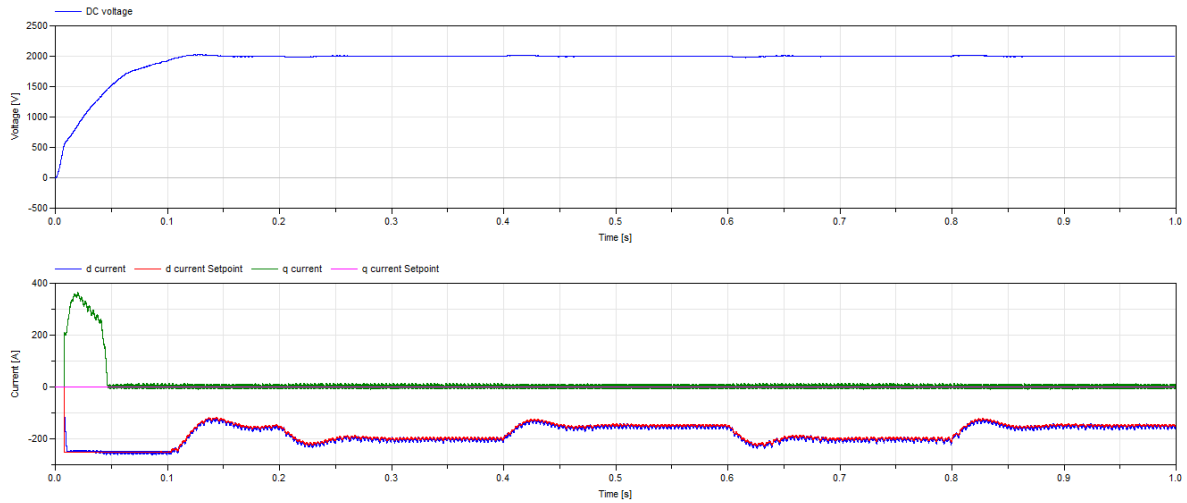


Figure 5.16 DC-link voltage of 2000 V in the top figure and in the lower figure the d, q currents of the DC voltage controller can be seen.

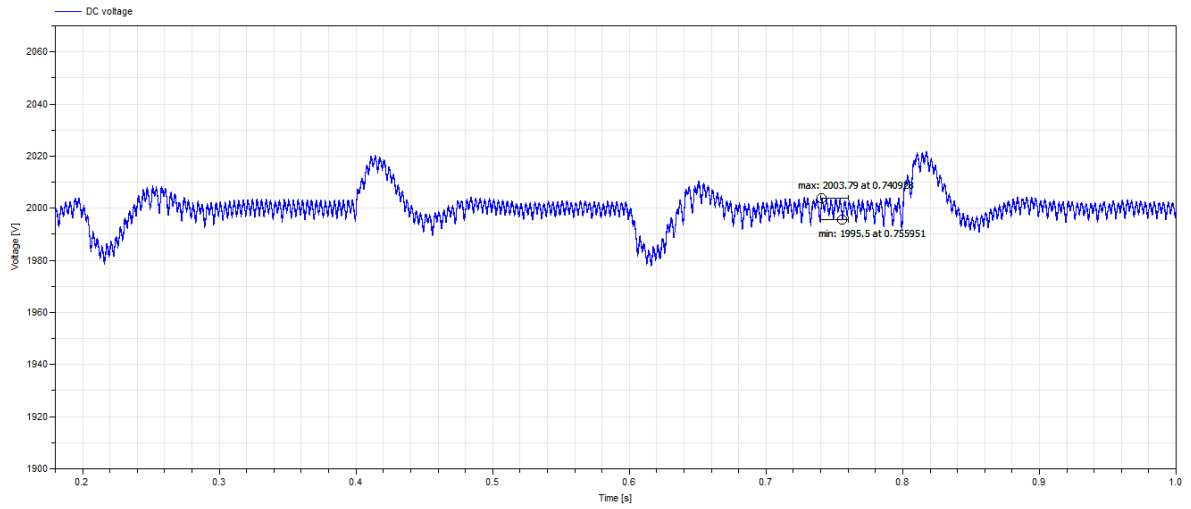


Figure 5.17 DC-link voltage in close up with minimum and maximum values of the ripple

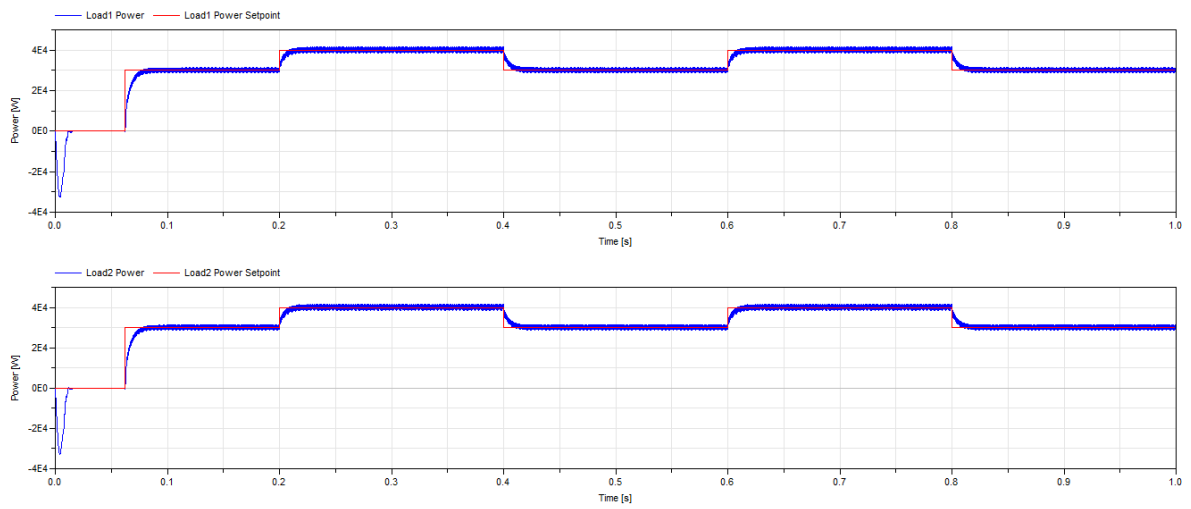


Figure 5.18 Produced and consumed power from the wind power unit and loads.

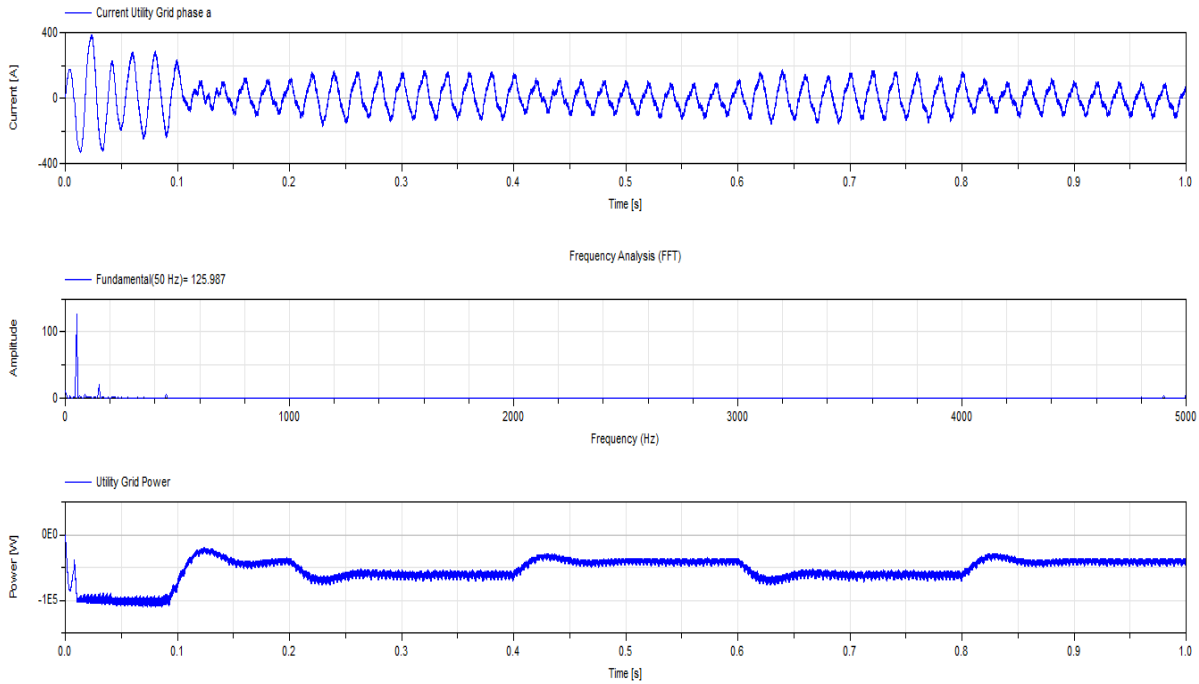


Figure 5.19 Top figures are showing the current (phase a) on the utility grid and a FFT analysis of the current in phase A performed in the time interval 0.25-0.39 s. The bottom figure is showing the power flow in the utility grid.

5.2.2.3.4 Discussion

Comments to the requirements:

- The DC voltage reaches the reference in approximately 150 ms which is reasonable. (See Figure 5.16).
- The maximum ripple of the DC voltage in steady state is 0.415 % which is below the requirements (1 %). (See Figure 5.17)
- The DC voltage controller is fast and robust and reacts quickly to changes when the power consumed by the loads is increased. (See Figure 5.17)
- The power controllers connected to the load and wind power units are reaching their references fast and accurately (see Figure 5.18).
- By studying the i_q current in Figure 5.16 it can be seen that it is controlled to zero which implies that no reactive power is drawn from the grid connection point.
- The AC current in phase A is almost sinusoidal. (see Figure 5.19)
- Studying the power flow in Figure 5.18 and Figure 5.19 it can be seen that consumed power of 80 kW is coming from the utility i.e. $P_{in} = P_{out}$.

The current in phase A looks quite good despite all the different dynamics in the system. A FFT analysis was made in the interval 0.25-0.39 seconds (see Figure 5.19) and it shows that there are harmonics especially of the 3rd order. But by studying figure A1 in appendix A it can be seen that the third order is $(\lambda \cdot 30) \%$ where λ is the power factor. Since the power factor is one the 3rd order harmonic can be 30 % of the fundamental. In this case it is 16.8 % which implies that for the small interval where the FFT was made the harmonics are filtered quite effectively. As mentioned in scenario 1 the analysis should be made for a longer steady state simulation however the obtained result is an indication that the AFE is working as intended.

5.2.2.3.5 MTDC Grid Scenario 3

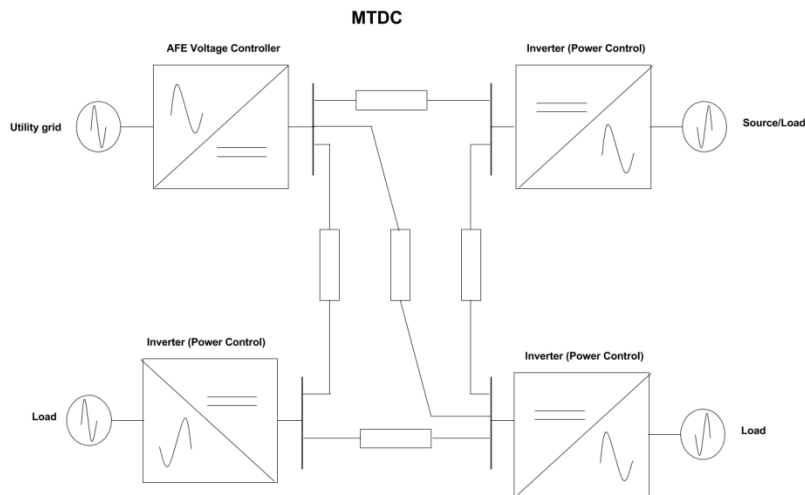


Figure 5.20 Scenario 3: MTDC for HVDC grid with an AFE controlling the DC voltage connected to the utility grid. DC voltage level is 50 kV. Three loads are connected to the power converters consuming a total power of 4MW. One of the loads is also regenerating 1 MW power. This could resemble a HVDC grid with one connection to the utility grid and different loads drawing and regenerating power

The third scenario is a HVDC grid with a DC link voltage of 50 kV. The setup is shown in figure 5.20. Three loads are connected to the power controlled converters consuming a total 4MW power. One of the loads is also regenerating power of 1 MW. The line resistances are set to $R = 0.1 \Omega$ which symbolizes a distance of maximum 10 km between the converters. The Dymola implementation is shown in figure 5.21.

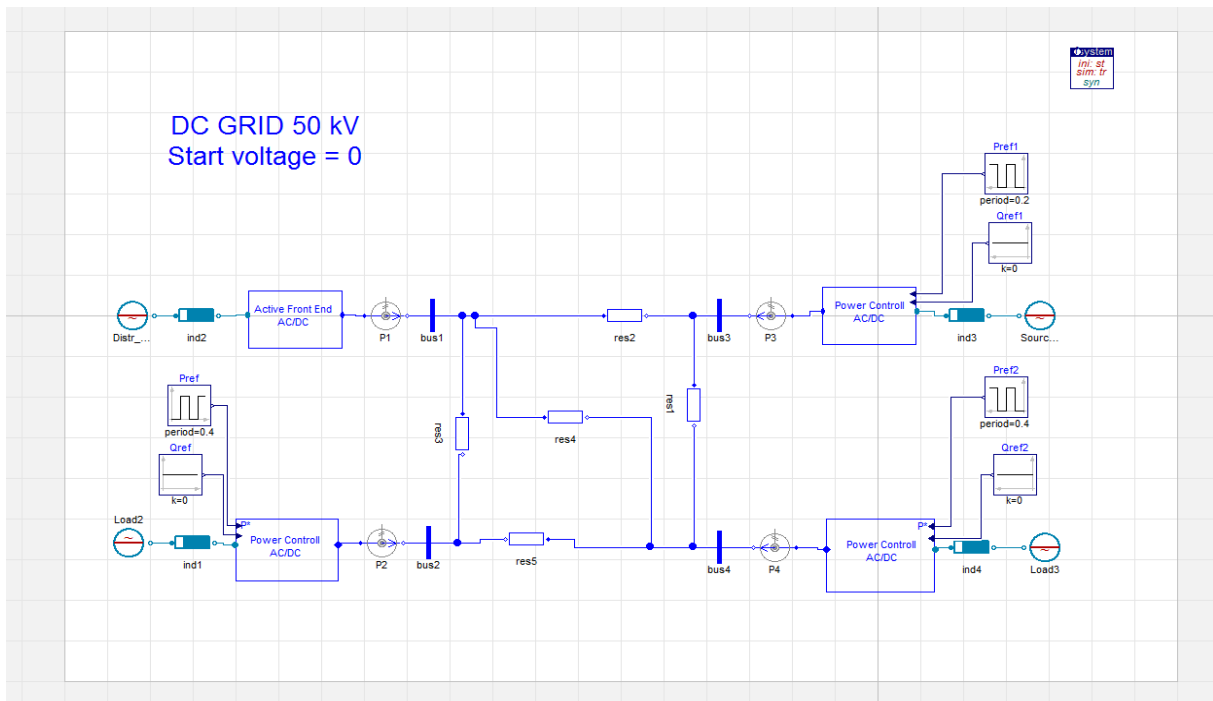


Figure 5.21 Dymola implementation of scenario 3.

The top figure in Figure 5.22 shows the DC link voltage and in the bottom figure the d, q currents on the three phase AC grid are plotted. In Figure 5.23 the ripple of the DC link voltage

can be seen and in Figure 5.24 and Figure 5.25 the power flow through each converter is shown. Figure 5.25 is also showing the AC grid current for phase A.

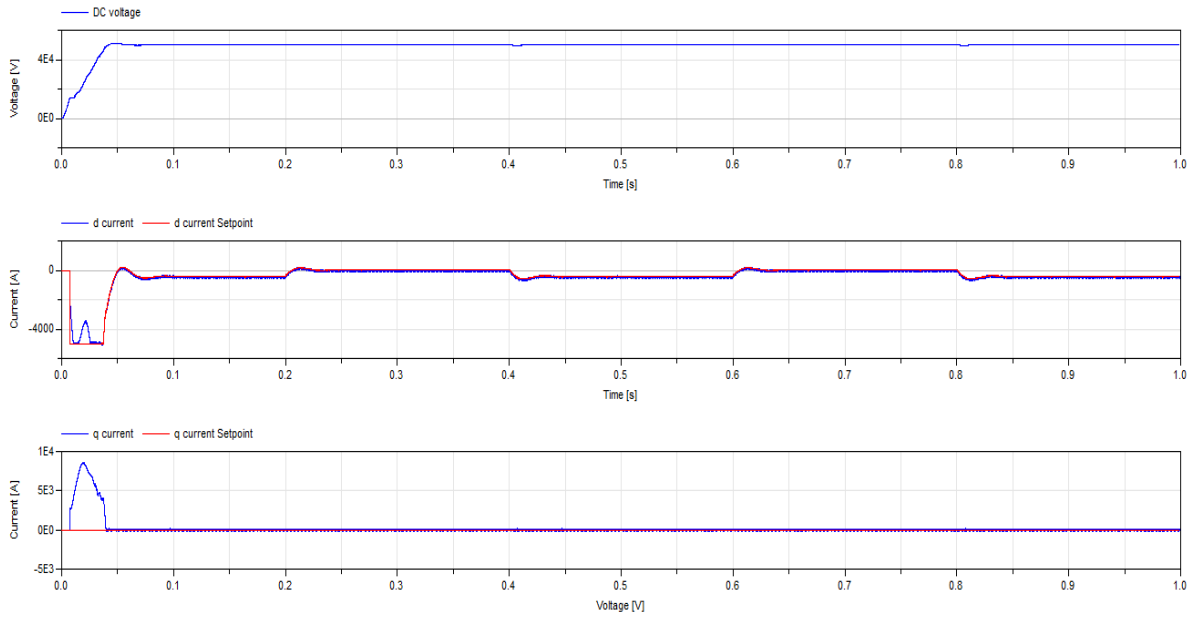


Figure 5.22 DC link voltage of 50 kV in the top figure and in the lower figures the d,q currents of the DC voltage controller can be seen.

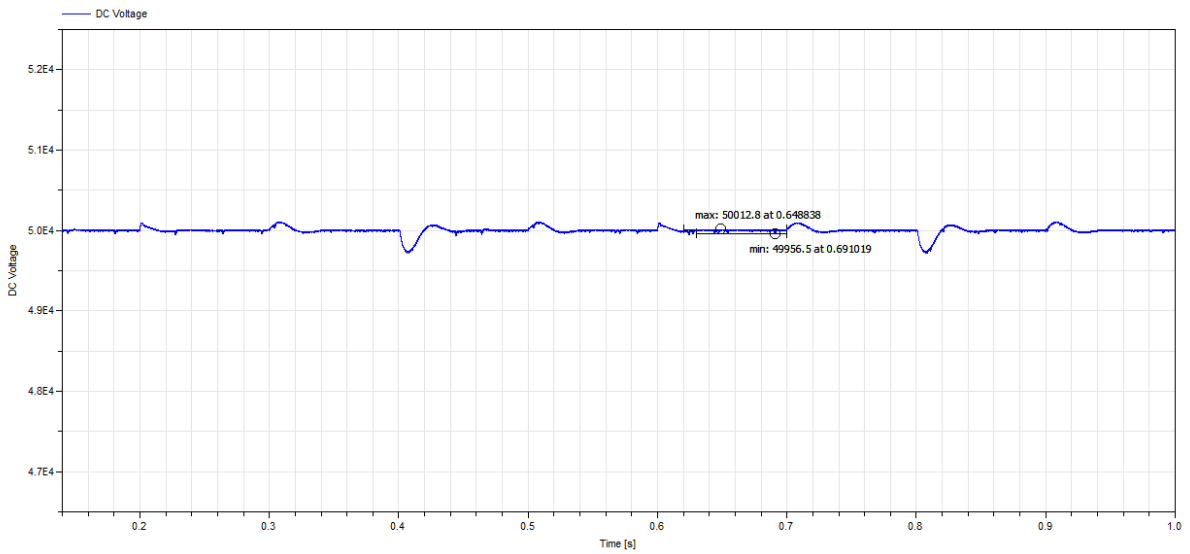


Figure 5.23 DC-link voltage in close up with minimum and maximum values of the ripple

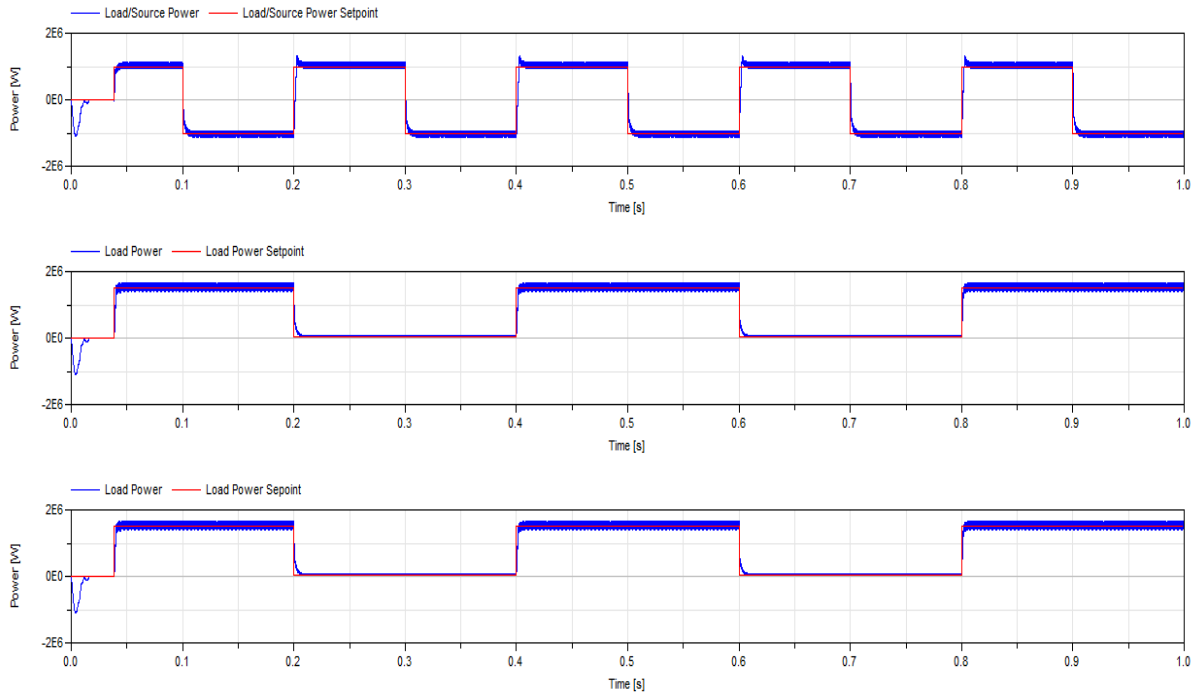


Figure 5.24 Consumed and produced power from the loads.

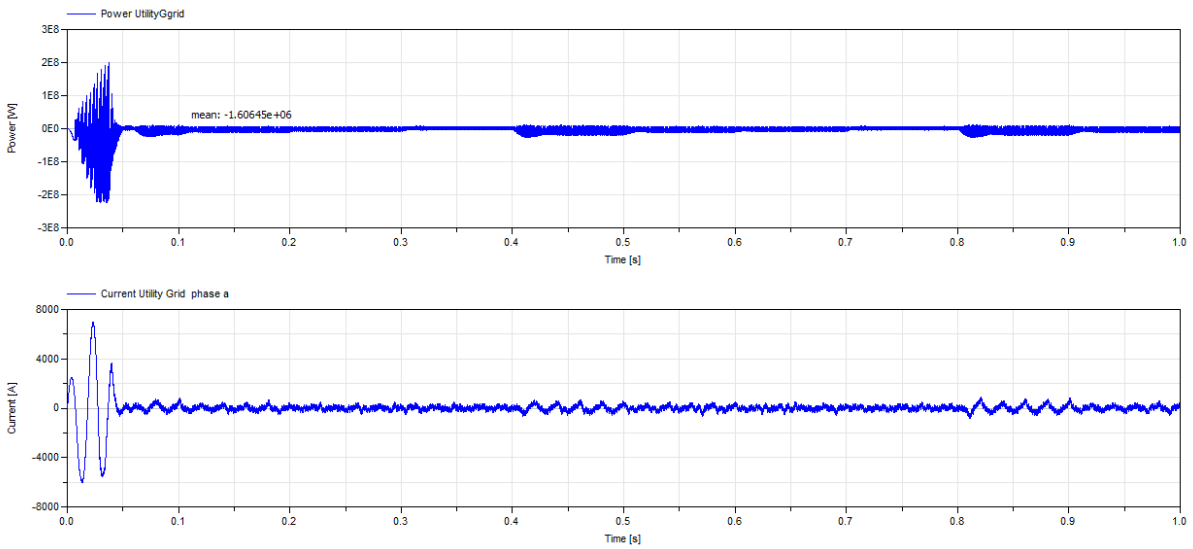


Figure 5.25 The figure is showing the power and phase A current on the three phase utility grid

5.2.2.3.6 Discussion

Comments to the requirements:

- The DC voltage reaches the reference in approximately 60 ms which is fast. (See Figure 5.22).
- The maximum ripple of the DC voltage in steady state is 0.13 % which is below the requirements (1 %). (See Figure 5.23)
- The DC voltage controller is fast and robust and reacts quickly to changes when power is produced and consumed by the loads. (See Figure 5.23)

- The power controllers connected to the loads are reaching their references fast and accurately see Figure 5.24.
- By studying the i_q current in Figure 5.22 it can be seen that it is controlled to zero which implies that no reactive power is drawn from the grid connection point.
- The AC current in phase A is not sinusoidal. (see Figure 5.25)
- Studying the power flow in Figure 5.24 and Figure 5.25 it is not easy to see that the relationship $P_{in} = P_{out}$ holds. The arithmetic mean value of the power flowing through the utility grid is -1.6 MW between 0.1 and 1 second. Studying Figure 5.24 it can be seen that the loads consume in average -1.5 MW which means that the power equation holds (neglecting losses).

The current in phase A is not sinusoidal. One of the reasons is already mentioned in scenario 1. Another pattern that has been noticed is that the current looks different depending whether the power is consumed or regenerated into the grid. When power is consumed the current looks better (see scenario 2). Scenario 3 could resemble a HVDC grid connected to a city where some of the inhabitants are producing energy locally. Of course it is not realistic to regenerate power in pulses of 1 MW but the simulations are done to stress the system and to see how it reacts on changes. Note that during startup the converters are not controlled since the transistors cannot operate when DC-link voltage is too low. Furthermore the capacitors on the DC-link have to be charged. This can be seen in first 0.03 s of the simulation.

5.3 DC GRID WITH WIND POWER AND SMART HOUSE LIBRARIES

To show that the created models of the converters and the grid structure can be connected to other libraries a new scenario is made in which a grid is implemented using the AC/DC converter with multi-control, the power controlled DC/DC converter and units from the Wind Power Library and the Smart Grid Library. These libraries were created in previous master theses and they have been developed in older versions of EPL [20][21]. These libraries use the time average converters already implemented in EPL and have implemented some additional features to them. Therefore the Time Average models created in this thesis are used when coupling to the external models. The models that are of interest in this thesis are alternating loads and wind power plants generating power according to wind speed input.

From the Smart Grid Library [20] a smart house model is used to represent a load. The smart house model is modified since the original smart house model included some generation. The generators are removed since the model is desired to be a purely alternating load and no generation should take place in the load. Also the loads inside the smart house model are set to consume a larger amount of power when active. An interface also needs to be created in order for the smart house model to be able to operate with symmetrical voltages. The voltage in the 2 kV DC-grid is -1 kV in the negative conductor and 1 kV in the positive connector resulting in 2 kV between the conductors. In the smart house model the negative conductor is grounded which means that the positive conductor should have 2 kV. The interface takes care of this problem moving the voltage to fit the demands of the smart house while maintaining power balance.

A wind power turbine model, from the Wind Power Library [21] is also used, together with a model generating wind speed. The wind power model is directly connected to the DC grid since inside the wind power plant model a power controlled AD/DC converter is already implemented. The power generated by the wind power plant is simply supplied to the DC grid.

5.3.1 DYMOLA IMPLEMENTATION OF THE DC GRID WITH EXTERNAL MODELS

The external models together with the models from this thesis are connected to form the grid shown in figure 5.26. As seen in figure 5.26 two wind turbines are connected to the DC grid and one smart house model is connected to the grid. The wind turbines have an installed capacity of 4 kW each. The AC distribution grid is connected to the DC grid through an AC/DC converter set to DC voltage control, which keeps the DC voltage of the DC grid to 2 kV. The AC distribution grid is represented by an AC source operating in 50Hz and 400 V line-line. Additionally a solar power plant is connected to the DC grid through a power controlled DC/DC converter. The solar power plant is represented by a DC source with voltage 100 V. The power generated by the solar plant varies sinusoidally between 0-2 kW with frequency 0.04 Hz. The lines are modeled with resistances set to 0.01 Ω representing a distance of 1 km or less. The inductance in the AC three phase grid is calculated according to equation 5.2 in chapter 5.1.2. The parameters for the AC/DC and DC/DC converters are listed in table C2 in appendix C. Note that all power sensors are oriented with reference power direction towards the DC grid except the power sensor connected the load.

Requirements for the simulation are:

- The models from different libraries should be able to work together.
- The voltage of the internal DC grid voltage should be kept constant when changing the load characteristics and with varying power supply.

- The power supplied should be consumed by the load when load is active.
- The residual power should be fed to the AC distribution grid.
- The AC distribution grid supplies power when the local generation is insufficient.

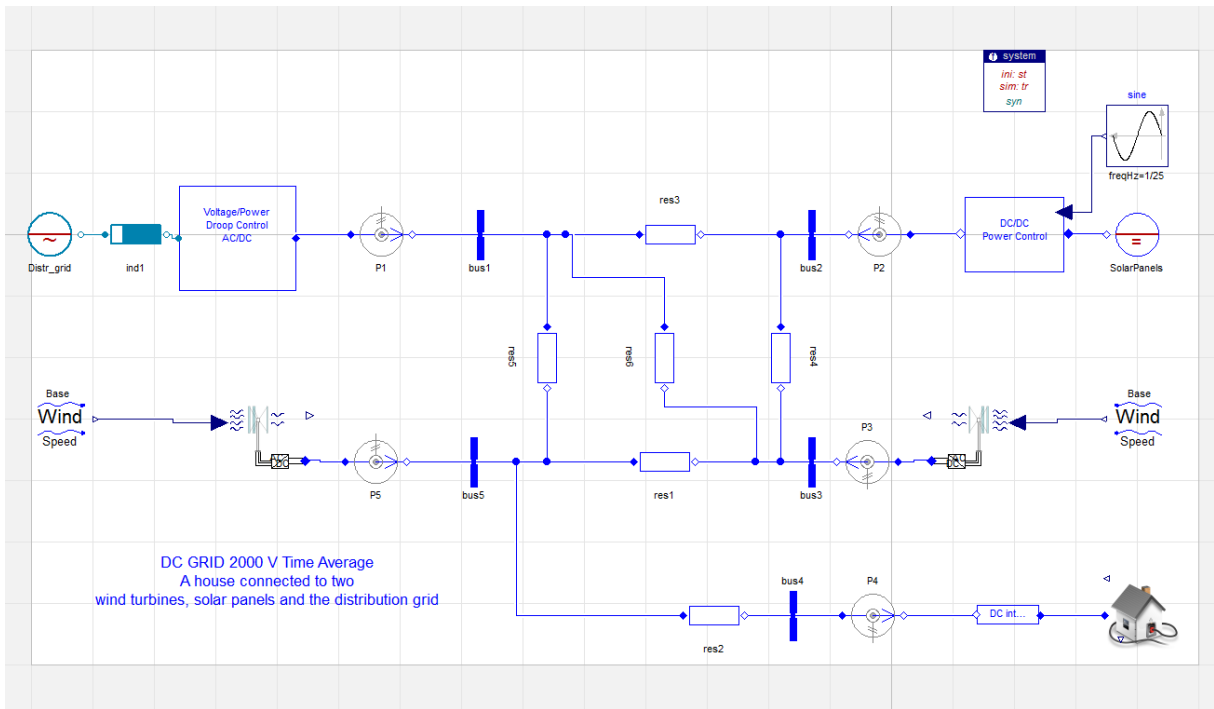


Figure 5.26 The grid setup for the DC grid with Smart Grid Library and Wind Power Library models connected.

In figure 5.27 the DC grid voltage is shown which should be kept at 2 kV. The power consumed by the load can be seen in figure 5.28 where the change in power consumption is clearly seen. In figure 5.28 power supplied to/consumed from the AC distribution grid can also be seen. In figure 5.29 the power generated by the wind turbines and the solar power plant can be seen.

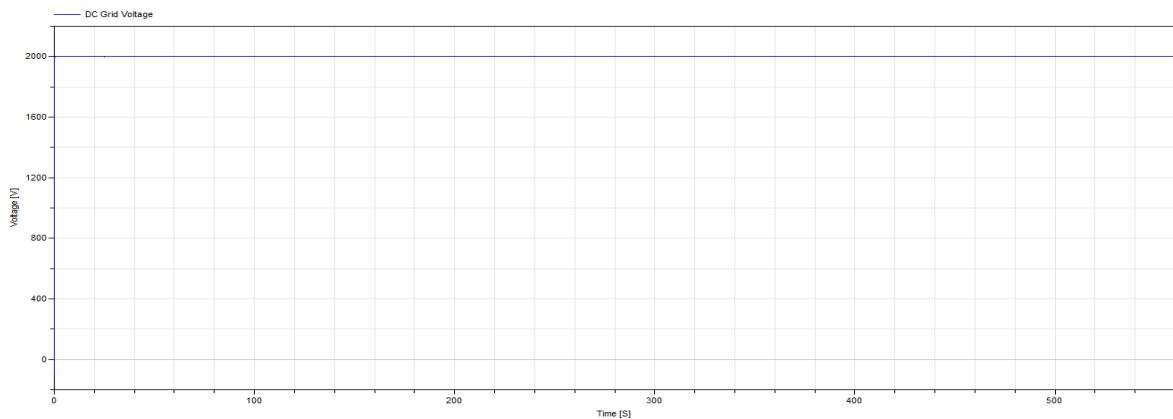


Figure 5.27 The voltage of the DC grid.

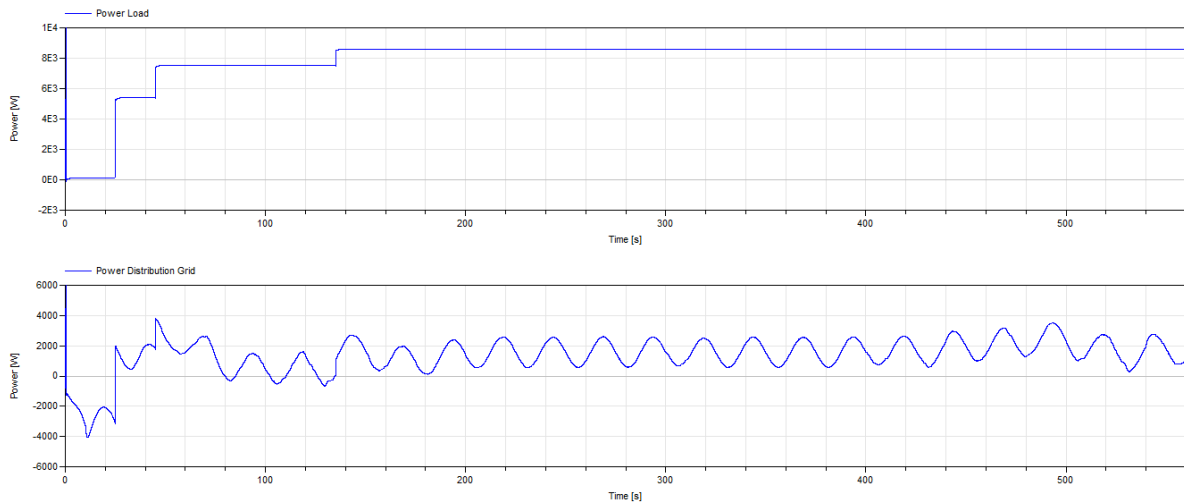


Figure 5.28 The power consumed by the load and the power supplied to/consumed from the AC distribution grid.

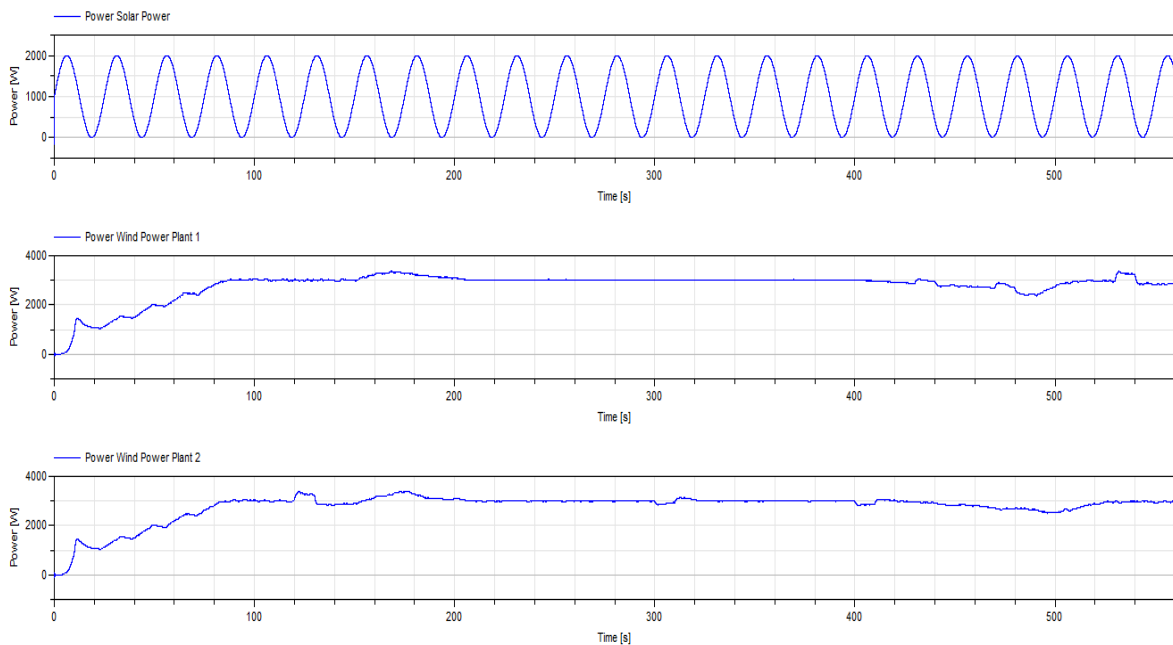


Figure 5.29 The power supplied by the generators, in the wind power plants and for the solar power plant.

5.3.2 DISCUSSION

From the figures 5.27-5.29 it is possible to evaluate the requirements set for the simulations. It is concluded that:

- The units from different libraries are compatible.
- The voltage of the DC grid is kept at 2 kV throughout the simulation as can be seen in figure 5.27.
- The amount of power consumed by load is generated by the wind and solar power plants when power can be generated by these units as shown through figures 5.28 and 5.29.
- The excess power is fed to the AC distribution grid as can be seen in figure 5.28 when the power flow is negative in the upper graph. Through this figure it is also seen that the AC distribution grid supplies the remaining power consumed by the load, in this case when the power flow is positive in the upper graph in figure 5.28.

Furthermore, it is notable that the power supplied by the grid varies sinusoidally as seen in figure 5.28. This is due to the solar power plants power variation. The frequency of this variation is not realistic and the solar power plant should be acting in a more constant manner. However, this frequency was chosen in order to see variations in the power supplied from the AC distribution grid clearly.

5.3.3 DROOP CONTROLLED DC GRID WITH EXTERNAL MODELS IN DYMOLA

The AFE connected to the grid is responsible in keeping the DC link voltage at the correct level. If something happens to the converter or if the utility grid suddenly is disconnected the DC link voltage will be out of control and after a while the DC grid will crash. To prevent this some of the other controllers can change their control mode and start regulating the DC voltage instead. This method is called droop control and has been explained earlier in the report, see chapter 3.5.

The following scenario is identical to the previous one but instead of solar panels connected to the DC grid there is a generator connected via an AC/DC converter with droop control. To test the droop controller a switch has been implemented between the voltage controller and the DC grid. The switch will turn off and on every second during a simulation time of 5 s. Two alternatives to droop control are presented in chapter 3.5. The later one is preferred and is therefore chosen in this scenario. The distance between the different components is less than 1 km thus $R = 0.01 \Omega$. The inductance in the AC three phase grid is calculated according to equation 5.2 in chapter 5.1.2. All control parameters can be seen in table C3 in appendix C. The Dymola implementation of the test bench is seen in figure 5.30.

The requirements are:

- The droop controller should be able to maintain the DC link voltage level when the AFE is disconnected from the grid.
- If the DC link voltage is too low the droop controller should increase the amount of power supplied by the generator to increase the DC link voltage.
- If the DC link voltage is on a reasonable level the droop controller should try to keep the power reference of 5 kW.

NOTE: The power sensors inside the controllers are pointing towards the AC side thus negative power is flowing to the DC grid.

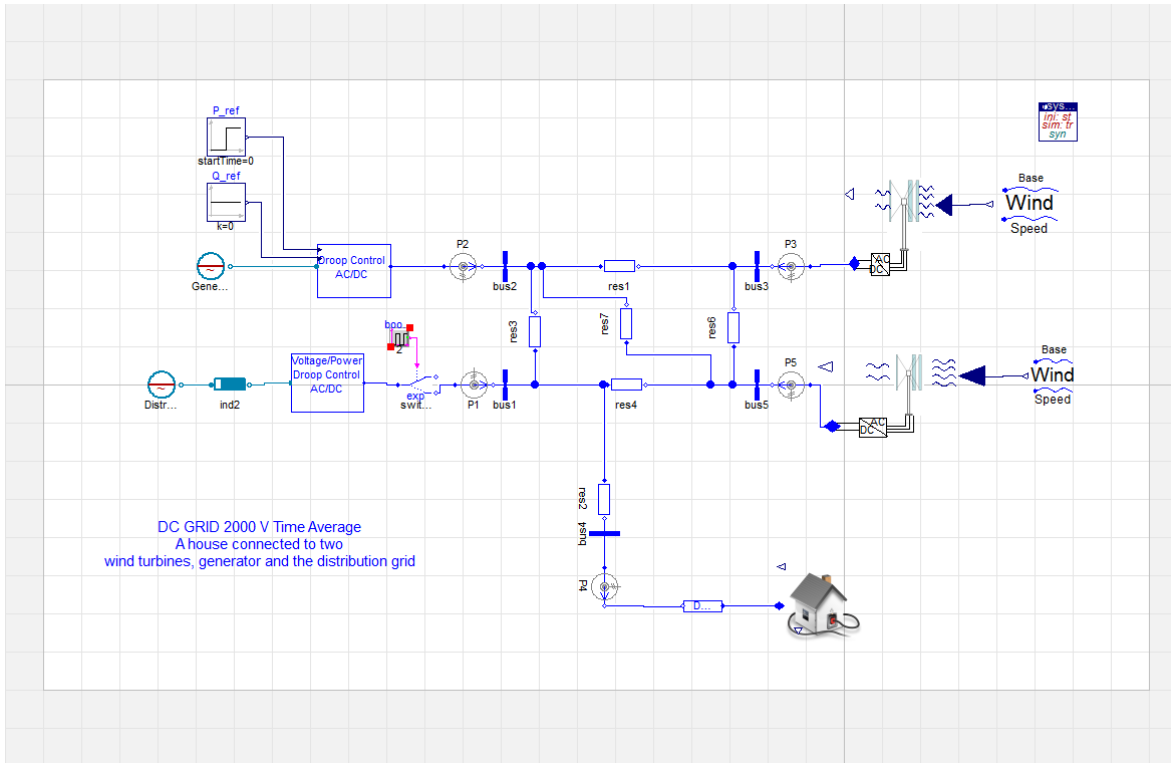


Figure 5.30 Dymola implementation of scenario 2.

In figure 5.31 the DC link voltage is plotted with and without droop controller. A close up of the DC link voltage together with the power from the generator both controlled by the droop controller can be seen in Figure 5.32.

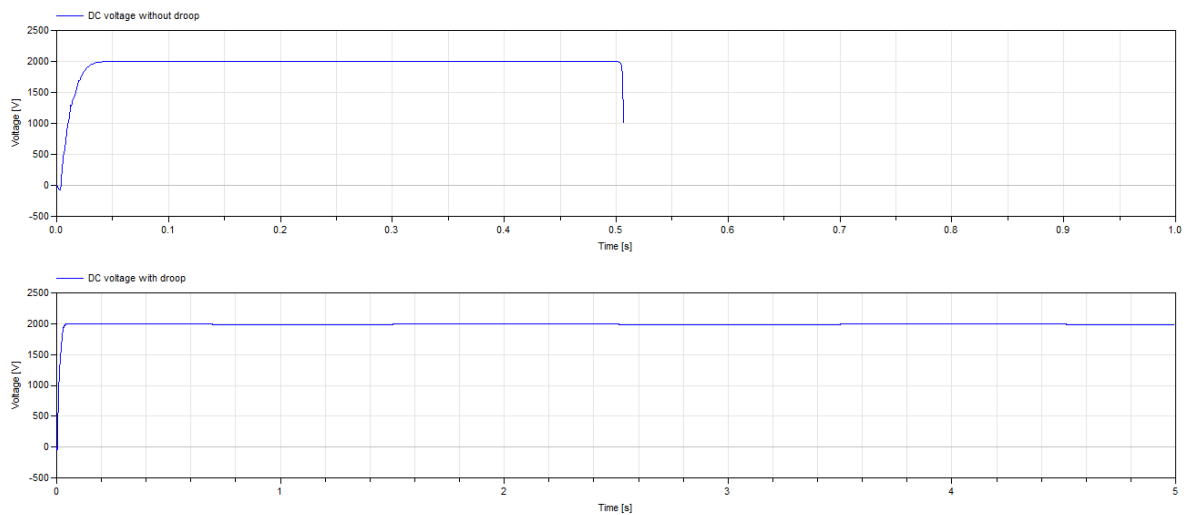


Figure 5.31 The DC link voltage with (bottom figure) and without droop control (top figure).

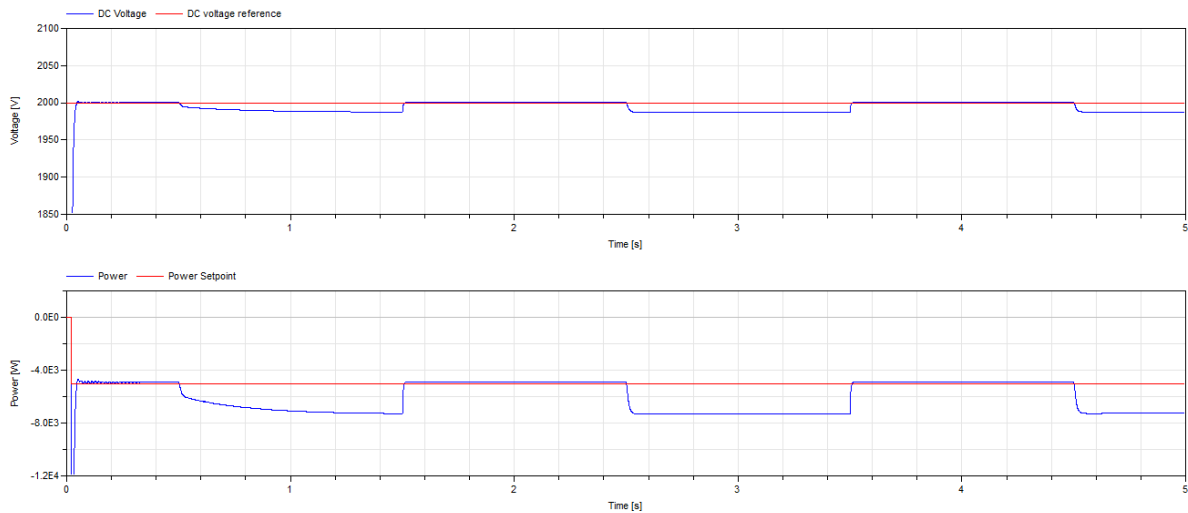


Figure 5.32 The DC link voltage and the power from the generator both controlled by the droop controller where the DC grid is disconnected from the utility grid every second.

5.3.4 DISCUSSION

From the figures 5.31 and 5.32 it is possible to evaluate the requirements set for the simulations. It is concluded that:

- After 0.5 seconds the AC grid is disconnected. The droop controller manages to keep the DC voltage level around 1986 V.
- When the grid is in islanding mode the droop controller increases the amount of power injected to the DC grid to increase the DC voltage.
- When the AC grid is connected again the droop controller starts controlling the power again and manages to control it to 4896 W.

The weights cause an inexact regulation since both voltage and power errors are scaled and added together and sent to the controller. This together with the fact that the controller is a P controller will cause stationary error. But with a well-tuned droop controller the error can be made quite small.

5.3.5 HIGH VOLTAGE SCENARIO

Another aspect of flexibility is that the models should be able to operate in many different levels as can be seen in figure 4.4 in chapter 4.2. In order to verify that the models are flexible in the latter manner a scenario for high voltage and large power flows is constructed. The scenario includes a large hydro power plant, two large wind power plants and the utility grid. The wind power plants consist of several wind turbines connected together in some internal grid and then connected to the water power plant and utility grid. The grid structure is shown in figure 5.33 and operates in DC.

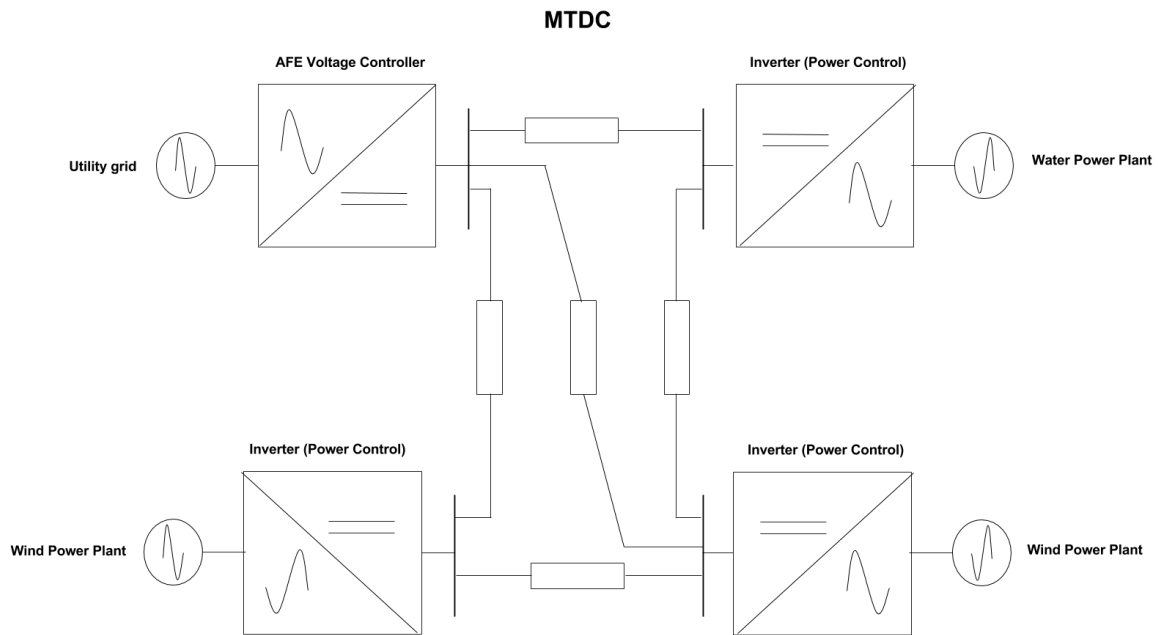


Figure 5.33 The grid structure of the high voltage scenario with large power flows.

5.3.5.1 Dymola Implementation of the High Voltage Scenario

The high voltage scenario is implemented with use of the Multi Controller. Four Multi Controller units are connected in the formation shown in figure 5.34. The unit connected to the utility grid is set in DC voltage control and is set to keep the DC voltage at the internal connection point to the grid to 130 kV. The units connected to the generators, i.e. hydro power plants and wind power plants, are set to power control. The generators and the utility grid are represented by AC sources with 50 kV line-line operating in 50 Hz. The installed power of the generators is set to be 150 MW and 100 MW for the two wind power plants and 150 MW for the hydro power plant. The wind power plants are set to generate full power initially and then vary its generation slowly using a low frequency sinusoidal reference. The larger wind power plants generated power varies between 80-150 MW with frequency 0.01 Hz and the smaller wind power plants generated power was varied between 60-100 MW with frequency 0.05 Hz. The hydro power plant generates full power and is shut down periodically every 40 s. This is implemented using a square wave as input to the power reference of the Multi Controller connected to it. The line resistances are set to 10 Ω and should roughly correspond to 1000 km cable length per line. The inductances in the AC three phase grid are calculated according to equation 5.6 in chapter 5.1.2.

The parameters of the converters are listed in table C4 in Appendix C. Note that the power reference direction of the power sensors is directed towards the AC sources.

The simulation should fulfill the requirements:

- The power controlled AC/DC converters should deliver the power generated by the power plant to the internal DC grid.
- The voltage at the internal DC grid connection point to the utility grid should be kept constant.
- The power generated by the power plants should be fed to the utility grid.

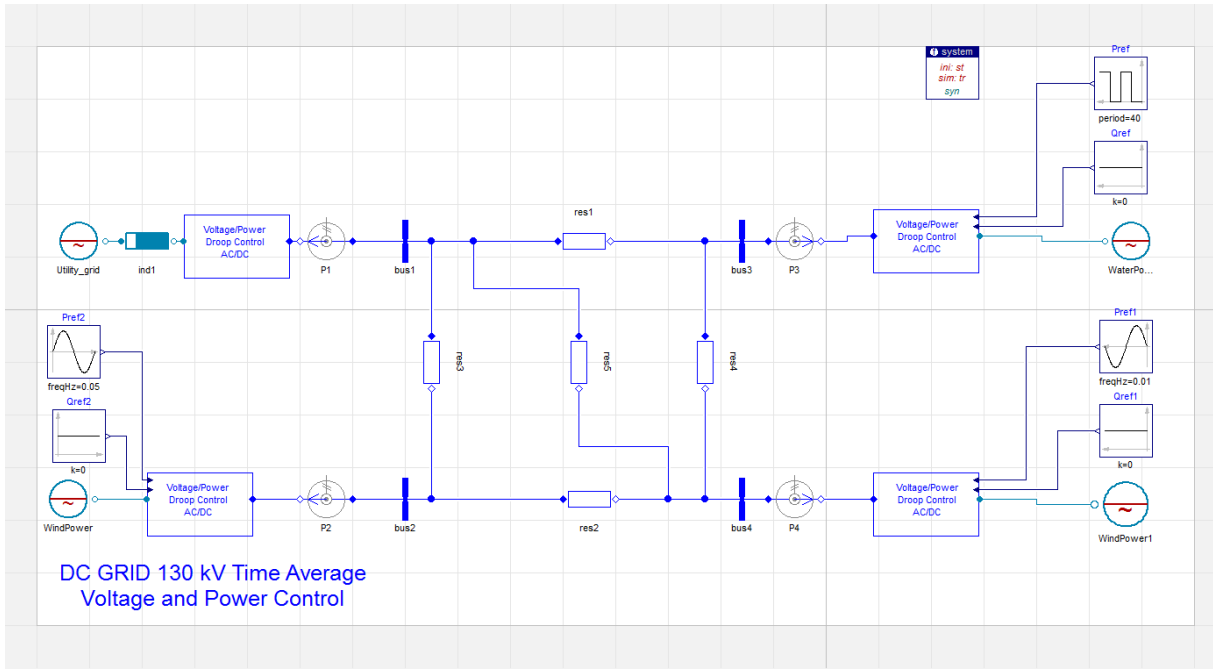


Figure 5.34 The grid structure of the high voltage scenario implemented in Dymola.

In figure 5.35 the power generated and supplied to the internal DC grid by the wind power plants is shown. In figure 5.36 the power generated by the hydro power plant is shown and also the power fed to the utility grid is shown. The voltage maintained by the DC voltage controller is shown in figure 5.37 throughout the changes in power supplied to the internal DC grid.

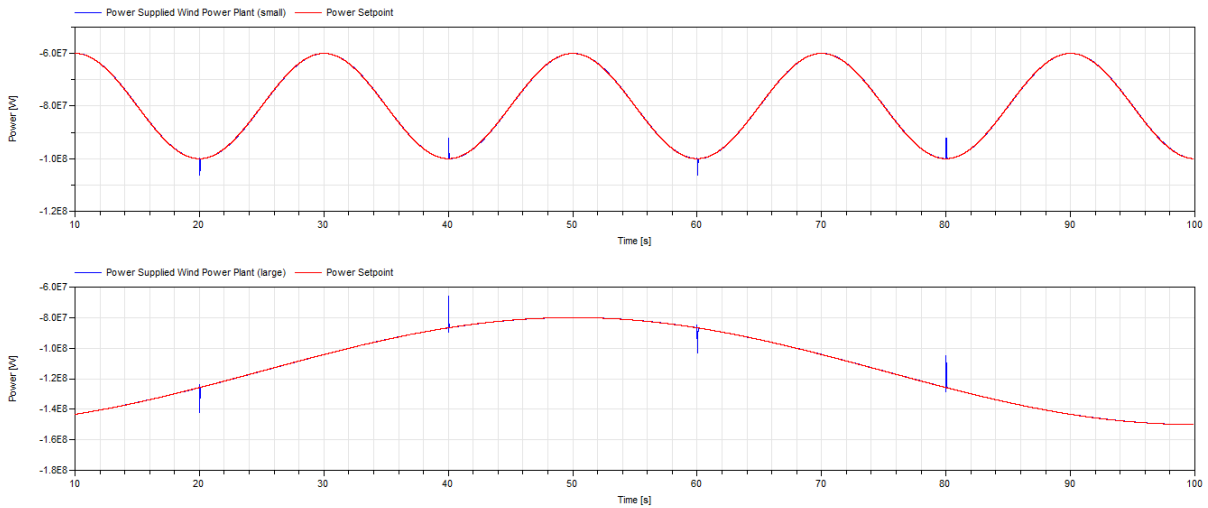


Figure 5.35 The power generated by the wind power plants fed to the internal DC grid.

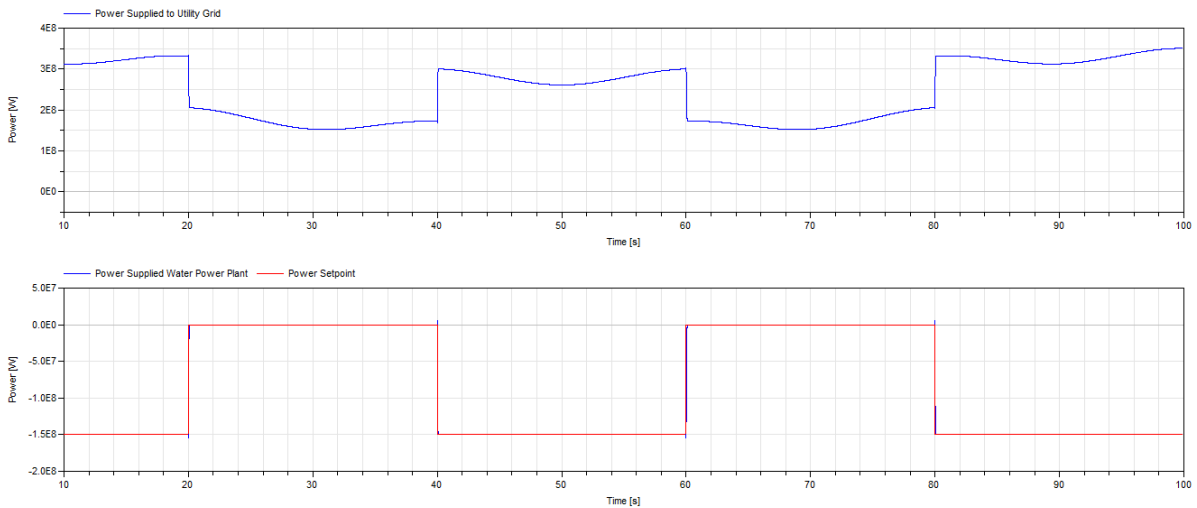


Figure 5.36 The power generated by the hydro power plant and the power supplied to the utility grid.

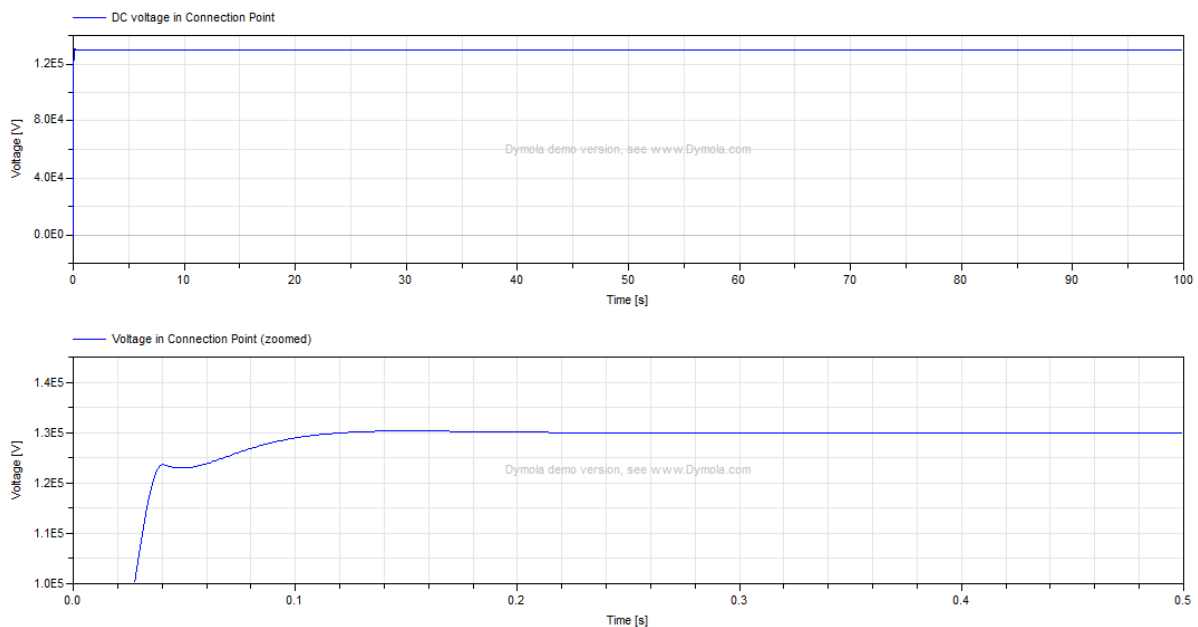


Figure 5.37 The voltage at the connection point of the DC grid to the utility grid.

5.3.5.2 Discussion

The requirements set for the simulation can be evaluated by figures 5.35-5.37. It is concluded that:

- The power generated is fed to the internal DC grid as can be seen in figure 5.35 for the wind power plants and in figure 5.36 for the hydro power plant. The limit lies in the speed of the power controller especially seen in figure 5.36 where the large change in power reference takes place momentarily. The power control respond very quickly to this change and the power control is considered adequate. The sudden changes in the hydro power plant reference affect the wind power plants. Such sudden changes in power will of course affect the current flowing through the circuit and thus the power supplied by the power controlled converter connected to the wind power plants will be affected. The recovery is however swift and the system is not pushed out of balance.

- The voltage in the connection point to the utility from the internal DC grid is kept throughout the simulation and is not affected considerably by the rapid changes in power flow as can be seen in figure 5.37.
- The power generated is supplied to the utility grid as can be seen in figure 5.36. Since the resistance of the line in this scenario is considerably larger than in previous scenarios and the fact that the current flowing in the system is also much larger there will be a considerable loss in power. A loss in power is unavoidable when having these long transmission lines. The losses can be minimized by raising the voltage of the DC grid, but this will put a larger demand on the power electronic equipment and also add to the investment cost of this equipment [6].

5.4 INTERNAL AC GRID

5.4.1 AC-GRID TOPOLOGY

The main focus of the thesis is the internal DC-grid because of its simpler regulation properties but also the plentiful research that are being done in this area. However, in order to make the converter models flexible, AC regulation is carried out implemented in these units as well. Another area which is highlighted in this report is the connection of power electronic converters to the internal grid. The first step in the implementation of the internal AC- grids is to connect converters to the internal AC-grid, where one converter is responsible for the voltage and frequency in the connection point of the AC-grid and the rest of the converters represent loads and generators connected in a back-to-back configuration operating in power control mode. The structure of the AC grid is the structure of the general grid described in chapter 1.2, but with back-to-back connected AC/DC converters as shown in figure 5.38.

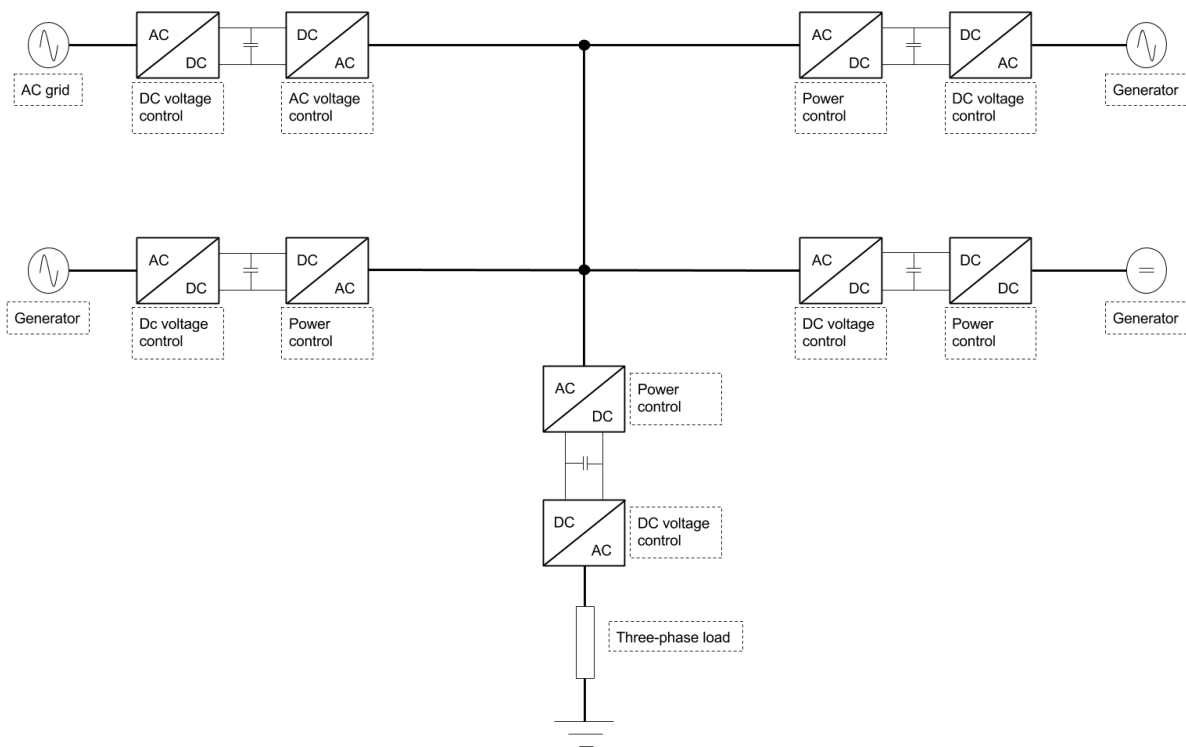


Figure 5.38 Internal AC grid with back to back connected converters.

When connecting a grid in this manner the frequency of the internal grid is not affected by changes in power, whether power is drawn from or supplied to the internal grid as mentioned in chapter 3.6. This means that no frequency control of the internal grid is required since the converter responsible for the AC voltage can operate in open loop AC voltage control described in chapter 3.6. Note that in figure 5.38 the line impedances in the internal AC grid are not included but will appear when running simulations. Due to this the reactive power compensation described in chapter 3.7 will also have to be implemented for the DC voltage controlled converters.

5.4.2 DYMOLA IMPLEMENTATION OF THE AC GRID

When implementing the internal AC grid in Dymola the Multi Controller described in chapter 4.1 is used in order to easily implement the different regulation loops described in chapter 3. The converters are connected in the back-to-back manner described in figure 5.38, as can be seen in figure 5.39. Note that in figure 5.39 yet another load is connected through a converter, this should however not pose a problem since the grid should be able to operate with any number of converters connected to it. The converters connected to the internal AC grid are set to power regulation, except one of the controllers which is set to open loop AC voltage regulation. The converters connected to the loads and generators are set to DC voltage control and the converter connected to the AC distribution grid is set to DC voltage control. The loads and generators are represented by AC sources which in turn represents another grid that consume or supply power.

The model shown in figure 5.39 is simulated for two scenarios and the specification for each scenario is listed in table 5.5. System parameters are presented in table C5 in appendix C. For the higher level simulations the DC generation is removed since DC power generation mostly takes place in lower levels. Common for both simulations is that the internal AC grid frequency is set to 50 Hz. The frequency of the generators/loads is also set to 50 Hz. The impedances of the lines are also set to have resistance of 0.1 Ω and inductance of 0.5 mH. The two top right back-to-back converter setups both correspond to loads that consume power in a pulsing manner, one pulsing with a frequency of 4 Hz and the other pulsing with a frequency of 5 Hz. The other two back-to-back converter setups supply power to the internal AC grid in a pulsing manner, one pulsing with a frequency of 5 Hz and the other pulsing with 6.67 Hz and delayed 0.15 s. The DC generation is only included in one scenario where it supplies power between 0-5 kW sinusoidally with frequency 0.1 Hz.

Requirements of the grid simulation:

- Voltage and current vectors should be aligned with the d-axis in the connection point.
- Voltage amplitude and frequency of the internal grid should be kept constant.
- Correct power should be consumed from the grid by the load power converters.
- Correct power should be supplied to the grid by the generator power converters.
- Residual power should be injected into the main grid.

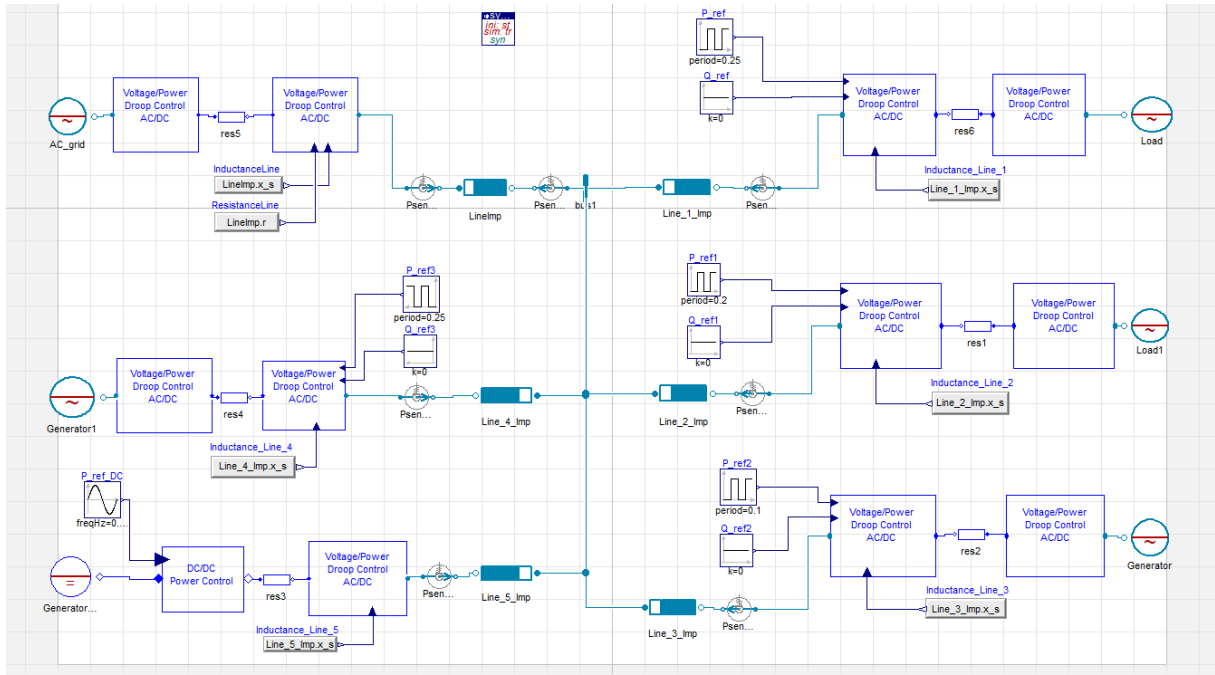


Figure 5.39 The simulation model of the AC grid setup implemented in Dymola.

	Scenario 1	Scenario 2
AC voltage amplitude (line-line) of the internal grid	400 V	20 kV
AC voltage amplitude (line-line) of the main AC-grid, loads and generators	400 V	10 kV
DC-link voltage	2000 V	50 kV
Consumed power by loads	20 kW	2 MW
Power supplied by generators	30 kW	3 MW

Table 5.5 Scenario specifications for the AC-grid.

5.4.2.1 AC Grid Scenario 1

In figure 5.41 the voltage and current vector alignment with the d-axis in the connection point is shown. Note that the current direction is dependent on the power flow direction and therefore the angle of the current vector switches between 180 degrees and -180 degrees when current flows in the opposite direction of the sensor reference direction. In figure 5.40 the phase voltage (peak) amplitude and frequency in the connection point are seen. Figures 5.42 and 5.43 shows how the loads and generators strive to achieve the correct power consumed/supplied to the grid. Figure 5.44 shows the power flow to the distribution grid.

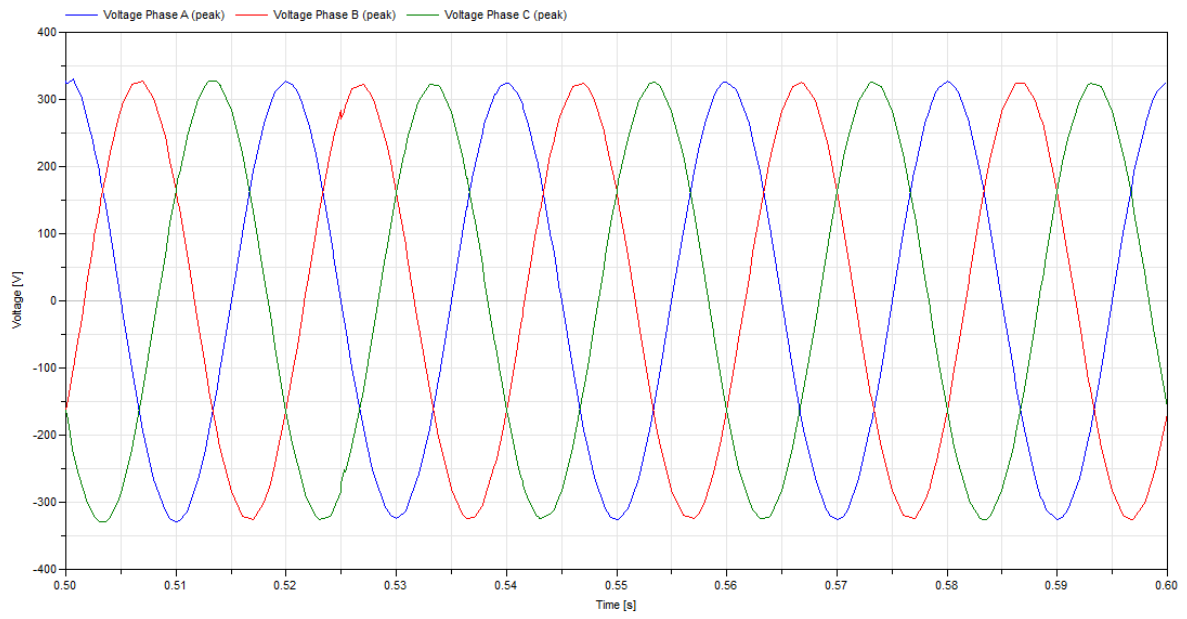


Figure 5.40 The voltage in the internal grid connection point.

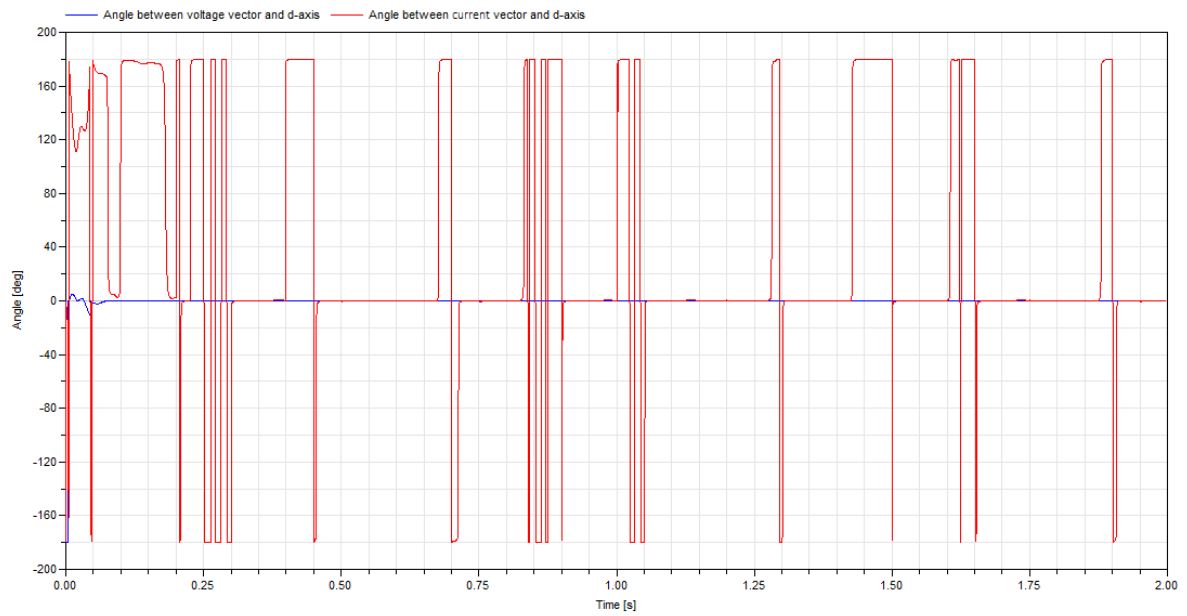


Figure 5.41 The alignment of the current and voltage vectors to the d-axis.

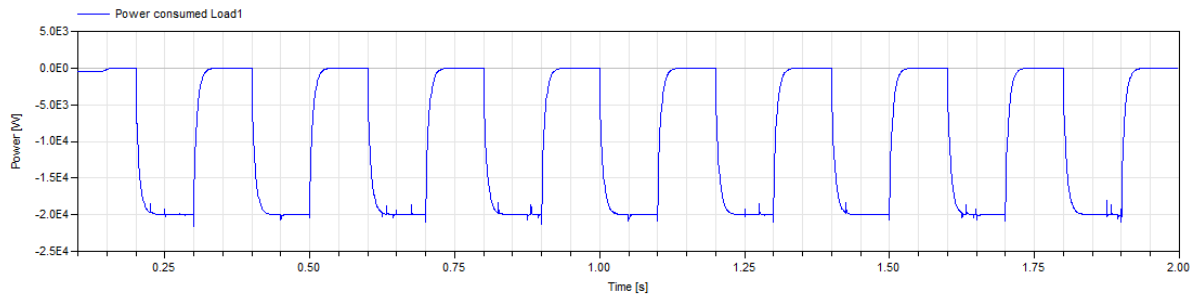
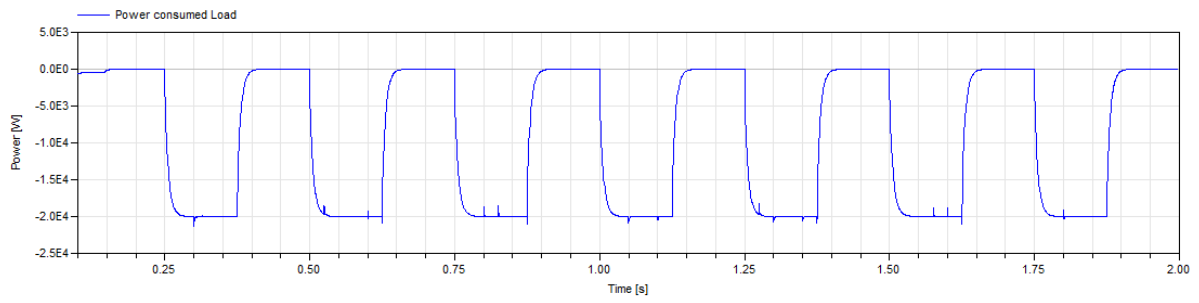


Figure 5.42 The consumed power from the internal AC grid

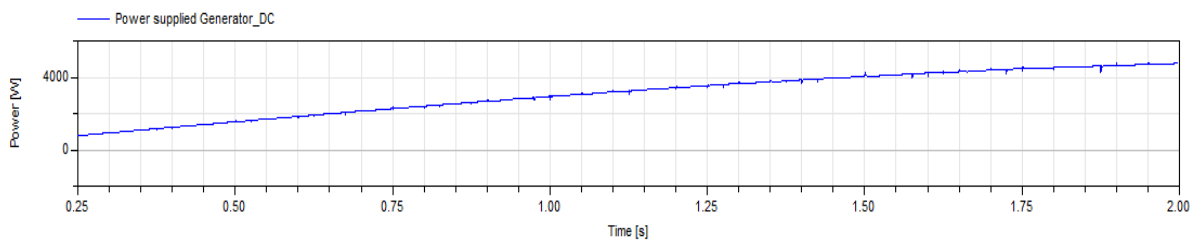
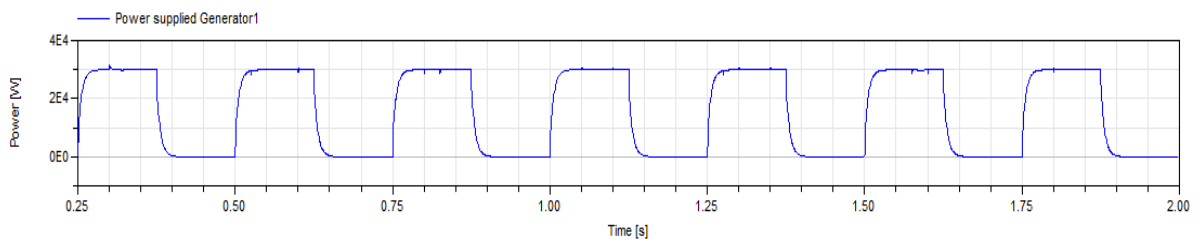
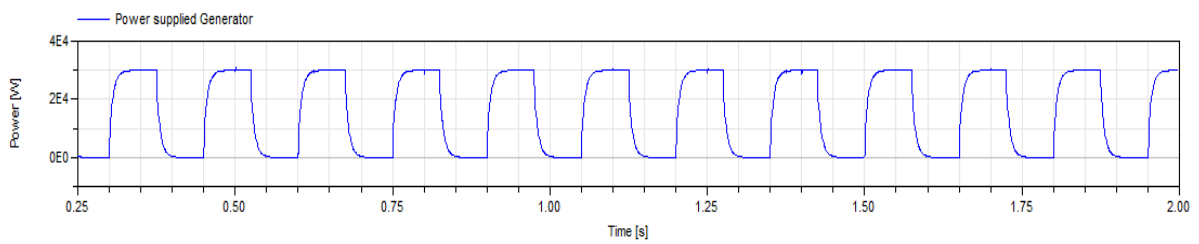


Figure 5.43 The supplied power to the internal AC grid.

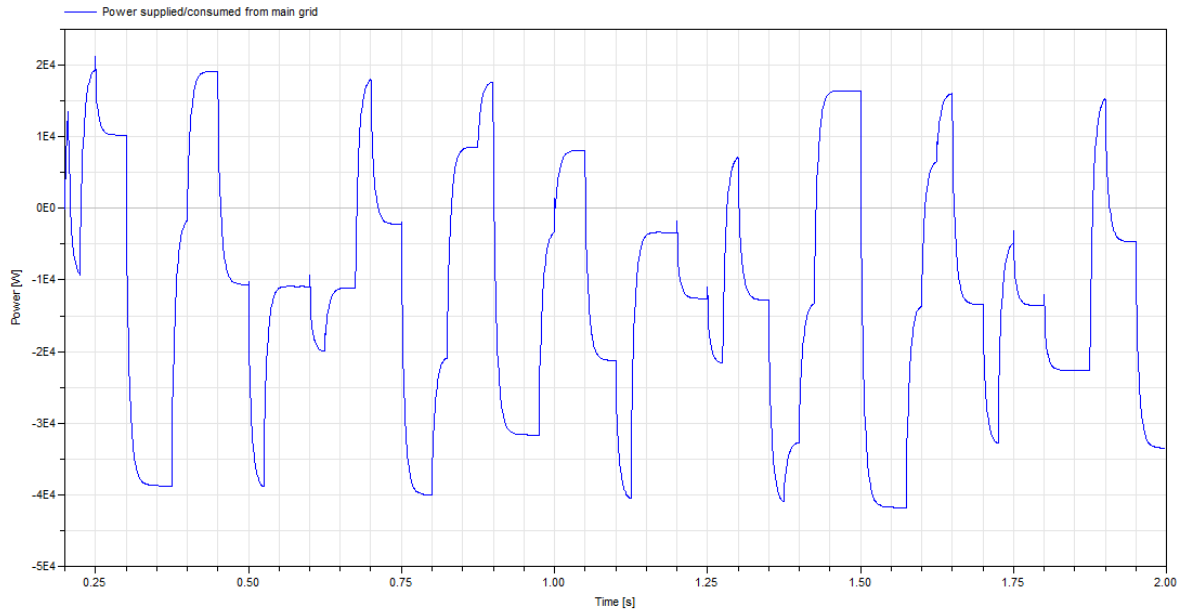


Figure 5.44 The power supplied/consumed to the distribution grid (negative corresponds to power fed to the distribution grid).

5.4.2.2 Discussion

In the first scenario the requirements of the simulation can be evaluated through figures 5.40-5.44:

- From figure 5.41 it is seen that both the current and voltage vectors are in line with the d-axis. Although the current vector seem quite unstable when power flows to the load this in not the case. In this situation the current vector is pointing in the opposite direction of the d-axis meaning that it is 180 degrees shifted. The current vector according to the graph is shifted 180 degrees and then -180 degrees which correspond to the same direction.
- In figure 5.40 the phase voltage amplitudes in peak value are shown and they are kept at 326-327 V. This corresponds to a line-line RMS voltage of ca 400 V. The frequency of the voltages can also be derived from figure 5.40, where the period of the voltages is 0.02 s which corresponds to 50 Hz frequency.
- Power consumed from the grid is seen in figure 5.42 where it is possible to conclude that the demanded power consumption is kept constant. The small ripple in power is caused by the other converters being switched on and off.
- Power supplied to the grid follows the same pattern as mentioned for the consumed power which can be seen in figure 5.43. The power generated by the DC generator also meets the reference. In this case, the generated power reference follows a low frequency sinusoidal which is why the power supplied by this unit looks a bit different.
- The remaining power needed is supplied from the distribution grid and vice versa as seen in figure 5.44. It is also possible to see that the open loop AC voltage control barely can react to the rapid changes. However, this is only for the small time intervals created by the over-lapsing of the square waves required from the power controlled converters.

5.4.2.3 AC Grid Scenario 2

The results corresponding to the second scenario can be viewed in figure 5.45-5.49. Note that in this simulation the DC generator was disconnected and removed from the simulation.

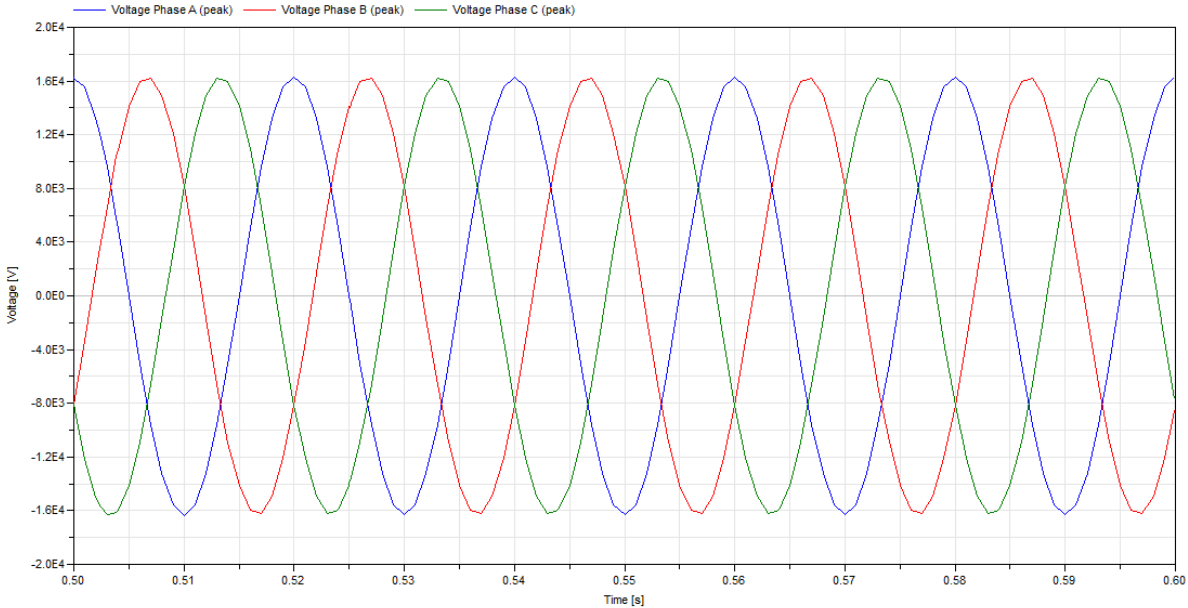


Figure 5.45 The phase voltages in the connection point.

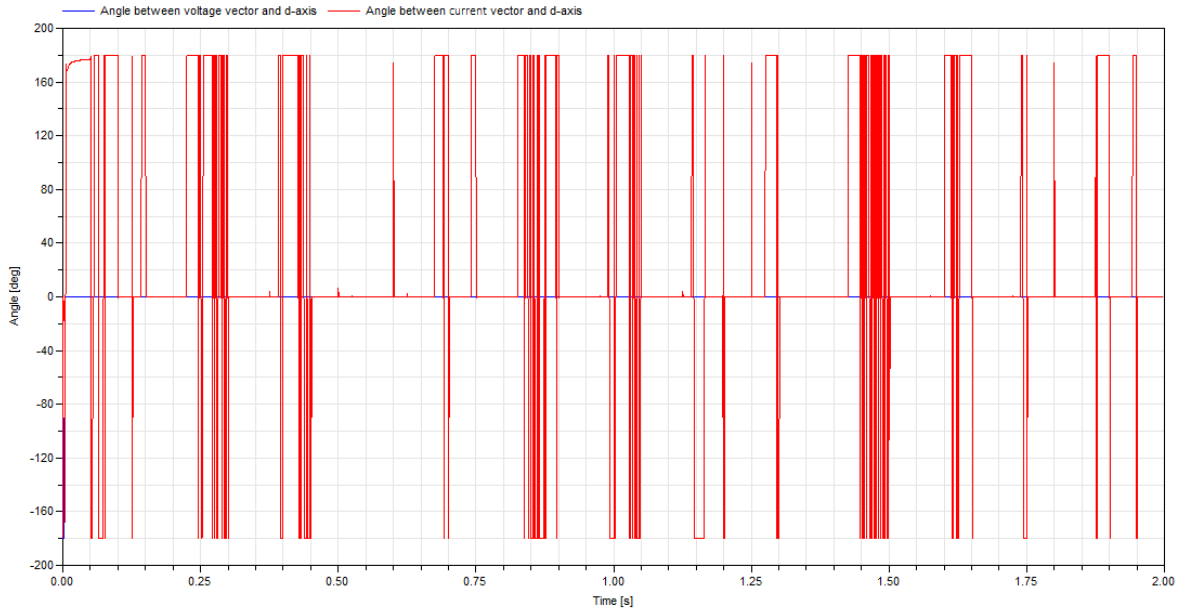


Figure 5.46 The alignment of the current and voltage vector with the d-axis.

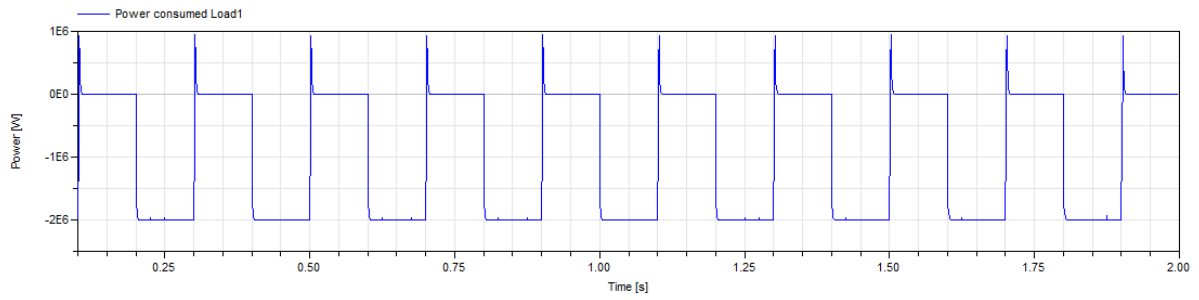
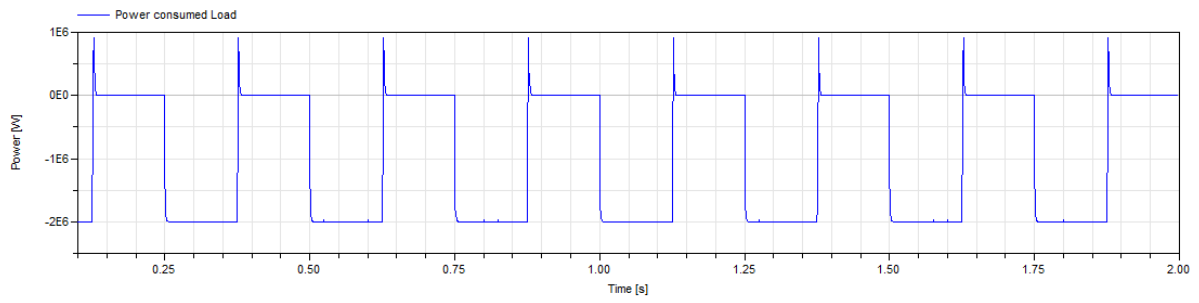


Figure 5.47 The power consumed from the internal AC grid by the loads.

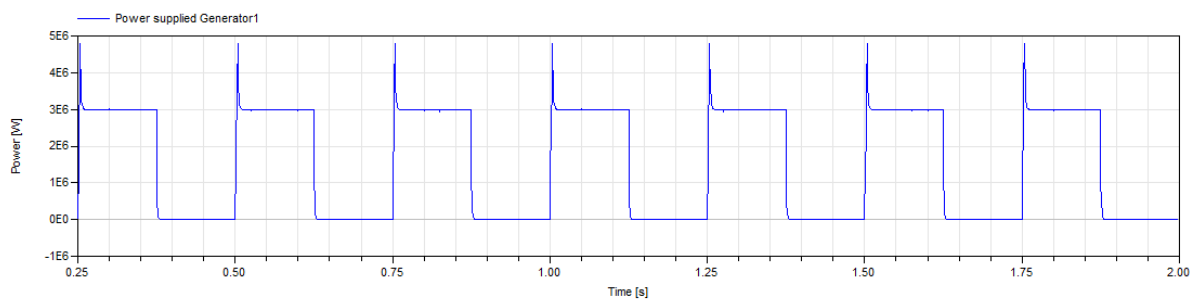
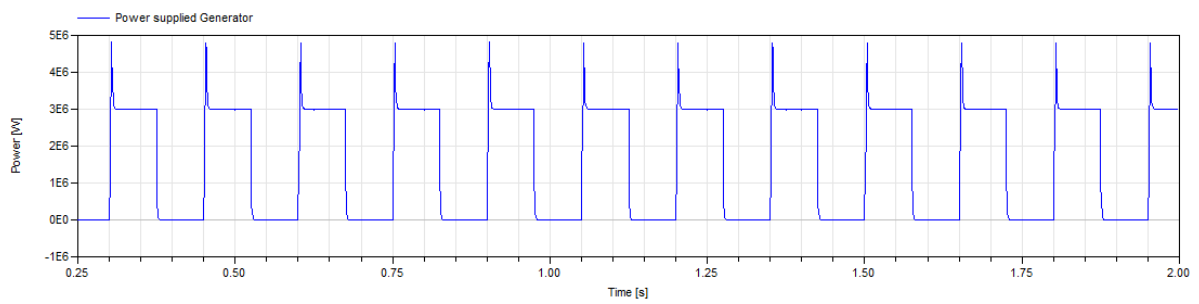


Figure 5.48 The power supplied to the internal AC grid by the generators.

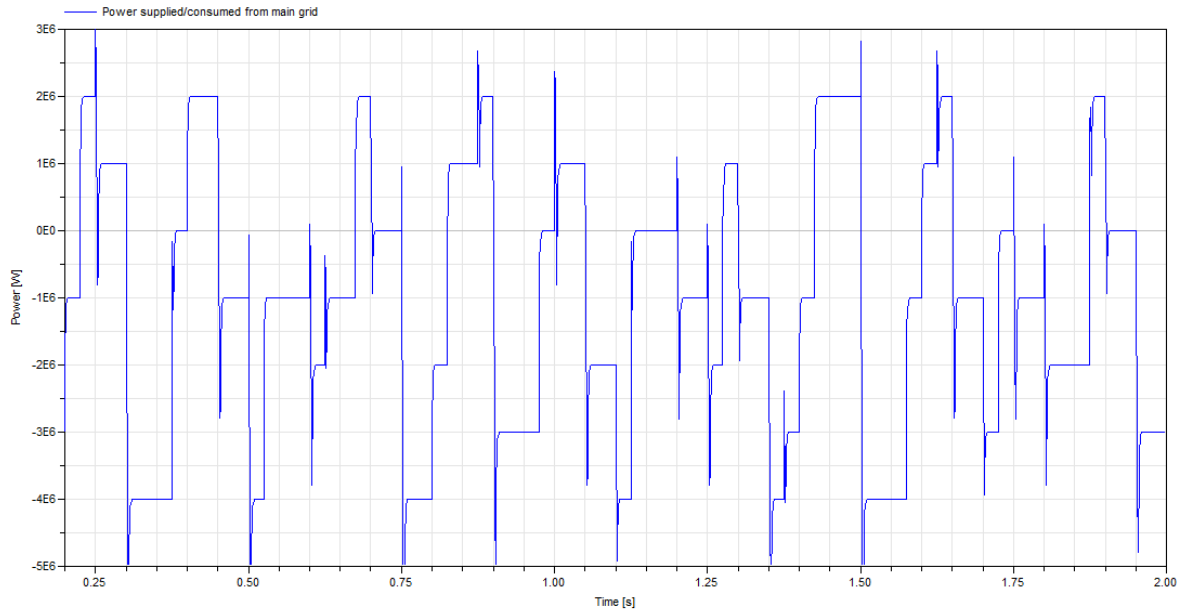


Figure 5.49 The remaining power needed to either output to the distribution grid or that has to be supplied to the internal AC grid.

5.4.2.4 Discussion

For the second scenario, the evaluation of the same requirements is done through figures 5.45-5.49:

- The current and voltage vectors are aligned in a similar manner as for the first scenario, seen in figure 5.46. The current vector exhibits the same behavior described for the first scenario.
- The phase voltage peak amplitudes are shown in figure 5.45 and are kept around 16330 V, which corresponds to 20 kV line-line voltages. The frequency of the voltage is also kept at 50 Hz as seen in the same figure.
- The consumed power from the internal AC grid meets the desired power consumption as seen in figure 5.47. By examining the figure closely, similar effects to those described for the first scenario are present when the other converters are switched on and off by the square wave references. There are however spikes in the measured power when changing the reference of the converter. This is due to a large value of the proportional gain in the power controller. By decreasing the gain these spikes can be eliminated, at the cost of a slower response which could be preferred.
- The power supplied to the internal AC grid is shown in figure 5.48 and it exhibits the same behavior as the consumed power.
- The residual power supplied to/consumed from the distribution grid is shown in figure 5.49, and it corresponds to the difference in power of the generators and loads.

5.4.2.5 Model Flexibility

The same converter model is used for all the converters operating in different control modes and on different power levels. This shows that model is flexible and can be used in many simulation applications. The grid is constructed by the user in Dymola and through the user interface the appropriate control and power level can be chosen.

6 CONCLUSIONS

The main purpose of the thesis was to implement a scalable, flexible and controllable grid. The term scalable implied that the grid could be used in many different voltage and power levels meaning that the grid could represent different applications. The grid was made scalable by implementing records where the parameters for the different power levels were set. The simulations from chapter 5 implemented scenarios of:

- DC grid with internal DC voltage of 1500 V and power flows of 11 kW
- DC grid with internal DC voltage of 2000 V and power flows of 80 kW in total
- DC grid with internal DC voltage of 50 kV and power flows of 4 MW
- DC grid with internal DC voltage of 130 kV and power flows 350 MW in total
- AC grid with internal AC voltage of 400 V line-line and power flows of 30 kW
- AC grid with internal AC voltage of 20 kV line-line and power flows of 3 MW

The grid can, by these varying scenarios, be considered scalable. The other goal was to implement controllability of the power electronic units used in order to set up the grid. This has been achieved by implementing different control options such as:

- AC/DC converter with current and DC voltage control
- AC/DC converter with AC voltage control
- AC/DC converter with droop control
- AC/DC converter with current and power control allowing bidirectional power flow
- DC/DC converter with current and power control allowing bidirectional power flow

The different control options were tested and evaluated in chapter 3. In chapter 5 the different converters were combined and tested in combination with each other in different grid structures showing that grid controllability was successful. In the grid simulations the additional system parameters such as cable representation were also taken into account.

All these simulations of grid and converter models show the flexibility of the constructed models. In addition the constructed models were tested together with external library models showing compatibility with these other libraries. To further improve the flexibility a Multi Controller model was implemented that combined all different control strategies, and which was also made scalable by implementing records for different scenarios.

In conclusion the goals that were set up for this thesis have been reached. The models were made flexible by using the Multi Controller and the records attached to it. The compatibility to other Modelica libraries has been successfully implemented, with this the scalability, flexibility and controllability of the grids were also ensured.

6.1 FUTURE WORK

In this thesis neither switching nor thermal losses were studied. In order to get more accurate and realistic results losses need to be included in the analysis. The EPL components used in the construction of the models support these kinds of losses, but due to time constraints and the extent of the thesis these aspects remain to be implemented.

Other control methods for controlling AC grids such as frequency control and a more elaborate AC voltage control can be implemented. Power control of the AC/DC converters has been

implemented already, and since the active and reactive powers affect the frequency and the AC voltage respectively, the step needed to implement frequency and voltage control is not that large. Again time issues led to that these controls were left unfinished.

The Multi Controller model is only implemented for Time Average converter models. A Multi Controller model for the switched models could also be implemented in order to get a more flexible switched grid structure.

Further work could also be done in the parameter optimization by setting up transfer functions for the full system. Thereby the optimal controller parameters could be derived mathematically for virtually any voltage and power level. This would improve the flexibility of the models but the pure extent of this work could probably be sufficient for a master thesis in itself.

The data for the power generated and supplied to the grid in the different scenarios was mostly based on estimations. Simulations with more realistic power generation could be done in order to get real examples how these kinds of grid operate in practical scenarios. More accurate representations of generators and external grids could further be implemented in order to account for the dynamics of these units.

The models developed in this thesis could also be tested and verified against other Modelica libraries except those that were included in the work of this thesis. This could be done to further verify the compatibility of the models to any library.

7 NOMENCLATURE

$\cos \theta$	Power factor
D	Duty cycle
$\frac{di}{dt}$	The current derivative
E_{PN}	The magnitude of the RMS phase-to-neutral voltage
E_{PP}	The magnitude of the RMS phase-to-phase voltage
e_a	Grid voltage phase a
e_b	Grid voltage phase b
e_c	Grid voltage phase c
\vec{e}_{dq}	Grid voltage in dq coordinates
\vec{e}_d	d-component of the grid voltage
\vec{e}_q	q-component of the grid voltage
$e(t)$	Measured error
Δi	Maximum current difference

Δi_{on}	The difference in between start and end value for the current when the transistor is conducting
Δi_{off}	The difference in between start and end value for the current when the transistor is not conducting
I_{DC}	DC link current in the three phase converter
$i_{\alpha\beta}$	Line current in $\alpha\beta$ coordinates
i_d	d-component of the dq current vector
i_q	q-component of the dq current vector
$ I_{max} $	Magnitude of the maximum current in one phase
I_N	Nominal current for the transformer
L	Inductance value
L_{conv}	Value of the grid inductance
K	Scaling constant
K_p	Proportional gain of the controller
m_a	Voltage reference in phase a
\hat{m}_a	Magnitude of the voltage reference in phase a
m_b	Voltage reference in phase b
\hat{m}_b	Magnitude of the voltage reference in phase b
m_c	Voltage reference in phase c
\hat{m}_c	Magnitude of the voltage reference in phase c
P_{grid}	Active power in the three phase grid
P_{AC}	Active Power on the AC side
P_{DC}	Power on the DC link
Q_{grid}	Reactive power in the three phase grid
R	Inductor resistance
\vec{S}_{grid}	Apparent power in the three phase grid
S_{line}	Apparent power through the line impedance
S_N	Rated power for the transformer
t_{on}	The time when the transistor is conducting

t_{off}	The time when the transistor is not conducting
T_{sw}	The switching period
T_i	Time constant for the integral part
Δt	Time during maximum current difference
U_{dc}	DC link voltage of the three phase converter
u_a	Voltage over the load of the three phase converter output phase a
u_b	Voltage over the load of the three phase converter output phase b
u_c	Voltage over the load of the three phase converter output phase c
u_α	Phase voltage expressed in the real component of the complex α, β vector.
u_β	Phase voltage expressed in the imaginary component of the complex α, β vector.
$\vec{u}_{\alpha\beta}$	Phase voltage expressed as the complex α, β vector
\vec{U}_{conv}	Output voltage vector of the three phase converter
U_{line}	Impedance voltage
\vec{u}_{dq}	Output voltage of the three phase converter in dq coordinates
\vec{u}_d	d-component of the output voltage of the three phase converter in dq coordinates
\vec{u}_q	q-component of the output voltage of the three phase converter in dq coordinates
u_{cc}	Parameter that describes the input voltage as a fraction of the nominal voltage V_N the transformer must have to be able to reach nominal current when short-circuited
v_a	Output voltage of the three phase converter phase a
v_b	Output voltage of the three phase converter phase b
v_c	Output voltage of the three phase converter phase c
V_{in}	Input voltage of the Boost Converter and Buck Converter
V_1	The potential in node 1 of the Buck converter
v_L	Voltage over the inductance
V_{DC}	Load voltage of the rectifier bridge
V_{out}	Output voltage
v_0	Zero potential of the three phase converter
V_N	Nominal voltage of the transformer

V_{LL}	Line-to-line voltage
$ \vec{x} $	Magnitude of the maximum output voltage vector of the three phase converter
$y_{ref}(t)$	Controller reference signal
$y_{act}(t)$	Measured value of the signal
$y_o(t)$	Output value of the controller
θ_{grid}	Grid phase shift
θ_{conv}	Phase shift of the three phase converter
ω	Grid frequency

8 LIST OF FIGURES

Figure 1.1 The figure illustrates the general grid structure with power electronic devices connected to it.....	6
Figure 1.2 The figure shows the conventional grid structure with generation at a common point and all consumers act as pure loads.....	9
Figure 1.3 The new grid structure that allows consumers to feed back power onto the grid.....	10
Figure 2.1 The figure show the simple modulation of a Buck converter.	12
Figure 2.2 The figure shows the electric schematic of the H-bridge.	13
Figure 2.3 The figure shows the modulation of the H-bridge when the H-bridge is used to create an AC voltage.	14
Figure 2.4 The electric schematic of the Buck converter.	15
Figure 2.5 The electric schematic of the Boost converter.	17
Figure 2.6 The electric schematic of the H-bridge.	18
Figure 2.7 The Dymola implementation of the H-bridge.....	19
Figure 2.8 The electric schematic of the one phase diode rectifier.....	20
Figure 2.9 The electric schematic of the three phase diode rectifier.	21
Figure 2.10 The electric schematic of the three phase converter connected to a load.....	22
Figure 2.11 In the illustration the different possible switch positions are shown [5].....	22
Figure 2.12 An illustrative figure showing the carrier wave and the sinusoidal voltage references together with the corresponding switching states over one switching period [5].....	23
Figure 2.13 An illustrative figure showing the 8 voltage vectors plotted in the complex plane [5].	24
Figure 2.14 An illustration of the maximum AC output voltage, shown in the circle, of the three phase converter.....	24
Figure 2.15 The figure illustrates the time average converter implemented in EPL with modulator.....	25
Figure 2.16 The figure shows the switched three phase converter implemented in EPL with modulator.....	25
Figure 2.17 The figure shows the AFE connected to the utility grid.	27

Figure 2.18 The figure shows connection point between the AFE and the grid with voltage phasors.	27
Figure 2.19 Phasor diagram showing the voltage phasors during regeneration (to the left) and rectification (to the right) while having the power factor equal to one.	28
Figure 2.20 The figure shows the Dymola implementation of the AFE.	32
Figure 3.1 The figure illustrates the Dymola implementation of the modified PID-controller block.	34
Figure 3.2 The figure shows the control block of the power controlled H-bridge.	35
Figure 3.3 The figure shows the Dymola implementation of the power controlled H-bridge.	36
Figure 3.4 The Dymola test bench for the power controlled H-bridge.	37
Figure 3.5 The graphs show the filtered power (top graph) and current (bottom graph) acting on their respective references.	38
Figure 3.6 The graph show the unfiltered power acting on its reference.	38
Figure 3.7 The figure shows the control loop with voltage control in the outer loop and current control in the inner loop.	40
Figure 3.8 The Dymola implementation of the voltage controlled AFE.	41
Figure 3.9 The inside of the voltage control block from figure 3.8.	42
Figure 3.10 The figure shows the content of the "Current Control"-block in figure 3.9.	43
Figure 3.11 The figure shows the test bench for the voltage controlled AFE.	44
Figure 3.12 The graphs shows the performance of the voltage controller (top graph) and also the change in resistive value of the load (bottom graph).	45
Figure 3.13 The figure shows a close up of the voltage controller with maximum and minimum values of the voltage ripple.	45
Figure 3.14 The figure shows the startup phase were the DC link voltage is controlled from 0 V to 2000 V. It can also be seen that the transistors are open until the DC link voltage reaches 550 V.	46
Figure 3.15. The figure shows the d, q currents and their setpoints.	46
Figure 3.16 The figure shows the corresponding power consumption in the load.	46
Figure 3.17 Shows the AC current in phase A with corresponding power consumption of 40 kW during steady state simulation.	47
Figure 3.18 The figure illustrates the current harmonics content for 40 kW load in phase A for frequencies up to 4800 Hz.	47
Figure 3.19 An illustration of the implemented power controller. The outer loop is controlling the power and the inner loop is controlling the current.	49
Figure 3.20 The Dymola implementation of the power controlled AC/DC converter.	50
Figure 3.21 The power control block model.	51
Figure 3.22 The current control block.	52
Figure 3.23 The test bench of the power controlled AC/DC converter connected to two stiff grids.	53
Figure 3.24 The graphs show the performance of the active (top graph) and reactive (bottom graph) power control. The signals are filtered in in this graphs.	54
Figure 3.25 The unfiltered active (top graph) and reactive (bottom graph) power is shown in the figure compared to the power references.	54
Figure 3.26 The current controllers responding to the reference generated by the active and reactive power controllers.	55
Figure 3.27 Illustration of the droop control structure.	57
Figure 3.28 Illustration of the AC/DC droop control loop implemented in Dymola.	58

Figure 3.29 The figure illustrates the inside of the “Droop Control”-block seen in figure 3.28.	59
Figure 3.30 The figure shows the power P-controllers.....	59
Figure 3.31 Test bench for droop control with a load connected to the DC grid consuming power in pulses of 30 kW.....	60
Figure 3.32 Test 1: DC voltage over the load and power generated by the source when the DC source is disconnected after 0.2 s.....	61
Figure 3.33 Load consuming power in pulses of approximately 30 kW for test 1.....	62
Figure 3.34 Test 2: DC voltage over the load and power generated by the source when the DC source is disconnected after 0.2 s.....	62
Figure 3.35 Load consuming power in pulsing of approximately 30 kW for test 2.	63
Figure 3.36 Typical line representation in an AC-grid.....	65
Figure 3.37 Illustration of the open loop AC voltage control setup.	66
Figure 3.38. The control block of the open loop AC voltage control implemented in Dymola.	67
Figure 3.39 The test bench for the open loop AC voltage control implemented in Dymola.	68
Figure 3.40 The length of the voltage d- and q-component and also the angle of the voltage/current vectors to the d-axis.....	69
Figure 3.41 The phase voltages and currents in the connection point.	69
Figure 3.42 The compensation made for reactive power shown in both DC voltage control and power control.....	71
Figure 3.43 The Dymola implementation of the reactive power compensation block.....	72
Figure 3.44 The test bench using power compensation for the power controlled AC/DC inverter.	73
Figure 3.45 The performance of the active (top graph) and reactive (bottom graph) power regulation.	74
Figure 3.46 The alignment of the current (bottom graph) and voltage (top graph) vector towards the d-axis.....	74
Figure 3.47 The phase peak voltages in the connection point.....	75
Figure 4.1 The Multi Controller that incorporate all control loops for the AC/DC converter implemented in Dymola.....	77
Figure 4.2 The content of the control block seen in figure 4.1.	78
Figure 5.1 The figure shows two power electronic converters connected in a Back-to-Back configuration.	83
Figure 5.2 Illustration of a MTDC grid.....	84
Figure 5.3 Test bench for the Back- to Back setup.....	85
Figure 5.4 The graphs show the DC link voltage (top graph), active power (bottom graph in blue) and reactive power (bottom graph in red) and references.....	86
Figure 5.5 The graph shows the active power on the AC side of the AFE DC voltage controller... ..	86
Figure 5.6 The top graph show the d-current control and the bottom graph shows q-current control used in the AFE.	86
Figure 5.7 The top graph show the d-current control and the bottom graph shows q-current control used with the power controller.	87
Figure 5.8 Scenario 1: MTDC for LVDC grid with an AFE DC voltage controller connected to the utility grid. DC voltage level is 1500 V. A wind power unit and solar panels are generating power of 11 kW and 2 kW. A load is connected to one of the converters consuming power between 1kW to 11 kW.....	88
Figure 5.9 Dymola implementation of scenario 1.	89

Figure 5.10 DC link voltage of 1500 V in the top figure and in the lower figure the d,q currents of the DC voltage controller can be seen.	89
Figure 5.11 DC-link voltage in close up with minimum and maximum values of the ripple.	90
Figure 5.12 Produced and consumed power from the wind power unit, solar panel and load.	90
Figure 5.13 Top figures are showing the power and current (phase A) on the utility grid. The bottom figure is showing a FFT analysis of the current in phase a performed in the time interval 0.4-0.55 s.....	91
Figure 5.14 Scenario 2: MTDC for MVDC grid with an AFE DC voltage controller connected to the utility grid. DC voltage level is 2000 V. Two loads are connected to two of the converters consuming a total power of 80 kW. This could resemble an industry with an internal DC grid. ..	92
Figure 5.15 Dymola implementation of scenario 2.	93
Figure 5.16 DC-link voltage of 2000 V in the top figure and in the lower figure the d,q currents of the DC voltage controller can be seen.	93
Figure 5.17 DC-link voltage in close up with minimum and maximum values of the ripple	94
Figure 5.18 Produced and consumed power from the wind power unit and loads.	94
Figure 5.19 Top figures are showing the current (phase a) on the utility grid and a FFT analysis of the current in phase A performed in the time interval 0.25-0.39 s. The bottom figure is showing the power flow in the utility grid.....	95
Figure 5.20 Scenario 3: MTDC for HVDC grid with an AFE DC voltage controller connected to the utility grid. DC voltage level is 50 kV. Three loads are connected to the power controllers consuming a total power of 4MW. One of the loads is also regenerating power of 1 MW. This could resemble a HVDC grid with one connection to the utility grid and different loads drawing and regenerating power	96
Figure 5.21 Dymola implementation of scenario 3.	96
Figure 5.22 DC link voltage of 50 kV in the top figure and in the lower figures the d,q currents of the DC voltage controller can be seen.	97
Figure 5.23 DC-link voltage in close up with minimum and maximum values of the ripple	97
Figure 5.24 Consumed and produced power from the loads.....	98
Figure 5.25 The figure is showing the power and phase A current on the three phase utility grid	98
Figure 5.26 The grid setup for the DC grid with Smart Grid Library and Wind Power Library models connected.	101
Figure 5.27 The voltage of the DC grid.....	101
Figure 5.28 The power consumed by the load and the power supplied to/consumed from the AC distribution grid.....	102
Figure 5.29 The power supplied by the generators, in the wind power plants and for the solar power plant.	102
Figure 5.30 Dymola implementation of scenario 2.	104
Figure 5.31 The DC link voltage with (bottom figure) and without droop control (top figure)...	104
Figure 5.32 The DC link voltage and the power from the generator both controlled by the droop controller where the DC grid is disconnected from the utility grid every fifth second.	105
Figure 5.33 The grid structure of the high voltage scenario with large power flows.	106
Figure 5.34 The grid structure of the high voltage scenario implemented in Dymola.	107
Figure 5.35 The power generated by the wind power plants fed to the internal DC grid.	107
Figure 5.36 The power generated by the water power plant and the power supplied to the utility grid.....	108
Figure 5.37 The voltage at the connection point of the DC grid to the utility grid.....	108

Figure 5.38 Internal AC grid with back to back connected inverters.	109
Figure 5.39 The simulation model of the AC grid setup implemented in Dymola.	111
Figure 5.40 The voltage in the internal grid connection point.....	112
Figure 5.41 The alignment of the current and voltage vectors to the d-axis.	112
Figure 5.42 The consumed power from the internal AC grid.....	113
Figure 5.43 The supplied power to the internal AC grid.	113
Figure 5.44 The power supplied/consumed to the distribution grid (negative corresponds to power fed to the distribution grid).....	114
Figure 5.45 The phase voltages in the connection point.	115
Figure 5.46 The alignment of the current and voltage vector with the d-axis.	115
Figure 5.47 The power consumed from the internal AC grid by the loads.	116
Figure 5.48 The power supplied to the internal AC grid by the generators.....	116
Figure 5.49 The remaining power that is needed to either output to the distribution grid or that has to be supplied to the internal AC grid.....	117

9 LIST OF TABLES

Table 3.1 The table lists the control parameters set to the test bench.	37
Table 3.2 The table lists the system parameters set to the test bench.....	37
Table 3.3 The control parameters for the test bench.	44
Table 3.4 The system parameters for the test bench.	44
Table 3.5 The parameters for the controllers in the test bench.	53
Table 3.6 The system parameters set for the test bench.....	53
Table 3.7 The control parameters for the droop control test bench.	61
Table 3.8 The system parameters for the droop control test bench.	61
Table 3.9 The voltage limits for the droop control.	61
Table 3.10 The weights of the droop control.....	62
Table 3.11 The system parameters for the open loop AC voltage control.	68
Table 3.12 The control parameters of the power controlled converter in the test bench.....	73
Table 3.13 The system parameters of the power controlled converter in the test bench.	73
Table 5.1 Power control parameters for the test bench.	85
Table 5.2 Voltage control parameters for the test bench.	85
Table 5.3 System parameters for the converters in the test bench.	85
Table 5.4 The specifications of the three scenarios.	88
Table 5.5 Scenario specifications for the AC-grid.....	111

10 ACRONYMS

AC – Alternating Current

AFE – Active Front End

DC – Direct Current

EPL – Electric Power Library

FFT – Fast Fourier Transform

GUI – Graphical User Interface

HVDC – High Voltage Direct Current

IEC – International Electrotechnical Commission

IGBT – Insulated Gate Bipolar Transistor

KVL – Kirchhoff's Voltage Law

LVDC – Low Voltage Direct Current

MTDC – Multi Terminal Direct Current

MVDC – Medium Voltage Direct Current

PWM – Pulse Width Modulation

RMS – Root Mean Square

11 REFERENCES

- [1] Fraunhofer, Juliane Segdi, Smart grid for electric vehicle fleet, <http://www.fraunhofer.de/en/press/research-news/2014/march/smart-grid.html>, [2014 05 14]
- [2] ABB, Onboard DC grid, <http://www.abb.com/cawp/seitp202/0f5012e931f12dabc12579ae00557dd2.aspx>, [2014 05 14]
- [3] Siemens, Connecting wind power to the grid, https://w3.siemens.com/powerdistribution/global/SiteCollectionDocuments/en/mv/switchgear/gas-insulated-medium-voltage-switchgear-wind-farms_en.pdf, [2014 05 14]
- [4] Garfield, How electric vehicles work, <http://www.garfieldcleanenergy.org/trans-EV-how-they-work.html>, [2014 05 14]
- [5] M Alaküla, P Karlsson, *Power Electronics: Devices, Converter, Control and Applications*, Department of Industrial Electrical Engineering and Automation.

- [6] M. Alaküla, L. Gertmar, O. Samuelsson, *Elenergiteknik*, (2011), Lund, Sweden, Lunds Tekniska Högskola, Department of Industrial Electrical Engineering and Automation.
- [7] B. Stenborg, *Elkraftsystem Del 1: Systemet och dess lugndriftstillstånd*, (1997), Göteborg, Sweden, Gothia Power.
- [8] T. M. Haileselassie; Control, Dynamics and Operation of Multi-terminal VSC-HVDC Transmission Systems, Norwegian University of Science and Technology Department of Electric Power Engineering Trondheim December 2012.
- [9] S. L. Sanjuan, Voltage Oriented Control of Three-Phase Boost PWM Converters Design, simulation and implementation of a 3-phase boost battery charger. Department of Energy and Environment ,Division of Electric Power Engineering CHALMERS UNIVERSITY OF TECHNOLOGY, Göteborg, Sweden, 2010.
- [10] A. Carlsson, The back to back converter control and design, Lund, Sweden, Department of Industrial Electrical Engineering and Automation Lund Institute of Technology, May 1998.
- [11] IEC 61000-3-2, Limits – Limits for harmonic current emissions (equipment input current ≤ 16 A per phase), Edition 3.0, 2005-11.
- [12] J. Petersson and P. Isaksson, Modelling and Simulation of a Vertical Wind Power Plant in Dymola/Modelica, Lund, Sweden, Division of Industrial Electrical Engineering and Automation Faculty of Engineering, Lund University 2011.
- [13] F. Mura and Rik. W. De Doncker ,Design Aspects of a Medium-Voltage Direct Current (MVDC) Grid for a University Campus, RWTH Aachen University, E.ON Energy Research Center, Aachen, Germany, 2011.
- [14] T. Hägglund, (2011), Reglerteknik AK Föreläsningar, Lund, Sweden: KFS I Lund AB.
- [15] T. Ogard and S. Persson, High Voltage Pulsed Power Converters for the ESS Linear Accelerator, Department of Electrical and Information Technology Faculty of Engineering, LTH, Lund University, Lund, Sweden. 2014.
- [16] Modelica, Modelica and the Modelica Association, <https://modelica.org/> , [2014 06 04]
- [17] Modelon AB, Dymola, <http://www.modelon.com/products/dymola/>, [2014 06 04]
- [18] Modelon AB, EPL, <http://www.modelon.com/products/modelica-libraries/electrical-power-library/> , [2014 06 04]
- [19] Modelica, Modelica Libraries, <https://modelica.org/libraries>, [2014 06 04]
- [20] J. Enerbäck, O. Nalin Nilsson, Modelling and Simulation of

Smart Grids using Dymola/Modelica, Division of Industrial Electrical Engineering and Automation, Faculty of Engineering, Lund University, Lund, Sweden, 2013

- [21] S. Andersson & J. Strömner, Model Calibration of a Vertical Wind Power Plant using Dymola/Modelica, Division of Industrial Electrical Engineering and Automation, Lund University, Lund Sweden, 2013

APPENDIX A

Limitations of the amount of current harmonics injected into the low voltage grid are set by the IEC 61000-3-2.

Harmonic order n	Maximum permissible harmonic current expressed as a percentage of the input current at the fundamental frequency %
2	2
3	$30 \cdot \lambda^*$
5	10
7	7
9	5
$11 \leq n \leq 39$ (odd harmonics only)	3

* λ is the circuit power factor

Figure A1 The figure is illustrating the limits for the current harmonic set by IEC 61000-3-2 [11].

A FFT analysis can be made to measure the amount of injected current harmonics into the grid. The FFT analysis shall be performed during 1.5 seconds and the first and last 10 seconds when the system is in start up or shut down shall not be included [11].

APPENDIX B

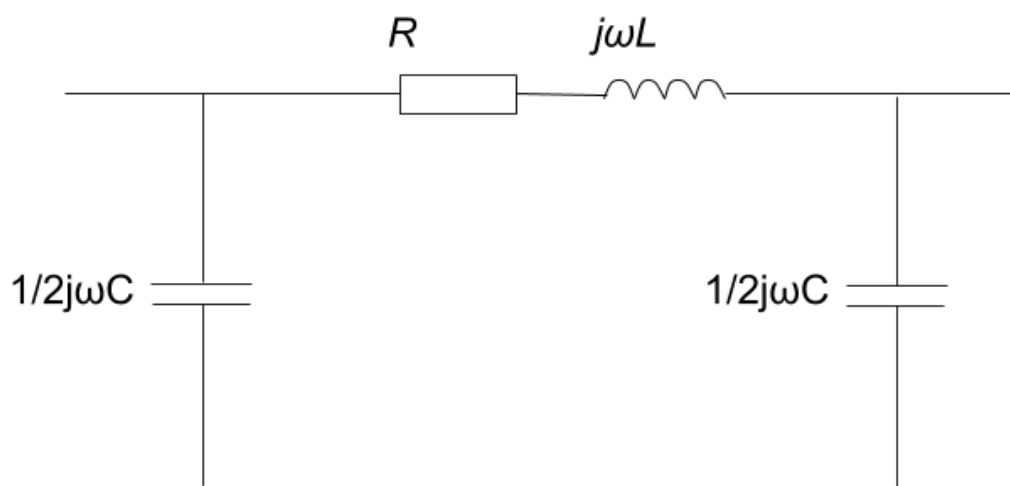


Figure B1 The π -circuit equivalent of a symmetrical three phase AC line.

APPENDIX C

Table for switched grid implementation:	Scenario 1	Scenario 2	Scenario 3
L_{grid}	0.101 mH	0.101 mH	1.58 mH
L_{load}	0.101 mH	0.101 mH	1.58 mH
$L_{wind\ power}$	0.101 mH	0.101 mH	1.58 mH
$L_{AFE\ conv}$	6.4 mH	6.4 mH	0.318 mH
$L_{power\ conv}$	47.7 mH	12.7 mH	0.223 H
$L_{DC/DC\ conv}$	50 mH	-	-
$C_{power\ conv}$	80 μF	80 μF	0.1 mF
$C_{AFE\ conv}$	800 μF	400 mF	1 mF
$C_{DC/DC\ conv}$	300 μF	-	-
AFE DC voltage controller/current controllers			
k_{AFE}	-0.8	-2	-1
Ti_{AFE}	0.01	0.01	0.005
k_{id}	5000	5000	5000
k_{iq}	100	100	100
Ti_{iq}	0.00001	0.00001	0.00001
AC/DC power controller/current controllers			
$k_{active\ power\ contr}$	0.0005	0.0005	0.00005
$Ti_{active\ power\ contr}$	0.001	0.001	0.001
$k_{reactive\ power\ contr}$	-0.0001	-0.0001	-0.0001
$Ti_{reactive\ power\ contr}$	0.0001	0.0001	0.0001
k_{id}	5000	5000	5000
k_{iq}	5000	5000	5000
DC/DC power controller/current controllers			
$k_{DC/DC\ power\ contr}$	0.0003	-	-
$Ti_{power\ contr}$	0.001	-	-
$k_{DC/DC\ current\ contr}$	15	-	-

Table C1 Table of parameters for the switched grid scenarios.

Power controlled DC/DC converter/Current Controllers		DC voltage controlled AFE converter/ Current Controllers	
K_P	0.0005	K_V	-3
$T_{i,P}$	0.001	$T_{i,V}$	0.008
L_{conv}	-	L_{conv}	3.18 mH
$C_{DC-link}$	-	$C_{DC-link}$	1.5 mF
k_i	20	k_{id}	500
		k_{iq}	500

Table C2 Table of parameters for the DC Grid with external models.

Droop controlled AC/DC converters/ Current Controllers		DC voltage controlled AFE converter/ Current Controllers	
K_P	5	K_V	-3
K_{RP}	-0.0001	$T_{i,V}$	0.008
$T_{i,RP}$	0.0001	-	-
L_{conv}	6.37 mH	L_{conv}	3.18 mH

$C_{DC-link}$	0.8 mF	$C_{DC-link}$	1.5 mF
k_{id}	500	k_{id}	500
k_{iq}	500	k_{iq}	500

Table C3 Table of parameters for the DC grid with external models using droop control.

Power controlled AC/DC converters/ Current Controllers		DC voltage controlled AFE converter/ Current Controllers	
K_P	0.005	K_V	-20
T_{iP}	0.02	T_{iV}	0.03
L_{conv}	31.8 mH	L_{conv}	0.16 mH
$C_{DC-link}$	1 mF	$C_{DC-link}$	0.1 F
k_{id}	500	k_{id}	500
k_{iq}	500	k_{iq}	500

Table C4 Table of parameters of the high voltage scenario.

Parameters	Scenario 1	Scenario 2
DC voltage controller connected to AC generators		
K_V	-3	-50
T_{iV}	0.008	0.01
L_{conv}	31.8 mH	0.16 mH
$C_{DC-link}$	1.5 mF	50 mF
DC voltage controller connected to distribution AC grid		
K_V	-3	-50
T_{iV}	0.008	0.01
L_{conv}	3.2 mH	0.16 mH
$C_{DC-link}$	1.5 mF	50 mF
DC voltage controller connected to internal AC grid		
K_V	-1	-
T_{iV}	0.008	-
K_{RP}	-0.0001	-
T_{iRP}	0.0001	-
L_{conv}	3.2 mH	-
$C_{DC-link}$	1.5 mF	-
Power controller connected to internal AC grid		
K_{AP}	0.0005	0.0005
T_{iAP}	0.001	0.001
K_{RP}	-0.0001	-0.0001
T_{iRP}	0.0001	0.0001
L_{conv}	31.8 mH	79.5 mH
$C_{DC-link}$	0.5 mF	1 mF
Power controller DC/DC converter		
K_P	0.0005	-
T_{iP}	0.001	-
$K_{current}$	20	-

Table C5 Table of parameters for the AC grid scenarios.

APPENDIX D

The Modelica code for the time average inverter model can be seen below.

```
model InverterAverage "Inverter time-average, 3-phase abc"
  extends Partials.SwitchEquation;
  extends ElectricPower.Common.Thermal.AddThermalIV(
    final m_thermal=1,
    final cT=par.cT,
    final T_ref=par.T_ref);

  constant Boolean needsModulator=false;
  // parameter Types.ModulationType modulation=Types.ModulationType.sin_PWM
  parameter Types.ModulationType modulation=1 "equivalent modulation";
  parameter Boolean syn=false "synchronous, asynchronous"
    annotation(Evaluate=true, Dialog(enable=modulation<3), choices(
      choice=true "synchronous",
      choice=false "asynchronous"));
  parameter Integer m_carr(min=1)=1 "f_carr/f, pulses/period"
    annotation(Evaluate=true, Dialog(enable=syn and modulation<3));
  parameter SI.Frequency f_carr=1e3 "carrier frequency"
    annotation(Evaluate=true, Dialog(enable=not syn and modulation<3));
  parameter Real width0=2/3 "relative width, (0 - 1)"
    annotation(Dialog(enable=modulation==3));
  parameter ElectricPower.Semiconductors.Ideal.SCparameters par "SC parameters"
    annotation (Placement(transformation(extent={{-100,-80},{-80,-60}},
      rotation=0)));
  Modelica.Blocks.Interfaces.BooleanInput[6] gates=fill(false, 6)
    "dummy gates, allow model being used in GenInverter";
  Modelica.Blocks.Interfaces.RealInput[2] u_alpha
    "reference voltage {abs(u) [pu], rotating-phase(u)}"
    annotation (Placement(transformation(
      origin={60,100},
      extent={{-10,-10},{10,10}},
      rotation=270), iconTransformation(
      extent={{-10,-10},{10,10}},
      rotation=270,
      origin={60,100})));
protected
  outer System system;
  final parameter SI.Resistance R_nom=par.V_nom/par.I_nom;
  final parameter Real M_factor=
    if modulation==Types.ModulationType_sin_PWM then 1 else
    if modulation==Types.ModulationType_SV_PWM then (4/3) else
    if modulation==Types.ModulationType_block_M then (4/pi)*sin(width0*pi/2) else 0
    annotation(Evaluate=true);
  SI.Voltage Vloss;
  Real iAC;
  Real hsw_nom;
  function transCinf = ElectricPower.Basic.Math.transientCinf;

equation
  Vloss = if par.Vf<1e-3 then 0 else transCinf(iDC1, 0.1*par.I_nom)*2*par.Vf*Tfactor[1];
  iAC = sqrt(ACterm.i*ACterm.i);
  hsw_nom = if syn then (2*par.Hsw_nom*m_carr/(pi*par.V_nom*par.I_nom))*der(ACterm.theta[1]) else
    4*par.Hsw_nom*f_carr/(par.V_nom*par.I_nom);

  switch_abc = M_factor*u_alpha[1]*cos(fill(u_alpha[2], 3) - ElectricPower.Basic.Constants.phaseShift);
  v_abc = (vDC1 - Vloss)*switch_abc;
  // passive mode?

  pThermal = if add_thermal then {(2*sqrt(6)/pi)*(par.Vf + hsw_nom*abs(vDC1))*Tfactor[1]*iAC} else zeros(m_thermal);
end InverterAverage;
```

The Modelica code for the switch inverter model can be seen below.

```

model InverterSwitch "Inverter switch equation, 3-phase abc"
extends Partial.SwitchEquation;
extends ElectricPower.Common.Thermal.AddThermalIV(
  final m_thermal=3,
  final cT=par.cT,
  final T_ref=par.T_ref);

constant Boolean needsModulator=true;
parameter SI.Time t_av = 0.1 "averaging time switching heat pulses" annotation(Dialog(tab="Thermal"), Evaluate=true);
parameter ElectricPower.Semiconductors.Ideal.SCparameters par "SC parameters"
  annotation (Placement(transformation(extent={{-100,-80},{-80,-60}},
    rotation=0)));
Modelica.Blocks.Interfaces.BooleanInput[6] gates
  "gate pairs {a_p, a_n, b_p, b_n, c_p, c_n}"
  annotation (Placement(transformation(
    origin={-60,100},
    extent={{-10,-10},{10,10}},
    rotation=270)));
Modelica.Blocks.Interfaces.RealInput[2] u_alpha
  "reference voltage {abs(u) [pu], rotating-phase(u)}"
  annotation (Placement(transformation(
    origin={60,100},
    extent={{-10,-10},{10,10}},
    rotation=270)));
protected
constant Integer[3] pgt={1,3,5} "positive gates";
constant Integer[3] ngt={2,4,6} "negative gates";
constant Integer[6] k = {1,1,2,2,3,3};
final parameter Real gamma = par.Hsw_nom/(2*t_av*par.V_nom*par.I_nom);
SI.Voltage[3] V;
SI.Voltage[3] V_s;
SI.Voltage[3] V_d;
SI.Voltage[3] i_sc "current scaled to voltage in abc representation";
Real[3] s "arc-length on characteristic";
discrete SI.Time[6] t_sw(final start=zeros(6)) "switching time (gate-change)";
discrete Real[6] p_sw(final start=zeros(6), fixed=true)
  "summed switching heat-pulses (recursion)";

equation
V = par.Vf*Tfactor;
V_d = fill(vDC1, 3) + V;
V_s = fill(vDC1, 3) - V;
i_sc = ACterm.i*par.V_nom/par.I_nom;

if initial() then // average values
  switch_abc = u_alpha[1]*cos(fill(u_alpha[2], 3) - ElectricPower.Basic.Constants.phaseShift);
  v_abc = vDC1*switch_abc;
  i_sc = s;
else
  for k in 1:3 loop
    if gates[pgt[k]] then // switched mode DC+ to AC
      switch_abc[k] = 1;
      if s[k] > V_d[k] then
        {v_abc[k],i_sc[k]} = {par.eps[1]*s[k] + (1 - par.eps[1])*V_d[k],s[k] - (1 - par.eps[2])*V_d[k]};
      elseif s[k] < V_s[k] then
        {v_abc[k],i_sc[k]} = {par.eps[1]*s[k] + (1 - par.eps[1])*V_s[k],s[k] - (1 - par.eps[2])*V_s[k]};
      else
        {v_abc[k],i_sc[k]} = {s[k],par.eps[2]*s[k]};
      end if;
    elseif gates[ngt[k]] then // switched mode DC- to AC
      switch_abc[k] = -1;
      if s[k] < -V_d[k] then
        {v_abc[k],i_sc[k]} = {par.eps[1]*s[k] - (1 - par.eps[1])*V_d[k],s[k] + (1 - par.eps[2])*V_d[k]};
      elseif s[k] > -V_s[k] then
        {v_abc[k],i_sc[k]} = {par.eps[1]*s[k] - (1 - par.eps[1])*V_s[k],s[k] + (1 - par.eps[2])*V_s[k]};
      else
        {v_abc[k],i_sc[k]} = {s[k],par.eps[2]*s[k]};
      end if;
    else // rectifier mode
      if s[k] > V_d[k] then // vDC+ < vAC

```

```

    {v_abc[k],i_sc[k]} = {par.eps[1]*s[k] + (1 - par.eps[1])*V_d[k], s[k] - (1 - par.eps[2])*V_d[k]};
elseif s[k] < -V_d[k] then // vAC < vDC-
    {v_abc[k],i_sc[k]} = {par.eps[1]*s[k] - (1 - par.eps[1])*V_d[k], s[k] + (1 - par.eps[2])*V_d[k]};
else // vDC- < vAC < vDC+
    {v_abc[k],i_sc[k]} = {s[k],par.eps[2]*s[k]};
end if;
switch_abc[k] = sign(s[k]);
end if;
end for;
end if;

pThermal = if add_thermal then (V.*abs(i_sc) + {sum(p_sw[1:2]),sum(p_sw[3:4]),sum(p_sw[5:6])})*(par.I_nom/par.V_nom)
    else zeros(m_thermal);

for i in 1:6 loop
    when change(gates[i]) then
        t_sw[i] = time;
        p_sw[i] = pre(p_sw[i])*exp(-(t_sw[i] - pre(t_sw[i]))/t_av) + gamma*(abs(v_abc[k]*pre(i_sc[k])) + abs(pre(v_abc[k])*i_sc[k]));
    end when;
end for;
end InverterSwitch;

```

The principal Modelica code structure for the wait blocks that has been used in the switch converter models can be seen below. The parameters seen in this code are for the AFE DC voltage converter.

model WaitUntil_hysteres

```

Modelica.Blocks.Interfaces.RealInput Vdc_ref
    annotation (Placement(transformation(extent={{-116,60},{-76,100}}),
        iconTransformation(extent={{-110,64},{-82,92}})));
Modelica.Blocks.Interfaces.RealInput Vdc
    annotation (Placement(transformation(extent={{-120,22},{-80,62}}),
        iconTransformation(extent={{-110,32},{-80,62}})));
Modelica.Blocks.Interfaces.RealInput id
    annotation (Placement(transformation(extent={{-120,-4},{-80,36}}),
        iconTransformation(extent={{-110,-2},{-80,28}})));
Modelica.Blocks.Interfaces.RealInput iq
    annotation (Placement(transformation(extent={{-120,-58},{-80,-18}}),
        iconTransformation(extent={{-110,-38},{-80,-8}})));
Modelica.Blocks.Interfaces.RealInput iqref
    annotation (Placement(transformation(extent={{-120,-84},{-80,-44}}),
        iconTransformation(extent={{-110,-74},{-84,-48}})));
Modelica.Blocks.Interfaces.RealOutput Vdc_ref_out
    annotation (Placement(transformation(extent={{90,58},{110,78}})));
Modelica.Blocks.Interfaces.RealOutput Vdc_out
    annotation (Placement(transformation(extent={{90,32},{110,52}})));
Modelica.Blocks.Interfaces.RealOutput id_out
    annotation (Placement(transformation(extent={{92,8},{112,28}})));

Modelica.Blocks.Interfaces.RealOutput iq_out
    annotation (Placement(transformation(extent={{90,-48},{110,-28}})));
Modelica.Blocks.Interfaces.RealOutput iq_ref_out
    annotation (Placement(transformation(extent={{90,-72},{110,-52}})));
parameter Real VoltageLimit = 550;
protected
    Boolean control;
equation
    if
        (Vdc > VoltageLimit) then
            control = true;
            id_out = id;
            iq_out = iq;
            Vdc_ref_out = Vdc_ref;
            Vdc_out = Vdc;
            iq_ref_out = iqref;
        elseif (Vdc <= VoltageLimit and Vdc > 0.95*VoltageLimit and pre(control)) then
            control = true;
            id_out = id;

```

```

iq_out = iq;
Vdc_ref_out = Vdc_ref;
Vdc_out = Vdc;
iq_ref_out = iqref;
elseif (Vdc <= VoltageLimit and Vdc > 0.95*VoltageLimit and not pre(control)) then
  control = false;
  id_out = 0;
  iq_out = 0;
  Vdc_ref_out = 0;
  Vdc_out = 0;
  iq_ref_out = 0;
elseif (Vdc <= 0.95*VoltageLimit) then
  control = false;
  id_out = 0;
  iq_out = 0;
  Vdc_ref_out = 0;
  Vdc_out = 0;
  iq_ref_out = 0;
else
  control = false;
  id_out = 0;
  iq_out = 0;
  Vdc_ref_out = 0;
  Vdc_out = 0;
  iq_ref_out = 0;
end if;

end WaitUntil_hysteres;

```

The Modelica code for the wait block that is used inside the EPL inverter can be studied below.

```
model Wait_hysteres
```

```

  Modelica.Blocks.Interfaces.RealInput compareSignal
  annotation (Placement(transformation(extent={{-120,-20},{-80,20}})));
  Modelica.Blocks.Interfaces.BooleanOutput[6] y
  annotation (Placement(transformation(extent={{100,-10},{120,10}})));

  Modelica.Blocks.Interfaces.BooleanInput[6] gates
  annotation (Placement(transformation(extent={{-120,26},{-80,66}})),
    iconTransformation(extent={{-120,26},{-80,66}}));
  parameter Real VoltageLimit = 550;
protected
  Boolean control;
equation
  if
    (compareSignal >= VoltageLimit) then
    control = true;
    y[1] = gates[1];
    y[2] = gates[2];
    y[3] = gates[3];
    y[4] = gates[4];
    y[5] = gates[5];
    y[6] = gates[6];
  elseif (compareSignal <= VoltageLimit and compareSignal > 0.95*VoltageLimit and pre(control)) then
    control = true;
    y[1] = gates[1];
    y[2] = gates[2];
    y[3] = gates[3];
    y[4] = gates[4];
    y[5] = gates[5];
    y[6] = gates[6];
  elseif (compareSignal <= VoltageLimit and compareSignal > 0.95*VoltageLimit and not pre(control)) then
    control = false;
    y[1] = false;
    y[2] = false;
    y[3] = false;
    y[4] = false;
    y[5] = false;
    y[6] = false;
  elseif (compareSignal <= 0.95*VoltageLimit) then

```

```

    control = false;
    y[1] = false;
    y[2] = false;
    y[3] = false;
    y[4] = false;
    y[5] = false;
    y[6] = false;
  else
    control = false;
    y[1] = false;
    y[2] = false;
    y[3] = false;
    y[4] = false;
    y[5] = false;
    y[6] = false;

  end if
end Wait_hysteres;

```

The Modelica code for a base record (where parameters are declared) can be seen below.

```

partial record BaseRecord_VoltageControl
  extends Modelica.Icons.Record;
  parameter Real Vdc_ref "Constant output value";
  parameter Real iq_ref "Constant output value";
  parameter Modelica.SIunits.Capacitance C "total capacitance";
  parameter Modelica.SIunits.Voltage Vstart_ACDC
    "start voltage for the DC link";
  parameter ElectricPower.Basic.Types.SIpu.Resistance r
    "resistance @T_ref [SI | pu]";
  parameter ElectricPower.Basic.Types.SIpu.Reactance x_s
    "self reactance [SI | pu]";
  parameter Real timeLimit "tid innan inverteraren kopplas på";
  parameter Real VoltageLimit;

  /// Voltage Controller
  parameter Real k_v "Gain of controller";
  parameter Modelica.SIunits.Time Ti_v "Time constant of Integrator block";
  parameter Modelica.SIunits.Time Td_v "Time constant of Derivative block";
  parameter Real wp_v "Set-point weight for Proportional block (0..1)";
  parameter Real wd_v "Set-point weight for Derivative block (0..1)";
  parameter Real Ni_v "Ni*Ti is time constant of anti-windup compensation";
  parameter Real Nd_v "The higher Nd, the more ideal the derivative block";
  parameter Modelica.Blocks.Types.InitPID initType_v
    "Type of initialization (1: no init, 2: steady state, 3: initial state, 4: initial output)";
  parameter Real yMax_v "Upper limit of output";
  parameter Real yMin_v "Lower limit of output";
  parameter Boolean limitsAtInit_v
    "= false, if limits are ignored during initialization";
  parameter Real xi_start_v
    "Initial or guess value value for integrator output (= integrator state)";
  parameter Real xd_start_v=0
    "Initial or guess value for state of derivative block";
  parameter Real y_start_v "Initial value of output";

  /// id controller

  parameter Real k_id "Gain of controller";
  parameter Modelica.SIunits.Time Ti_id "Time constant of Integrator block";

  parameter Modelica.SIunits.Time Td_id "Time constant of Derivative block";

  parameter Real wp_id "Set-point weight for Proportional block (0..1)";
  parameter Real wd_id "Set-point weight for Derivative block (0..1)";
  parameter Real Ni_id "Ni*Ti is time constant of anti-windup compensation";

  parameter Real Nd_id "The higher Nd, the more ideal the derivative block";
  parameter Modelica.Blocks.Types.InitPID initType_id
    "Type of initialization (1: no init, 2: steady state, 3: initial state, 4: initial output)";

  parameter Boolean limitsAtInit_id

```

```

    "= false, if limits are ignored during initialization";
parameter Real xi_start_id
    "Initial or guess value for integrator output (= integrator state)";
parameter Real xd_start_id
    "Initial or guess value for state of derivative block";
parameter Real y_start_id "Initial value of output";

/// iq controller

parameter Real k_iq "Gain of controller";
parameter Modelica.SIunits.Time Ti_iq "Time constant of Integrator block";

parameter Modelica.SIunits.Time Td_iq "Time constant of Derivative block";

parameter Real wp_iq "Set-point weight for Proportional block (0..1)";
parameter Real wd_iq "Set-point weight for Derivative block (0..1)";
parameter Real Ni_iq "Ni*Ti is time constant of anti-windup compensation";

parameter Real Nd_iq "The higher Nd, the more ideal the derivative block";
parameter Modelica.Blocks.Types.InitPID initType_iq
    "Type of initialization (1: no init, 2: steady state, 3: initial state, 4: initial output)";

parameter Boolean limitsAtInit_iq
    "= false, if limits are ignored during initialization";
parameter Real xi_start_iq
    "Initial or guess value value for integrator output (= integrator state)";
parameter Real xd_start_iq
    "Initial or guess value for state of derivative block";
parameter Real y_start_iq "Initial value of output";

end BaseRecord_VoltageControl;

```

Scenario parameters are fitted into the base record through an extended model seen below.

```

record Scenario1
    "Switched Grid 2000 V load 11 kW (Suitable for 400 V AC Source)"
    extends BaseRecord_VoltageControl(
        Vdc_ref=2000,
        iq_ref=0,
        C=0.0008,
        Vstart_ACDC=0,
        r=0.00005,
        x_s=2,
        timeLimit=0,
        VoltageLimit=550,
        k_v=-3,
        Ti_v=0.001,
        Td_v=1,
        wp_v=1,
        wd_v=1,
        Ni_v=0.1,
        Nd_v=0.2,
        initType_v=.Modelica.Blocks.Types.InitPID.DoNotUse_InitialIntegratorState,
        yMax_v=10000,
        yMin_v=-100,
        limitsAtInit_v=true,
        xi_start_v=0,
        xd_start_v=0,
        y_start_v=0,
        k_id=5000,
        Ti_id=0.1,
        Td_id=0.1,
        wp_id=1,
        wd_id=1,
        Ni_id=0.01,
        Nd_id=1,
        initType_id=.Modelica.Blocks.Types.InitPID.DoNotUse_InitialIntegratorState,
        limitsAtInit_id=true,
        xi_start_id=0,
        xd_start_id=0,
        y_start_id=0,

```

```
k_iq=100,  
Ti_iq=0.00001,  
Td_iq=1,  
wp_iq=1,  
wd_iq=1,  
Nd_iq=0.1,  
Ni_iq=0.01,  
initType_iq=Modelica.Blocks.Types.InitPID.DoNotUse_InitialIntegratorState,  
limitsAtInit_iq=true,  
xi_start_iq=0,  
xd_start_iq=0,  
y_start_iq=0);  
end Scenario1;
```